ENGINEERED WATER REPELLENCY FOR FROST HEAVE MITIGATION: DECOUPLING THE RELATIVE INFLUENCE OF MATRIC AND OSMOTIC SUCTION

by

Micheal Uduebor

A dissertation submitted to the faculty of
The University of North Carolina at Charlotte
in partial fulfillment of the requirements
for the degree of Doctor of Philosophy in
Civil Engineering

Charlotte

2023

Approved by:

_____
Dr. John L. Daniels

_____
Dr. Vincent O. Ogunro

_____
Dr. Milind Khire

_____
Dr. Bora Cetin (MSU)

_____
Dr. Yunesh Saulick

ABSTRACT

MICHEAL UDUEBOR. Engineered Water Repellency for Frost Heave Mitigation: Decoupling the Relative Influence of Matric and Osmotic Suction
(Under the direction of DR. JOHN L. DANIELS)

This dissertation, stemming from a substantial research endeavor funded by the U.S. National Science Foundation (Award #1928813), stands as an essential exploration of Engineered Water Repellency (EWR) in mitigating frost heave. Combining laboratory experiments, field investigations, and numerical analyses, this interdisciplinary study aims to disentangle the impact of matric and osmotic potentials on this phenomenon, marking a significant leap in our comprehension of frost heave mechanisms. Frost-susceptible soils (FSS) present challenges in construction due to their dynamic thermal and mechanical properties. The detrimental effects of frost heave on infrastructure, particularly road pavements, prompt immense costs—over two billion US dollars annually—attributed to recurrent maintenance and structural damage. Extensive research, from as early as the 17th century, has grappled with the complexities of frost heaving, highlighting the transport of moisture to freezing fronts as a key factor. While prevailing studies have centered on matric effects, the influence of solutes on ice lensing has been noted, underscoring the need for further investigation. Engineered Water Repellency (EWR) emerges as a promising solution. By treating soils with environmentally compatible polymers, the transport of water through frost-susceptible soils can be limited, offering a viable alternative to combat frost action. Experimental assessments revealed that increasing EWR treatment led to higher hydrophobicity, with contact angles surpassing 110° and Water Drop Penetration Test times exceeding 3600 seconds. However, optimal treatment concentrations varied by

organosilane, demonstrating plateauing trends in hydrophobicity. Exploration of grain size effects on water-repellent soils showcased reduced contact angles with increasing grain size, influencing the effectiveness of treatment. This indicated the necessity of considering soil properties for successful implementation in infrastructure. Further analyses unveiled the impact of salt concentrations on EWR treatment efficacy. Salts, common in cold regions for road maintenance, proved to diminish the water-repellent properties, requiring careful consideration in treatment strategies. The interplay between water repellency and hygroscopicity highlighted treatment dosage, drying conditions, and soil properties as crucial factors. While silanes and siloxanes limit moisture absorption, they don't eradicate it, emphasizing the complexity of soil performance. Evaluation of breakthrough pressure in water-repellent soils offered insights for using these materials as moisture barriers in construction. Automated tests indicated that treated soils could sustain hydrostatic heads of up to 36kPa. Frost heave mitigation, using EWR treatment, was proven effective even after multiple freeze-thaw cycles. A systematic exploration of osmotic potential in freezing soils paved the way for a refined understanding of freezing soil processes, shedding light on factors influencing water migration and frost heave. This dissertation serves as a milestone in comprehending frost heave mechanisms and the potential of EWR treatment in geotechnical applications. The comprehensive exploration of soil treatment, the impact of soil properties, and the complexities of water repellency underpin a promising avenue for addressing frost heave challenges in construction and infrastructure.

ACKNOWLEDGEMENTS

I would like to express my profound gratitude to my advisor, Dr. John L. Daniels, for his unwavering support, invaluable guidance, constant encouragement, and exceptional mentorship throughout my academic journey at UNC Charlotte. His expertise and dedication have played a pivotal role in shaping the direction and success of my doctoral dissertation. I am immensely grateful to the esteemed members of my doctoral dissertation committee, Dr. Vincent O. Ogunro, Dr. Milind Khire, Dr. Bora Cetin, and Dr. Yunesh Saulick, for their valuable contributions and insightful feedback on my research. Their expertise and rigorous review have significantly strengthened the quality and rigor of my work. I would also like to express my heartfelt appreciation to my fellow research assistants in the Civil Engineering doctoral program at UNC Charlotte, particularly Emmanuel Adeyanju, and Adams Familusi for their camaraderie, stimulating discussions, and enduring friendship. Their presence has enriched my academic experience and provided a supportive network within the department. I owe a debt of gratitude to the other members of the Daniels Research Lab Team - Rui, Mackenzie, Mya, and David - for cultivating a conducive and collaborative research environment. Their teamwork, cooperation, and shared passion for knowledge have been indispensable in fostering my growth and development as a researcher. I wish to acknowledge the financial support that has made this research possible. The National Science Foundation and the Iowa Highway Research Board deserve special recognition for their funding contributions. Additionally, I am grateful for the grants, fellowships, scholarships, and travel support I have received from the UNCC Graduate School, UNCC GCLL, UNCC GPSG, ASCE Geo-Institute, and the Civil & Environmental Engineering Department. Their financial assistance has alleviated

the burdens associated with conducting research and attending academic conferences. I would like to extend my sincere appreciation to the Engineers from Charlotte Douglas International Airport, NCDOT and IowaDOT for their logistical support in providing soil samples and log data from field sites. Their collaboration has been invaluable in obtaining essential data for my research. Lastly, I am indebted to my loving family, the Uduebor, Olajide, Imoh, and Ugbaja Families, as well as my dear friends, for their immeasurable love, unwavering support, and constant encouragement throughout this interesting journey.

DEDICATION

…for Aan and Hizo.

TABLE OF CONTENTS

LIST OF TABLES

LIST OF FIGURES

LIST OF SYMBOLS AND ABBREVIATIONS

AK-FB	Alaska Fairbanks
ASTM	American Society for Testing and Materials
BP	Breakthrough Pressure
BTV	Breakthrough Pressure
CA	Contact Angle
CaCl2	Calcium Chloride
CEC	Cation Exchange Capacity
CRM	Capillary Rise Method
CRREL	Cold Regions Research and Engineering Laboratory
DCMS	Dimethyldichlorosilane
DDL	Diffuse Double Layer
DOT	Department of Transportation
EC	Electrical Conductivity
EDX	Energy-dispersive X-ray spectroscopy
EWR	Engineered Water Repellency
FHWA	Federal Highway Administration
FSS	Frost-susceptible soils
GB	Glass Beads
HDPE	High-Density Polyethylene
IA-PC	Iowa Pottawattamie
IowaDOT	Iowa Department of Transportation
kPa	kilopascal
L/S	Liquid-to-solid ratio
NaCl	Sodium Chloride
NC-AS	North Carolina Asheville
NC-BO	North Carolina Boone
NCDOT	North Carolina Department of Transportation
NH-HS	New Hampshire Hanover Silt
^{o}	Degrees

OMC	Optimum Moisture Content
OS	Organosilane
OTS	Trichloro(octadecyl)silane
PA	Atmospheric Pressure
Pa	Pressure due to air
PD	Applied Pressure
PDMS	Polydimethylsiloxane
PO	Pressure due to the weight of the frozen soil above the freezing front
Ps	Pressure due to Diffuse layer
Pw	Pressure due to pore water
RH	Relative Humidity
SDM	Sessile Drop Method
SSA	Specific Surface Area
THM	Thermo-Hydraulic-Mechanical
UCS	Unconfined Compressive Strength
WDPT	Water Drop Penetration Test
WEP	Water Entry Pressure
Wh	Hygroscopic Moisture Content
ΔP	Change in Pressure
ΔV	Change in Volume

CHAPTER 1: INTRODUCTION

This dissertation constitutes an integral part of a comprehensive, multi-year research project generously funded by the U.S. National Science Foundation (Award #1928813). The project encompasses an interdisciplinary approach, combining laboratory experiments, field investigations, and numerical analyses, with the overarching goal of exploring the innovative application of Engineered Water Repellency (EWR) for frost heave mitigation. Additionally, it aims to decouple the distinct influences of matric and osmotic potentials on frost heave, representing a significant advancement in our understanding of this phenomenon.

This chapter serves as an introduction to the dissertation and provides essential background information. It will outline the research hypothesis, objectives, and thematic areas to be addressed. Furthermore, it will elucidate the intellectual merit of the study, highlighting its contributions to the existing body of knowledge and lastly present the organization and structure of the dissertation, providing a clear roadmap of what to expect in subsequent chapters.

1.1 Background

The continuing freezing and thawing of frost susceptible soils (FSS) make them undesirable in construction due to the dramatic changes in thermal and mechanical properties, which have detrimental effects on structures constructed on them (Lein *et al*, 2019). Particularly in road pavements, frost susceptible soils when exposed to moisture and cold conditions, heave (Ahammed, 2018). Frost swelling of soils is widespread in

many climate zones (Figure 1-1) and seasonal frost heaving and freeze-thaw weakening have a significant effect on construction and transportation infrastructure. Shallow, intermediate, and deep foundations are adversely impacted by frost action as are airfields, railroads, and pipelines. Figure 1-2 shows damage to infrastructure caused by frost heaving.

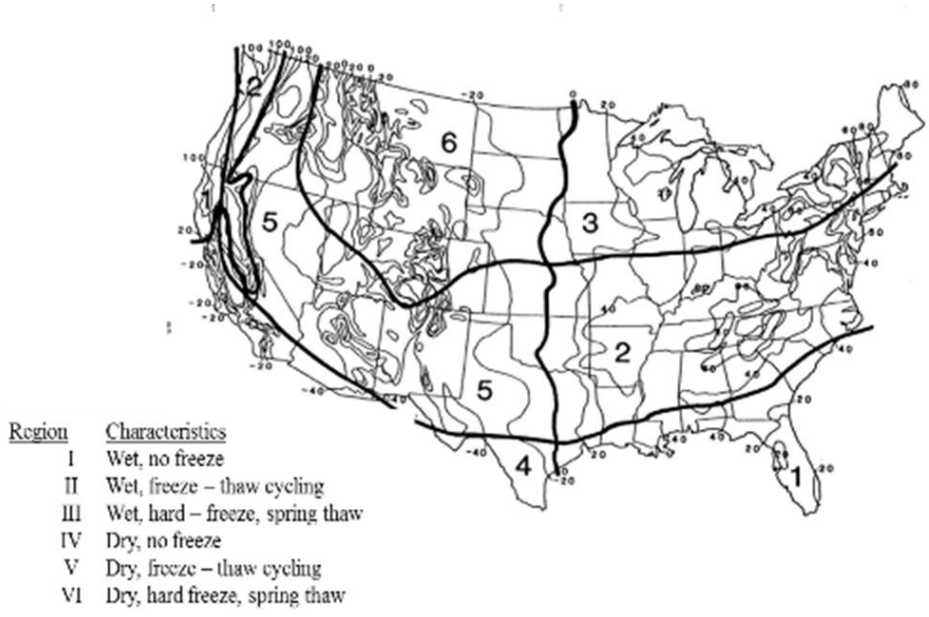

Figure 0-1 Climatic regions in the U.S. (USACE)

One widely accepted definition of FSS, presented by the Highway Research Board Committee on Frost Heave and Frost Action in Soil (1955) is “one in which significant ice segregation will occur when the appropriate moisture and freezing conditions are present”. The presence of these soils coupled with freezing temperatures and the availability of a water source either within these soils or a high groundwater table provides suitable conditions for frost action. This leads to substantial damage due to large changes in stress, strains, and moisture content from frost heave and freeze-thawing. Government transportation engineers have estimated that over half of the costs associated with road maintenance in cold regions can be credited to the effects of seasonal freezing and thawing

(Henry & Holtz, 2001), and recurring maintenance costs due to frost heave damage are estimated at over two billion US dollars annually (FHWA, 1999). There is no indication that these costs have decreased since the FHWA report.

A lot of work and theories have been done to understand the process of frost heaving since it was recognized as a phenomenon as early as the 17th century (Beskow 1935). MacKay *et al.* (1979), Loch (1981), and Smith (1985) presented their studies and reviews of different theories relating to frost heaving and frost action in soils. While they all focus on different aspects of the phenomenon, the transport of moisture from the unfrozen soil zone to the freezing front has been credited to a causative agent in frost heave during soil freezing, and potential difference (thermal, osmotic, matric) between the two points within a freezing soil moves the pore water to migrate to the frozen region, leading to water redistribution (Xue *et al.*, 2017). While much of the relevant literature has focused on matric effects, data indicate that solutes may control the extent and nature of ice lensing (Marion, 1995). Very little is known about the influence of osmotic suction and the practical effects of pore fluid composition on ice lensing. Early studies indicate that as pore water freezes, ions are mostly excluded and further concentrated in the remaining unfrozen water. This exclusion of ions results in the highest concentrations being found immediately in front of the freezing front (e.g. Hallet, 1983). Kay and Groenevelt (1983) estimate the solute concentration at the freezing front rise to 80 times the original pore fluid concentration. This change in the equilibrium of precipitation/dissolution and cation exchange reactions creates an osmotic gradient that further attracts water toward the freezing front.

Figure 0-2 Frost heave damage to foundations (ECP, 2011) and roadways (Ystenes, 2013)

Also, the formation of ice within the pore spaces (pore ice) results in the reduction of the pore space available, increasing capillary action within the freezing soil. This results in a net increase in matric potential due to cryogenic action (cryogenic suction). Most frost heave theories have largely focused on matric (capillary) suction as the primary mode of migration of water to a freezing front with a lot of them still unable to account for sub-phenomenon like layered or discrete ice lens creation. At best, they are a good estimation of what can be expected. There is a paucity of inquiry into the relative effect of osmotic and cryogenic suction in moisture transport within freezing soils. By understanding the relative contributions of matric and osmotic potentials, we can understand the process of frost heave better and how to mitigate it.

Remedial techniques against frost heaving such as stripping and replacement, thermo-siphoning, soil stabilization using lime and/or cement or increasing pavement thickness are generally cost-prohibitive, time-consuming, or unfeasible. Engineered Water Repellency (EWR) is an innovative technology that offers an effective low-cost approach to environmental geotechnology challenges (Debano, 1981; Daniels, 2020) that is gaining significance in infiltration control (Daniels et al, 2019), landfill barriers (Subedi et al.,

2012) and slope covers (Zheng et al, 2017) and has proven efficient in the treatment of soils and coal combustion residuals (Feyyisa et al, 2019; Dumenu et al, 2017). By treating FSS with cost-effective and environmentally compatible polymers making them hydrophobic (water repellent), we can limit the transport of water through these soils and mitigate frost heaving. This method can prove to be a viable alternative or complement to already existing methods of tackling frost action in soils.

This dissertation investigates the feasibility of using EWR as a viable technique to mitigate the effects of frost action, develop a systematic framework for evaluating EWR, and create new laboratory procedures that can be adopted for other geotechnical applications. It also explores the relative influence of osmotic and matric suctions in the migration of water through frost susceptible soils under freezing conditions to better understand the phenomenon of frost heaving.

1.2 Research Hypotheses and Themes

Ice lens development and subsequent heaving within frost susceptible soils is a result of water migration towards the ice lens which is a function of both osmotic and matric potential. The relative role of both potentials is of scientific and engineering relevance. Being able to understand and quantify the effects of these potentials on water transport in freezing soils will give insights into how to mitigate damage caused by frost heave to allied infrastructure, particularly using Engineered Water Repellency (Daniels *et al.*, 2021).

Hypothesis (1) states that water-repellent additives will result in significant

reductions in ice lens formation. Hypothesis (2) states that changes in osmotic potential have a predictable effect on frost heaving.

To test these hypotheses, this research study focuses on two major themes.

1. Water repellency treatment of soils and dosage optimization
    a. explore and select OS treatment, methods, and techniques best suited for laboratory and field studies
    b. determine optimal dosage concentrations for maximum hydrophobicity of soils
2. Osmotic suction potential estimations and sensitivity analysis
    a. explore the effect of osmotic potential relative to matric potential on frost heave
    b. explore the relationship between osmotic potential, DDL, EWR, and frost heaving

1.3 Intellectual Merit

Engineered Water Repellency is a viable alternative and/or complement to existing mitigation techniques for frost heaving and this study will help understand the effect of hydrophobizing soils on the transport of water through them, especially under freezing conditions. This has implications for developing knowledge of other challenges related to soil moisture transport. It will also extend the potential of engineered water repellency in geotechnical engineering extending beyond the present focus to improvements in strength, reductions in swelling (e.g., (Daniels and Hourani, 2009)), and control of infiltration and

leachability for waste containment applications (e.g., (Daniels *et al*, 2009, Daniels *et al.* 2018)).

Organosilanes, as a class of chemicals, utilized in imparting water repellency to soils are in their infancy with respect to the current knowledge base on their use for geotechnical applications. This study provides needed baseline information on optimal dosage concentrations, treatment techniques, micro and macro soil interactions, characteristics, and other relevant information needed to address the current knowledge deficit in the literature.

By exploring the subject matter in detail, this dissertation sheds light on the potential of EWR as a novel solution for mitigating frost heave. It endeavors to unravel the complex interplay between matric and osmotic potentials, which has hitherto remained insufficiently understood. The results of this study have the potential to revolutionize current practices and enhance our ability to combat frost heave effectively.

1.4 Dissertation Outline

This dissertation comprises several chapters, each contributing to a comprehensive understanding of the research topic. The subsequent chapters are organized as follows:

Chapter 2: Literature Review. This chapter provides a concise but thorough review of the pertinent literature pertaining to the dissertation. It encompasses a comprehensive examination of various aspects, including frost susceptible soils, their characterization techniques, the intricate process of frost heaving, experimental investigation

methodologies, and relevant models utilized in the field. Additionally, it offers an overview of the process of water transport and moisture migration during the frost heave phenomenon. It also identifies existing knowledge gaps that will be addressed in this dissertation.

Chapter 3: Engineered Water Repellency in Frost Susceptible Soils (4 Articles). This chapter delves into the realm of Engineered Water Repellency (EWR) treatment of frost susceptible soils, presenting a collection of six articles that contribute to a comprehensive understanding of this innovative approach. These articles focus on various aspects of EWR treatment and its impact on soil behavior. The chapter encompasses the following key components:

Article 1: Optimization of Water Repellency in Soils for Geotechnical Applications

This article outlines the experimental plan implemented to optimize the application of water-repellency treatment using different organosilanes. It describes the specific methodologies, techniques, and parameters utilized to achieve the desired outcomes in treating frost susceptible soils. The article sheds light on the innovative approaches employed to enhance the effectiveness and durability of EWR treatment.

Article 2: Effect of Grain Size on Water-Repellent Soils

This article focuses on the behavior and performance of water-repellent soils, with particular emphasis on the influence of grain size properties. It delves into the relationship between grain size, porosity, and the effectiveness of water-repellency treatment. The study aims to shed light on the impact of different organosilane concentrations and surface

roughness on soil properties and performance. Understanding the interplay between grain size properties and water-repellency treatment is essential for comprehending the underlying mechanisms that govern soil behavior. By investigating this relationship, it seeks to contribute to a deeper understanding of how grain size influences the effectiveness and durability of water-repellent treatments.

Article 3: Effect of Varying Salt Concentrations on EWR Treatment

This article explores the effects of varying salt concentrations within the soil, which arise because of deicing operations in cold regions. It investigates how the presence of salts influences the treatment, performance, and stability of EWR-treated soils. The research findings provide valuable insights into the challenges posed by salt within soils and its impact on the efficacy of EWR treatment.

Article 4: Impact of EWR Treatment on Hygroscopic Potential in Soils

This article focuses on the impact of EWR treatment on the hygroscopic potential of soils. It examines how the water-repellency treatment affects the moisture absorption and desorption characteristics of treated soils. The findings shed light on the changes in soil-water interactions induced by EWR treatment and contribute to a deeper understanding of its implications for moisture control in frost susceptible soils.

Through this collection of articles, Chapter 3 provides a comprehensive examination of EWR treatment in frost susceptible soils. The presented research offers valuable insights into the optimization of treatment strategies, improved testing

methodologies, and the effects of salt concentrations and hygroscopic potential. By investigating these crucial aspects, this chapter contributes to the broader understanding of EWR's potential as a sustainable and effective solution for mitigating frost heave.

Chapter 4: Hydraulic, and Strength Properties of EWR-Treated Frost Susceptible Soils (2 Articles). In this chapter of the dissertation, the focus is on comprehensively characterizing the hydraulic, and strength properties of both untreated and Engineered Water Repellency (EWR) treated frost susceptible soils. Tests such as the Water Entry Pressure (WEP) and Unconfined Compressive Strength (UCS) tests are conducted on compacted soil samples. These tests serve to ascertain the hydraulic properties of the soils, as well as the strength properties of treated soils under repeated freeze-thaw cycles. This chapter encompasses the following articles, which contribute to a comprehensive understanding of the subject matter:

Article 1: An Automated Technique for Measurement of Water Entry Pressure in Hydrophobic Soils

This article introduces an improved test method for evaluating the engineering performance of treated soils. It highlights the limitations of existing testing techniques and proposes innovative modifications to overcome these limitations. The enhanced test method enables a more accurate and comprehensive assessment of the effectiveness and stability of EWR-treated soils.

Article 2: Effect of Freeze-Thaw Cycles on Strength Properties of Engineered Water Repellent Soils

This article explores the strength properties of untreated and EWR-treated soils under repeated freeze-thaw cycles. It highlights the advantages of treatment – increased density and strength, reduced moisture, and heave – over several cycles. It answers questions raised by many engineers and researchers regarding the effect of treatment on strength and the durability of the treated soil.

By undertaking a comprehensive analysis of the hydraulic, and strength characteristics of untreated and EWR-treated frost susceptible soils, this chapter provides valuable knowledge for researchers, engineers, and professionals in the field. The findings presented in these articles contribute to the advancement of soil engineering practices and pave the way for more effective strategies in managing frost susceptible soils.

Chapter 6: Osmotic and Matric Potential in Freezing Soils. In this chapter of the dissertation, the focus is on investigating the relative contributions of osmotic potential to the frost heave phenomenon. Building upon previous knowledge and leveraging instrumented frost heave tests, the study examines frost susceptible soils subjected to varying salt concentration regimes. This chapter consists of the following article:

Article 1: Osmotic Potential in Freezing Soils

This article presents an experimental analysis of the evolution of osmotic and matric potential in freezing soils. Instrumented frost heave tests are conducted on frost susceptible soils, subjected to varying salt concentrations while maintaining a constant matric suction. The study establishes a relationship between Osmotic Suction, Electrical

Conductivity (EC), and salt concentration. The findings offer valuable insights into the changes occurring within freezing soils.

The research conducted in this chapter advances our understanding of osmotic and matric potential in freezing soils, offering insights into the frost heave process. This article contributes to the broader field of geotechnical engineering and paves the way for more effective models in describing the frost heave phenomenon.

CHAPTER 2: LITERATURE REVIEW

2.1 Introduction

The literature on frost action is vast and extends nearly a century, with early reports by Taber (1929) and Beskow (1935). It is difficult to summarize such a mature field defined by hundreds of monographs, technical papers, and textbooks. However as noted by Darrow (2007), there are many excellent summaries, with varying focus on theory, experimentation, and numerical modeling. A more recent change that contemporary researchers can leverage is the variety of innovations in laboratory testing and computational modeling, both of which have advanced significantly. As part of this dissertation, this review focuses on gaps in select theoretical frameworks, experimental methods, and numerical models, specifically as it relates to the effects of osmotic and matric potential as well as engineered water repellency.

2.2 Frost Heaving in Frost Susceptible Soils

2.2.1 Frost Susceptibility of Soils

Frost-susceptible soils are typically silts, but soils with a larger number of fine particles, such as clays, are also known to heave (Michalowski and Zhu, 2006). According to Jessberger (1973), criteria for determining frost-susceptibility can be divided into 3 main groups based on the following:

1. Gradation curves and particle size,
2. Frost-heave rate, and

3. Phase-interface relation.

Criteria determining frost susceptibility based on grain size and particle gradation are the widely utilized methods for determining frost susceptibility of soils (National Research Council, 1973). Basically, the gradation curve compares the content of fines against some fixed values. The most common of these methods is the Casagrande and Schiable criteria. Several Departments of Transportation (DOTs) and several other countries utilize the Casagrande criterion in the design of pavement (Chamberlain, 1981). However, several DOTs have developed their own criteria based on experience and field investigations because even though their soils meet the Casagrande criterion, under local climatic conditions, they still have detrimental frost effects. The criterion also does not consider other factors like soil minerals, chemical conditions, surcharge loads, water table, and temperature gradients. Other factors to be considered include temperature, surcharge load, and availability of water to or within the frost susceptibility soil.

2.2.2 Frost Heave Theories

The study of frost heave dates to the early 1900s, with initial approaches primarily treating soil freezing as a thermodynamic issue. By the 1930s, there was a shift towards considering it as the interaction of water and heat transfer across a freezing boundary (MacKay et al. 1978; Loch 1981; Smith 1985). Nevertheless, many of these early theories left ambiguity regarding the influence of soil properties, particularly the impact of suction forces due to the diffuse layer (Konrad and Morgenstern 1983; O'Neill and Miller 1985). Some early explanations for frost heave, considering the electric double layer, were

proposed by Cass and Miller (1959). Horiguchi (1987), using the secondary frost heave theory, introduced a model that incorporated osmotic pressure, which forms in saturated soil due to the diffuse double layers on mineral surfaces. A more recent study conducted by Torrance and Schellekens (2006) expanded on this osmotic pressure model. A brief overview of major frost heave theories is presented below.

The Capillary Theory, as discussed by Gold (1957), Everett (1961), Penner (1966, 1967), Jackson and Chalmers (1958), Jackson and Uhlmann (1966), Vignes and Dijkema (1974), Vignes (1977), and Ozawa and Kinosita (1989), presents the formation of an ice lens as a process initiated at the freezing front. According to this theory, pore size plays a pivotal role in ice lens development, with temperature, temperature gradient, freezing rate, and the presence of ions in the solution being disregarded as significant factors. Furthermore, the model does not accommodate the occurrence of ice lens formation in intermittent layers, which is commonly observed in field conditions. This capillary model faced criticism from Takagi (1979) due to its applicability to static conditions, while the freezing of pore water is a kinematic effect requiring a distinct thermodynamic approach.

The Secondary Frost Heave Theory, extensively discussed by Miller (1978), Miller and Koslow (1980), Gilpin (1980), Hopke (1980), O'Neill and Miller (1982, 1985), is a widely recognized and applied model that builds upon the capillary theory. Miller (1972) introduced the concept of a "frozen fringe," which represents a partially frozen region located between the surface of ice lens growth and the freezing front, assumed to be colder than the freezing front. According to this theory, an ice lens forms when the effective stress of soil particles within this frozen region reaches zero. Notably, this theory is the sole one capable of explaining the development of intermittent layers of ice lenses.

The Segregation Potential Concept, as discussed by Konrad and Morgenstern (1980, 1981), Nixon (1982), Konrad (1987, 1989), and Konrad and Duguennoi (1993), approaches the issue of frost heave as a matter of ensuring an adequate water supply to ice lenses. The rate of moisture migration is determined through calculations involving the expansion ratio of water, porosity, and the quantity of unfrozen water at the anticipated temperature for ice lens segregation. This Segregation Potential concept has been employed as a method to categorize the frost susceptibility of soil, as seen in the work of Kujala (1991).

The Adsorption Force Theory, developed by Takagi (1980), offers a unique perspective on the mechanism of ice lens formation. Building upon earlier studies by Taber (1929, 1930) and Beskow (1935) that established the existence of a thin water film at the freezing front, Takagi (1979) postulated that the adsorbed "film" water on soil particles could create internal solid-like stress. He argued that the flow within this film water differed from that in pore water. As temperatures decreased, the adsorbed water froze, causing the water film on the particles to thin and its ionic concentration to increase. This, in turn, generated a suction potential that facilitated the transport of water to the freezing front, giving rise to what Takagi termed the Adsorption Force Theory. Takagi's theory challenged the fundamental premise of the capillary force theory, which neglected the role of adsorption force due to the diffuse layer in frost heaving. Instead, he proposed that adsorption force was the primary factor driving frost heaving. A key outcome of his work was the distinction between pore and film (adsorbed) water, with the suction force necessary for the advancement of the freezing front into an elevating ice lens arising from

the solid-like stress accumulated in the film water. He also suggested ideal experiments for validating this theory.

The Osmotic Model, as proposed by Horiguchi (1987), offers a distinct perspective on the Secondary Frost Heave theory, focusing on the role of the diffuse double layer surrounding soil particles. While the Secondary Frost Heave theory assumes that effective stress propagates through soil particles, this model questions the connectivity of soil particles in highly frost-susceptible soils, where there exists a thin film of bound unfrozen water around the particles, known as the Diffuse Double Layer.

Within this osmotic model, pressure conditions are examined, considering osmotic pressure resulting from concentration differences between the ice lens, the diffuse double layer, and pore water. Furthermore, the model assesses the impact of overburden pressure, as well as the heat and water fluxes on the rate of heaving. Horiguchi's (1977) earlier experimental work in demonstrated that powdery materials with substantial surface charges exhibit higher frost susceptibility compared to those with smaller surface charges, even when the surface area per unit volume is identical. This experimental evidence underscores the significance of the electric double layer surrounding soil particle surfaces in the frost heaving process, as particles with higher charges tend to possess thicker double layers. Horiguchi (1986) expanded on this by presenting an osmotic model for saturated, normally consolidated soil, establishing a balance between the suction force within the diffuse layer and the heaving pressure (see Figure 0-1).

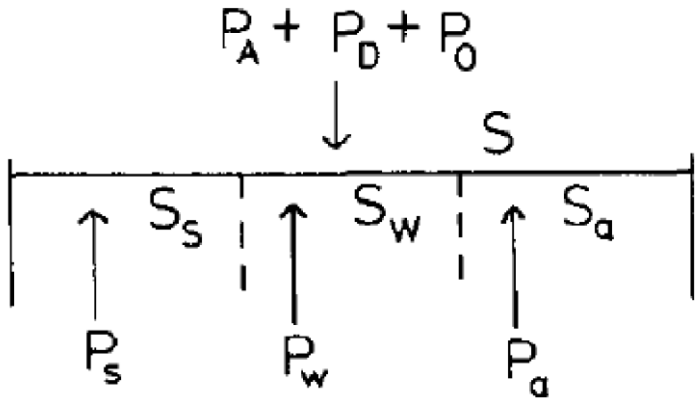

Figure 0-3 Force balance at the freezing front (Horiguchi, 1986)

where P_A, P_D, and P_O are the atmospheric pressure, the applied pressure, and the pressure due to the weight of the frozen soil above the freezing front while Ps, Pw, and Pa are the forces due to the diffuse layer, pore water, and air respectively.

Hence, we have

$$(P_A + P_D + P_O)S = P_s S_s + P_w S_w + P_a S_a$$

Since the soil is saturated, S_a is zero and since the surface area covered by the diffuse layer is very large compared with that of the pore water for the consolidated soil, we have;

$$P_s = P_A + P_D + P_O$$

For an unsaturated soil, Sa is not zero and the effects of capillarity due to the narrowing of the pore spaces within the soil particles need to be considered. It is therefore important to determine the relative contributions of both the forces in the pore water (matric suction due to capillarity) and the adsorbed water layer (osmotic suction).

2.2.3 Experimental Investigation

Experimental investigation into the phenomenon of frost heaving can be broadly classified into two categories: Laboratory Frost Heave Experiments and Full-Scale Field experiments.

Laboratory Frost Heave Experiments

Taber (1929, 1930) and later Beskow (1935) conducted pioneering laboratory experiments on frost heaving, challenging the prevailing notion that heaving was primarily the result of the expansion of water turning into ice. Their experiments demonstrated that heaving was chiefly caused by the migration of pore fluids, leading to the formation of segregated ice, which grew with a continuous supply of water. To emphasize this, Taber used liquid benzene as the pore fluid, which contracts upon freezing. His experiments confirmed that the soil-benzene mixture heaved and produced ice lenses upon freezing.

The uniaxial testing principle, involving an insulated soil sample (typically cylindrical) with controlled thermal and hydraulic conditions at both ends, as employed by Taber and Beskow, remains a widely adopted approach for studying frost heaving in soils under freezing conditions (Chamberlain 1981). The sample mold is designed to expand, allowing for displacement monitoring, and an axial force is applied to simulate the overburden stress. Heat exchangers are placed at the top and bottom of the specimen with coolant lines connected to circulating baths. In open system setups, water is introduced at the warm end of the sample to facilitate ice lens growth, and uptake is monitored. Frost heaving in this test is typically measured by total surface displacement, the volume of water uptake per unit area over a specific time frame, or the heave rate at a steady state. The

ASTM D5918 standardizes this setup, but various modifications have been employed by different researchers for specific experimental testing.

According to Konrad (1988), the thermal gradient applied in laboratory tests often exceeds in-situ values, with typical gradients ranging from 10 to 40 °C/m, in contrast to the 1 to 5 °C/m reported in nature. Smaller gradients would necessitate longer sample lengths and extremely precise temperature control systems, which are often impractical. They would also result in small displacement rates and longer test durations. Test durations generally span from 1 to 10 days, although some tests have extended up to 100 days (Eigenbrod et al. 1996). Sample heights range from 50 mm to 1 m, and diameters range from 50 to 200 mm. The tested soils may either be undisturbed or compacted undisturbed soil tailored to the desired density.

Laboratory frost heave tests typically employ two categories of thermal boundary conditions: stepped and ramped temperature variation (Konrad 1994). In a stepped freezing test, the temperatures at the top and bottom of the soil sample are initially equalized, usually slightly above 0°C. Then, the temperature at one end is rapidly decreased to a value below 0°C and maintained, resulting in quick frost penetration through the sample followed by a period of a constant temperature profile. Ramped freezing, on the other hand, involves linearly varying the temperatures at the top and bottom while maintaining a consistent temperature gradient throughout the sample, leading to a constant frost penetration rate. Stepped freezing is more common as it requires less complex temperature controllers, although it doesn't offer precise control of the frost penetration rate. Stepped tests result in high concentrations of segregated ice around the final position of the frozen fringe, while ramped tests yield more evenly distributed ice lenses.

Additional thermal boundary conditions include multi-stepped boundaries (Seto and Konrad 1994) and those outlined in the Japanese Geotechnical Standard Test (JGST), which involve a constant warm boundary and a linearly decreasing cold boundary, though these are less commonly reported in the literature (Japanese Geotechnical Society 2003).

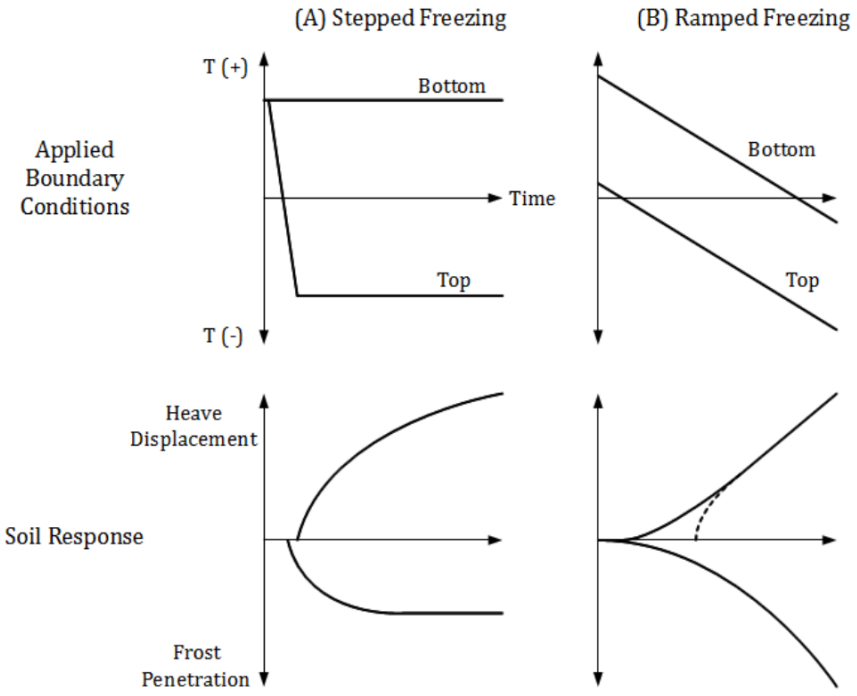

Figure 0-4 Stepped and Ramped Freezing Boundary Conditions in 1D Laboratory Frost Heave Tests with Typical Soil Response (After Tiedje, 2015)

Full-Scale Frost Heave Studies

While laboratory experiments can offer valuable insights into the frost heave behavior of specific soils, it is essential to conduct full-scale tests and field observations to assess the impact of frost heave on geotechnical systems that involve complex interactions

between soil and structures. These systems often comprise multiple soil types, various geometries, and different boundary conditions. Field-scale tests are typically tailored to address specific construction scenarios, particularly those where frost heave can lead to damage or structural failure. Examples include cases involving road pavements (Doré and Zubeck 2008), transmission line poles (Lyazgin et al. 2004), and piles (Penner, 1974).

In addition to full-scale testing, researchers and engineers also employ centrifuge modeling (Clark and Phillips, 2003) to investigate frost heave. This method involves constructing scaled models and subjecting them to increased gravitational forces by placing them within a large centrifuge. By doing so, researchers can physically observe the stresses within the model. Centrifuge modeling has been successfully applied to analyze frost heaving in buried gas pipelines (Piercy et al. 2011).

2.2.4. Empirical Models

In cases where conducting laboratory or field tests is not feasible, engineers have often turned to empirical relationships based on soil properties, historical behavior, or previous testing results. One straightforward method involves using the freezing index, typically defined as the average degree-days of freezing in a particular climate (Boyd 1976). When combined with prior observations of frost susceptibility for a specific soil, this approach can provide estimates for uplift pressures, displacements, and associated pavement distress. Frost susceptibility can be roughly estimated using the Unified Soil Classification System, with silts and clayey silts generally considered the most susceptible,

while clean coarse materials are typically the least susceptible (Andersland and Ladanyi, 1994).

Konrad and Morgenstern (1980) introduced a model based on the segregation potential theory. This approach establishes a relationship between the water flux across the frozen fringe and the temperature gradient across the same region when the frost penetration rate is held at a low, constant value. This concept can be expressed mathematically as

$$q_f = SP\left(\frac{\partial T}{\partial z}\right)_f \quad (1)$$

where the subscript "f" denotes the frozen fringe, while the segregation potential (SP) is a material parameter known to be sensitive to various factors, including stress levels and the rate of cooling, as described by Konrad and Morgenstern (1981). Additionally, it can vary based on factors that influence overall soil frost susceptibilities, such as particle size distribution and void ratio. The segregation potential model offers the advantage of being relatively simple to determine and implement, while still providing sufficiently accurate results for many engineering applications. However, its accuracy tends to decrease when there are variations in frost penetration rates, as noted by Nixon (1991) and Fukuda et al. (1997). Despite this limitation, the segregation potential concept remains one of the most widely utilized models for addressing frost heave in current engineering practice, as indicated by Kujala (1997).

Michalowski (1993) introduced the porosity rate function, which estimates frost heave by establishing a correlation between volumetric soil expansion and thermal

gradient, as well as temperature, using empirical material parameters. The porosity rate function conceptualizes frost heave as a localized alteration in soil porosity, distinguishing it from the segregation potential, which focuses on the flux of pore water entering the frozen fringe, as discussed by Tiedje (2015).

2.2.5. Physical Models

Numerous models have been developed to describe the phenomenon of frost heave. Despite the diversity of available research, these models can be broadly categorized into four major physical models. These categories encompass the hydrodynamic model, the fully coupled thermo-hydro-mechanical model, the rigid ice model, and the premelting dynamics approach. While these models share a fundamental principle, which involves offering solutions for the governing equations governing heat and mass transport during the freezing and heaving process, their distinctions primarily arise from the assumptions they make about these transport mechanisms.

Hydrodynamic Model

The hydrodynamic model approaches the development of segregated ice as a groundwater flow problem within frozen and partially saturated soil, as described by Hansson et al. (2004). This model employs the generalized Clapeyron equation to establish the pressure differential between pore ice and unfrozen pore water. It assumes that the pressure within the ice is zero, and osmotic pressure is not taken into account. To describe the flow of water to the active ice lens, the model relies on Darcy's law. It operates under the assumption that the position and size of the frozen fringe fall within a specific temperature range, with no consideration for the initiation of ice lenses. An essential

requirement for this model is an accurate representative value of frozen, partially saturated hydraulic conductivity, which explicitly quantifies the frost susceptibility and the resulting moisture migration associated with the frost heave process.

Thermal-Hydraulic-Mechanical (THM) Frost Heave Model

Coupled thermal-hydraulic-mechanical (THM) models for frost heave have seen widespread development, extending the principles of the hydrodynamic model to incorporate mechanical responses during the frost heaving process, as outlined by Nishimura et al. (2009). Similar to the hydrodynamic model, the THM approach utilizes Darcy's law to define mass transport but doesn't account for soils under partially saturated conditions. The hydraulic conductivity of frozen soil is derived from unsaturated conductivity using the van Genuchten (1980) function of relative permeability. Liquid water pressure is determined relative to temperature and ice pressure through the Clapeyron expression. Ice pressure is characterized by the total stress, employing a stress partitioning function identical in form to that used in the rigid ice model. The resulting effective stress serves as the basis for defining elasto-plastic deformation, offering a mechanical representation of frozen soil's behavior. However, it's important to note that the THM model also necessitates an accurate characterization of frozen soil hydraulic conductivity.

Rigid Ice Model

While both the hydrodynamic and THM models rely on Darcy's law to explain heave, the rigid ice model approaches soil displacement by considering the concept of regelation. Regelation is a phenomenon involving continuous melting and freezing, leading to the gradual deformation of ice bodies, as elucidated by Miller (1978). During this

process, the unfrozen soil remains fixed in its position, while pore ice moves along the temperature gradient toward colder areas. The velocity of the ice is determined in relation to the temperature gradient, and this relationship is expressed using the formulation introduced by Gilpin (1980).:

$$v_i - v_s = -A\frac{\partial T}{\partial z} \qquad (2)$$

where $\upsilon_i - \upsilon_s$ is the relative ice velocity and A is an empirical material property. In the rigid ice model, mechanical equilibrium is maintained between ice and liquid water through the use of a stress partitioning function, allowing for the characterization of effective soil particle stress. This concept enables the description of the formation of individual ice lenses, similar to the THM model. Algebraically, the rigid ice model shares similarities with the segregation potential theory, as frost heave is linearly proportional to the temperature gradient. One notable feature of the rigid model is its decoupling of thermal and hydraulic processes, permitting separate but concurrent analysis of hydraulic characteristics as influential factors in frost heaving. The rigid model has gained wide acceptance and remains the most used among physically based models, having been introduced by O'Neil and Miller (1982), and subsequently elaborated upon by Gilpin (1980), Nixon (1991), Fowler and Krantz (1994), and Noon (1996). Its appeal lies in its ability to provide designers with an estimate of the maximum possible heave achievable under the assumption of an unlimited water supply to the ice lens.

Premelting Dynamics Model

Similar to the rigid ice model, the premelting dynamics concept operates under the assumption that frost heave is primarily driven by the relative deformation of pore ice, as outlined by Rempel et al. (2004). However, it deviates from the rigid ice model in its explanation of the mechanism behind freezing-induced potentials. The process involves a reduction in pore pressure within the liquid water films situated between pore ice and adjacent soil grains due to repulsive forces acting between them. This pressure disparity, under the influence of a temperature gradient, leads to a corresponding pressure gradient, as described by Rempel et al. (2001). In comparison to the empirical characterization in the rigid ice model equation, the premelting dynamics model offers a more comprehensive physical depiction of regelation-induced ice velocity. Algebraically, the implementation of the premelting dynamics model aligns with that of the rigid ice model, as established by Rempel (2007).

Physical models are generally considered more robust than empirical models, although their utility is constrained by the quality and availability of the required input parameters. Most physical models depend on simplifying assumptions or empirical characterizations of processes involved in frost heaving. Consequently, physically derived models do not inherently surpass empirically based counterparts; their performance is contingent on the quality and appropriateness of the parameters used.

2.2.6 Water Transport and Moisture Migration during Frost Heaving

Beskow (1935) delved into frost damage conditions and offered insights into water transport within freezing soils. Beskow's explanation relied on capillary suction related to

soil interface properties in confined regions. He highlighted that soils most susceptible to heave are those that are fine-grained enough to retain significant quantities of liquid water above the water table due to capillary forces. Simultaneously, they must be permeable enough to allow a steady flow of unfrozen water to reach the segregated ice when freezing occurs.

While pore size plays a critical role, capillarity and surface energy are insufficient to explain liquid transport during freezing, as demonstrated by a study conducted by Wilen and Dash (1995). They observed a membrane's gradual upward swelling over several days as a disk of ice on a slide, with its center cooled below freezing, received a continuous supply of ice growth from liquid flow through a thin premelted film separating the membrane from the ice below. The absence of significant curvature in the ice-liquid interface ruled out curvature as the cause of liquid transport. Frost heaving has also been observed in gravel soil, with the frost-heave ratio increasing with higher moisture content, as reported by Long et al. (2018), Akagawa et al. (2017), and Liu et al. (2017).

Several factors influence the phase composition of freezing soil, including specific surface area, temperature, applied pressure, the osmotic pressure of the soil solution, pore size distribution, particle packing geometry, and exchangeable adsorbed ions, as noted by Anderson and Tice (1972) and Nersesova and Tsytovitch (1963). Beskow emphasized the importance of 'adsorbed' water films as liquid conduits between soil grains and ice crystals during freezing. It's well-established that when fine-grained soil freezes, not all the water in the soil pores solidifies at 0°C. In air- and solute-free soils, water coexisting with ice is presumed to exist as thin films of adsorbed water and capillary water that remains unfrozen because it occupies spaces too narrow for a curved ice-water interface to penetrate. This

dynamic range of freezing temperatures has a significant impact on water migration. Observations on specimens frozen under a temperature gradient indicate that even when much of the pore water is frozen, water transport still occurs within the frozen soil beyond the pore freezing front, as reported by Freden (1965), Hoekstra (1969), Penner and Goodrich (1981), and Konrad and Morgenstern (1982).

Therefore, it is crucial to distinguish between the various transport mechanisms contributing to frost heaving in soils. While many models concentrate on temperature and meso- and macro soil properties, explaining transport using generalized Clayperon's and Darcy's equations, including the relative impact of osmotic pressure and micro soil properties, such as specific surface area and exchangeable ions, will yield a more comprehensive model for understanding water migration during the frost heaving process.

2.3 Engineered Water Repellency (EWR)

2.3.1 Engineered Water Repellency in Soils

Soil water repellency is defined as a reduction in the ability to get wet and retain water by soil resulting from the existence of hydrophobic coatings on the surface of soil particles (Hallet, 2007). This decrease in the attraction of soils such that they prevent wetting for periods can range from a few seconds to weeks (King, 1981). Hydrophobicity in soils was first established in agricultural and soil science (Schreiner and Shorey, 1910), but with advances and improvements in water-repellent chemistry and polymer technologies, engineered water repellency is being further studied and potential applications researched (Daniels *et al.*, 2009). To date, a variety of substances have been tested for their water-repellent behavior; natural substances, such as organic materials

produced by plant root exudates, certain species of fungi, waxes from the surface of plant leaves, and decaying soil organic matter (Mainwaring *et al.* 2004; Hallett *et al.* 2006; Lamparter *et al.*, 2009); fluorinated compounds, oils, and paraffin/wax, for textiles (Schuyten *et al.*, 1948) and silanes utilized in the coating of glass (Tripp & Hair, 1995). Other research carried out into hydrophobicity in soils has made use of a variety of chemicals like Dimethyldichlorosilane (DMDCS) and Alkylsiloxanes.

Silanes are among the most suitable chemicals for imparting hydrophobicity as they induce high and stable water repellency (Bachmann *et al.*, 2003). Treatment of soil with organo-silanes (OS) through a process of silanization, forms a covalent -Si-O-Si- irreversible bond with a silica-based substrate increasing its hydrophobicity (Chan and Lourenco, 2016). As quartz (SiO_2) is a major component within most soils, it is a very suitable chemical for engineering water repellency in soils.

2.3.2. Water Repellency Assessment

There are numerous methods to measure water repellency in soil. Hallet et al (2011), identify major tests that can be carried out; Contact Angle (CA) tests, a direct measurement of the soil-water contact angle based on the sessile drop method using a Goniometer ((Bachmann *et al.*, 2000; Diehl and Schaumann, 2007, Feyyisa *et al.* 2017; Keatts *et al.*, 2018) and is a widely utilized method for determining the degree of hydrophobicity of solid surfaces by determining the inter-phasal angle (Adamson, 1990). The Capillary Rise Method (CRM) which compares the infiltration rates of water and a known liquid not influenced by hydrophobicity (e.g. hexane) (Bachmann *et al.*, 2003),

intrinsic sorptivity test, comparing the sorptivity of water and ethanol measured with tension infiltrometers (Schulte *et al.*, 2007), molarity of an ethanol droplet test (MED) suitable for field measurements and indicates how strong a water droplet is repelled by the soil at the time of application (King, 1981) and the Water Drop Penetration Time Test (WDPT) which is the most commonly used because of its simplicity and versatility (Dekker *et al.*, 2009, Lee *et al.*, 2015; Liu *et al.*, 2012). There is a positive correlation between contact angle, WDPT, and the Water Entry Point/Breakthrough Pressure (WEP/BP) test (Feyyisa 2017; Keatts *et al.*, 2018; Lee *et al.*, 2015), and the dosage/concentration of the water repellent chemical/solution Daniels *et al.,* (2019). So, the BP test is also a good indicator of the degree of water repellency of the treated soil.

2.3.3. EWR in Frost Heave Mitigation

Established techniques geared toward frost heaving reduction involve removing FSS, limiting or cutting water flow, and insulating the soil against freezing temperature. However, they do not provide a permanent solution as clogging, soil deposition, and changing soil boundary temperature have reduced their efficiency (Henry, 1996). Also, many of these techniques are costly and labor-intensive, requiring extensive cost and life-cycle analysis before their execution. Engineered Water Repellency is a cost-effective approach where existing soil is made hydrophobic, thereby preventing water migration. Studies by Sage and Porebska (1993), and Keatts *et al.* (2018) have demonstrated that OS-treated soils achieve higher contact angles than untreated soils. These studies also showed that hydrophobic soils take far less water than FSS layers, corresponding to reduced water

flow, lower moisture changes, and lower deformation. Therefore, the heaving rate or height is negligible; the treated soil can be classified either as low or negligible potential soil.

CHAPTER 3: ENGINEERED WATER REPELLENCY IN FROST SUSCEPTIBLE SOILS

ARTICLE 1: OPTIMIZATION OF WATER REPELLENCY IN SOILS FOR GEOTECHNICAL APPLICATIONS

ABSTRACT

Water repellency in soils can be achieved by applying water-repellent additives known as organo-silanes (OS). This technique enhances soil properties, making them suitable for use as moisture barriers in various infrastructures like road pavements, landfills, and tunnels exposed to seasonal wet-dry and freeze-thaw effects. To explore the potential of this approach, four soil samples and glass beads were treated with three OS products at varying dosages (ranging from 1:1 to 1:1000). The study included laboratory tests of contact angle, water drop penetration, and breakthrough pressure. A comprehensive parametric study encompassing multiple variables was conducted on 216 samples. The results demonstrated that increasing OS treatment led to higher hydrophobicity, with contact angles exceeding 110^{o} and Water Drop Penetration Test times exceeding 3600s. However, this trend plateaued at specific dosage concentrations (varying by OS), evident from changes in electrical conductivity and pH measurements, which are practical indicators for field assessment. The primary factors influencing treatment efficacy (~94.6%) were identified as soil type, organosilane product, dosage, and drying condition. Conversely, variables such as reaction time, and leaching/washing, accounted for a minor contribution (~5.4%) to the variance in the results. Breakthrough Head tests on treated soils showed an ability to sustain a hydrostatic head of up to 17 kPa. These findings give insights for implementing water-repellency treatment in soils, particularly for capillary barriers in geotechnical applications. By understanding these influences, practitioners can optimize water-repellency treatments for enhanced soil performance and long-term infrastructure durability.

Keywords

Hydrophobic, Contact Angle, Breakthrough Pressure, Grain Size

1. Introduction

Moisture changes result in significant stress on all elements of the pavement system, resulting in the need for maintenance or failure. The problem is further exacerbated when these changes in moisture conditions are seasonal and become even more problematic in roads built on poor subgrade material like frost-susceptible soils, which under suitable conditions keep absorbing moisture under the influence of suction forces resulting in frost heaving (Daniels et al., 2021; Mahedi et al., 2020a; Uduebor et al., 2022). Repeated frost heaving and thaw weakening within these soils result in damage, leading to annual recurrent maintenance expenditure, road closures, weight restrictions, poor riding experience, and other economic impacts (Brooks et al., 2022; Uduebor et al., 2022; Wasif et al., 2022). Seasonal freezing and thawing can contribute up to 75% of pavement degradation (Dore et al., 2005; Yuan et al., 2021), and it is estimated that over 2 billion is spent annually on pavement maintenance and restoration due to frost action in the US (FHWA,1999).

Traditional frost mitigation techniques focus on controlling either one or more of the three basic requirements for frost heaving; 1. The presence of frost-susceptible soils (FSS) (silt-sized fractions), which are soils that promote the migration of water towards a freezing front resulting in the formation of an ice lens. 2. Sub-freezing temperatures result in the freezing of water within the soil pores (Daniels et al., 2021; Uduebor, et al., 2022). Methods employed include increasing pavement thickness when designing with such soils (usually considering reduced strength due to moisture weakening and frost action), replacing with more suitable backfill material, preventing/intercepting water by use of barrier, and drainage systems (low and/or high permeability soils, geosynthetics) and

modifying such soils using lime and/or cement (Baldovino et al., 2021). While such methods have been majorly successful, they result in significant labor, time, and resource costs.

Water repellency has been recently explored for use in civil and geotechnical engineering where it can find utility in engineering construction, particularly where removing, resisting, and retaining water is required for the stability and safety of civil infrastructure (Brooks et al., 2022; Mahedi et al., 2020; Uduebor, et al., 2022; Uduebor et al., 2023). Barrier systems prevent the infiltration of water into areas where it is undesirable (landfill sites, road pavement foundations, tunnels, etc.), and engineered water repellency (EWR) can be a solution.

EWR is a technique for imparting water-repellent properties to soils and is an innovative method for mitigating moisture migration and frost action in road pavements. Soils can be artificially made water-repellent by treating them with water-repellent additives called organo-silanes (OS), which form a covalent, irreversible bond with silica and metal-based substrates, a major component of soil. Figure 1-1 shows the bonding between OS and a sand particle's surface (substrate). The modification is permanent as the bond which binds the organic functional groups (R) is the same siloxane (Si-O-Si) bond found in other minerals such as silicon dioxide.

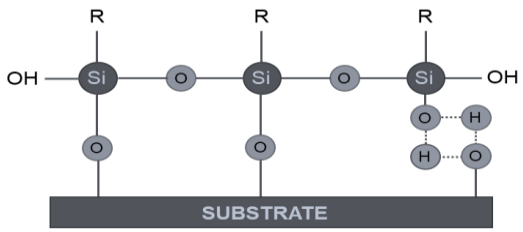

Figure 1-1 Silane Reaction Bond with Soil Surface (Substrate)

This approach of direct soil modification follows efforts by (Lambe, 1951; Lambe et al., 1969), which indicated that four types of water-repellent chemicals yielded a reduction in heave for Boston Blue clay, New Hampshire silt, and Fort Belvoir sandy clay. Several studies carried out using OS such as Dimethyldichlorosilane (DMDCS) and trichloro(octadecyl)silane (OTS), polydimethylsiloxane (PDMS) is available in the literature, and water-repellent chemistry (Choi et al., 2016; Debano, 2015; Lin et al., 2019; Lourenço et al., 2018). Organosilanes come in diverse types and have benefits suitable for particular use cases. Water soluble OS can be mixed with water used to mold and compact soils. This is particularly important when ensuring treatment is carried out effectively and is compatible with current road pavement construction methods. OS that can be utilized directly is more effective for topical spray applications, where only a thin top layer is required to be hydrophobic. They have the advantage of direct utilization and not requiring "activation" before use.

Other materials used to impart soil hydrophobic properties include Tung oil, Linseed oil (Lin et al., 2019), and wax (Bardet et al., 2015). Advancements in OS and water-repellent additives manufacturing have led to their availability at lower costs, safe application, and use, e.g., as used in food applications (Bautista-Gallego et al., 2017). Recent formulations which are water-soluble mixtures allow for concentration dilution and effective treatment when applied at the surface or molded with soils during compaction (Daniels & Hourani, 2009) with the bonding reaction and hydrophobicity developing as the soil dries.

To successfully establish engineered water repellency as a means for moisture control and frost heave mitigation by designers and engineers, there is a need to develop

treatment specifications, obtain optimal OS dosage concentrations, and explore the effects of varying treatment conditions (drying, reaction time, leaching/washing) on treatment outcome. This paper explores EWR in frost susceptible soils and examines the influence of treatment variables on its optimization in frost susceptible soils. It also establishes baseline criteria for using water repellency in geotechnical applications.

2. Materials and Methodology

2.1 Soil

Natural soils and glass beads were utilized in this study for testing and analysis. Four soils were collected from different locations in the US; Fairbanks in Alaska (AK-FB), Pottawatomie County in Iowa (IA-PC), Asheville in North Carolina (NC-AS), and Hanover silt (NH-HS) from the U.S. Army Cold Regions Research and Engineering Laboratory (CRREL) in New Hampshire. Samples received were air dried and prepared for testing and analysis. Glass beads (Soda Lime, type S) of grain sizes ranging from 0.05 mm to 1.85 mm were mixed in proportion to model an average of all the four soil samples given.

2.1.1 Material Characterization

Index property and other tests were performed according to the standard ASTM procedures (ASTM D4318; ASTM D854; ASTM D7928; ASTM D698; ASTM D6913). A summary of the index properties, material classifications, and frost susceptibility

classification from the U.S. Army Corps of Engineers (U.S. Army Corps of Engineers, 1965) is given in Table 1-1.

Table 1-1 Summary of soil index properties and classifications

Soil Property	**SOIL**			
	AK-FB	**IA-PC**	**NC-AS**	**NH-HS**
Specific Gravity, Gs	2.67	2.74	2.65	2.68
#4 Sieve (4.75 mm)	97.6	100	89.51	79.8
#10 Sieve (2mm)	96.0	99.8	73.32	74.18
#40 Sieve (0.425 mm)	93.4	99.6	67.08	52.69
#200 Sieve (0.075 mm)	84.5	98.4	30.52	42.41
Silt content (%) (75μm–2μm)	75.65	86.67	26.47	37.52
Clay content (%) (< 2μm)	8.87	11.69	4.05	4.88
Liquid Limit, LL	41.0	33.73	38.44	41.8
Plastic Limit, PL	NP	NP	NP	NP
Optimum Moisture Content (%)	20.7	17.5	18.50	10.6
Max. Dry Unit Weight (kN/m^3)	14.1	16.3	15.02	19.5
USCS Classification	ML	CL	SM/SC	ML
AASHTO Classification	A-5	A-6	A-4	A-4
Frost Susceptibility Classification	F4	F3	F3	F4

2.2 Organosilane Selection

While several products abound to impart hydrophobic properties to materials, three (3) organosilane chemicals were selected for this study based on ease of use, environmental considerations, and cost. The organosilanes were broadly grouped into two categories; (i) “water-soluble,” requiring dilutions in water to achieve water repellency (through a process of hydrolysis), and (ii) “use-as-is” which do not require any additional mixing and can be directly mixed in with soil.

2.2.1 Water-Soluble OS Products

DOWSIL™ IE 6683 (OS1) is a water-based silane/siloxane emulsion that can be used as supplied or diluted further in water for water-repellency treatment of surfaces. It is particularly suited to porous construction materials and bonds with the substrate to produce a durable hydrophobic treatment.

Terrasil (OS2) from Zydex Industries is a viscous, water-soluble, and reactive soil modifier that permanently modifies the soil surface, making it hydrophobic. OS2 is safe and has been utilized in previous studies as a soil modifier and performance enhancer, particularly in stabilization for pavement applications (Oluyemi-Ayibiowu and Uduebor, 2019)

2.2.2 “Use-as-is” OS product

SIL-ACT® ATS-100 (OS3) is a clear, durable silane treatment product utilized in masonry, concrete, and stone waterproofing. Treated surfaces become repellent to water, chloride, waterborne contaminants, and weathering elements. They have been utilized by the Departments of Transportation (DOTs) of many states for the treatment of parking decks, bridges, airport pavements, and highways (Khanzadeh Moradllo et al., 2016; Behravan et al., 2022a).

Table 1-2 Summary of treatment products and active chemicals

Type	ID	Product Name	Active compound	Composition in Solution (%)	Color	Specific Gravity (@25ºC)	pH	Density (g/cm$^{3)}$
Water Soluble	S1	DOWSIL™ IE 6683	Alkoxysilane, Polydimethylsiloxane	40.0	Milky white	1.0	4.0 - 6.0	
	S2	TERRASIL	Alkoxy-Alkylsilyl Compounds	65.0 -70			Neutral to acidic	1.01 – 1.05
Use-as-is	S3	SIL-ACT® ATS-100	Alkyltrialkoxysilane (Isobutyltrimethyoxysilane)	90 – 100	Clear	0.92		0.92

2.3 Treatment protocol

Initial treatment was carried out at a dosage concentration of 1:10 (OS: Soil, batched by weight), to determine the relative effectiveness of the products and select the most effective three (two. water-soluble and one use-as-is). While higher concentrations of some products could prove more effective, there is a need to account for the associated costs of the increased volume of material required. Further treatment at varying dosage concentration ratios was carried out to determine optimal dosage concentrations. For the use-as-is product (OS3), the soil and OS were manually mixed for one minute in a 250ml (8.45 oz) HDPE bottle and set up on a tumbler to react for 24 hours (30 cycles/min). For water-soluble OS (OS1, OS2), the OS product was mixed with DI water to achieve a Liquid/Solid Ratio of 1:1 to ensure maximum coverage of the soil samples. Therefore, for 50g (0.11lb) of soil at 1:10 dosage, 5g (0.011lb) of the OS was diluted in DI water to make up 50g for mixing.

To observe the impact of drying conditions, the resulting mixture was then split into two parts placed into cans, and dried under two different drying conditions: air drying in an air-conditioned laboratory (temperature 22^{o}C, relative humidity ~21%) and an electric oven at 60°C. While air-dried samples simulated conditions closest to field results, the oven-dried samples gave the maximum possible drying conditions available. Oven-dried samples were dried for 24 - 48 hours (about 2 days) and then cooled for 24 hours in a desiccator to prevent an enhancement of the water repellency during measurement (Roy et al., 1992).

2.4 Water Repellency Assessment

2.4.1. Contact Angle (CA) Test

Contact angle measurement was carried out following protocols by Feyyisa et al. (2017) which described a dynamic approach to improve the repeatability of tests carried out on coal fly ash after Bachmann et al. (2000). A double-sided adhesive tape was attached to a glass slide and dried samples were sprinkled on the other coated side and compressed for 10s using a 10g weight. The slide was then tapped carefully to remove any excess soil grains, creating a monolayer of soil on the tape surface. This process of application was repeated twice to ensure full coverage of the tape and duplicate slides were also prepared for each test. The soil specimen was placed on a goniometer (Ramehart Instruments, 260-U1, standard goniometer, #150512) made up of a microscopic camera, along with a fiber optic backlighting source and an adjustable sample holding table (Fig. 1-2). Drops of deionized water were placed on the surface of the specimen utilizing a FlowTrac II

(Geocomp Products) in volume increments of 20µl. The drop was gradually advanced with continual horizontal image capturing and measurements were taken for each drop size. The drop advancement was continued until a stable contact angle is observed which is taken as the apparent contact angle of the sample. Contact angle measurements less than 90^o are considered wettable/hydrophilic, while angles measured between 90^o and 150^o are considered hydrophobic. Contact Angles above 150^o are taken to be superhydrophobic (King, 1981). The observed minimum and maximum are also given as standard deviations from this value.

Figure 1-2 (a) Contact Angle measurement (b) Hydrophilic (<90^o) (c) Hydrophobic (>90^o)

While laboratory tests provide optimal conditions for the treatment of soils using a different OS, there is a need to investigate the effect of varying treatment variables on the resulting hydrophobicity of engineered soils. A number of variables were considered; Soil type (S) (IA-PC (fine-grained), NH-HS (coarse-grained), GB (coarse-grained)), Organosilane Product (OS) (OS1, OS2, OS3), Dosage (D) (1:10, 1:50, 1:100), Reaction Time (R) (0.25, 4, 12, 24 hours), Leached Condition (Washed, Unwashed), to determine the effect of changes on the water repellency imparted to the soil sample. A total of 216 samples were tested using a parametric study comprising the various variables and the results were analyzed using a two-step analysis of variance (ANOVA) test.

2.4.2 Water Drop Penetration Time (WDPT) Test

20g of dried samples were utilized for the WDPT measurements. The samples were placed in aluminum cans and tapped lightly on the side to get a uniform surface. This is to prevent the rolling of the water droplets after placement. Three drops of deionized water ($50 \pm 1\mu L$ volume) were placed on the soil surface with a pipette. The tests were conducted under a constant temperature of ~25^{o}C, and RH of ~21% without draft to minimize evaporation during the experiment. Any penetration less than or equal to 1 second was taken as instantaneous. All measurements were terminated after 1 hour (3600s), and WDPTs exceeding 3600s (1 hour) were assigned as extremely water-repellent.

2.4.3 Breakthrough Head Tests

While CA and WDPT tests indicate the degree of water repellency of soils using a planar surface, they do not give information about the ease with which water can penetrate the pore space between particles. Breakthrough head tests offer a good correlation for water repellency concerning the treatment and provide more insights into the performance of the treated material under practical use conditions. According to (Carrillo et al., 1999), if the CA is greater than 90° (i.e., hydrophobic), a positive pressure is required to force liquid into the capillary space. The pressure required to force the liquid is referred to as the breakthrough pressure head.

The method established by (Feyyisa et al., 2019) using a flexible wall permeameter setup as described in ASTM D5084 was adopted. It shares a similar operational concept to the rigid wall permeameter approach reported in previous studies (Carrillo et al., 1999; Fink, 1970; Letey et al., 2000). It avoids side wall leakage using a confining pressure on a flexible membrane. The breakthrough pressure is identified as the pressure corresponding

to the maximum rate of change of the pressure-time data series. This correlates with the results of (Fink and Myers, 1969), who identified the breakthrough pressure as the point where a change in the slope of the linear section of the pressure-time series plot occurs. Oven-dried soil samples (35 mm (1.38 inches) by 70mm (2.76 inches)) compacted at Optimum Moisture Content (OMC) were mounted on a triaxial cell. A constant cell pressure of 138 kPa was applied using a FlowTrac II system (Geocomp) to prevent preferential flow between the flexible membrane and the soil sample. The soil sample was mounted on a porous stone and the bottom was flushed to remove entrapped air. The input flow line was set up with a pressure transducer (PX409-030GUSBH from Omega Engineering, Inc.) via the inflow valve to determine the pressure applied while the outflow valve was kept open to allow pore air to escape during water infiltration. DI water was supplied at incremental pressures, with successive pressure increments of 1kPa, using another FlowTrac II. Each pressure increment was maintained for 300s and the volume of water passing through the sample at constant pressure was monitored. The pressure and volume response were logged every second using software paired with the pressure transducer. Breakthrough pressure was selected based on the pressure/volume-time series plot. The breakthrough pressure test ended after water penetrated through the sample (indicated by volume change).

Electric Conductivity (EC) and pH measurements were carried out on untreated and treated samples using a Mettler Toledo probe. The dried samples were mixed with Deionized water (~1μS/cm) at a liquid-to-solid ratio of 2:1 for 24 hours and the supernatant was extracted for testing.

3. Results and Discussion

3.1 Contact Angle

The results of contact angle tests carried out on soil samples treated at an OS: Soil ratio of 1:10 using three (3) selected organosilane products are presented in Figure 3. Soils treated have very high contact angles (>110^{o}) and are all hydrophobic after treatment. An observable result was the effect of drying on the contact angle results. Air-dried samples had a lower contact angle compared to sample oven-dried samples. This is because the water-repellent properties of the soil are affected by dry conditions (Lee et al., 2015). While oven-dried samples provide the maximum possible contact angle measurement for a given soil sample, air-dried samples provide what is obtainable under field conditions.

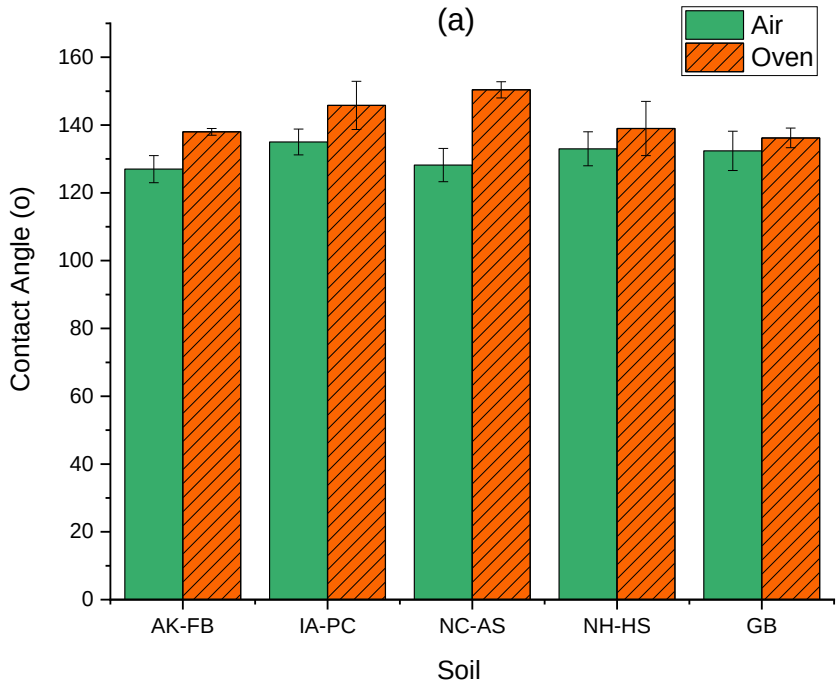

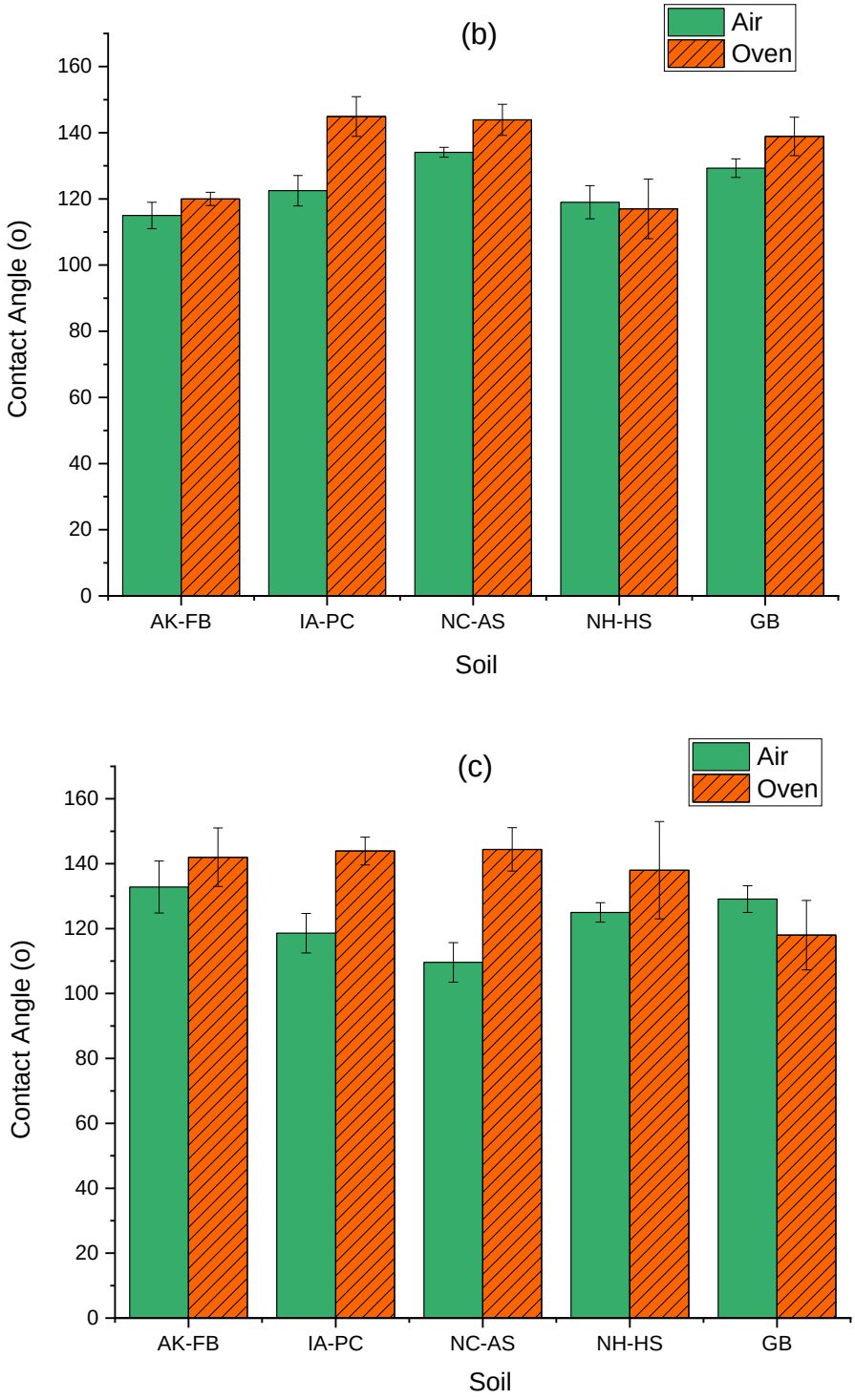

Figure 1-3 Contact Angles of soils under two drying conditions after treatment (1:10, OS:Soil, g/g) with (a) OS1 (b) OS2 (c) OS3

Figures 1-4 shows the change in contact angle concerning dosage concentration. There is a gradual decrease in the contact angle with decreasing OS concentration. Treatment with OS2 achieves a higher CA even at lower concentrations (1:1000) due to the high concentration of the active ingredients (65 - 70%) compared to OS1 (40%). There was an insufficient quantity of OS3 to saturate and treat the soil samples by the “use as is” product at lower concentration ratios resulting in poor treatment of the soil surface. Results from Choi et al. (2016) indicate that only approximately 40% of the soil particle surface is required to be treated for measurable hydrophobicity. This means a high contact angle does not necessarily mean full surface treatment. This characteristic is also observed by the marginal increment in contact angle with increased dosage.

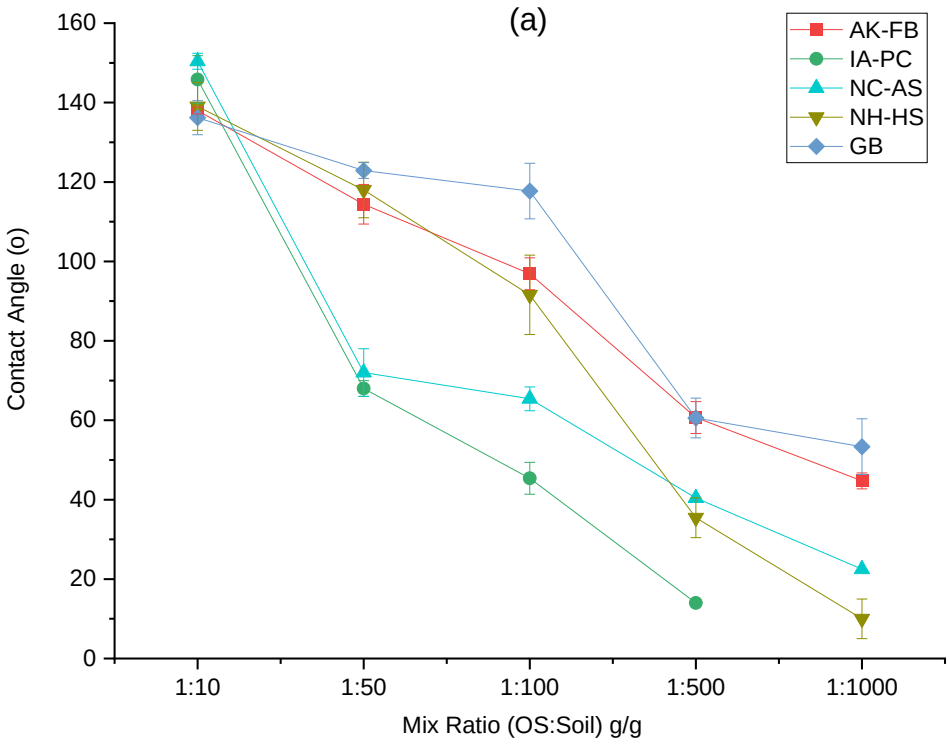

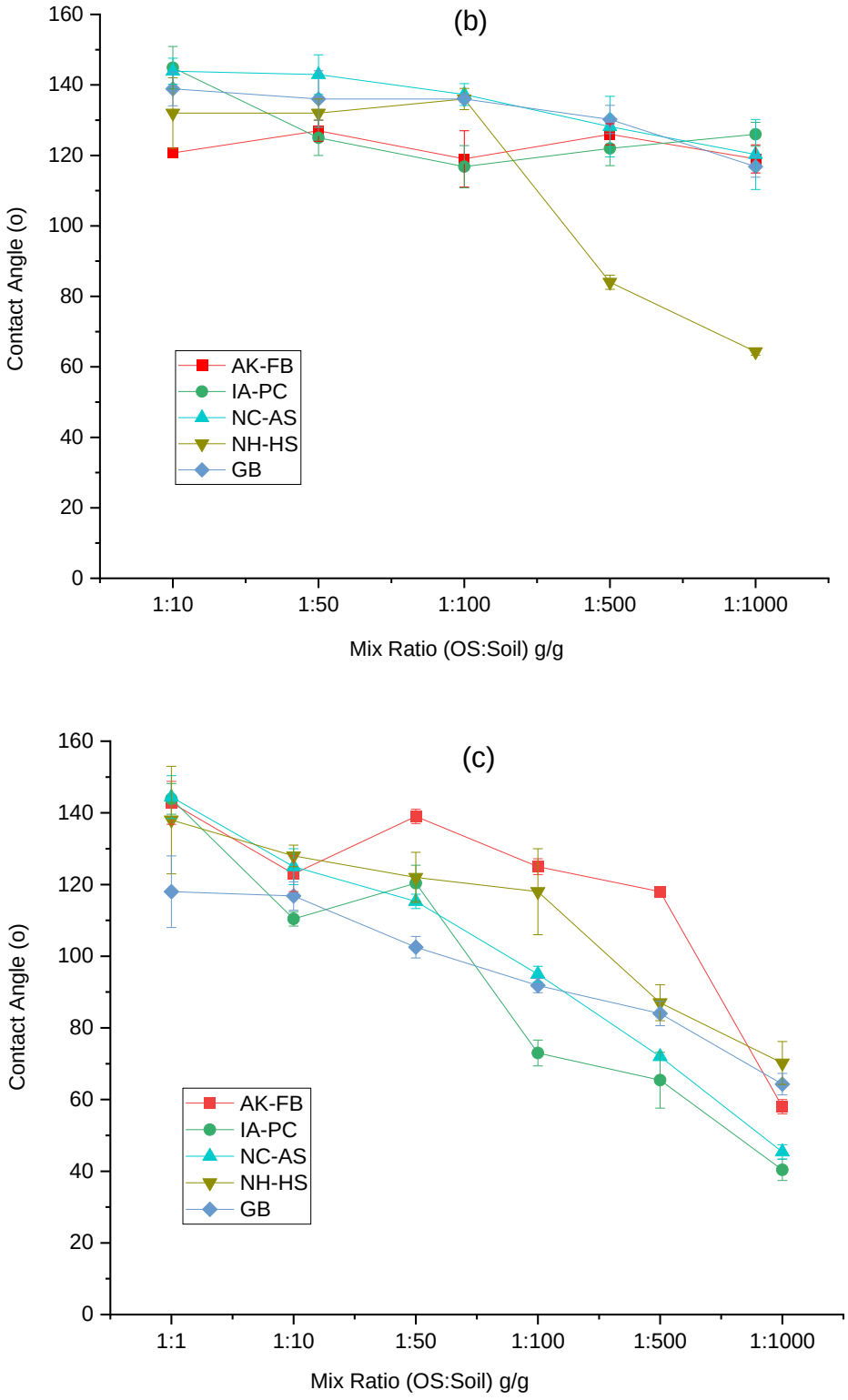

Figure 1-4 Contact Angles of soils with varying treatment dosage concentrations (a) OS1 (b) OS2 (c) OS3

Energy-dispersive X-ray spectroscopy (EDX) analysis performed (See Table 1-3) shows that the soils possess some quantity of silica which is favored for silanization (15.48 - 33.47%). The soils also have a large amount of Iron (5.58 - 17.57%), except for glass beads. Studies have also shown good adsorption of organosilanes by Iron and Aluminum oxide surfaces, with better adsorption on iron oxide surfaces than aluminum at lower concentrations (Quinton et al., 1997). At lower dosage concentrations (1:500, 1:1000), there is a marked difference between the contact angles of different soil samples, with soils (AK-FB, GB) performing better than others. Different products also have different compositions as indicated in Table 1-2 and this may also be responsible for the variation in results, as different products bond differently with soils.

Table 1-3 Elemental composition of soils from EDX analysis

Element	**NC-AS**	**IA-PC**	**GB**	**NHHS**	**AK-FB**
Carbon (C)	11.44	8.92	21.18	9.63	20.85
Oxygen (O)	34.89	42.5	41.71	40.98	29.35
Sodium (Na)	3.87	13.82	8.24	-	-
Aluminum (Al)	7.6	9.06	0.24	12.23	6.99
Silicon (Si)	23.89	19.72	24.66	15.48	33.47
Calcium (Ca)	1.49	1.25	2.05	-	1.35
Iron (Fe)	16.84	13.82	-	17.57	5.58
Zinc (Zn)	-	0.73	-	0.96	-
Magnesium (Mg)	-	2.3	1.93	1.75	1.06
Potassium (K)	-	1.7	-	1.4	1.35

3.1.1 Effect of Varying Treatment Variables on the Contact Angle of Engineered Soils

Different variables - soil type, organosilane product, dosage, leaching and drying condition - and their effect on treatment effectiveness were investigated. All possible interactions between the testing variables were considered and the resulting sum of squares

indicated the resulting variance in the contact angle was obtained. The resulting percentage of each combination as part of the total variance was then plotted into a pie chart (See Fig 5). It can be observed that there is a variation in the values of the contact angle with changes in soil type, OS, and dosage (a total of 94.59%). Other considerations including reaction time and leaching condition did not contribute much to the variance in the contact angle (5.40%). Drying effects on the contact angle have been established already and were not considered. There was also a correlation between Soil ($p = 4.97e-07 < 0.05$), OS ($p=1.52e-09<0.05$), and Dosage ($p=2.28e-09<0.05$) with the contact angle, while there is no correlation between Reaction Time ($p=0.993>0.05$) and Washing ($p=0.143>0.05$). In terms of field application, this means, there is no significant need to pause operations to "cure" or allow for treatment.

The variation in the contact angle results due to soil type can be explained by the differences in their mineralogical composition which affects the available ions and pH of the resulting mixture. The varying oxide compositions in their respective proportions allow for preferential bonding with the silane-forming siloxane (-Si-O-Si) and -Si-O-Metal bonds. In addition, the available surface area for treatment makes the treatment of finer-grained soils more effective. Studies carried out by Saulick et al. (2018) have shown that particle size, shape, and roughness can affect the contact angle of treated soils. OS and dosage effects can be explained by the difference in composition of the three OS utilized in this study which reacts and bond differently with material surfaces. Their performance can also be affected by the pH of the soil, while the amount of the active ingredient available based on dosage will affect the contact angle results up to a limiting value where

the soil properties indicated above predominantly affect the resulting contact angle measurement.

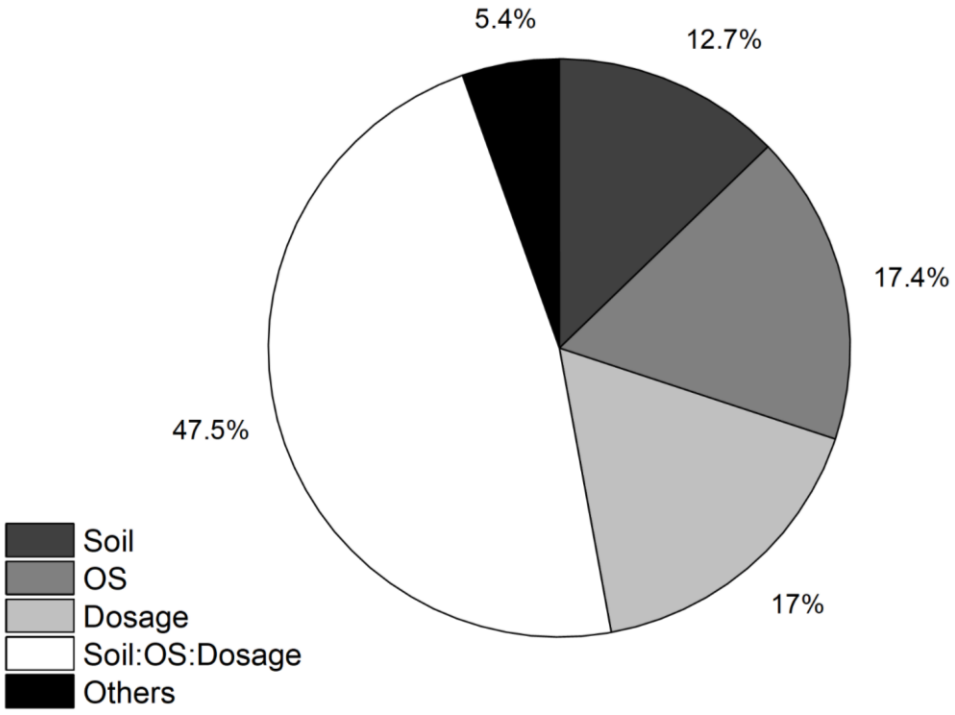

Figure 1-5 Percentage contribution of variables to the variance in Contact Angle Results

A Tukey test carried out with a 95% confidence level showed a similarity between contact angle results obtained for NH-HS and GB ($p = 0.389 > 0.05$) while there was no similarity between those for IA-PC and the other two materials tested ($p = 2.225e-04, 7.00e-07 < 0.05$) indicating that the glass bead material had similar contact results to the NH-HS sample. Dosage, Washing, and Reaction Time showed no similarities in the results obtained from their varying test conditions.

3.2 Effect of Treatment on Chemical Properties

3.2.1 EC

Electrical conductivity was used to track ionic activities in solution and to establish the excess or decrease of ions following treatment. An increase in EC after treatment relates to excess chemical addition to achieve water repellency. There is a marked change in EC at 1:50 dosage concentration for OS1, 1:100 for OS2, and 1:10 for OS3. EC is also a good indicator of excess ions in solution or a measure of excess OS left in solution after treatment. From Figure 1-6, EC drops after treatment except for treatment with ZD and XA, which have higher EC values indicating an excess in solution. This trend is not repeated in NC-AS where all treatment EC is higher than untreated soil. This could be indicative of excess OS for all treatments or the material composition. Increased conductivity could also indicate increased osmotic potential which will result in moisture absorption by the excess salt in the treated soil. This will impact the water-repellent performance of the treated soil and inhibit its ability to serve as a capillary barrier or sustain hydrostatic head.

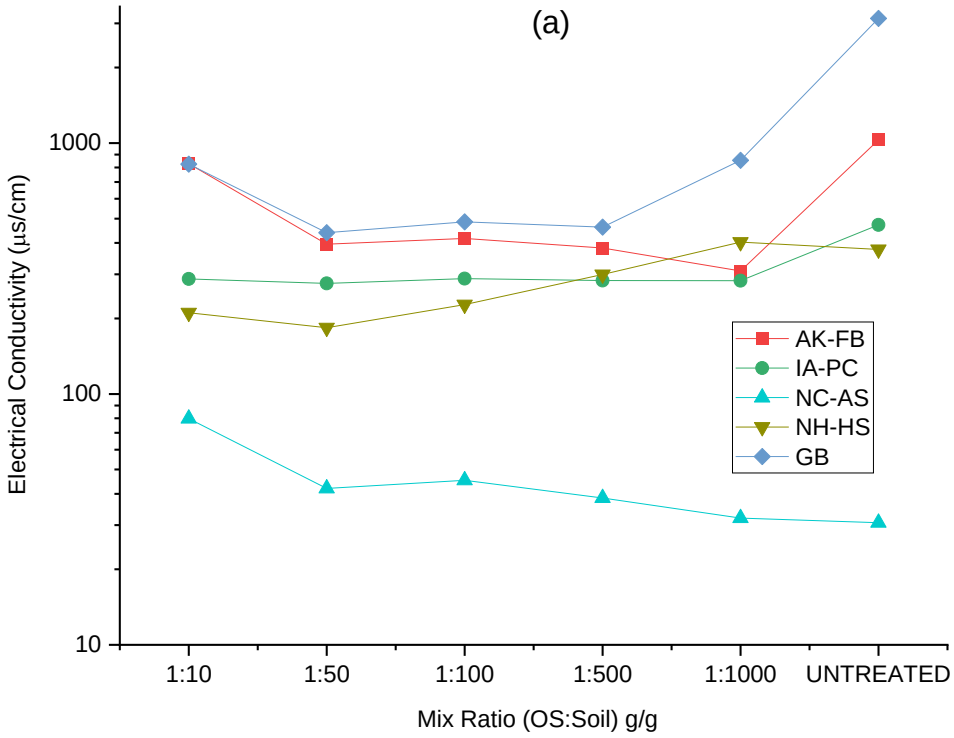
(a)
Electrical Conductivity (µs/cm)
1000
100
10
1:10
1:50
1:100
1:500
1:1000
UNTREATED
Mix Ratio (OS:Soil) g/g
AK-FB
IA-PC
NC-AS
NH-HS
GB

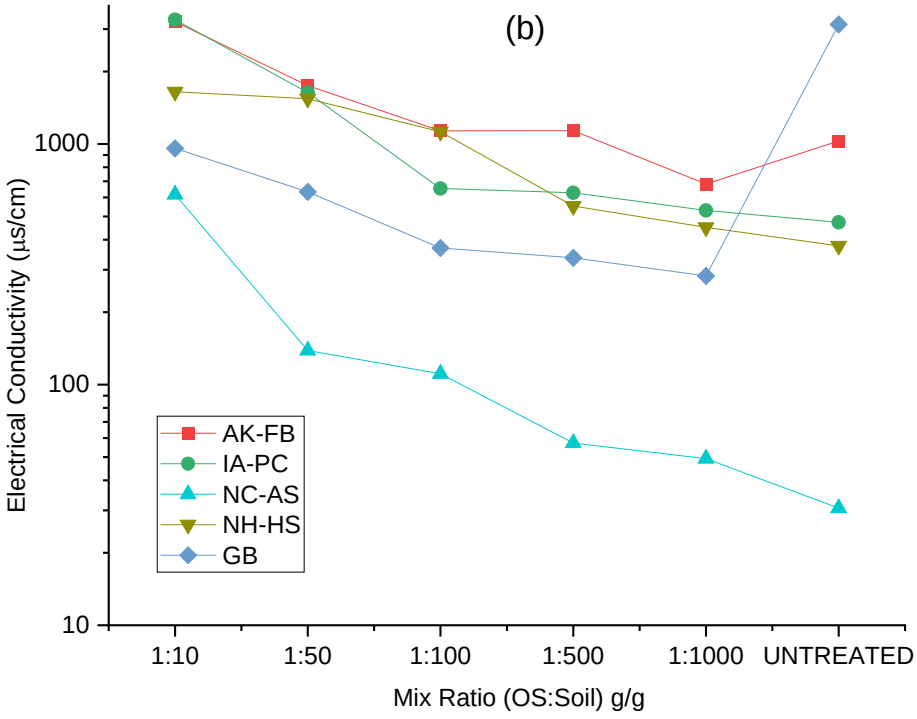
(b)
Electrical Conductivity (µs/cm)
1000
100
10
1:10
1:50
1:100
1:500
1:1000
UNTREATED
Mix Ratio (OS:Soil) g/g
AK-FB
IA-PC
NC-AS
NH-HS
GB

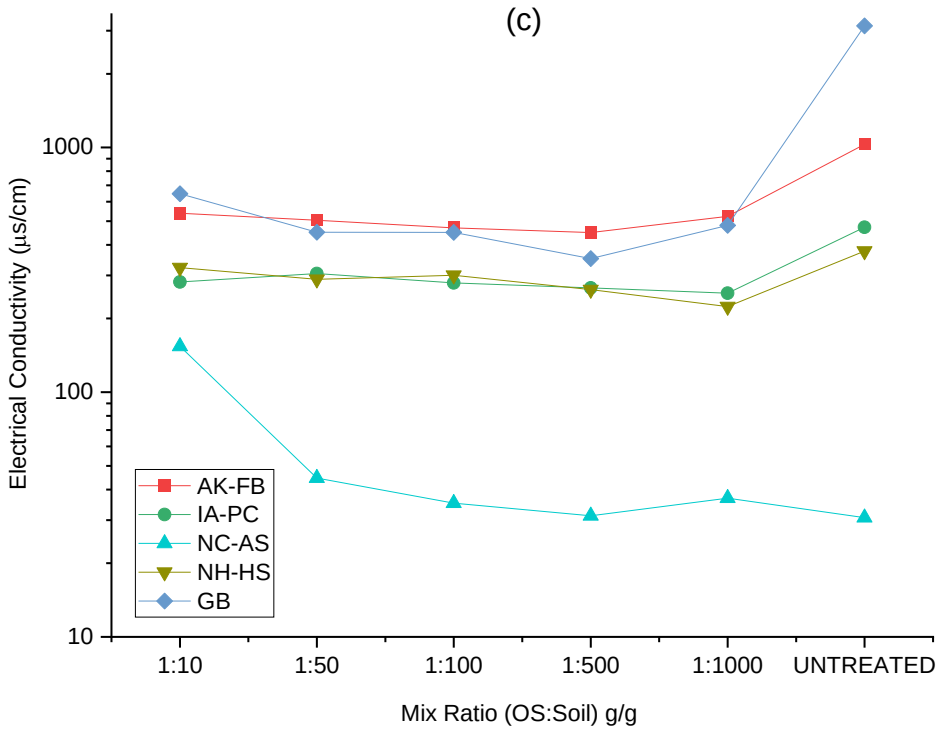

Figure 1-6 Electric Conductivity of soils with varying dosage concentrations (a) OS1 (b) OS2 (c) OS3

3.2.2 pH

The results of pH tests carried out on treated and untreated samples are presented in Figure 1-7. There is a good correlation between the EC and pH of treated samples, and both could serve as good indicators for determining optimal treatment. Where there is sufficient utilization of OS, pH remains stable. In cases where the OS is in excess (1:50 for OS1, 1:100 for OS2, and 1:10 for OS3), pH changes based on the composition of the OS to become more acidic. This could be important to note when optimizing treatment in certain applications where the effects of excess OS could impact agricultural land or waterways is a major concern.

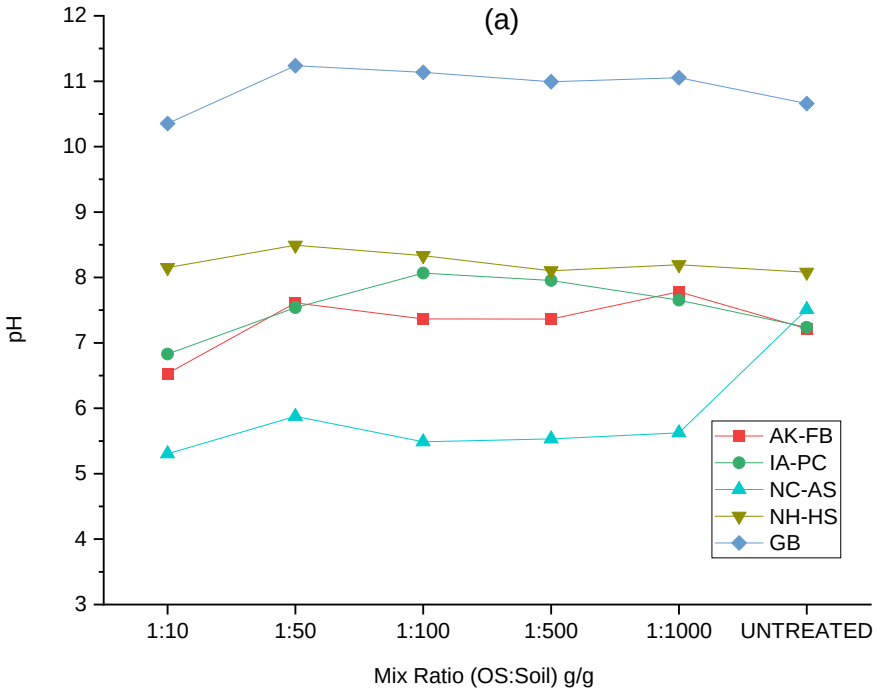
(a)
pH
12
11
10
9
8
7
6
5
4
3
1:10
1:50
1:100
1:500
1:1000
UNTREATED
Mix Ratio (OS:Soil) g/g
AK-FB
IA-PC
NC-AS
NH-HS
GB

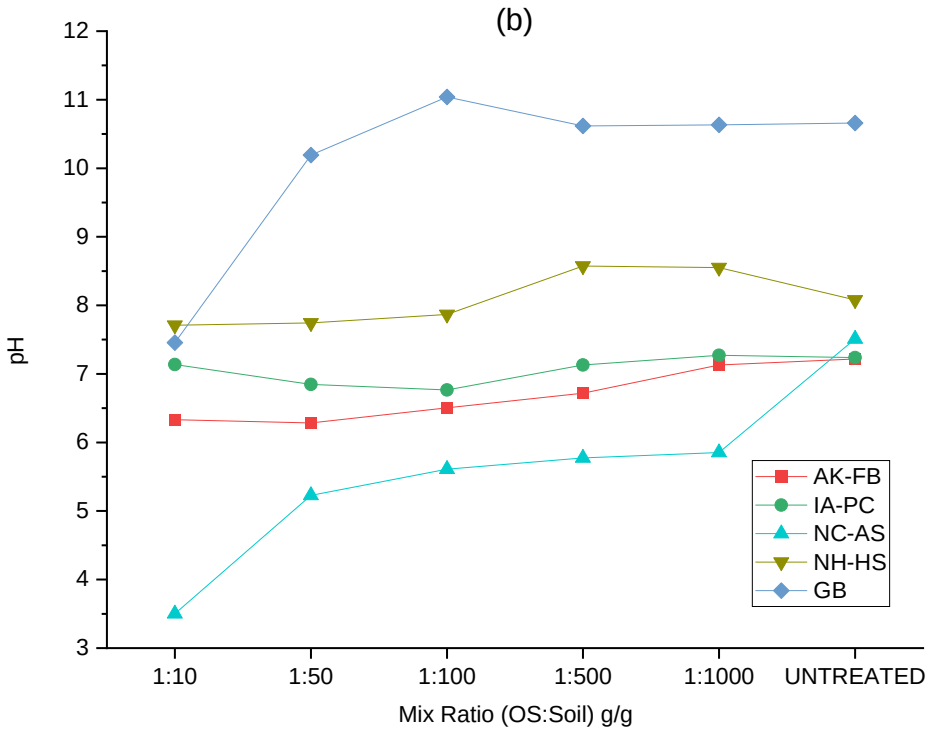
(b)
pH
12
11
10
9
8
7
6
5
4
3
1:10
1:50
1:100
1:500
1:1000
UNTREATED
Mix Ratio (OS:Soil) g/g
AK-FB
IA-PC
NC-AS
NH-HS
GB

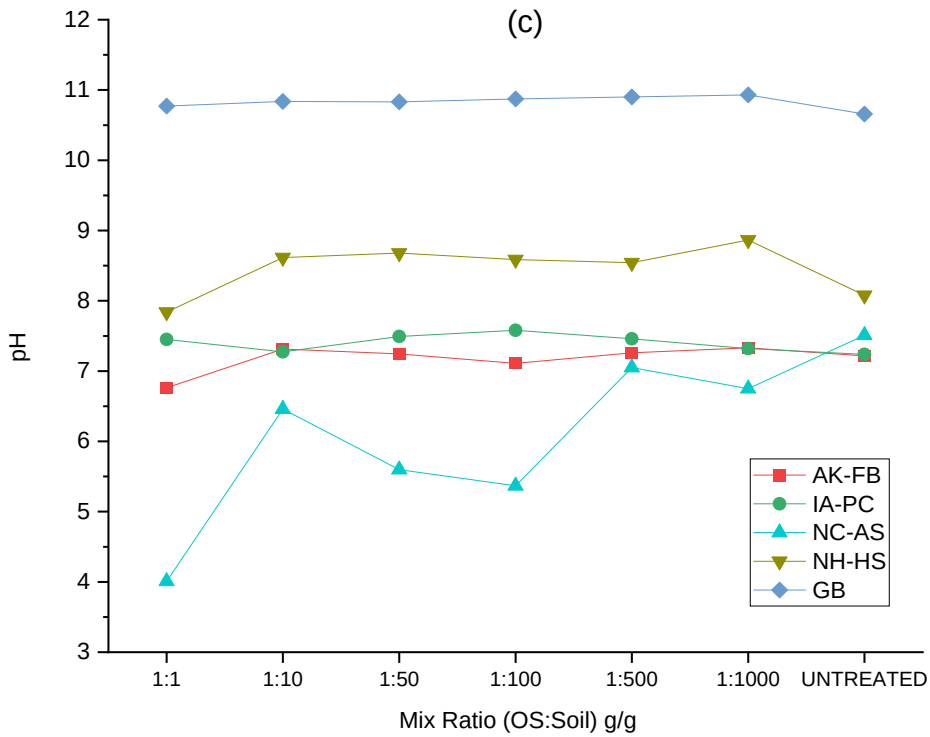

Figure 1-7 pH of soils with varying dosage concentrations (a) OS1 (b) OS2 (c) OS3

3.3 Water Drop Penetration Time Test

The results of the WDPT tests carried out are shown in Figure 8a-c. Some untreated soils (AK-FB, GB) were slightly water repellent with penetration times of 128s and 2s respectively. The AK-FB sample possesses large quantities of decayed organic matter and is humic in nature. This results in an apparent hydrophobicity that disappears after mixing. The glass beads are made up of soda lime, which in the amorphous state possesses some form of repellency. For treated samples, there is a marked increase in penetration times with increasing dosage concentration. All samples treated with OS2 were extremely water repellent even at lower concentrations (1:1000). There is a good correlation between the contact angle results and the WDPT as shown in figure 8d. Some studies have developed

relationship equations for contact angle and WDPT (Feyyisa et al., 2019; Keatts et al., 2018), but the models developed cannot be easily transferred across soil samples due to the variations in material and other test conditions as established earlier.

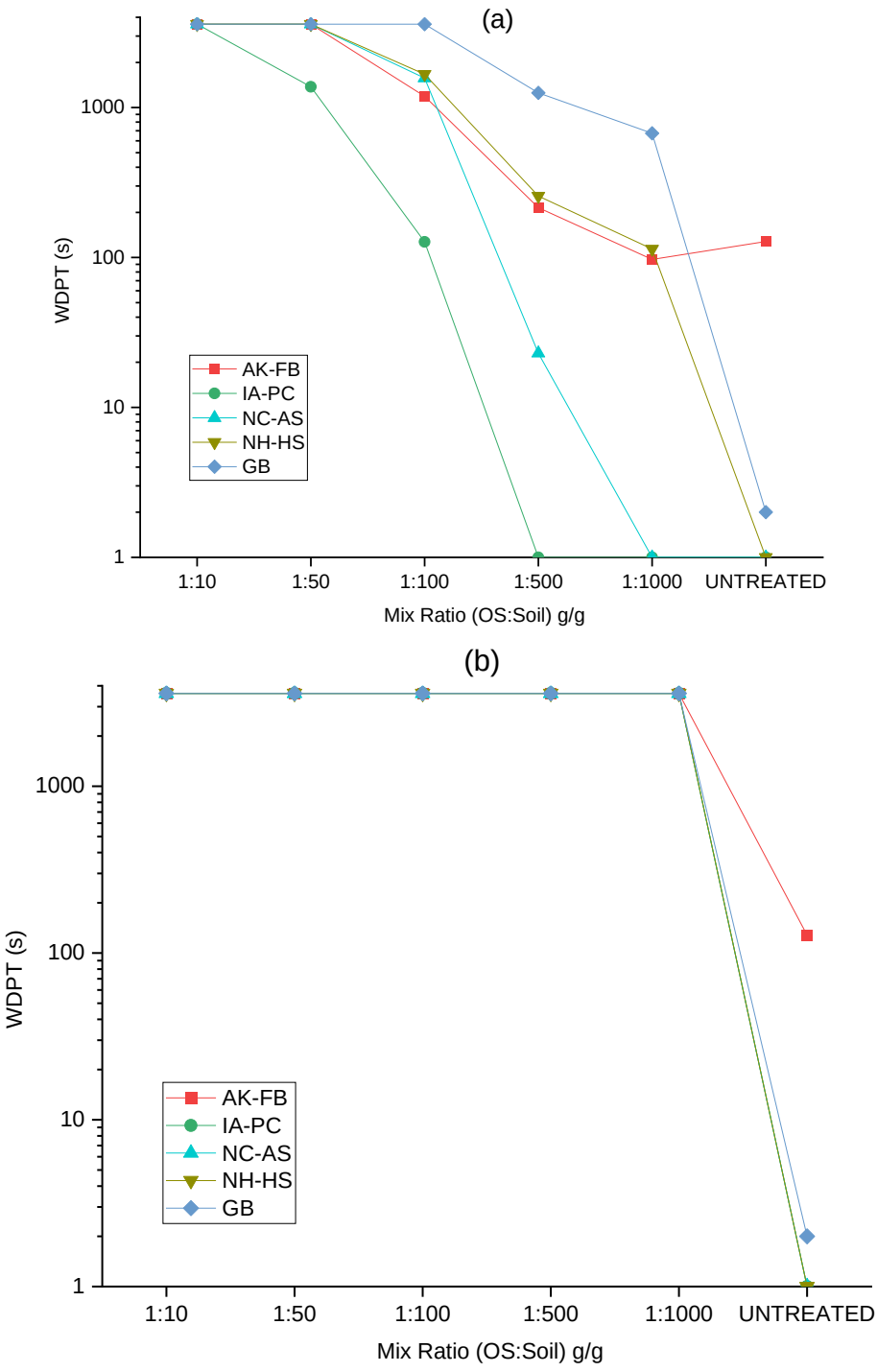

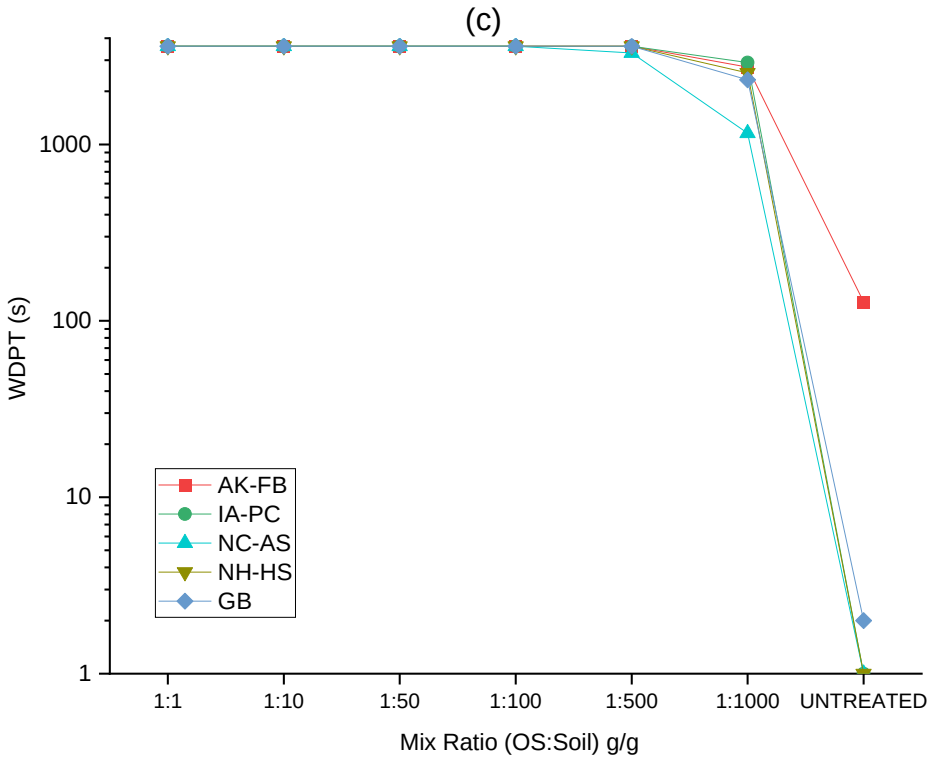

Figure 1-8 Water Drop Penetration Times of soils with varying dosage concentrations (a) OS1 (b) OS2 (c) OS3

3.4 Breakthrough Pressure Test

While the WDPT gives a good correlation with the contact angle of water-repellent soils, it does not provide any information on the performance of these soils under a pressure head since the water droplet does not impart any considerable pressure on the surface of the soil. The breakthrough pressure test provides relevant information useful for engineers in design and construction. Figure 9 shows the water entry (breakthrough pressure) of tested soils under varying dosage concentrations. There is a marked increase in the pressure required to infiltrate the treated soil with dosage. Breakthrough pressures of up to 23 kPa were measured for treated samples.

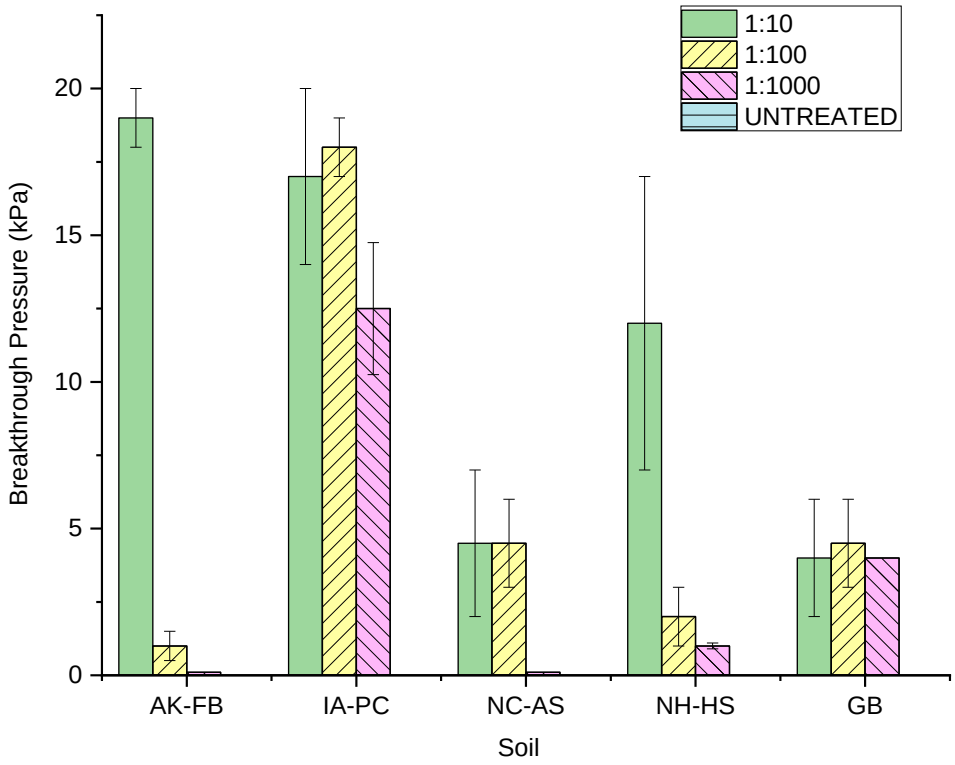

Figure 1-9 Breakthrough Pressure of soils with varying dosage concentrations using OS2

It can be observed that there was higher breakthrough pressure for the fine-grained sample (IA-PC) even at lower dosages compared to the others. This is because soil properties like grain size affect the results with fine-grained soils possessing larger surface areas treatable by the OS and also smaller void spaces within the compacted sample. The smaller capillary pore that otherwise would have aided the transport of water through the frost susceptible soil is now shut down due to the particle surface being water-repellent. This shows that treatment improves the water repellency properties of frost susceptible soils and makes them suitable for use as capillary barrier materials, preventing the transport of water through them and mitigating the effects of frost action.

4. Conclusion

EWR in soils can be an effective solution for moisture control and improving the water-repellency properties of in-situ soil. This study was carried out to determine the optimal treatment dosage and treatment protocols affecting water repellency in soils. The conclusions of this study are given below.

- Major factors influencing water repellency in soils include soil type, OS (Organosilane) product, dosage, and drying conditions. Other factors like reaction time and leaching do not significantly impact water repellency. For field operations, engineers and designers should consider soil type, OS selection, and dosage as key factors for treatment decisions.
- CA test results indicate a positive correlation with dosage concentration, with OS2 treatment proving effective even at lower concentrations (1:1000) and minimal marginal increase in CA measured after 1:50. Due to varying OS types, engineers should specify a target CA to be met rather than a fixed dosage concentration for engineering applications. Optimal dosage concentrations can be preliminarily accessed in the field by monitoring EC and pH changes post-treatment.
- CA and WDPT (Water Drop Penetration Time) are useful but do not provide any information on engineering performance. Breakthrough tests provide some data on the engineering performance of treated soils. OS2-treated soil samples demonstrated increased breakthrough pressures with dosage increases at uniform density, making them suitable for moisture control applications. Fine-

grained soils exhibit higher breakthrough pressures due to larger surface areas and smaller void spaces.

These results suggest that treated soils can serve as effective barriers or moisture control materials in geotechnical applications. By modifying in-situ soils with EWR treatment frost susceptibility can be eliminated and costly soil replacement can be avoided, saving limited resources. EWR can also be utilized to manage moisture and mitigate shrink-swelling in expansive soils by limiting water transport into the soil matrix.

REFERENCES

ASTM. (2000). D5084 - Standard Test Methods for Measurement of Hydraulic Conductivity of Saturated Porous Materials Using a Flexible Wall Permeameter. *Astm D5084*, *04*(October 1990).

ASTM. (2012). ASTM D698: Standard Test Methods for Laboratory Compaction Characteristics of Soil Using Standard Effort (12 400 ft-lbf/ft3 (600 kN-m/m3)). *ASTM International*, *3*.

ASTM D 854. (2002). ASTM D854 Standard Test Methods for Specific Gravity of Soil Solids by Water Pycnometer. *ASTM International*, *04*.

ASTM D7928. (2021). Standard Test Method for Particle-Size Distribution (Gradation) of Fine-Grained Soils Using the Sedimentation (Hydrometer) Analysis. *ASTM International*, *May 2016*.

ASTM International. (2017a). D6913: Standard Test Methods for Particle-Size Distribution (Gradation) of Soils Using Sieve Analysis. *ASTM International*, *D6913*(17).

ASTM International. (2017b). ASTM D4318-17. *Standard Test Methods for Liquid Limit, Plastic Limit, and Plasticity Index of Soils*.

Bachmann, J., Ellies, A., & Hartge, K. H. (2000). *Development and application of a new sessile drop contact angle method to assess soil water repellency*. www.elsevier.com/locate/jhydrol

Bardet, J. P., Jesmani, M., Jabbari, N., & Lourenco, S. D. N. (2015). Permeability and compressibility of wax-coated sands. *Https://Doi.Org/10.1680/Geot.13.P.118*, *64*(5), 341–350. https://doi.org/10.1680/GEOT.13.P.118

Bautista-Gallego, J., Iacumin, L., Cabello, A. B., Gkana, E. N., Doulgeraki, A. I., Chorianopoulos, N. G., & Nychas, G.-J. E. (2017). *Anti-adhesion and Anti-biofilm Potential of Organosilane Nanoparticles against Foodborne Pathogens*. https://doi.org/10.3389/fmicb.2017.01295

Behravan, A., Aqib, S. M., Delatte, N. J., Ley, M. T., & Rywelski, A. (2022). Performance Evaluation of Silane in Concrete Bridge Decks Using Transmission X-ray Microscopy. *Applied Sciences (Switzerland)*, *12*(5). https://doi.org/10.3390/app12052557

Brooks, T., Asce, S. M., Daniels, J. L., Asce, F., Uduebor, ; Micheal, Cetin, B., Asce, M., Naqvi, M. W., & Student, P. D. (2022). *Engineered Water Repellency for Mitigating Frost Action in Iowa Soils*. 448–456. https://doi.org/10.1061/9780784484012.046

Carrillo, M. L. K., Yates, S. R., & Letey, J. (1999). Measurement of Initial Soil-Water Contact Angle of Water Repellent Soils. *Soil Science Society of America Journal*, *63*(3), 433–436. https://doi.org/10.2136/SSSAJ1999.03615995006300030002X

Choi, Y., Choo, H., Yun, T. S., Lee, C., & Lee, W. (2016). Engineering characteristics of chemically treated water-repellent Kaolin. *Materials*, *9*(12). https://doi.org/10.3390/ma9120978

Daniels, J. L., & Hourani, M. S. (2009). Soil Improvement with Organo-Silane. *U.S.-China Workshop on Ground Improvement Technologies 2009*, 217–224. https://doi.org/10.1061/41025(338)23

Daniels, J. L., Langley, W. G., Uduebor, M., & Cetin, B. (2021). Engineered Water Repellency for Frost Mitigation: Practical Modeling Considerations. *Geo-Extreme 2021*, 385–391. https://doi.org/10.1061/9780784483701.037--

de Jesús Arrieta Baldovino, J., dos Santos Izzo, R. L., & Rose, J. L. (2021). Effects of Freeze–thaw Cycles and Porosity/cement index on Durability, Strength and Capillary Rise of a Stabilized Silty Soil Under Optimal Compaction Conditions. *Geotechnical and Geological Engineering*, *39*(1), 481–498. https://doi.org/10.1007/S10706-020-01507-Y/FIGURES/12

Debano, L. F. (2015). Infiltration, evaporation, and water movement as related to water repellency. *Soil Conditioners*, 155–164. https://doi.org/10.2136/SSSASPECPUB7.C15

Dore, G., Drouin, P., Pierre, P., & Desrochers, P. (2005). *Estimation of the Relationships of Road Deterioration to Traffic and Weather in Canada*. http://www.bv.transports.gouv.qc.ca/mono/0965375.pdf

Feyyisa, J. L., Daniels, J. L., & Pando, M. A. (2017). Contact Angle Measurements for Use in Specifying Organosilane-Modified Coal Combustion Fly Ash. *Journal of Materials in Civil Engineering*, *29*(9). https://doi.org/10.1061/(asce)mt.1943-5533.0001943

Feyyisa, J. L., Daniels, J. L., Pando, M. A., & Ogunro, V. O. (2019). Relationship between breakthrough pressure and contact angle for organo-silane treated coal fly ash. *Environmental Technology and Innovation*, *14*. https://doi.org/10.1016/j.eti.2019.100332

Fink, D. H. (1970). Water Repellency and Infiltration Resistance of Organic-Film-Coated Soils. *Soil Science Society of America Journal*, *34*(2), 189–194. https://doi.org/10.2136/SSSAJ1970.03615995003400020007X

Fink, D. H., & Myers, L. E. (1969). *Synthetic Hydrophobic Soils for Harvesting Precipitation*.

Keatts, M. I., Daniels, J. L., Langley, W. G., Pando, M. A., & Ogunro, V. O. (2018). Apparent Contact Angle and Water Entry Head Measurements for Organo-Silane Modified Sand and Coal Fly Ash. *Journal of Geotechnical and Geoenvironmental Engineering*, *144*(6). https://doi.org/10.1061/(ASCE)GT.1943-5606.0001887

Khanzadeh Moradllo, M., Sudbrink, B., & Ley, M. T. (2016). Determining the effective service life of silane treatments in concrete bridge decks. *Construction and Building Materials*, *116*, 121–127. https://doi.org/10.1016/J.CONBUILDMAT.2016.04.132

King, P. M. (1981). Comparison of methods for measuring severity of water repellence of sandy soils and assessment of some factors that affect its measurement. *Australian Journal of Soil Research*, *19*(3). https://doi.org/10.1071/SR9810275

Lambe, T. William. (1951). *Soil testing for engineers.* Wiley.

LAMBE TW, KAPLAR CW, & LAMBIE TJ. (1969). EFFECT OF MINERALOGICAL COMPOSITION OF FINES ON FROST SUSCEPTIBILITY OF SOILS. *U S Engr Dept-Cold Regions Research & Eng Laboratory-Tech Report 207*.

Lee, C., Yang, H.-J., Yun, T. S., Choi, Y., & Yang, S. (2015). Water-Entry Pressure and Friction Angle in an Artificially Synthesized Water-Repellent Silty Soil. *Vadose Zone Journal*, *14*(4). https://doi.org/10.2136/vzj2014.08.0106

Leelamanie, D. A. L., Karube, J., & Yoshida, A. (2008). Characterizing water repellency indices: Contact angle and water drop penetration time of hydrophobized sand. *Soil Science and Plant Nutrition*, *54*(2). https://doi.org/10.1111/j.1747-0765.2007.00232.x

Letey, J., Carrillo, M. L. K., & Pang, X. P. (2000). Approaches to characterize the degree of water repellency. *Journal of Hydrology*, *231–232*. https://doi.org/10.1016/S0022-1694(00)00183-9

Lin, H., Lourenço, S. D. N., Yao, T., Zhou, Z., Yeung, A. T., Hallett, P. D., Paton, G. I., Shih, K., Hau, B. C. H., & Cheuk, J. (2019). Imparting water repellency in completely decomposed granite with Tung oil. *Journal of Cleaner Production*, *230*, 1316–1328. https://doi.org/10.1016/J.JCLEPRO.2019.05.032

Lourenço, S. D. N., Saulick, Y., Zheng, S., Kang, H., Liu, D., Lin, H., & Yao, T. (2018). Soil wettability in ground engineering: fundamentals, methods, and applications. In *Acta Geotechnica* (Vol. 13, Issue 1). Springer Verlag. https://doi.org/10.1007/s11440-017-0570-0

Mahedi, M., Satvati, S., Cetin, B., & Daniels, J. L. (2020a). Chemically Induced Water Repellency and the Freeze–Thaw Durability of Soils. *Journal of Cold Regions Engineering*, *34*(3), 04020017. https://doi.org/10.1061/(ASCE)CR.1943-5495.0000223

Mahedi, M., Satvati, S., Cetin, B., & Daniels, J. L. (2020b). Chemically Induced Water Repellency and the Freeze–Thaw Durability of Soils. *Journal of Cold Regions Engineering*, *34*(3), 04020017. https://doi.org/10.1061/(ASCE)CR.1943-5495.0000223

Oluyemi-Ayibiowu, B. D., & Uduebor, M. A. (2019). Effect of Compactive Effort on Compaction Characteristics of Lateritic Soil Stabilized With Terrasil. *Journal of Multidisciplinary Engineering Science Studies (JMESS)*, *5*(2), 2458–2925. www.jmess.org

Quinton, J., Thomsen, L., & Dastoor, P. (1997). Adsorption of Organosilanes on Iron and Aluminium Oxide Surfaces. In *SURFACE AND INTERFACE ANALYSIS* (Vol. 25).

Roy, W. R. *., Krapac, I. G. *., Chou, S.-F. J. *., & Griffin, R. A. (1992). Technical Resource Document: batch-type procedures for estimating soil adsorption of chemicals. In *Report* (Issue 87).

Saulick, Y., Lourenço, S. D. N., Baudet, B. A., Woche, S. K., & Bachmann, J. (2018). Physical properties controlling water repellency in synthesized granular solids. *European Journal of Soil Science*, *69*(4), 698–709. https://doi.org/10.1111/EJSS.12555

Uduebor, M., Adeyanju, E., Saulick, Y., Daniels, J., & Cetin, B. (2022). A Review of Innovative Frost Heave Mitigation Techniques for Road Pavements. *International Conference on Transportation and Development 2022*. https://doi.org/10.1061/9780784484357

Uduebor, M., Adeyanju, E., Saulick, Y., Daniels, J., & Cetin, B. (2023). Engineered Water Repellency for Moisture Control in Airport Pavement Soils. *Airfield and Highway Pavements 2023*, 92–102. https://doi.org/10.1061/9780784484906.009

Uduebor, M., Daniels, J., Mohammad, N., & Cetin, B. (2022). *Engineered Water Repellency in Frost Susceptible Soils*. 457–466. https://doi.org/10.1061/9780784484012.047

Uduebor, M., Daniels, J., Naqvi, M. W., & Cetin, B. (2022). *Engineered Water Repellency in Frost Susceptible Soils*. 457–466. https://doi.org/10.1061/9780784484012.047

U.S. Army Corps of Engineers. (1965). Soils and geology- Pavement design for frost conditions. *Department of the Army Courses Department of Civil Engineering, University of New Technical Manual TM 5-818-2*.

Wasif Naqvi, M., Sadiq, Md. F., Cetin, B., Uduebor, M., & Daniels, J. (2022). Investigating the Frost Action in Soils. *Geo-Congress 2022*, 257–267. https://doi.org/10.1061/9780784484067.027--

Yuan, G., Che, A., & Tang, H. (2021). Evaluation of soil damage degree under freeze–thaw cycles through electrical measurements. *Engineering Geology*, *293*, 106297. https://doi.org/10.1016/J.ENGGEO.2021.106297

ARTICLE 2: EFFECT OF GRAIN SIZE ON BEHAVIOR AND PERFORMANCE OF WATER-REPELLENT SOILS

ABSTRACT

Water-repellent soils are being used in engineering applications. Their behavior and performance are largely governed by the grain size properties of the soils regardless of treatment. This study explores the effect of grain and pore size on water repellency to improve performance. Soils, collected from different locations in the United States as well as glass beads were treated with a commercially available organosilane. Various tests were performed to assess the level of water repellency imparted to the soils and their performance. The results revealed that the water-repellency treatment was effective, with contact angles ranging from 119.5^{o} to 148.5^{o}. The contact angle decreased with increasing grain size, while the surface roughness increased the contact angle. Water drop penetration test results showed no recorded penetration even after 2 hours (7200s), regardless of grain size. Breakthrough pressure values ranged from 0.1kPa to 2kPa, decreasing with increasing grain size. This study shows that water-repellent soils can help achieve a sustainable low-carbon future by reducing road pavement damage caused by moisture-related distress. It is however important to consider the effect of grain size and porosity on the performance of water-repellent soils before use in pavement construction.

Keywords:

Pavements, Engineered Water Repellency, Carbon Emissions, Soils, Hydrophobicity, Maintenance, Breakthrough Pressure

1. Introduction

Soil water repellency, also known as soil hydrophobicity, refers to the phenomenon where certain organic compounds coat soil particles, causing them to repel water. This results in a decreased affinity to water, impeding wetting for durations ranging from seconds to hours (Doerr, Shakesby, and Walsh 2000). Naturally occurring water repellency in some organic soils has been discussed in the fields of agriculture and soil science for a long time (Bonanomi et al. 2016; Capriel et al. 1995; Dymov, Milanovskii, and Kholodov 2015). It has also been found to negatively affect plant growth, reduce infiltration capacity, accelerate soil erosion, and cause preferential flow in soils in the field of soil science (Dekker et al. 2009; Imeson et al. 1992; Ritsema et al. 1993; 1997; Shakesby et al. 1993). However, recent studies have demonstrated the benefits of water repellency in civil engineering applications, such as improving the freeze-thaw durability of pavements, leachate barriers, surface protection, slope protection, and coal combustion residual management (Mahedi et al. 2020; Bardet, Jesmani, and Jabbari 2015; DeBano 1981; Dumenu et al. 2017; Feyyisa, Daniels, and Pando 2017; Oluyemi-Ayibiowu and Uduebor 2019).Water repellency offers an effective solution for preventing frost-heaving-related damage in foundations, concrete slabs, and basement walls by limiting water migration, with the potential to reduce both energy consumption and CO_2 emissions. By reducing the need for frequent maintenance and new construction, soil water repellency can lower the demand for raw materials and energy-intensive production processes, ultimately contributing to a more sustainable construction with a significantly lower carbon footprint. In addition, adjusting the water repellency of soil can create an impermeable or semi-

permeable seepage barrier, suitable for various engineering applications (Daniels 2020; Daniels and Hourani 2009; Lin et al. 2019; Uduebor, Daniels, Mohammad, et al. 2022).

Soil water repellency can be achieved by treating the soil with natural or synthetic water-repellent substances. Natural water repellency has been observed in soils exposed to wildfires and the presence of organic materials. On the other hand, synthetic substances like wax coatings, Tung Oil, Paraffin Oils, and Silanes have been used to engineer water repellency in soils (Bardet, Jesmani, and Jabbari 2014; Chan and Lourenço 2016; Ng and Lourenço 2016). Silanes and siloxanes are very effective in making soils hydrophobic, with studies showing that adding 2.5% or less by mass can induce water repellency (Brooks et al. 2022; Y. Choi et al. 2016; Uduebor, Daniels, Naqvi, et al. 2022).

An accurate assessment of the effectiveness of various treatment methods for inducing soil water repellency is essential. Various methods are available for measuring water repellency in soil, including the Contact Angle (CA) test, the Capillary Rise Method (CRM), the intrinsic sorptivity test, the molarity of an ethanol droplet test (MED), and the Water Drop Penetration Time Test (WDPT) (Hallett, Baumgartl, and Young 2001; Bachmann, Ellies, and Hartge 2000; Bachmann et al. 2003; Schulte, Culligan, and Germaine 2007; King 1981; Dekker et al. 2009). Among these methods, the CA test using the sessile drop method with a Goniometer and the WDPT are commonly used due to their simplicity and versatility (Bachmann, Ellies, and Hartge 2000; Diehl and Schaumann 2007; Feyyisa, Daniels, and Pando 2017; Keatts et al. 2018; Lee et al. 2015; Letey, Carrillo, and Pang 2000; Liu et al. 2012). The contact angle measurement is based on Young's equation (Equation 1), which describes the equilibrium of a water drop on a solid surface with three interfacial tensions, solid-air, solid-liquid, and liquid-air.

$$cos\theta = \frac{\gamma_{sa} - \gamma_{al}}{\gamma_{la}}$$ - Equation 1

Where γ_{sa} is the tension force between solid and air, γ_{al} is that between air and liquid and γ_{la} is the tension between liquid and air (Figure 2-1).

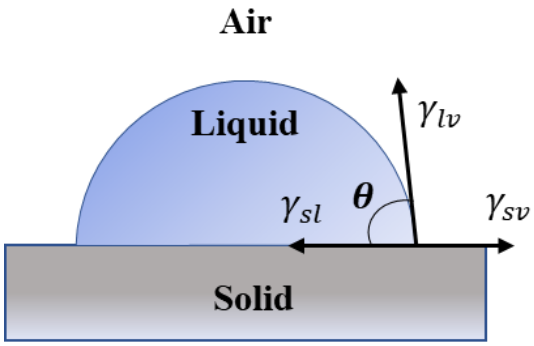

Figure 2-1 Schematic of Water Drop Showing Solid Liquid Air Interface

A CA value greater than 90° indicates low wettability or water repellency, while a CA value less than 90° indicates high wettability (Goebel et al. 2011). Among the various methods available for determining the contact angle, the Sessile Drop Method (SDM) is preferred due to its ability to directly measure the contact angle at the solid-liquid-vapor interface, providing a reliable estimate of soil wettability. All the contact angle measurement methods have their flaws and drawbacks including multiple and varying CA values, swelling of the soil sample when immersed, and irregularity of the tested soil surface aside from user error (Y. Saulick, Lourenço, and Baudet 2017). Advancements have been made to ensure repeatability, including testing uniform-grained samples (Y. Choi et al. 2016), employing semi-automated techniques (Y. Saulick, Lourenço, and Baudet 2017), and automating the test procedure using defined drop volumes, height, and plane thickness. Despite these advancements, most studies have carried out tests only on

uniform soil grains or materials, which do not represent the real composition of the soil, as it is made up of different particle sizes. Saulick et al. (2016) reported that finer materials exhibit a greater contact angle than coarse granular materials. The SDM procedure only tests the fine-grained portion of the soil that is usually left on the double-sided tape after sample preparation and does not necessarily represent the bulk mass. This can provide an erroneous value of the contact angle, particularly for soils where the fines are little and do not affect the overall soil characteristics. Therefore, there is a need to estimate the contact angle of the bulk soil mass based on the values of the individual grains of the soil sample.

In this study, an experimental program was carried out to understand the relationship between grain size and the water-repellent properties and behavior of soils.

2. Materials and Methods

2.1 Materials

Sand and fine-size glass beads and four naturally occurring frost-susceptible soils were chosen, including loess from Iowa (IA-PC), as well as silt from New Hampshire (NH-HS), North Carolina (NC-BO), and Alaska (AK-FB). Glass beads (GB) made of silica oxide (soda lime, type S) in various grain sizes were obtained from Carl Stuart Ltd. in Dublin, Ireland. The glass beads were proportioned to model an average grain size of all four soils and provide an idealized particle size distribution. The natural soils were selected even though they are non-homogenous and prone to large variations because they provide real results that can be expected and compared to field conditions and predictions. The soils

were oven-dried and sieved through the #4 Sieve. This was done to remove gravelly soil fractions and prevent variations in the sample specimens. Contact angle measurements are difficult to obtain from gravel-sized particles and the large pore space between them makes it unlikely that making the particles water-repellent will result in any meaningful hindrance to the flow of water through them.

Figure 2-2 Soils and Glass Beads Utilized in this Study; AK-FB, IA-PC, NC-BO, NH-HS, and GB (Uduebor et al., 2023)

2.1.1 Water Repellent Chemical

Commercially available IE6683 from Dow Corning was utilized for the treatment of the soil samples. It is a water-based silane-siloxane emulsion blend with 40% active ingredients (alkoxysilane and polydimethylsiloxane) by weight. It has been used in previous research carried out by (Brooks et al. 2022; Feyyisa, Daniels, and Pando 2017; Keatts et al. 2018; Uduebor, Daniels, Mohammad, et al. 2022). Silanes provide a very stable -Si-O- bond to the surface of soil particles by the reaction of a silicon hydride (-Si-H) with water to yield a reactive silanol (-Si-OH). Alkoxysilanes have the added benefit of coupling organic polymers to inorganic materials providing increased adhesion of the water-repellent molecule and improved surface modification (Arkles et al. 1992) Siloxanes

have the added benefit of an extra silicon atom. This significantly improves its resistance to oxidation, and UV exposure and prevents any biodegradation (Ley et al., 2015)

2.1.2 Characterization

Table 1 presents a summary of the index properties of the soils utilized in this study. Specific gravity was carried out according to ASTM D854 and ranged from 2.65 to 2.80. The particle size distribution was determined in accordance with (ASTM D7928 and showed betweeen 38 to 98% passing through the #200 sieve. The soils were majorly Silty Sand, Silts, or Lean Clays. Atterberg limits tests; plastic limit (PL) and liquid limit (LL), were performed in accordance with ASTM D4318. Soils had a liquid limit ranging from 33% to 42%. All the soils were non-plastic (NP) except the Pottawatomie County (Iowa) Soil which had a plastic limit of 23%.

Table 2- 2 Summary of Soil Index Properties and Classifications (Uduebor et al., 2023)

Soil Property	**SOIL**			
	AK-FB	**IA-PC**	**NC-BO**	**NH-HS**
Specific Gravity, Gs	2.67	2.74	2.67	2.68
% Passing #4 Sieve (4.75 mm)	97.6	100	95.32	79.8
% Passing #10 Sieve (2mm)	96.0	99.8	91.84	74.18
% Passing #40 Sieve (0.425 mm)	93.4	99.6	86.88	52.69
% Passing #200 Sieve (0.075 mm)	84.5	98.4	38.88	42.41
Silt content (%) (75μm–2μm)	75.65	86.67	34.31	37.52
Clay content (%) (< 2μm)	8.87	11.69	4.57	4.88
USCS Classification	ML	CL	SM/SC	ML
AASHTO Classification	A-5	A-6	A-4	A-4
Frost Susceptibility Classification	F4	F3	F3	F4

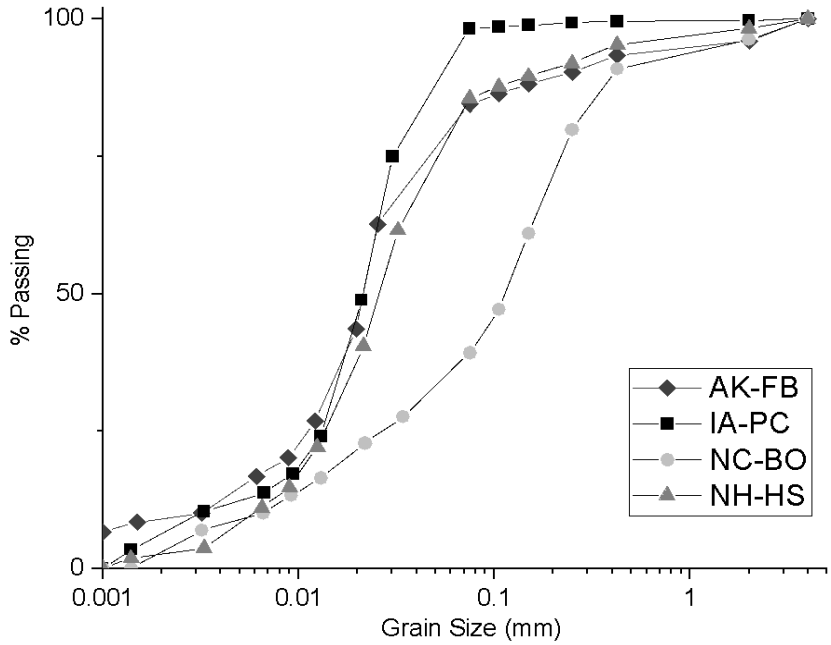

Figure 2- 3 Grain Size Distribution of Soils (Uduebor et al., 2023)

2.2 Methods

2.2.1 Treatment

A uniform dosage concentration ratio of 1:10 (OS: Soil, batched by weight) was selected for surface modification of the soil sample because it has been proven to induce sufficient water repellency in soils (Brooks et al. 2022; Uduebor, Daniels, Mohammad, et al. 2022). The OS was first dissolved with deionized water (~1µs/cm) and mixed with the soil to achieve a liquid-to-solid (L/S) of 2, ensuring complete saturation of the soil. This means for a 200g sample of soil, 20g of OS was mixed with water to make up 400mL utilized to treat the soil. The mixing was done in a 1000mL HDPE bottle mounted on a rotary tumbler to react for 24 hours. Studies carried out by Uduebor et al. (2022) have shown there is sufficient treatment even after 0.25 hours. At the end of the reaction time,

the mixture was allowed to settle and then decanted. Excess OS within the mixture was washed out by adding DI water and agitating the bottle repeatedly and decanting after settling until the OS concentration was negligible. The resulting residue from the washing and decanting was split into two portions, one for air drying and the other for oven drying. The air-dried sample was placed in a fume cupboard in the laboratory with temperature and humidity at a relatively stable value of 22-24^{o}C and 40-45% respectively. Oven drying was done using a small lab oven at 60^{o}C. Samples were dried till there was no further weight loss. Oven-dried samples were stored in a desiccator to cool down before testing.

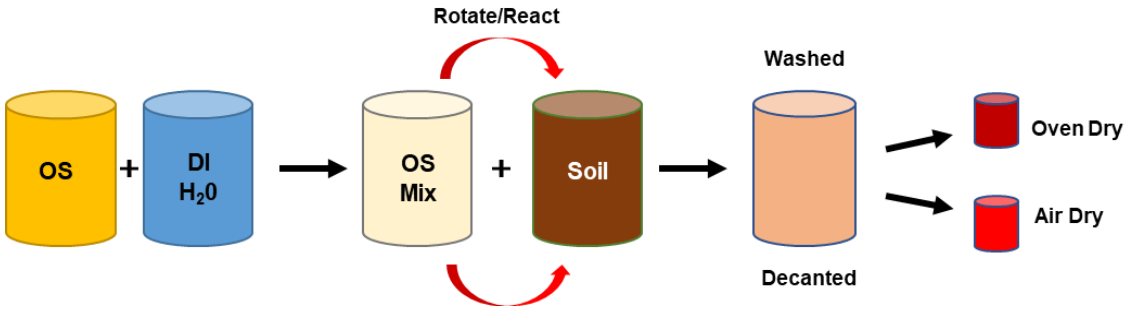

Figure 2- 4 Schematic Showing Treatment Procedure (Uduebor et al., 2023)

2.2.2 Contact Angle Test

Assessment of the water repellency of treated samples was carried out using the Sessile Drop Method (SDM) using a static measurement. Air and oven-dried samples were placed in a mortar and any agglomerations were broken up with the aid of a rubber end pestle. Where required, the soil sample was passed through sieves to provide a uniform range and test surface. A double-sided adhesive tape was affixed to a glass slide and the treated soil was placed on the other end with the aid of a spatula. A slight weight of about 100g was placed on the soil for about 2 minutes after which the excess loose material

unattached to the tape was removed by flipping it and lightly tapping the sides of the glass slide. This process was repeated until there was full coverage of a monolayer of treated material over the surface of the adhesive tape.

The glass slide was placed on a goniometer and a water droplet was tittered to the surface of the soil using a Flow-Trac II, set with a predetermined flow rate of 0.0095l/s. Contact angle measurements were taken by capturing the water-soil-air interface for 10s with images taken at 1s intervals which were analyzed using the drop image analysis software, ASDA. To ensure consistency of results, the drop size was advanced as described in (Feyyisa, Daniels, and Pando 2017), until the contact radius reached equilibrium resulting in a constant angle measurement. Duplicate specimens were tested for each sample to evaluate variability in the results obtained.

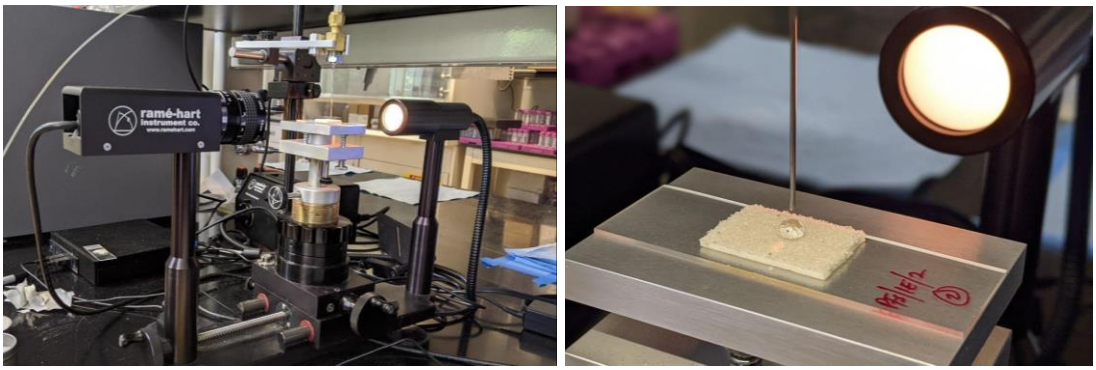

Figure 2- 5 (a) Goniometer for Measuring Contact Angle (b) Water Drop on Test Sample (Uduebor et al., 2023)

For aspects of the tests where sieving was required, the soils were passed through a set of sieves (#10, #16, #20, #40, #60, #80, #100, #160, #200) and the mass retained on

each sieve, stored separately for testing. Studies have asserted that uniform soil grains for the test make for a better, repeatable test. (Choi et al., 2016).

Figure 2- 6 Sieved Soil Sample (NC-BO) Showing different grain sizes. (Uduebor et al., 2023)

2.2.3 Water Drop Penetration Test

The water drop penetration time (WDPT) method measures the degree of soil water repellency by evaluating the infiltration rate of water droplets into the soil (Letey, Carrillo, and Pang 2000). The Water Drop Penetration Time (WDPT) test involves placing water drops on the surface of an exposed surface of the soil with subsequent measurement of the time taken to infiltrate into the soil. Usually, an average is taken over some drops (typically three) and the mean is utilized in determining the degree of water repellency based on a given classification (King 1981; Liu et al. 2012). In this study, about 20g samples of the air-dried soil material were measured into a can and three drops of deionized water (50 ± 1 μL) were measured on the surface of the soil with a pipette. The time taken to complete the penetration of the water droplet was recorded with a timecode stamp to determine the time interval.

.

2.2.4 Breakthrough Head Tests

Breakthrough head tests were carried out to determine the water-repellent performance of a range of grain sizes. The samples were first dried in a desiccator until there was no further change in the mass of the samples. 100g of treated samples were compacted within a rigid walled tube lined with a rubber membrane for support and placed on a porous stone upon the base of the triaxial cell. O-rings were placed with an O-ring expander to seal the membrane to the base and the top cap. The cell was set up and filled with distilled water and a confining pressure was applied while the valve to the top cap remains open to allow the outflow of excess air from the sample within the membrane. An initial "flushing" pressure (0.5kPa) is applied through the base of the setup using a FLOWTRAC II (Geocomp) to ensure there is no air trapped between the porous stones and the sample. A "back pressure of 0.1kPa was applied to the sample using the FLOWTRAC II and kept constant for 5 minutes and the volume of water flowing into the specimen was measured. The pressure was incrementally increased at 0.1 kPa intervals till 1kPa and at 1kPa intervals till the breakthrough volume was reached. A breakthrough volume of 0.1cc (cm^3) was utilized for this test. The test was ended after breakthrough has occurred within the sample.

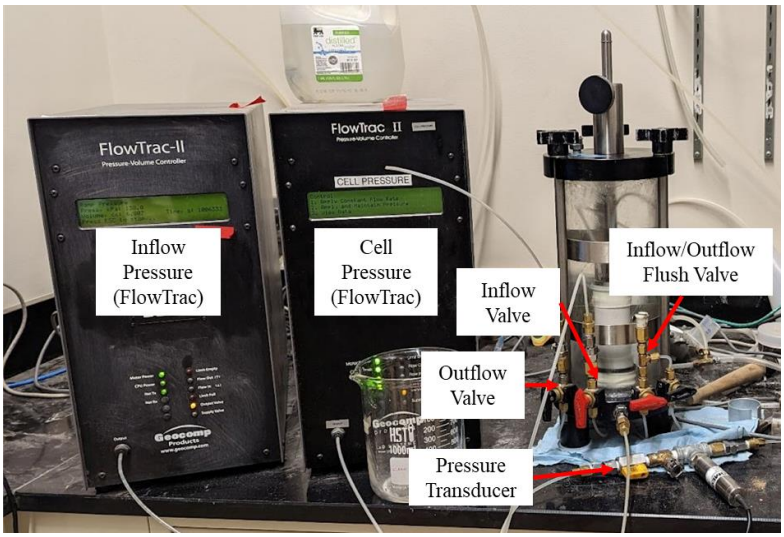

Figure 2- 7 Setup for Breakthrough Test (Uduebor et al., 2023)

3. Results and Discussion

3.1 Contact Angle Test

3.1.1 Contact Angle Using Bulk Mass.

Results from Contact Angle tests carried out using the bulk soil mass are given in Fig 2-8 below. Water repellency treatment was effective with contact angles ranging from 119.5^{o} to 148.5^{o}. Based on the classification from (Goebel et al. 2011; McHale, Newton, and Shirtcliffe 2005), the soils can be considered hydrophobic (>90^{o}) and close to superhydrophobicity (150^{o}). Treated NC-BO soil can be classified as superhydrophobic. There was a slight increase in the CA values of the oven-dried soil. This can be attributed to the hygroscopic nature of the fine-grained portion of the soil. Oven-dried CA values represent the maximum possible CA of the treated soil sample for that dosage concentration while air-dried CA values are more representative of obtainable values after sufficient drying in the field (Uduebor, Daniels, Naqvi, et al. 2022). It must also be noted that values

obtained from the contact angle tests are not the maximum CA possible for the treated soil. Johnson & Dettre, 1964 analyzed water-repellent treated heterogeneous surfaces and reported that a constant contact angle was obtainable after over 40% of the total surface area has been made non-wettable. Therefore, increasing OS concentration will impact the performance of the treated material and not necessarily its contact angle as more surfaces of the material will be made non-wettable.

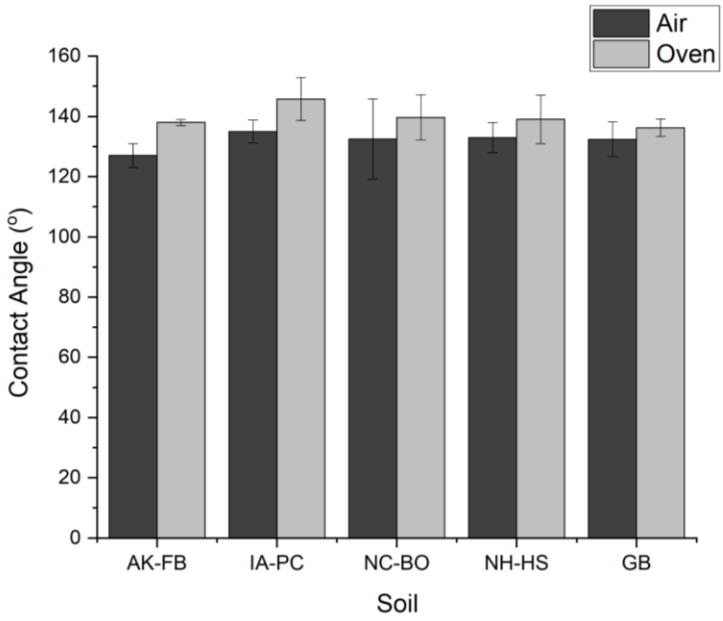

Figure 2- 8 Contact Angle for different soils treated with organosilane (1:10, OS: Soil) (Uduebor et al., 2023)

3.1.2 Contact Angle with Grain Size

Results of contact angle measurements of sieved grain sizes indicate a reduction in CA values with increasing grain size Fig 2-9a-e. This is due to a decrease in the treated total surface area. Finer-grained soils have a larger specific surface area than coarse-grained particles. Also, as grain sizes get coarser or rougher the contact angle also

increases. This is noticeable in all soil particles except glass beads which have a uniform spherical shape and no rough edges. This marked increase in surface roughness has also been observed in previous studies carried out by (Yunesh Saulick, Lourenço, and Baudet 2016). This marked increase is noticeable around ~1mm. It is therefore important to note that no singular grain size is sufficient to characterize the CA of the bulk mass. Hence it is imperative to have a good knowledge of the grain size distribution of the soil mass and the relative effect of the major and minor constituents and their properties on the CA of the bulk mass. For example, soil with less than 5% fines if mounted for the CA test could give higher contact angle values from the fines that may not be representative of the CA of the bulk mass.

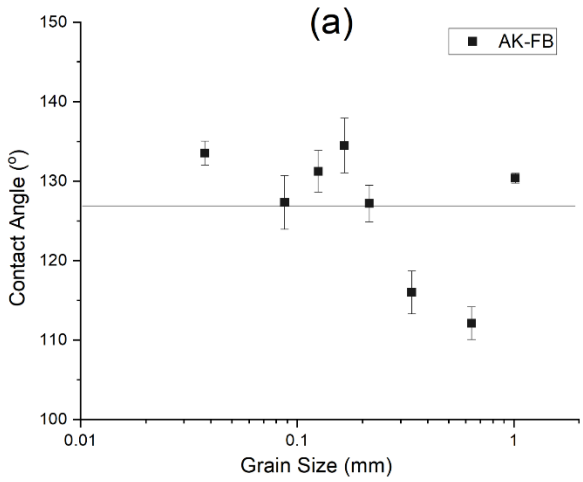

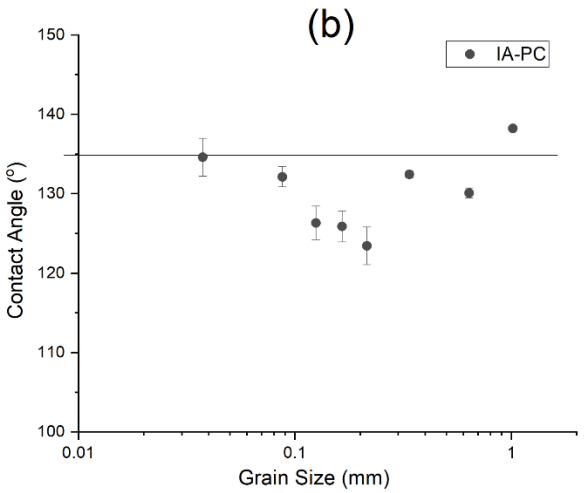
(b)
IA-PC
Contact Angle (°)
Grain Size (mm)
150
140
130
120
110
100
0.01
0.1
1

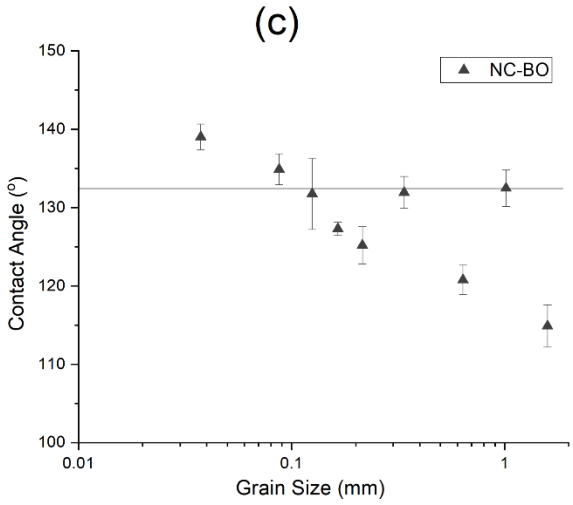
(c)
NC-BO
Contact Angle (°)
Grain Size (mm)
150
140
130
120
110
100
0.01
0.1
1

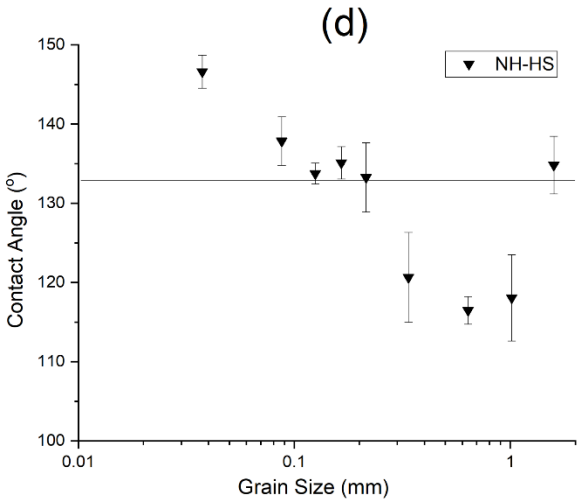
(d)
NH-HS
Contact Angle (°)
Grain Size (mm)
150
140
130
120
110
100
0.01
0.1
1

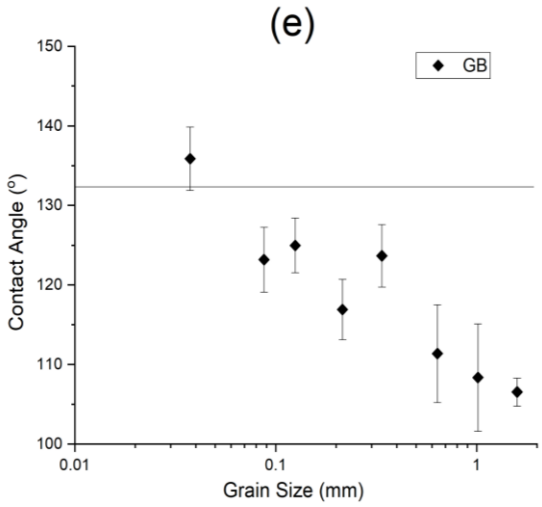

Figure 2- 9 Contact Angles with Respect to Average Grain Size for Treated Soil Samples (lines show the Contact Angle of Bulk Mass) (Uduebor et al., 2023)

3.1.3 Normalized Contact Angle with grain size

A normalized graph plot of the CA results is given in Fig 2-10 below. The maximum obtained CA is given a value of 1 and the other values are expressed as a fraction of the maximum value. It can be observed minimum CA values obtained are within 0.8 - 0.9 of the maximum value. This could form a standardized factor of safety for expressing CA values obtained using fine grains from the bulk mass only. Results obtained using bulk mass can be multiplied by 0.8 to give a range of values or utilized as a safe value for calculations.

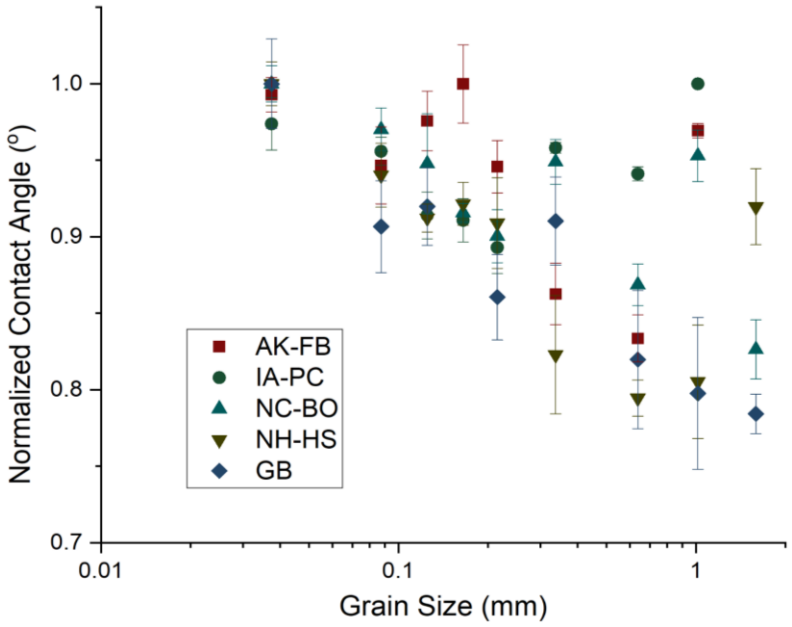

Figure 2- 10 Normalized Contact Angle Values with Respect to Grain Size (Uduebor et al., 2023)

3.2 Water Drop Penetration Test

All untreated soil samples had instantaneous penetration (<1s), except AKFB (~128s) and GB (~2s). AKFB possesses some humic properties that give it a pseudo-water-repellency that disappears after mixing with water, while the water droplet lagged before infiltrating into the glass bead sample. All treated samples did not get any infiltration, regardless of grain size, and penetration was not recorded even after 2 hours (7200s). This indicates that the surface of each particle was sufficiently treated and water-repellent regardless of particle size.

3.3 Breakthrough Pressure Test

As versatile as the contact angle and water drop penetration test time are, they only provide an empirical estimation of what the performance of the treated soil as a barrier will be. In many cases, other factors like densification, fluid type, and viscosity play an

important role in determining the performance of water-repellent soils. The breakthrough pressure tests result is shown in Fig 2-11 below. There is a noticeable decrease in the breakthrough pressure values with an increase in the grain size of the samples.

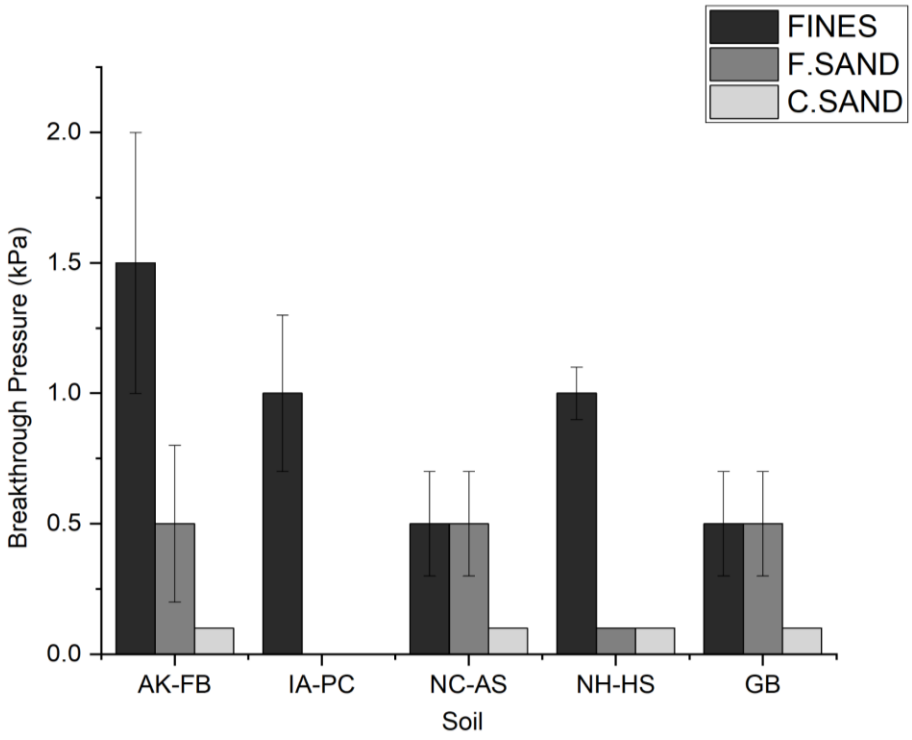

Figure 2- 11 Breakthrough Pressure Test Results (Uduebor et al., 2023)

This reveals the impact of pore size openings on the ability of treated water-repellent soil to sustain a hydrostatic head. While the particle surfaces themselves are water-repellent, as confirmed by the WDPT tests, the pore spaces are open, and their size ultimately determines the infiltration of water into the soil.

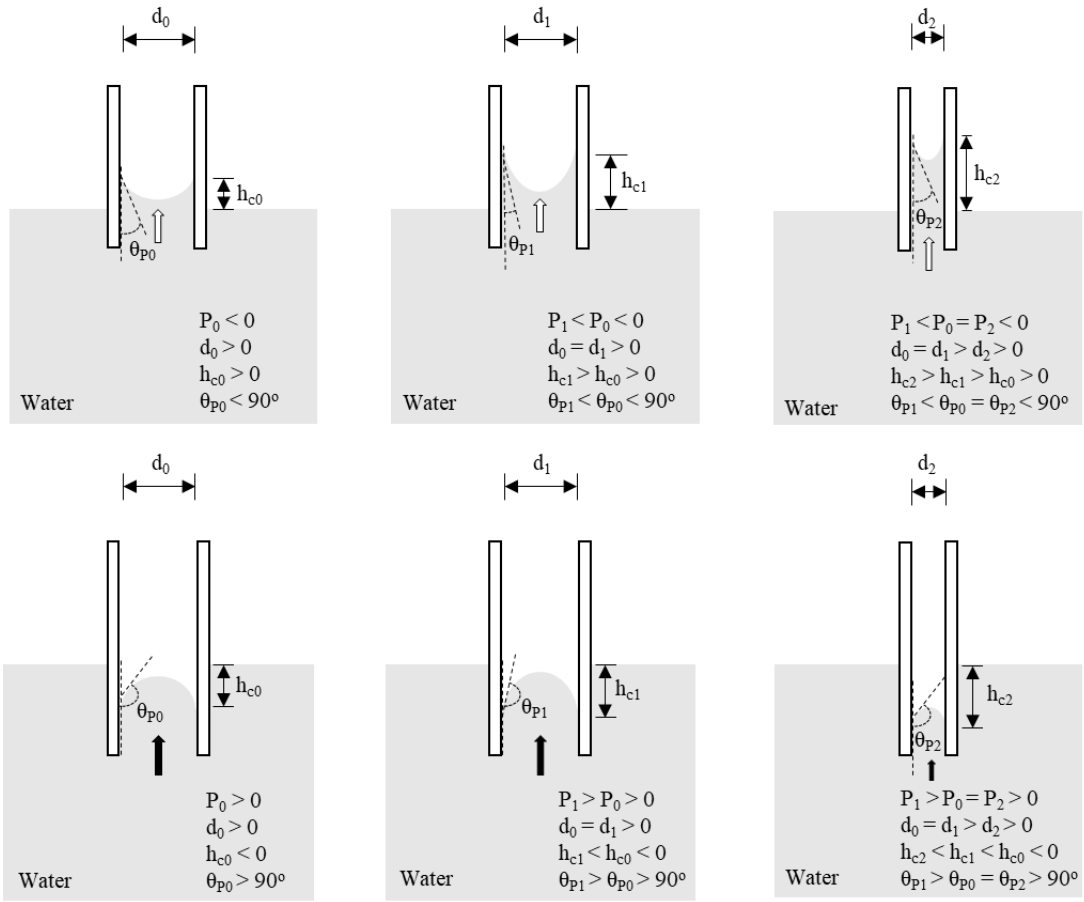

Figure 2- 12 Idealized Sketch of The Difference in Capillary Rise in Hydrophilic and Hydrophobic Pore Spaces (Uduebor et al., 2023)

Figure 2-12 shows an idealized sketch of the difference in the capillary rise in hydrophilic and hydrophobic pore spaces and the effect of changing pore diameter. For a hydrophilic pore, with a contact angle, $\theta_{P0} < 90^o$, the capillary rise within it can be increased by increasing the wettability (reducing the contact angle, $\theta_{P1} < \theta_{P0} < 90^o$) of the surface at a similar pore diameter ($d_1 = d_0 > 0$), or by decreasing the pore diameter, ($d_0 > d_2 > 0$), at the same degree of wettability ($\theta_{P0} = \theta_{P2} < 90^o$). Alternatively, for the hydrophobic pore, increasing the contact angle reduces the capillary rise ($\theta_{P1} > \theta_{P0} > 90^o$) at a similar pore diameter and a corresponding decrease is achieved at the same degree of hydrophobicity

by reducing the pore size. This reveals that at a uniform level of hydrophobicity of soil particles, the breakthrough pressure is dependent on the size of the pore space openings. Smaller openings will result in higher breakthrough pressure values and vice versa (Fig 11.)

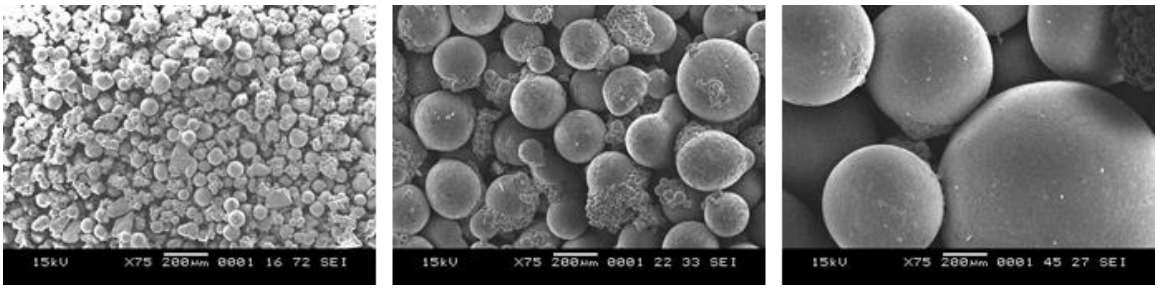

Figure 2- 13 SEM images (at x75 Magnification) of glass beads showing the various particle sizes and their pore space openings (a.) Fines (b.) Fine Sand, (c.) Coarse Sand (Uduebor et al., 2023)

4. Conclusion

Engineering Water Repellency in soils is a sustainable solution to mitigating moisture-related problems, particularly in road pavements where moisture conditions can be kept uniform, allowing for better design, and long-term performance, saving construction and maintenance costs, and reducing global warming. This innovative technology requires the right knowledge and testing protocols to assess both its efficacy and performance, particularly in soils where treatment results vary for different soil grains and types within a soil mass due to mineralogy, size, and surface area. The conclusions from this study are summarized in the points below.

1. Conventional tests like the Sessile Drop Method (Contact Angle) tests developed in soil science are more suited for uniform-sized material to obtain repeatable and

reliable results. Engineering soil is a mixture of different grain-sized materials; hence it is important to consider the effect of the treatment of each grain size type in determining the overall contact angle for the soil. Test carried out indicates higher contact values are obtained for the finer-grained portion of the soils and gradually reduce with an increase in grain size (up to 20% decrease).

2. There is also a marked increase with increase in surface roughness (noticeable after a certain grain size of ~1mm). Therefore, contact angle determination for civil engineering applications should be given either as a range of values or as the least observable measurement based on individual particle size or surface characteristics. Contact angle measurements should be determined for major soil constituents, particularly grain sizes greater than 10%, as they affect the overall contact angle of the bulk soil mass.

3. While Contact Angle tests are simple and useful ways of determining the efficacy of water-repellent treatment, it does not give any behavioral or performance information useful to the engineer. Breakthrough Pressure tests provide a measure of the ability of the treated soil to sustain a hydrostatic head. Test results indicate that there is a higher breakthrough pressure for finer-grained soil compared to soils with larger grain sizes. This is due to the reduced pore space within them that limits the transport of moisture through the water-repellent soil.

4. There is a strong correlation between the pore size of the treated soil compared to the breakthrough pressure with an inverse relationship between them.

REFERENCES

Arkles, B., J. R. Steinmetz, J. Zazyczny, and P. Mehta. 1992. “Factors Contributing to the Stability of Alkoxysilanes in Aqueous Solution.” *Journal of Adhesion Science and Technology* 6 (1): 193–206. https://doi.org/10.1163/156856192X00133.

ASTM D 854. 2002. “ASTM D854 Standard Test Methods for Specific Gravity of Soil Solids by Water Pycnometer.” *ASTM International* 04.

ASTM D7928. 2021. “Standard Test Method for Particle-Size Distribution (Gradation) of Fine-Grained Soils Using the Sedimentation (Hydrometer) Analysis.” *ASTM International*, no. May 2016.

ASTM D4318-17.” In *Standard Test Methods for Liquid Limit, Plastic Limit, and Plasticity Index of Soils*. *ASTM International*

Bachmann, J, A Ellies, and K H Hartge. 2000. “Development and Application of a New Sessile Drop Contact Angle Method to Assess Soil Water Repellency.” www.elsevier.com/locate/jhydrol.

Bachmann, J., S. K. Woche, M. O. Goebel, M. B. Kirkham, and R. Horton. 2003. “Extended Methodology for Determining Wetting Properties of Porous Media.” *Water Resources Research* 39 (12). https://doi.org/10.1029/2003WR002143.

Bardet, J. P., M. Jesmani, and N. Jabbari. 2014. “Permeability and Compressibility of Wax-Coated Sands.” *Geotechnique* 64 (5): 341–50. https://doi.org/10.1680/GEOT.13.P.118.

Blomberg, Timo, Jeff Barnes, Frédérick Bernard, P. Dewez, S. Le Clerc, M. Pfitzmann, and R. Taylor. 2011. “Life Cycle Inventory: Bitumen.” Brussels, Belgium.

Bonanomi, Giuliano, Salvatore A Gaglione, Vincenzo Antignani, and Gaspare Cesarano. 2016. “Unimodal Pattern of Soil Hydrophobicity along an Altitudinal Gradient Encompassing Mediterranean, Temperate, and Alpine Ecosystems.” *Plant and Soil* 409: 37–47. https://doi.org/10.1007/s11104-016-3020-0.

Brooks, Ty, S M Asce, John L Daniels, F Asce, ; Micheal Uduebor, Bora Cetin, M Asce, Mohammad Wasif Naqvi, and Ph D Student. 2022. “Engineered Water Repellency for Mitigating Frost Action in Iowa Soils,” March, 448–56. https://doi.org/10.1061/9780784484012.046.

Capriel, Peter, Theodor Beck, Heinz Borchert, Jörn Gronholz, and Günter Zachmann. 1995. “Hydrophobicity of the Organic Matter in Arable Soils.” *Soil Biology and Biochemistry* 27 (11): 1453–58. https://doi.org/10.1016/0038-0717(95)00068-P.

Chan, C. S.H., and S. D.N. Lourenço. 2016. “Comparison of Three Silane Compounds to Impart Water Repellency in an Industrial Sand.”

Https://Doi.Org/10.1680/Jgele.16.00097 6 (4): 263–66. https://doi.org/10.1680/JGELE.16.00097.

Choi, Jae ho. 2019. “Strategy for Reducing Carbon Dioxide Emissions from Maintenance and Rehabilitation of Highway Pavement.” *Journal of Cleaner Production* 209 (February): 88–100. https://doi.org/10.1016/J.JCLEPRO.2018.10.226.

Choi, Youngmin, Hyunwook Choo, Tae Sup Yun, Changho Lee, and Woojin Lee. 2016. “Engineering Characteristics of Chemically Treated Water-Repellent Kaolin.” *Materials* 9 (12). https://doi.org/10.3390/ma9120978.

Daniels, John L. 2020. “Engineered Water Repellency for Applications in Environmental Geotechnology.” *Lecture Notes in Civil Engineering* 89: 39–46. https://doi.org/10.1007/978-3-030-51350-4_6/COVER.

Daniels, John L, and Mimi S Hourani. 2009. “Soil Improvement with Organo-Silane.” In *U.S.-China Workshop on Ground Improvement Technologies 2009*, 217–24. American Society of Civil Engineers. https://doi.org/10.1061/41025(338)23.

DeBano, LF. 1981. *Water Repellent Soils: A State-of-the-Art*. https://books.google.com/books?hl=en&lr=&id=D_0TAAAAYAAJ&oi=fnd&pg=PA1&ots=SWVTEVJDWR&sig=vz2Yx4NP4Bzszu4B9xFLM6gkN6s.

Dekker, Louis W., Coen J. Ritsema, Klaas Oostindie, Demie Moore, and Jan G. Wesseling. 2009. “Methods for Determining Soil Water Repellency on Field-Moist Samples.” *Water Resources Research* 46 (4). https://doi.org/10.1029/2008WR007070.

Diehl, Doerte, and Gabriele E. Schaumann. 2007. “The Nature of Wetting on Urban Soil Samples: Wetting Kinetics and Evaporation Assessed from Sessile Drop Shape.” *Hydrological Processes* 21 (17). https://doi.org/10.1002/hyp.6745.

Doerr, S. H., R. A. Shakesby, and R. P.D. Walsh. 2000. “Soil Water Repellency: Its Causes, Characteristics and Hydro-Geomorphological Significance.” *Earth-Science Reviews* 51 (1–4): 33–65. https://doi.org/10.1016/S0012-8252(00)00011-8.

Dumenu, Livingstone, Miguel A. Pando, Vincent O. Ogunro, John L. Daniels, Merhab I. Moid, and Carlos Rodriguez. 2017. “Water Retention Characteristics of Compacted Coal Combustion Residuals,” March, 403–13. https://doi.org/10.1061/9780784480434.044.

Dymov, A., E. Milanovskii, and V.A. Kholodov. 2015. “Composition and Hydrophobic Properties of Organic Matter in the Densimetric Fractions of Soils from the Subpolar Urals. .” *Eurasian Soil Science* 48 (11): 1212–21. https://link.springer.com/content/pdf/10.1134/S1064229315110058.pdf.

Espinoza, Marianela, Noelia Campos, Rebekah Yang, Hasan Ozer, José P Aguiar-Moya, Alejandra Baldi, Luis G Loría-Salazar, and Imad L Al-Qadi. 2019. “Carbon

Footprint Estimation in Road Construction: La Abundancia-Florencia Case Study." *Sustainability (Switzerland)* 11 (8): 1–13. https://doi.org/10.3390/su11082276.

Feyyisa, Jenberu L., John L. Daniels, and Miguel A. Pando. 2017. "Contact Angle Measurements for Use in Specifying Organosilane-Modified Coal Combustion Fly Ash." *Journal of Materials in Civil Engineering* 29 (9). https://doi.org/10.1061/(asce)mt.1943-5533.0001943.

France-Mensah, Jojo, and William J O'brien. 2019. "Developing a Sustainable Pavement Management Plan: Tradeoffs in Road Condition, User Costs, and Greenhouse Gas Emissions." *Journal of Management in Engineering* 35 (3). https://doi.org/10.1061/(ASCE)ME.1943-5479.0000686.

Goebel, Marc O., Jörg Bachmann, Markus Reichstein, Ivan A. Janssens, and Georg Guggenberger. 2011. "Soil Water Repellency and Its Implications for Organic Matter Decomposition – Is There a Link to Extreme Climatic Events?" *Global Change Biology* 17 (8): 2640–56. https://doi.org/10.1111/J.1365-2486.2011.02414.X.

Hallett, P.D., T. Baumgartl, and I.M. Young. 2001. "Subcritical Water Repellency of Aggregates from a Range of Soil Management Practices." *Soil Science Society of America Journal* 65 (1): 184–90. https://doi.org/10.2136/SSSAJ2001.651184X.

Imeson, A. C., J. M. Verstraten, E. J. van Mulligen, and J. Sevink. 1992. "The Effects of Fire and Water Repellency on Infiltration and Runoff under Mediterranean Type Forest." *CATENA* 19 (3–4): 345–61. https://doi.org/10.1016/0341-8162(92)90008-Y.

Johnson, Rulon E., and Robert H. Dettre. 1964. "Contact Angle Hysteresis. III. Study of an Idealized Heterogeneous Surface." *Journal of Physical Chemistry* 68 (7). https://doi.org/10.1021/j100789a012.

Keatts, Matthew I., John L. Daniels, William G. Langley, Miguel A. Pando, and Vincent O. Ogunro. 2018. "Apparent Contact Angle and Water Entry Head Measurements for Organo-Silane Modified Sand and Coal Fly Ash." *Journal of Geotechnical and Geoenvironmental Engineering* 144 (6). https://doi.org/10.1061/(ASCE)GT.1943-5606.0001887.

King, P. M. 1981. "Comparison of Methods for Measuring Severity of Water Repellence of Sandy Soils and Assessment of Some Factors That Affect Its Measurement." *Soil Research* 19 (3): 275–85. https://doi.org/10.1071/SR9810275.

Lee, Changho, Heui-Jean Yang, Tae Sup Yun, Youngmin Choi, and Seongyeong Yang. 2015. "Water-Entry Pressure and Friction Angle in an Artificially Synthesized Water-Repellent Silty Soil." *Vadose Zone Journal* 14 (4): 1–9. https://doi.org/10.2136/VZJ2014.08.0106.

Letey, J., M. L.K. Carrillo, and X. P. Pang. 2000. “Approaches to Characterize the Degree of Water Repellency.” In *Journal of Hydrology*. Vol. 231–232. https://doi.org/10.1016/S0022-1694(00)00183-9.

Ley, T., Moradllo, M. K., & Oklahoma Department of Transportation Materials and Research Division Office of Research & Implementation. (2015). *Expected Life of Silane Water Repellent Treatments on Bridge Decks Phase 2*.

Lin, H., S. D.N. Lourenço, T. Yao, Z. Zhou, A. T. Yeung, P. D. Hallett, G. I. Paton, K. Shih, B. C.H. Hau, and J. Cheuk. 2019. “Imparting Water Repellency in Completely Decomposed Granite with Tung Oil.” *Journal of Cleaner Production* 230 (September): 1316–28. https://doi.org/10.1016/J.JCLEPRO.2019.05.032.

Liu, Hui, Zhaoqiang Ju, Jörg Bachmann, Robert Horton, and Tusheng Ren. 2012. “Moisture-Dependent Wettability of Artificial Hydrophobic Soils and Its Relevance for Soil Water Desorption Curves.” *Soil Science Society of America Journal* 76 (2): 342–49. https://doi.org/10.2136/SSSAJ2011.0081.

Mahedi, Masrur, Sajjad Satvati, Bora Cetin, and John L Daniels. 2020. “Chemically Induced Water Repellency and the Freeze–Thaw Durability of Soils.” *Journal of Cold Regions Engineering* 34 (3): 04020017. https://doi.org/10.1061/(ASCE)CR.1943-5495.0000223.

McHale, G., M. I. Newton, and N. J. Shirtcliffe. 2005. “Water-Repellent Soil and Its Relationship to Granularity, Surface Roughness and Hydrophobicity: A Materials Science View.” *European Journal of Soil Science* 56 (4): 445–52. https://doi.org/10.1111/J.1365-2389.2004.00683.X.

Ng, S. H.Y., and S. D.N. Lourenço. 2016. “Conditions to Induce Water Repellency in Soils with Dimethyldichlorosilane.” *Geotechnique* 66 (5). https://doi.org/10.1680/jgeot.15.T.025.

Oluyemi-Ayibiowu, Bamitale Dorcas, and Micheal Abiodun Uduebor. 2019. “Effect of Compactive Effort on Compaction Characteristics of Lateritic Soil Stabilized With Terrasil.” *Journal of Multidisciplinary Engineering Science Studies (JMESS)* 5 (2): 2458–2925. www.jmess.org.

Ritsema, Coen J., Louis W. Dekker, Erik G.M. Van Den Elsen, Klaas Oostindie, Tammo S. Steenhuis, and John L. Nieber. 1997. “Recurring Fingered Flow Pathways in a Water Repellent Sandy Field Soil.” *Hydrology and Earth System Sciences* 1 (4): 777–86. https://doi.org/10.5194/HESS-1-777-1997.

Ritsema, Coen J., Louis W. Dekker, J. M.H. Hendrickx, and W. Hamminga. 1993. “Preferential Flow Mechanism in a Water Repellent Sandy Soil.” *Water Resources Research* 29 (7): 2183–93. https://doi.org/10.1029/93WR00394.

Sadiq, Fyaz, Mohammad Wasif Naqvi, Bora Cetin, and John Daniels. 2023. “Role of Temperature Gradient and Soil Thermal Properties on Frost Heave.” *Journal of the Transportation Research Board*. https://doi.org/10.1177/03611981221147261.

Saulick, Y., S.D.N. Lourenço, and B.A. Baudet. 2017. “A Semi-Automated Technique for Repeatable and Reproducible Contact Angle Measurements in Granular Materials Using the Sessile Drop Method.” *Soil Science Society of America Journal* 81 (2). https://doi.org/10.2136/sssaj2016.04.0131.

Saulick, Yunesh, Sergio Lourenço, and Béatrice Baudet. 2016. “Effect of Particle Size on the Measurement of the Apparent Contact Angle in Sand of Varying Wettability under Air-Dried Conditions.” *E3S Web of Conferences* 9 (September): 09003. https://doi.org/10.1051/E3SCONF/20160909003.

Schulte, K. E., P. J. Culligan, and J. T. Germaine. 2007. “Intrinsic Sorptivity and Water Infiltration into Dry Soil at Different Degrees of Saturation,” October, 1–11. https://doi.org/10.1061/40907(226)5.

Shakesby, Richard A., Celeste De O.A. Coelho, Antonio D. Ferreira, James P. Terry, and Rory P.D. Walsh. 1993. “Wildfire Impacts on Soil-Erosion and Hydrology in Wet Mediterranean Forest, Portugal.” *International Journal of Wildland Fire* 3 (2): 95–110. https://doi.org/10.1071/WF9930095.

Uduebor, Micheal, John Daniels, Naqvi Mohammad, and Bora Cetin. 2022. “Engineered Water Repellency in Frost Susceptible Soils,” March, 457–66. https://doi.org/10.1061/9780784484012.047.

United Nations Environment Programme. 2022. “Global Status Report for Buildings and Construction: Towards a Zero-emission, Efficient and Resilient Buildings and Construction Sector.” Nairobi.

Wasif Naqvi, Mohammad, Md. Fyaz Sadiq, Bora Cetin, Micheal Uduebor, and John Daniels. 2022. “Investigating the Frost Action in Soils,” March, 257–67. https://doi.org/10.1061/9780784484067.027.

Wu, Peng, Bo Xia, and Xianbo Zhao. 2014. “The Importance of Use and End-of-Life Phases to the Life Cycle Greenhouse Gas (GHG) Emissions of Concrete – A Review.” *Renewable and Sustainable Energy Reviews* 37 (September): 360–69. https://doi.org/10.1016/J.RSER.2014.04.070.

ARTICLE 3: EFFECT OF VARYING SALT CONCENTRATIONS ON EWR TREATMENT

ABSTRACT

Engineered Water Repellency (EWR) treatment has emerged as a promising solution for managing moisture in soils, with applications in geotechnical and soil engineering. One of its critical use cases is in mitigating frost action in cold climate regions, where freezing and thawing cycles can pose significant challenges to infrastructure and soil stability. EWR treatment, achieved through the process of silanization, involves the bonding of hydrophobic silane molecules to soil particles, creating a water-repellent protective layer. However, the interaction between salt concentrations and EWR treatment in soils remains a largely unexplored area. In regions with cold climates, salt applications are common for road maintenance, which can influence the effectiveness of EWR treatment. Sodium chloride (NaCl) and calcium chloride ($CaCl_2$) are frequently used salts, but their impact on EWR treatment and treated soils remains uncertain. Moreover, the relationship between pH levels and the silanization process, which is crucial for EWR treatment efficacy, is disrupted by salt concentrations. Natural soils and glass beads were collected and subjected to EWR treatment using different organosilane (OS) dosages. The impact of salt concentration was evaluated in both contact angle measurements and Water Drop Penetration Time (WDPT) tests. Additionally, electrical conductivity (EC) and pH measurements were taken to assess the chemical changes in treated soils. Findings reveal that the presence of salts, leads to decreased contact angles, indicating a loss of water-repellent properties. Only at very high OS concentrations and low salt concentrations were strong repellency characteristics retained. The EC and pH results indicated that the addition of salts significantly altered the chemical properties of the soils, making them less suitable indicators of the optimal EWR treatment concentration for salted soils. The presence of salts had a clear impact on pH levels, affecting the silanization process and the bonding of silane molecules to soil particles. This study highlights the crucial role of salt concentration in influencing the effectiveness of EWR treatment and the necessity of considering salt content, particularly in cold climate regions where salts are commonly applied. Engineers and researchers must carefully evaluate soil salt levels and tailor EWR treatment strategies accordingly to ensure optimal performance.

1. Introduction

Engineered Water Repellency (EWR) treatment has emerged as a promising and innovative approach for controlling moisture in soils – useful for addressing various challenges in geotechnical and soil engineering (Lourenço et al., 2018; Daniels et al., 2021). One prominent use case of EWR treatment is its ability to mitigate frost action in soil, where it has demonstrated its effectiveness in reducing the detrimental effects, making it a valuable tool in regions prone to cold climates (Mahedi et al., 2020; Uduebor et al., 2022). Frost action, which occurs when soil undergoes freezing and thawing cycles, can lead to significant damage to infrastructure and soil stability. EWR treatment has been applied to address moisture control challenges in (Brooks et al., 2022; Uduebor et al., 2023). The ability to repel water effectively can help prevent excessive soil saturation, which can lead to issues like soil erosion and instability, helping in stabilizing slopes and embankments.

EWR treatment is carried out via a process called silanization (Arkles, 2011). Silanization involves the bonding of silane molecules to the surface of soil particles, altering their surface properties. Silane molecules possess hydrophobic characteristics, making them effective in repelling water. When applied to soils, these silane molecules form a protective layer that reduces water infiltration and absorption, effectively rendering the treated soil water-repellent. Evaluating the performance of EWR-treated soils is crucial to understanding the efficacy of this treatment method. Various test methods have been developed to assess the effectiveness of EWR treatment and its impact on soil behavior. One common approach involves measuring the water repellency of treated soils using methods like the Water Drop Penetration Time (WDPT) test or the Contact Angle

Measurement. These tests help quantify the degree of water repellency achieved after EWR treatment.

In many regions where EWR treatment is applied, the soil is exposed to salt applications before and after treatment. This is particularly relevant in areas with cold climates, where road maintenance practices often involve the use of salt to reduce ice formation and enhance road drivability. Two commonly used salts in such applications are sodium chloride (NaCl) and calcium chloride ($CaCl_2$). While the application of salt on road surfaces is an established practice to mitigate the hazards of cold weather, its interaction with EWR treatment and treated soils remains poorly understood. Manufacturers of EWR products often claim that their treatments are designed to withstand chloride attacks, but the real-world effectiveness of these treatments in the presence of salts remains uncertain. One key factor complicating this issue is the relationship between pH and the silanization process. The efficacy of EWR treatment heavily depends on maintaining the proper pH conditions during application. Salt concentration can disrupt pH levels, potentially impacting the bonding of silane molecules to soil particles. Moreover, salt-induced changes to the properties of clay minerals in soils can further complicate the interaction between EWR treatment and salt (Arkles et al., 1992).

This paper aims to address the critical knowledge gap concerning the effect of salt concentration on Engineered Water Repellency treatment and treated soils. Specifically, it seeks to provide comprehensive insights into how salt concentration influences the performance of EWR treatment and its effectiveness in moisture control.

2. Materials and Methods

2.1 Materials

Natural soils and glass beads were utilized in this study for testing and analysis. Four soils were collected from different locations in the US; Fairbanks in Alaska (AK-FB), Pottawatomie County in Iowa (IA-PC), Asheville in North Carolina (NC-AS), and Hanover silt (NH-HS) from the U.S. Army Cold Regions Research and Engineering Laboratory (CRREL) in New Hampshire. Samples received were air dried and prepared for testing and analysis. Glass beads (Soda Lime, type S) of grain sizes ranging from 0.05 mm to 1.85 mm were mixed in proportion to model an average of all the four soil samples given.

Index property and other tests were performed according to the standard ASTM procedures (ASTM D4318; ASTM D854; ASTM D7928; ASTM D698; ASTM D6913). A summary of the index properties, material classifications, and frost susceptibility classification from the US Army Corps of Engineers (U.S. Army Corps of Engineers, 1965) is given in Table 1.

Table 3-1 Summary of Soil Index Properties and Classifications

Soil Property	**Soil**		
	IA-PC	**NC-AS**	**NH-HS**
Specific Gravity, Gs	2.74	2.65	2.68
#4 Sieve (4.75 mm)	100	89.51	79.8
#10 Sieve (2mm)	99.8	73.32	74.18

#40 Sieve (0.425 mm)	99.6	67.08	52.69
#200 Sieve (0.075 mm)	98.4	30.52	42.41
Silt content (%) (75µm–2µm)	86.67	26.47	37.52
Clay content (%) (< 2µm)	11.69	4.05	4.88
Liquid Limit, LL	33.73	38.44	41.8
Plastic Limit, PL	10.7	NP	NP
Optimum Moisture Content (%)	17.5	18.50	10.6
Max. Dry Unit Weight (kN/m^3)	16.3	15.02	19.5
USCS Classification	CL	SM/SC	ML
AASHTO Classification	A-6	A-4	A-4
Frost Susceptibility Classification	F3	F3	F4

2.2 Salts and Organosilane

Laboratory grade (99.99% Purity) Sodium Chloride (NaCl) was utilized in this study. The salt was obtained from Spectrum Chemical (S1529-500GM). Commercially available Terrasil from Zydex Industries was selected for organosilane treatment. It is a viscous, water-soluble, and reactive soil modifier that permanently modifies the soil surface, making it hydrophobic. It is safe and has been utilized in previous studies as a soil modifier and performance enhancer, particularly in stabilization for pavement applications (Oluyemi-Ayibiowu and Uduebor, 2019)

2.3 Treatment

To induce varying hydrophobicity in the soil, treatment was done at three dosage concentrations (1:1000, 1:100 and 1:10). The organosilane was first dissolved with deionized water (~1μs/cm) and mixed with the soil to achieve a liquid-to-solid (L/S) of 2, ensuring complete saturation of the soil. The mixing was done in a 1000mL HDPE bottle mounted on a rotary tumbler to react for 24 hours. At the end of the reaction time, the mixture was allowed to settle and then decanted. The samples were placed in a fume cupboard to air-dry in the laboratory with temperature and humidity at a relatively stable value of 22-24ºC and 40-45% respectively. Samples were dried till there was no further weight loss.

Untreated and treated samples were split into smaller portions and mixed with NaCl solutions prepared at 0.001, 0.01, 0.1 and 1M molar concentrations. The mixture was done at a liquid-to-solid (L/S) of 1 and poured into a small lab tray to air-dry. The air-dried samples were collected and stored for testing. Labelling was done indicating the OS and Salt treatment respectively.

2.4 Testing

2.4.1 Contact Angle Test

Assessment of the water repellency of treated samples was carried out using the Sessile Drop Method (SDM) using a static measurement. Air and oven-dried samples were placed in a mortar and any agglomerations were broken up with the aid of a rubber end pestle. Where required, the soil sample was passed through sieves to provide a uniform

range and test surface. A double-sided adhesive tape was affixed to a glass slide and the treated soil was placed on the other end with the aid of a spatula. A slight weight of about 100g was placed on the soil for about 2 minutes after which the excess loose material unattached to the tape was removed by flipping it and lightly tapping the sides of the glass slide. This process was repeated until there was full coverage of a monolayer of treated material over the surface of the adhesive tape.

The glass slide was placed on a goniometer and a water droplet was tittered to the surface of the soil using a Flow-Trac II, set with a predetermined flow rate of 0.0095l/s. Contact angle measurements were taken by capturing the water-soil-air interface for 10s with images taken at 1s intervals which were analyzed using the drop image analysis software, ASDA. To ensure consistency of results, the drop size was advanced as described in (Feyyisa, Daniels, and Pando 2017), until the contact radius reached equilibrium resulting in a constant angle measurement. Duplicate specimens were tested for each sample to evaluate variability in the results obtained.

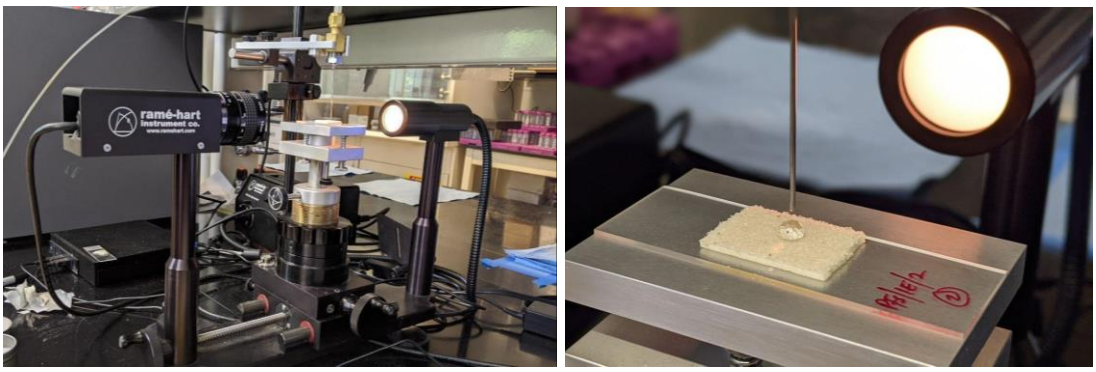

Figure 3-1 (a) Goniometer for Measuring Contact Angle (b) Water Drop on Test Sample

2.4.2 Water Drop Penetration Test

The water drop penetration time (WDPT) method measures the degree of soil water repellency by evaluating the infiltration rate of water droplets into the soil (Letey, Carrillo, and Pang 2000). The Water Drop Penetration Time (WDPT) test involves placing water drops on the surface of an exposed surface of the soil with subsequent measurement of the time taken to infiltrate into the soil. Usually, an average is taken over some drops (typically three) and utilized in determining the degree of water repellency based on a given classification (King 1981; Liu et al. 2012). In this study, about 20g samples of the air-dried soil material were measured into a can and three drops of deionized water (50 ± 1 μL) were measured on the surface of the soil with a pipette. The time taken to complete the penetration of the water droplet was recorded with a timecode stamp to determine the time interval.

2.4.3 EC and pH

Electric Conductivity (EC) and pH measurements were carried out on untreated and treated samples using a Mettler Toledo probe. The dried samples were mixed with Deionized water (~1μS/cm) at a liquid-to-solid ratio of 2:1 for 24 hours and the supernatant was extracted for testing.

3. Results and discussions

3.1 Contact Angle

Contact angles for the different soils at varying salt concentrations and OS dosage treatments are given in the figure below. There is a decrease in contact angle with

increasing salt concentration, while it increases with increasing OS Dosage treatment. In soils with larger grain sizes (NHHS, GB), the contact angles are lower than untreated values even at high-dosage treatments (1:10) and are more affected by the salt concentration than the hydrophobic treatment. In the finer-grained soils, the OS Dosage influences the contact angle results more. This behavior is likely due to the quantity of fine-grained material, which has more surface area and can be treated more by the organosilane to impart hydrophobicity. Also, salts in coarser-grained material increase the ionic concentration of their fine-grained portion – usually utilized in contact angle testing. This can influence the results obtained from the tests.

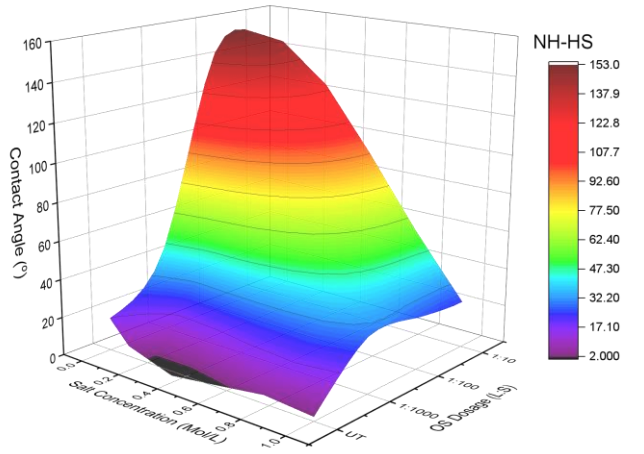
NH-HS
Contact Angle (°)
160
140
120
100
80
60
40
20
0
153.0
137.9
122.8
107.7
92.60
77.50
62.40
47.30
32.20
17.10
2.000
Salt Concentration (Mol/L)
0.0
0.2
0.4
0.6
0.8
1.0
GS Dosage (L/g)
UT
1:1000
1:100
1:10

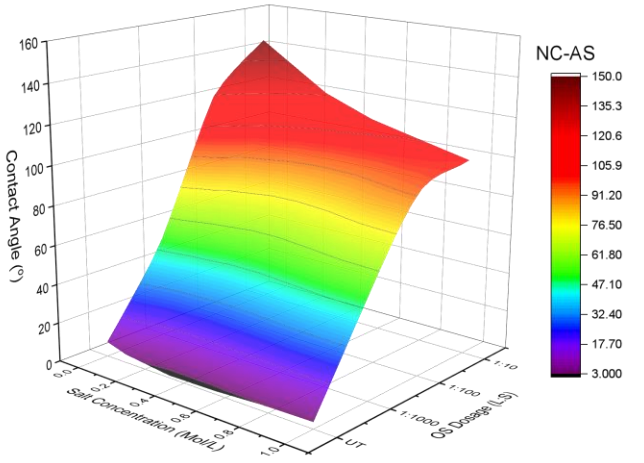
NC-AS
Contact Angle (°)
160
140
120
100
80
60
40
20
0
150.0
135.3
120.6
105.9
91.20
76.50
61.80
47.10
32.40
17.70
3.000
Salt Concentration (Mol/L)
0.0
0.2
0.4
0.6
0.8
1.0
GS Dosage (L/g)
UT
1:1000
1:100
1:10

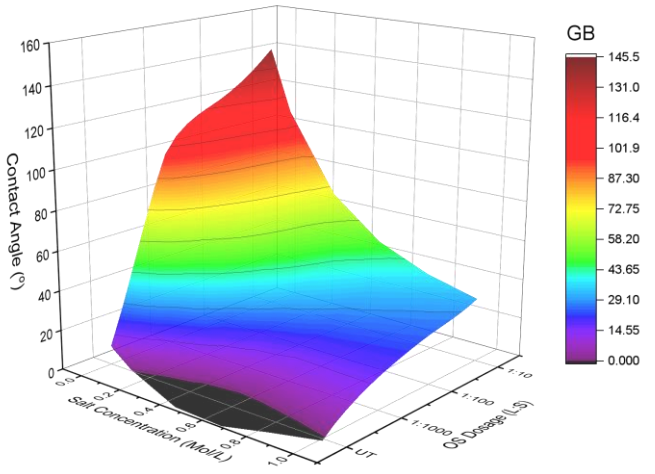
GB
Contact Angle (°)
160
140
120
100
80
60
40
20
0
145.5
131.0
116.4
101.9
87.30
72.75
58.20
43.65
29.10
14.55
0.000
Salt Concentration (Mol/L)
0.0
0.2
0.4
0.6
0.8
1.0
GS Dosage (L/g)
UT
1:1000
1:100
1:10

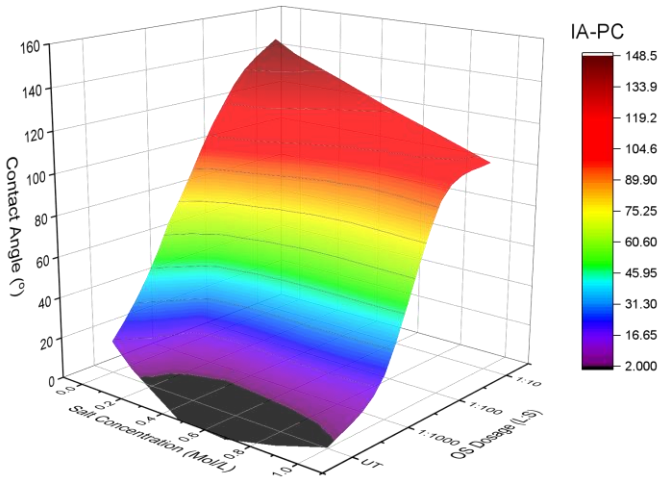

Figure 3-2 Contact angle values as a function of salt concentration and OS dosage

In all cases a higher concentration of improved the hydrophobicity of the treated soils up to a ratio of 1:100 after which there was no marginal increase in the contact angle values. For practical purposes, soils to be utilized for treatment will need to be assessed for their salt content and the impacts on hydrophobicity treatment prior to use.

3.2 WDPT

The waterdrop penetration test results correlated well with contact angle results but skewed more toward the salt concentration. Results were highly influenced by the salt concentration within the soil samples with OS-treated samples having slight (1-60s) to strong (600 – 3600) repellency. Only treated (above 1:1000) unsalted soils (less than 0.1M) had penetration times above 3600. This indicates that the water-repellent properties of the treated material are inhibited by the ionic potential of the salts present within them. WDPT results provide a measure of the persistence of a water droplet on the surface of a treated material, hence the results indicate that the presence of salts will be disadvantageous to

water repellency treatment regardless of the attainment of substantial hydrophobicity of the material surface.

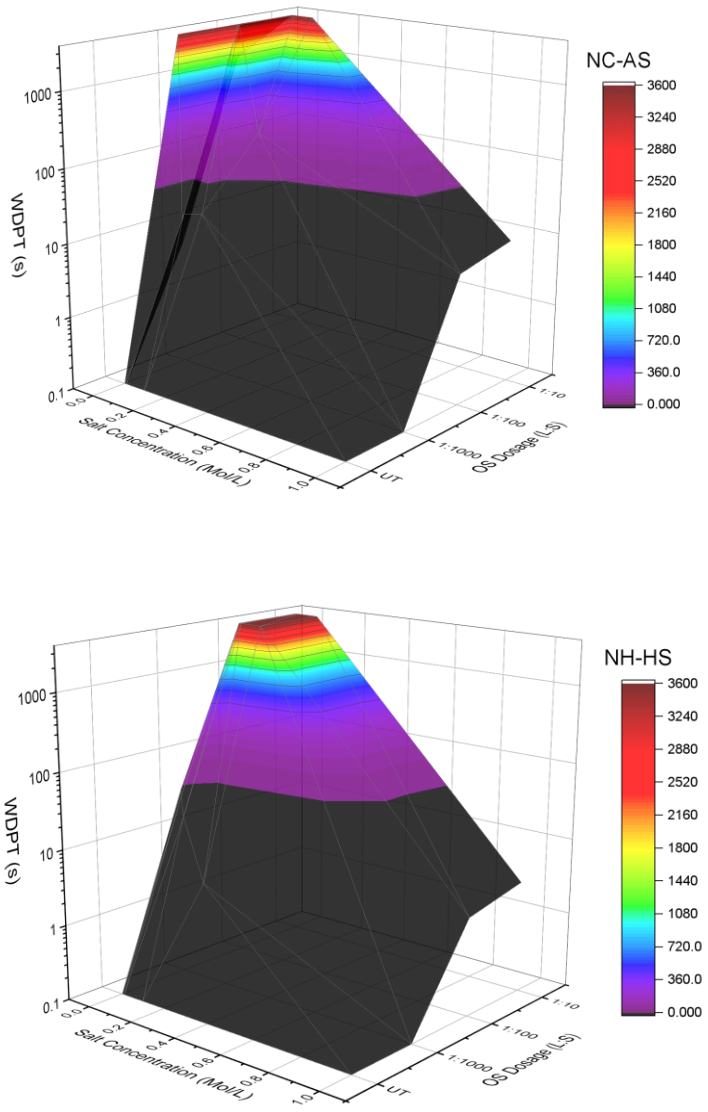

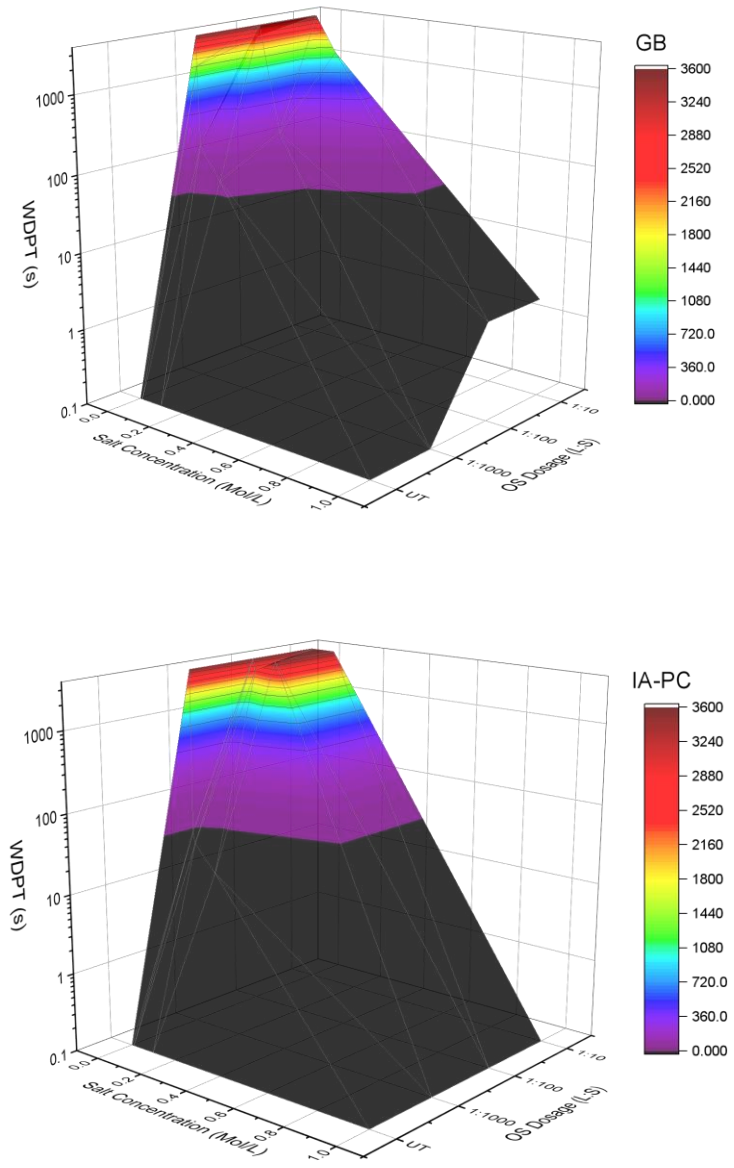

Figure 3-3 WDPT times as a function of salt concentration and OS dosage

3.3 EC

Electrical conductivity test results indicate that the EC value of the soil is governed by the NaCl added. All salted soils had a similar trend in the increase of EC which was not affected by treatment. This indicates that treatment will not alter the EC of previously salted salts and maybe a poor indicator of optimal treatment as described in earlier tests by

Uduebor et al (2023). For already salted soils laboratory tests (CA, WDPT, WEP) combined with field trials would provide a better understanding of the optimal dosage concentration as well as treatment method to be utilized.

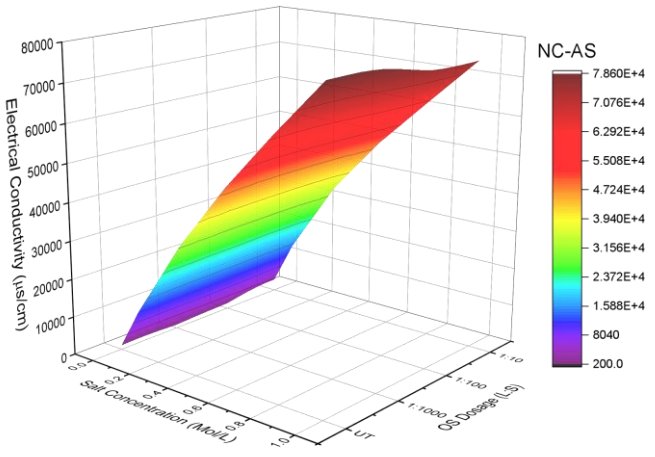

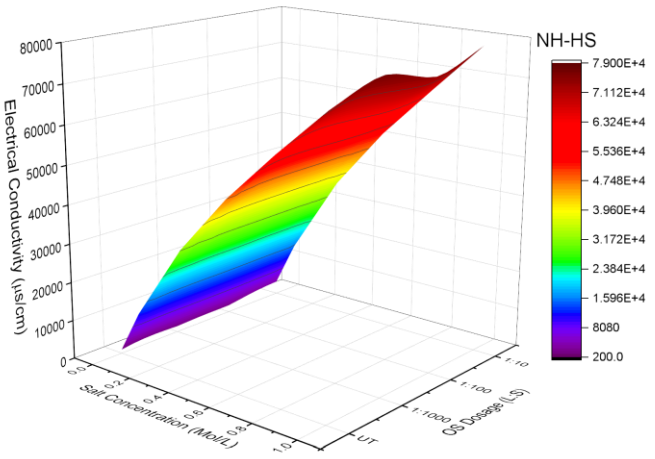

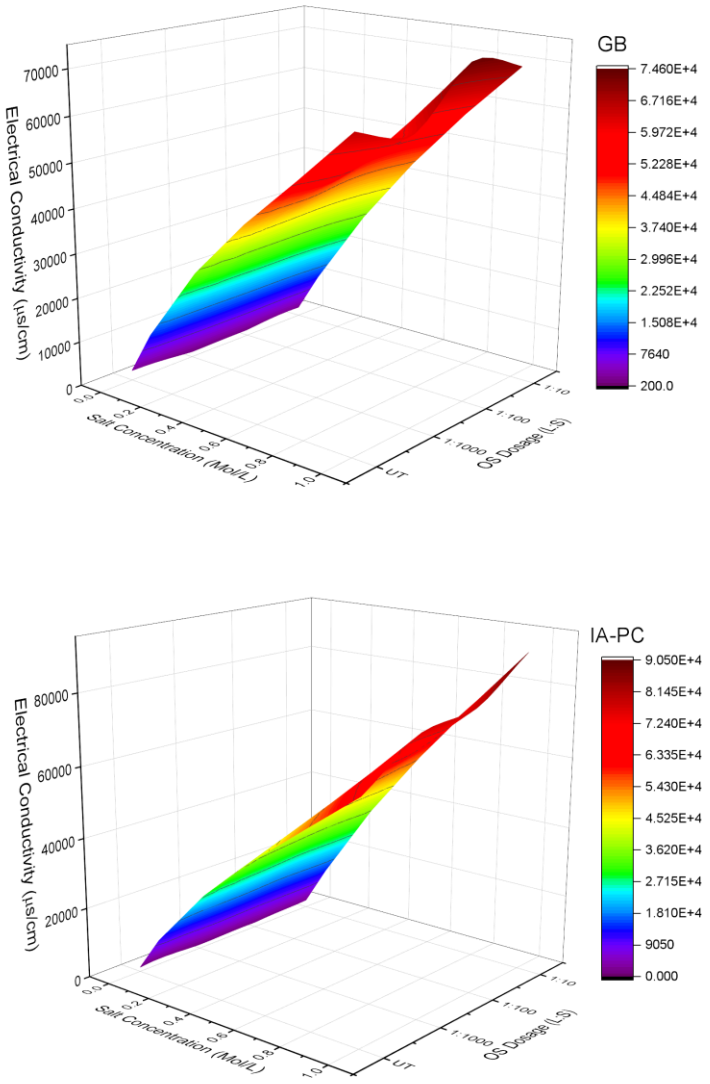

Figure 3-4 EC as a function of salt concentration and OS dosage

3.4 pH

Ph values correlated with EC and were inversely proportional, dropping with increasing salt concentration. For untreated soils, the salted solution gradually moves towards a neutral solution. pH can be affected by the presence of salts in the solution, which ultimately affects the hydrolysis reaction of the organosilane polymer. By lowering the pH and making it more acidic there is formation of more

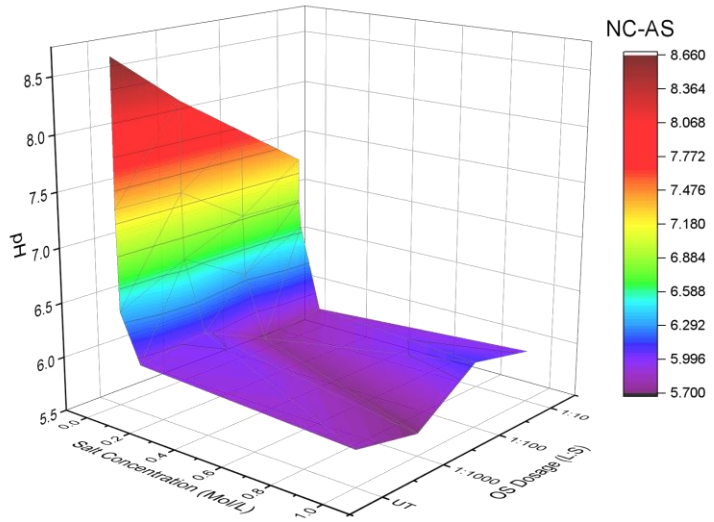
NC-AS
8.660
8.364
8.068
7.772
7.476
7.180
6.884
6.588
6.292
5.996
5.700
pH
8.5
8.0
7.5
7.0
6.5
6.0
5.5
Salt Concentration (Mol/L)
0.0
0.2
0.4
0.6
0.8
1.0
GS Dosage (L/g)
UT
1:1000
1:100
1:10

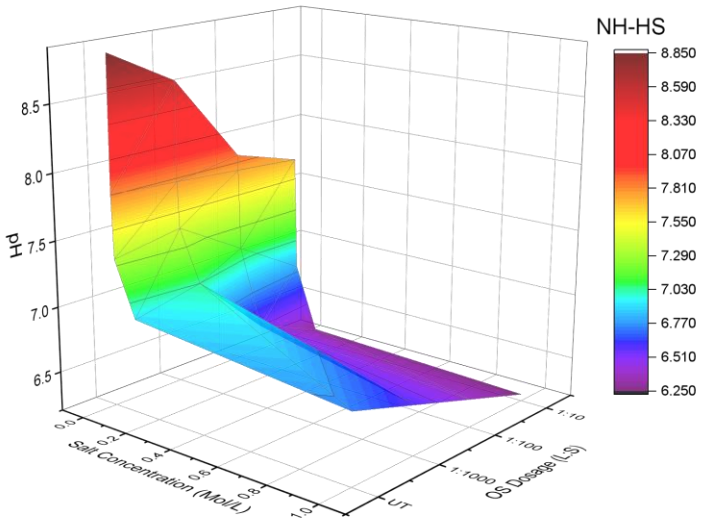
NH-HS
8.850
8.590
8.330
8.070
7.810
7.550
7.290
7.030
6.770
6.510
6.250
pH
8.5
8.0
7.5
7.0
6.5
Salt Concentration (Mol/L)
0.0
0.2
0.4
0.6
0.8
1.0
GS Dosage (L/g)
UT
1:1000
1:100
1:10

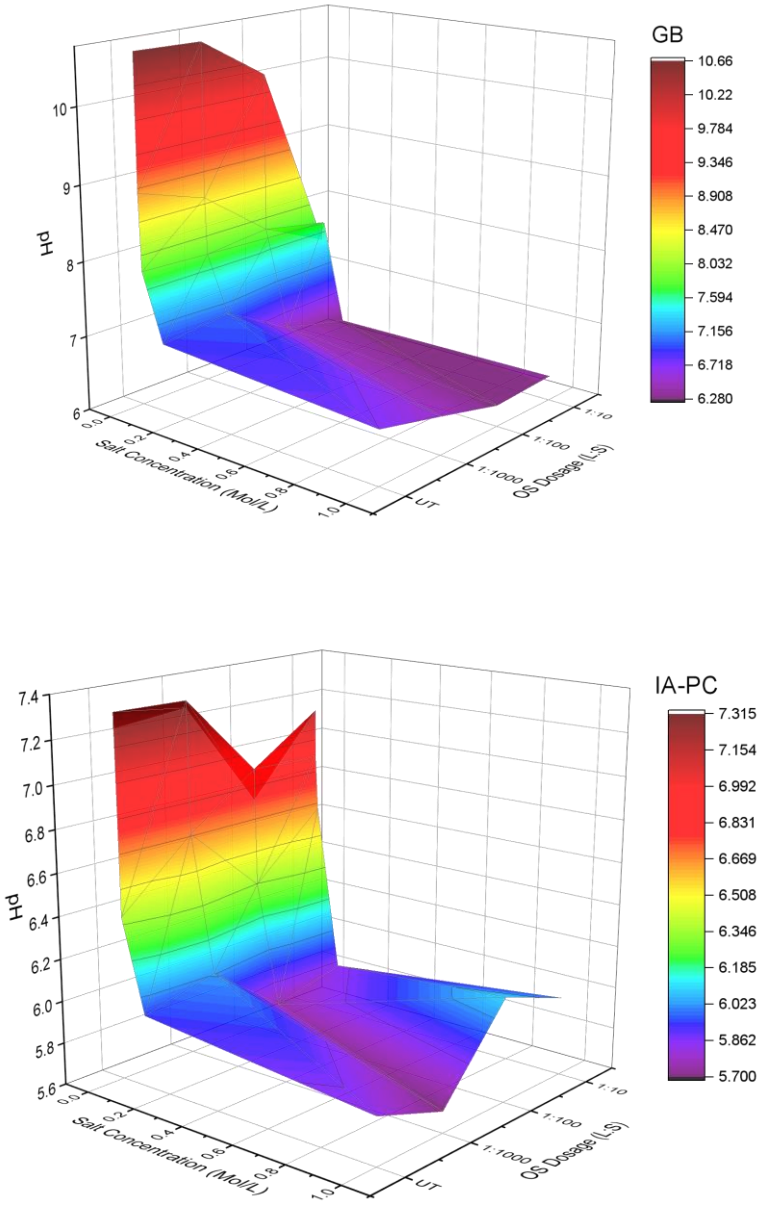

Figure 3-5 pH as a function of salt concentration and OS dosage

4. Conclusions

This study explored the impacts of salt concentrations on Engineered Water Repellency (EWR) treatment and its effectiveness for use in moisture control for different soil types. Several key findings are highlighted below.

1. EWR treatment effectively increased hydrophobicity in soils, with higher organosilane (OS) dosages leading to improved water repellency. However, the effectiveness of this treatment was compromised by increasing salt concentrations, particularly in soils with larger grain sizes. This was observed with decreasing contact angles as well as water drop penetration time test results that indicate that the ionic potential of salts can hinder the effectiveness of EWR treatment in repelling water.
2. EC and pH results indicated the presence of added salts, drastically change the chemistry of soils. Their treatment with organosilanes did not change this in any drastic way. Therefore, EC and pH are not good indicators of the optimal EWR treatment concentration for salted soils.
3. The presence of salts impacts the pH of the pore fluid and or mixing solution. This affects the silanization process potentially influencing the bonding of the silane molecules to the soil particles.

In conclusion, this study highlights the significant influence of salt concentration on EWR treatment and treated soils. It presents the need to consider salt content in soil, particularly in regions with cold climates where salt applications are common. Engineers and researchers should carefully assess salt levels in soils and tailor EWR treatment strategies accordingly to ensure optimal performance.

REFERENCES

Arkles, B., 2011. Hydrophobicity, Hydrophilicity and Silane Surface Modification. Morrisville, PA.

Arkles, B., Steinmetz, J.R., Zazyczny, J., Mehta, P., 1992. Factors contributing to the stability of alkoxysilanes in aqueous solution. J Adhes Sci Technol 6, 193–206. https://doi.org/10.1163/156856192X00133

ASTM. (2000). D5084 - Standard Test Methods for Measurement of Hydraulic Conductivity of Saturated Porous Materials Using a Flexible Wall Permeameter. *Astm D5084*, *04*(October 1990).

ASTM. (2012). ASTM D698: Standard Test Methods for Laboratory Compaction Characteristics of Soil Using Standard Effort (12 400 ft-lbf/ft3 (600 kN-m/m3)). *ASTM International*, *3*.

ASTM D 854. (2002). ASTM D854 Standard Test Methods for Specific Gravity of Soil Solids by Water Pycnometer. *ASTM International*, *04*.

ASTM D7928. (2021). Standard Test Method for Particle-Size Distribution (Gradation) of Fine-Grained Soils Using the Sedimentation (Hydrometer) Analysis. *ASTM International*, *May 2016*.

ASTM International. (2017a). D6913: Standard Test Methods for Particle-Size Distribution (Gradation) of Soils Using Sieve Analysis. *ASTM International*, *D6913*(17).

ASTM International. (2017b). ASTM D4318-17. *Standard Test Methods for Liquid Limit, Plastic Limit, and Plasticity Index of Soils*.

Brooks, T., Daniels, J.L., Uduebor, M., Cetin, B., Wasif Naqvi, M., 2022. Engineered Water Repellency for Mitigating Frost Action in Iowa Soils. https://doi.org/10.1061/9780784484012.046

Daniels, J.L., Langley, W.G., Uduebor, M., Cetin, B., 2021. Engineered Water Repellency for Frost Mitigation: Practical Modeling Considerations. Geo-Extreme 2021 385–391. https://doi.org/10.1061/9780784483701.037--

Feyyisa, J.L., Daniels, J.L., Pando, M.A., 2017. Contact Angle Measurements for Use in Specifying Organosilane-Modified Coal Combustion Fly Ash. Journal of Materials in Civil Engineering 29. https://doi.org/10.1061/(asce)mt.1943-5533.0001943

King, P.M., 1981. Comparison of methods for measuring severity of water repellence of sandy soils and assessment of some factors that affect its measurement. Australian Journal of Soil Research 19. https://doi.org/10.1071/SR9810275

Letey, J., Carrillo, M.L.K., Pang, X.P., 2000. Approaches to characterize the degree of water repellency. J Hydrol (Amst) 231–232, 61–65. https://doi.org/10.1016/S0022-1694(00)00183-9

Liu, H., Ju, Z., Bachmann, J., Horton, R., Ren, T., 2012. Moisture-Dependent Wettability of Artificial Hydrophobic Soils and Its Relevance for Soil Water Desorption Curves. Soil Science Society of America Journal 76, 342–349. https://doi.org/10.2136/SSSAJ2011.0081

Lourenço, S.D.N., Saulick, Y., Zheng, S., Kang, H., Liu, D., Lin, H., Yao, T., 2018. Soil wettability in ground engineering: fundamentals, methods, and applications. Acta Geotech. https://doi.org/10.1007/s11440-017-0570-0

Mahedi, M., Satvati, S., Cetin, B., Daniels, J.L., 2020. Chemically Induced Water Repellency and the Freeze–Thaw Durability of Soils. Journal of Cold Regions Engineering 34, 04020017. https://doi.org/10.1061/(ASCE)CR.1943-5495.0000223

Oluyemi-Ayibiowu, B.D., Uduebor, M.A., 2019. Effect of Compactive Effort on Compaction Characteristics of Lateritic Soil Stabilized With Terrasil. Journal of Multidisciplinary Engineering Science Studies (JMESS) 5, 2458–925.

Uduebor, M., Adeyanju, E., Saulick, Y., Daniels, J., Cetin, B., 2023. Engineered Water Repellency for Moisture Control in Airport Pavement Soils. Airfield and Highway Pavements 2023 92–102. https://doi.org/10.1061/9780784484906.009

Uduebor, M., Adeyanju, E., Saulick, Y., Daniels, J., Cetin, B., 2022. A Review of Innovative Frost Heave Mitigation Techniques for Road Pavements. International Conference on Transportation and Development 2022. https://doi.org/10.1061/9780784484357

ARTICLE 4: EFFECT OF WATER REPELLENT TREATMENT ON HYGROSCOPIC PROPERTIES OF FINE-GRAINED SOILS

ABSTRACT

In this study, the relationship between water repellency and hygroscopicity in fine-grained soils is explored, shedding light on crucial factors such as treatment dosage, drying conditions, grain size, and the presence of organic content. Hygroscopicity, which reflects a material's ability to absorb moisture from the atmosphere, plays a pivotal role in fine-grained soils, particularly those rich in clay minerals. Results from assessment of water repellency treatments show significant reduction in the hygroscopic moisture content (W_h), with W_h diminishing as the treatment dosage and concentration increase. A strong correlation is established between W_h and other essential water repellency parameters, including contact angle and water drop penetration time. W_h is also observed to be influenced by treatment concentration and drying conditions, underlining the importance of these variables in soil performance. The study emphasizes that silanes and siloxanes, which permit vapor migration, inherently limit the complete elimination of moisture absorption in treated soils, with significant implications for engineering applications.

1. Introduction

Hygroscopy is the tendency of materials to absorb water from the atmosphere. This is typical with fine-grained soils that contain clay mineral particles (particularly montmorillonite and illite groups). The absorbed water is a consequence of the negative surface charges of the clay minerals composing the soil (Prakash et al., 2016). The hygroscopic or absorbed water held by the soil is referred to as hygroscopic moisture content (w_h) and represents the water absorbed by the negatively charged clay particles when exposed to different levels of humidity.

Hygroscopy is a valuable soil property that can be utilized in characterizing other physical and physicochemical characteristics of soils. Correlations have been made to cation exchange capacity (CEC) (Torrent et al., 2015) and specific surface area (SSA) (Moiseev, 2008). Investigations into the adsorption phenomenon carried out by (Kuron, 1930; Kuhn, 1932; Kelley et al., 1936) revealed that the exchange capacity and vapor retention capacity are closely correlated. Other correlations include Water Capacity (Chen et al., 2020), clay content (Wuddivira et al., 2012), Atterberg limits, retention curves (Chen et al., 2014),and permittivity (Robinson et al., 2002), etc.

The hygroscopic moisture content of soils is usually determined by air drying under a defined relative humidity. This is important because relative humidity affects the interaction between water and soil (Shah and Singh, 2006). The variation of W_H with respect to time and R_h is documented in the literature. There are no hygroscopic studies carried out on water-repellent soils but available literature on fine-grained soils present uniform W_H results after 7 days of using an R_h between 45% and 90% (Robinson et al., 2002; Shah and Singh, 2006) with the W_H obtained at R_h of 90% considered as the optimal

hygroscopic moisture content. Hygroscopic moisture content measurements can be made quickly and easily. Moreover, such measurements correlate with other properties (e.g. CEC, SSA) that are more time-consuming to obtain (Wuddivira et al., 2012). The hygroscopicity of soil is also indicative of the soil particle's effectiveness in holding bound or adsorbed water, and by extension, its hydrophobicity.

Previous studies for determining hydrophobicity in water-repellent soils – contact angle, and water drop penetration time test do not often correlate to geotechnical system performance (e.g., infiltration) which is largely affected by soil type, grain size, and pore size (M. A. Uduebor et al., 2023). Performance tests such as breakthrough pressure take a longer time and process to determine and are largely without a defined standard for determination (M. Uduebor et al., 2023). By contrast, there are standard procedures for measuring hygroscopic water content, which makes it a better measure of performance.

Water-repellent soils occur naturally from several processes including wildfires, organic compounds obtained from decomposing organic matter, and waxes from plant matter (Doerr et al., 2000). They can also be engineered in soils by treating them with various naturally occurring and synthetic compounds and/or chemicals (Daniels and Hourani, 2009; Uduebor et al., 2022b). Silanes and siloxanes have been found to be very effective in making soils hydrophobic, with 2.5% or less by mass, inducing water repellency (Brooks et al., 2022; Malisher et al., 2023).

Water repellency has been explored in engineering applications with success in applications such as slopes (Lourenço et al., 2018), road pavements and embankments (Uduebor et al., 2022a), barrier systems, etc. It has been proposed as a solution for a wide

variation of civil engineering problems where other treatment alternatives are cost- or labor-prohibitive (Brooks et al., 2022; M. A. Uduebor et al., 2023; M. Uduebor et al., 2023). Improvements have been observed in terms of moisture stability and control (keeping the moisture content uniform or dry), increased compaction, and strength (Oluyemi-Ayibiowu and Uduebor, 2019; Malisher et al., 2023; M. Uduebor et al., 2023). One characteristic that makes water repellency innovative is the ability to keep the soil matrix in its unsaturated state – one in which thermo-hydro-mechanical properties of the soil are optimal for construction. It has the potential to improve resilience and reduce design and construction costs as well as carbon emissions due to a reduced factor of safety required and increased lifespan of built infrastructure (M. A. Uduebor et al., 2023).

While engineered water repellency offers a radical change in hydraulic properties, questions remain about the long-term stability and durability of these changes. Tests carried out by (Uduebor et al., 2022b; M. A. Uduebor et al., 2023) indicate there is a marked difference of about 10% between the Contact Angle (CA) of air-dried and oven-dried soil subjected to the same treatment. Other studies have shown a reduction in the water-repellent properties of soils after being ponded for a while (Zaman et al., 2022). This represents a significant limitation, particularly when water-repellent soils are used as capillary barriers or within containment systems. Exploring this is important because CA doesn't ultimately translate to performance. It takes 40% of treated particles within a soil sample for a constant CA to be obtained, but water repellent performance could still be improved with higher OS concentration (Choi et al., 2016). Measuring hygroscopic properties could better give insight into the long-term wettability and/or non-wettability of soil samples.

While water repellency treatment binds water repellent long chain organic polymers to the particle surface not all bonding sites may be occupied, rendering unbonded sites available for subsequent reaction. Silane treatment on surfaces permits vapor migration through the pore space while keeping the treated surface water repellent (Arkles, 2011). This permits sufficient adsorption in clay particles under sufficient relative humidity. Figure 1 shows a surface before (a) and after treatment (b). After treatment, the water molecules are prevented from reaching the surface by the silane coating. Moisture adsorption of the fine particles is still possible due to the creation of a high humidity zone at the surface which creates a gradient causing the migration of moisture vapor through the pore space and ultimately permits wetting of the particle even though still hydrophobic (c).

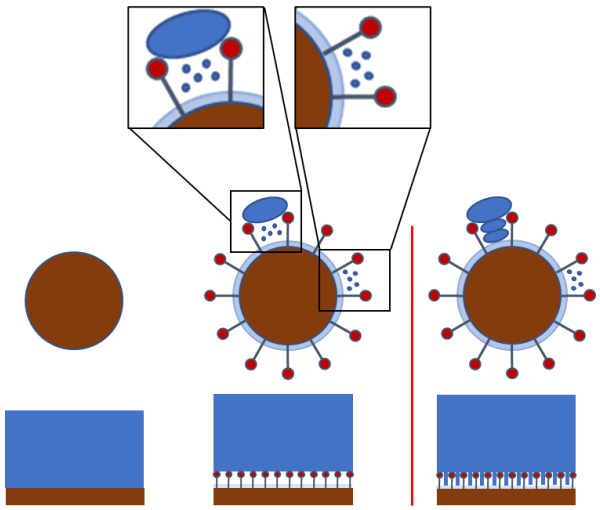

Figure 4-1 Schematic Showing Untreated and Treated Surfaces

Very little is understood about this relationship and this study will explore the relationship between water repellency and hygroscopy in fine-grained soils. It will explore the effect of different drying and wetting conditions on different grain sizes and hygroscopy of fine-grained water-repellent soil. It also seeks to explain the wetting behavior of water-

repellent soil over time under high humidity and provide insights on preventing this from reducing the effectiveness of such soils in engineering practice.

2. Methodology

2.1 Materials

2.1.1 Soil

Four soil samples were selected for this study collected from Pottawatomie County Iowa (IA-PC), Hanover, New Hampshire (NH-HS), Boone County, North Carolina (NC-BO), and Fairbanks, Alaska (AK-FB). Soils were selected to represent different climatic regions of the United States and present material with varying grain size fractions as well as distributions. Natural soils were utilized to obtain results corresponding to field performance. Previous studies carried out on water-repellent soils have utilized standard sands, crushed glass, and silica (Saulick et al., 2018, 2019) but do not represent actual soil types or their behaviors in practice. Also, there is no presence of clay fractions within the samples to model the adsorption behaviors of engineering soils. The four samples were characterized according to the test methodology outlined in different ASTM standards. A summary of the test results as well as the soil classification is presented in Table 1. Specific gravity was carried out according to ASTM D854 and grain size distributions were determined using sieve analyses and hydrometer testing (ASTM D6913; ASTM D7928). Atterberg limits (liquid limit, plastic limit, and plasticity index) were determined using the multipoint liquid limit and the hand-rolling method (ASTM International, 2017a). According to the USCS classification, the soils are primarily fine-grained with a significant

silt percentage (~34 – 87%); IA-PC is a Silty Clay (CL), while NH-HS and AK-FB are Silty Sand and Silt (ML) respectively. NC-BO is a Silty/Clayey Sand (SM/SC). AK-FB had visible organic content made up of decayed roots and other plant matter. Its Organic content was determined to be between 1.3 -1.4% (ASTM D2974)

Table 4-1 Summary of soil index properties and classification

Soil Property	**Soil**			
	NC-BO	**IA-PC**	**NH-HS**	**AK-FB**
% Passing #4 Sieve (4.75 mm)	96.50	100.0	79.80	97.60
% Passing #10 Sieve (2mm)	92.60	99.80	74.18	96.00
% Passing #40 Sieve (0.425 mm)	82.00	99.60	52.69	93.40
% Passing #200 Sieve (0.075 mm)	38.20	98.40	42.41	84.50
Silt content (%) (75μm–2μm)	34.00	86.67	37.52	75.65
Clay content (%) (< 2μm)	4.60	11.69	4.88	8.870
Liquid Limit, LL	38.37	33.73	41.80	41.00
Plasticity Index, PI	NP	10.70	NP	NP
USCS Classification	SC/SM	CL	ML	ML

2.1.2 Organosilane

Samples were treated with commercially available organosilane (OS) Terrasil ® from Zydex Industries. It is a viscous, water-soluble, and reactive soil-modifying polymer with 65-70% active ingredients (Alkoxy-Alkylsilyl Compounds) by weight. This product has been employed in previous research studies (Brooks et al., 2022; Malisher et al., 2023) to create a stable hydrophobic surface on soil particles and has been successfully used for stabilizing soft clays and expansive soils in various studies (Daniels and Hourani, 2009), as well as improving compaction properties (Oluyemi-Ayibiowu and Uduebor, 2019). Terrasil's unique composition, including an additinal silicon atom, enhances resistance to degradation (Arkles et al., 1992).

2.2 Preparation and Treatment

The collected soil samples were air-dried in the laboratory and sieved through a #4 sieve to remove large fractions of the soil. Coarse sands and gravels have relatively low hygroscopy and do not contribute to the bulk adsorption behavior of soils. Removal of large fractions also allows for a relatively consistent material and reduces large variations in results. Soils were treated at mix ratios of 1:10, 1:100, and 1:1000 utilizing the treatment protocol from previous tests carried out by (Uduebor et al., 2022b) to impart varying levels of hydrophobicity to the soil samples. The required OS for each ratio was mixed with deionized water (~1μs/cm) to allow for hydrolysis and activation of the silane after which the resulting mixture was added to soil measured into a 500ml HDPE bottle to achieve a liquid-to-solid (L/S) of 2. The bottle was mounted on a rotary tumbler and the mixture dried after 24 hours. This was done instead of decanting the supernatant carried out in previous studies to obtain near-field results of treatment and determine the possible impacts of having excess OS in the soil. When required, samples were either air-dried in the laboratory (~25ºC, R_h ~45%) or oven-dried in a small lab oven at 110°C. Soils were also separated after treatment into different grain sizes using a set of sieves. The retained mass on each sieve was collected and stored separately. This was done to determine the relative contributions of soil fractions to the bulk mass.

2.3 Water Repellency Assessment

Two tests were employed to assess the water repellency imparted by the treatment. The contact angle test is an established method for measuring solid surface water repellency via the sessile drop contact angle method (SDM) developed by Bachmann et al.

(2000). A glass slide was affixed with double-sided adhesive tape after which samples were applied and compressed onto the tape's coated side, creating a soil monolayer. This application process was repeated twice for full tape coverage. The prepared slide was placed on a goniometer attached to a digital microscope (AVEN model #26700-200, Ann Arbor, Michigan) with backlighting and an adjustable sample table after Uduebor et al. (2023) (Fig. 4-2). Deionized water drops are gradually added to the specimen's surface, capturing images, and taking measurements within 10s for each drop size. Angles below 90° signify wettable/hydrophilic, 90° to 150° are hydrophobic, and above 150° are super hydrophobic.

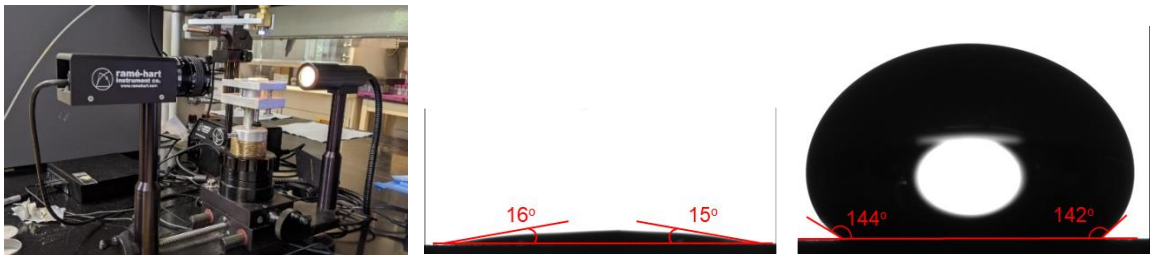

Figure 4-2 Goniometer b. Contact angle measured from a drop on the soil surface.

The Water Drop Penetration Time (WDPT) method assesses soil water repellency by measuring water droplet infiltration rate (Letey et al., 2000). The test involves placing water drops on exposed soil and measuring the time for infiltration. Typically, an average of three drops is used to classify repellency. Water repellency categories based on King (1981) are as follows; ≤ 1s (Non-repellent/Completely wettable); 1–60s (Slightly repellent); 60–600s (Strongly repellent); 600–3600s (Severely repellent); ≥3600s (Extremely repellent). In this study, 20g air-dried soil was placed in a can, and three 50 ±

1 µL deionized water drops were pipetted onto the surface. Droplet penetration time was recorded with a timecode stamp for interval determination.

2.4 Humidification/Conditioning

5g, 10g, and 20g samples of oven-dried samples were spread out on wide aluminum cans and air-dried in the laboratory until a uniform weight was obtained. This was taken to be the air-dry value of the hygroscopic moisture content. The samples were then stored in a humidification chamber maintained at a relative humidity (R_h) of ~100% (Fig. 4-3). This was obtained by placing distilled water at the bottom of the chamber and keeping it airtight. Temperature and humidity were measured with the aid of a HOBO temperature and humidity data logger (UX100-011A). Because of the nature of the test, removing samples from the desiccation chamber lowered the humidity within the chamber, so it was important to determine the optimal storage time for carrying out the tests.

Figure 4-3 Desiccation chamber utilized for humidification process.

Tests carried out by (Prakash et al., 2016) utilized a R_h of 100%. In this study, samples were initially stored for 2 weeks with the masses of the cans with the soil samples obtained at different elapsed time intervals (1, 3, 7, 10, and 14 days) to determine the optimal test time and reduce the need to keep the chamber open. It was observed that all the soil samples reached their equilibrium state, indicating that a maximum W_H was obtained on average, at 7 days (Fig. 4-4). This was selected as the duration for further tests.

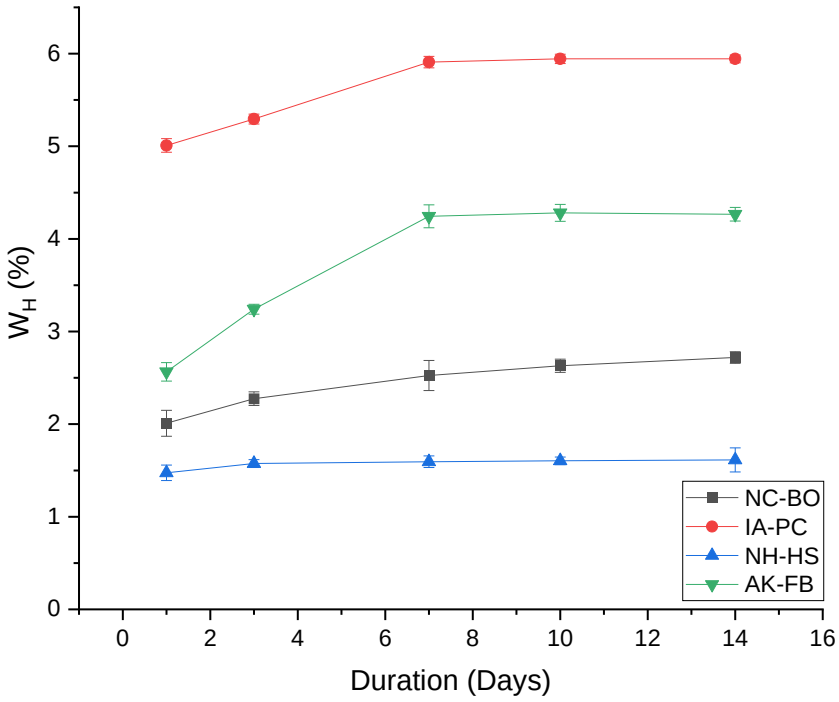

Figure 4-4 Hygroscopic moisture content of untreated soils with time

2.4.1 Hygroscopic Moisture Content Determination

Hygroscopic moisture content was determined for the four soils at three treatment dosages and two drying conditions. Samples were only obtained for testing after achieving and maintaining the maximum humidity for 7days. The samples were weighed on an

analytical balance (OHAUS Adventurer AX224N) sensitive to 0.1mg with a draft shield to determine the moisture adsorbed by the sample. Hygroscopic moisture content was determined using Equation 1 below.

$$W_H(\%) = \frac{M_w}{M_s} \times 100 \quad -eqn1$$

Where M_w is the mass of water (g), M_s, the average mass of oven-dried soil (g) obtained before and after the test, and W_H is the hygroscopic moisture content (%).

3. Results and Discussion

3.1 Assessment of Water Repellency

Results from contact angle tests indicate considerable water repellency was imparted from the organosilane treatment. Contact angles increased with increasing dosage concentration (53.4 to 141.2^o), with 1:10 dosage treatment having the highest apparent contact angles (Fig. 4-5). Values obtained at 1:100 for all soils were comparable to those obtained at 1:10 with very few variations in results obtained. This is important for cost considerations, where increased costs in concentration will mean more than any increase in contact angle. Previous tests carried out by (Feyyisa et al., 2019) have proven there is no marginal increase in contact angle values after a certain treatment concentration.

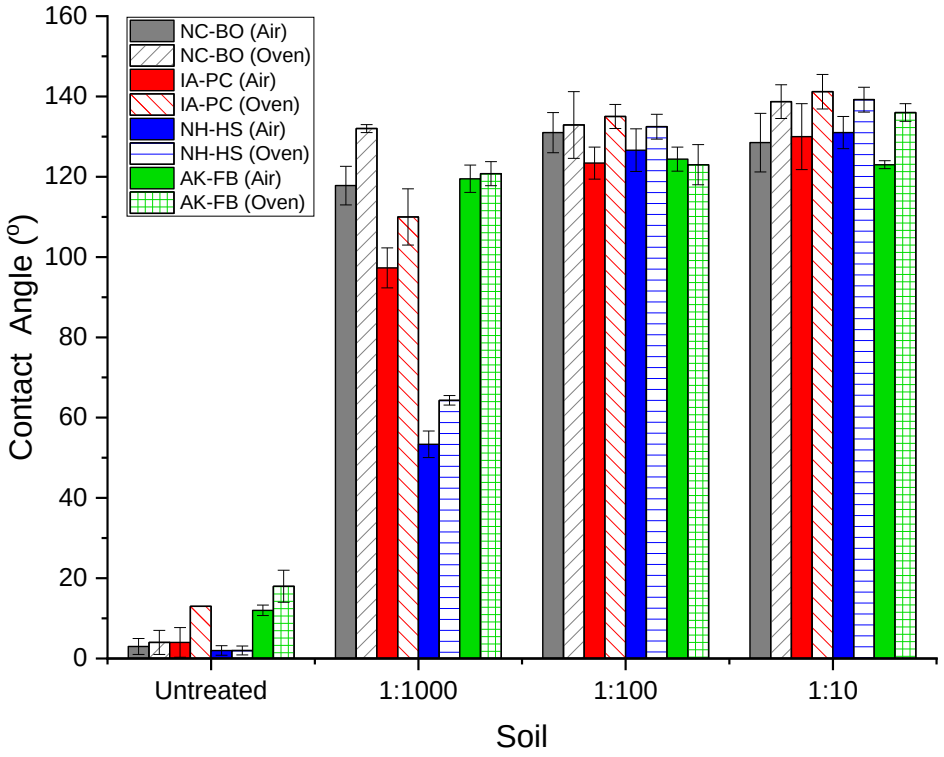

Figure 4-5 Contact angle results of soils with varying treatment dosage concentrations.

There is also an increase in the contact angle values with drying conditions. Oven-dried samples possess a slightly higher value when compared to air-dried samples. While oven-dried samples give the maximum obtainable values for the treated soils, air-dried samples provide a value more representative of field conditions (Uduebor et al., 2022b; M. Uduebor et al., 2023). It also presents the importance of considering the effect of humidity on the performance of treated soils.

Water drops penetration test results indicate all untreated soils as completely wettable (≤ 1s) except AK-FB which was slightly repellent (1-60s). This is due to the humic nature of the soil and the presence of decaying matter which imparts some form of water repellency to the soil (DeBano, 1981). All treated soil samples were severely repellent (600 – 3600s) at 1:1000 treatment except AK-FB which was extremely repellent (>3600s).

Treatments at 1:100 and 1:10 for all soils made them extremely water-repellent. The results correlate very well with the contact angle tests carried out. This relationship has been obtained in previous studies carried out by (Keatts et al., 2018; Feyyisa et al., 2019). It describes the persistence of the hydrophobicity of the treated surface. Previous studies carried out show that it does not represent the performance of the treated samples under hydrostatic pressure, which is governed by other factors including grain size, pore size as well as fluid properties. While these play a considerable role, the humidity behavior (adsorption) of the soil surface will also impact the performance of these soils in the long term, where the other properties seem to be in place.

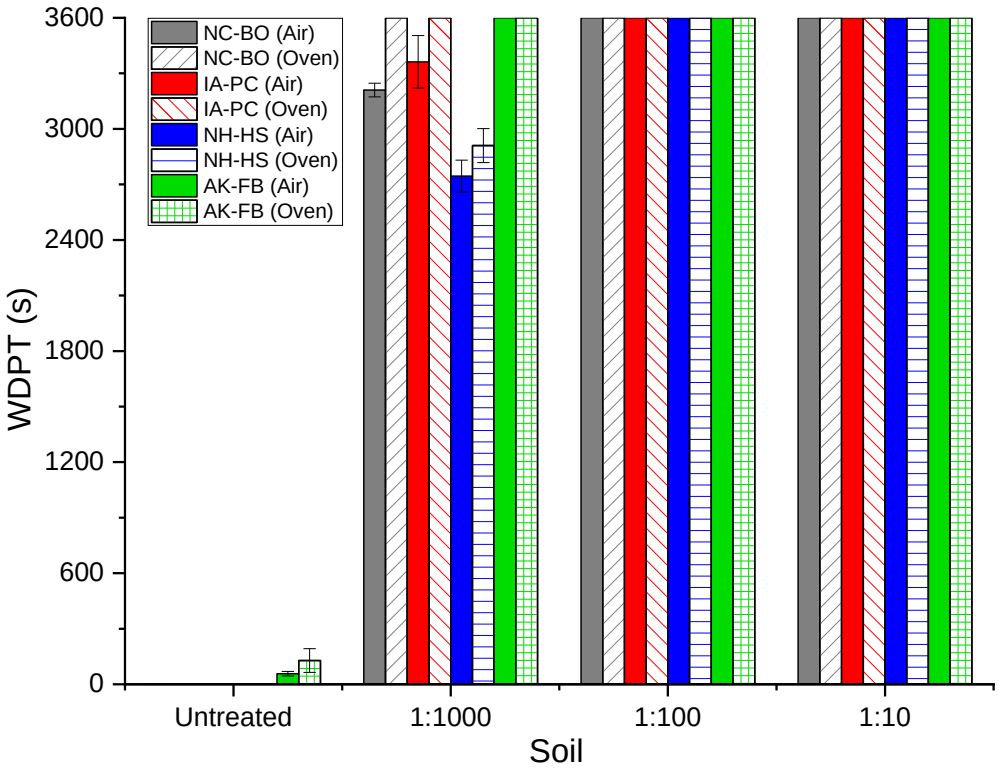

Figure 4-6 Water Drop Penetration Times of soils with varying dosage concentrations

3.2 W_H- Effect of humidity, treatment dosage.

Results from hygroscopic moisture tests show that all soils regardless of treatment are hygroscopic, with reducing moisture contents with increasing dosage treatment. There is significant moisture absorbed in air which confirms the reduction in contact angle and WDPT results obtained between the oven and air-dried samples. These values increase considerably under Rh100 with comparable percentages across all treatment dosages (Fig 4-7). This adsorption behavior is important to note because it places a limitation on the practical engineering usage of water-repellent soils. Adsorption of moisture will result in wetting of the material under sufficient humidity or over time and may reduce performance and the ability of treated soils to prevent infiltration. Further studies into this wetting time as well as retardation factors of treated materials will provide engineers and material scientists with the possible limits of their application. Higher values of Wh are also observed for soil material with higher clay content (IA-PC, AK-FB). The presence of organic content in AK-FB could also contribute to its high hygroscopy even after treatment.

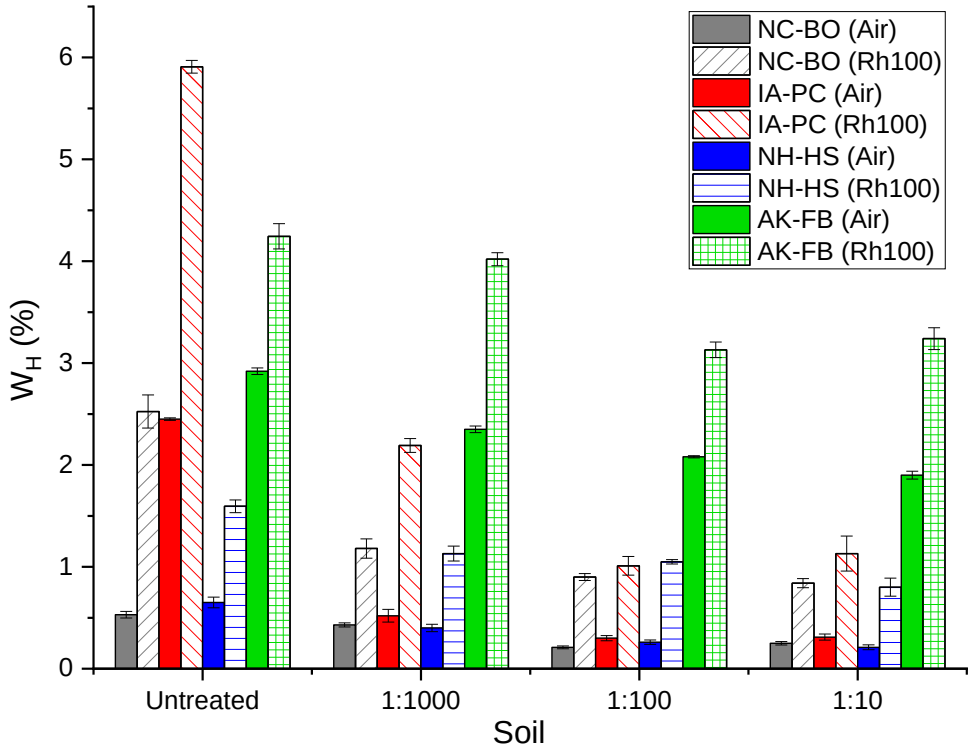

Figure 4-7 Hygroscopic moisture content for untreated and treated samples at various dosage concentrations

The effectiveness of silanes and siloxanes is determined by the mineralogical composition of the substrate (soil) as well as the available ions and pH of the resulting mixture, with bonding favoring the formation of (-Si-O-Si) and -Si-O-Metal bonds (M. A. Uduebor et al., 2023). The presence of organic material will considerably reduce the performance of the soil under humid conditions. As mentioned in previous studies, silanes and siloxanes permit vapor migration and are 100% breathable (Arkles, 2011), which means with a reduction in humidity, there is a reverse operation with the treated sample releasing the moist vapor to the surrounding ((M. Uduebor et al., 2023)). This opens treatment to applications where there is a variation in wetting. For example, using it in pavement systems that experience wetting and drying cycles would be an ideal use case,

as the treated sample ensures moisture balance within the treated section, preventing welling while wet and shrinkage cracking in the dry period. Also, it can be used as a liner for ponds temporarily storing low-impact waste materials.

3.3 WH – Correlation with treatment dosage, W_H

There is a comparable relationship between the hygroscopic moisture content and soil surface water repellency and fines content at the two humidity values as shown in Figure 4-8. The slopes for similar soils are uniform except IA-PC, which experiences more adsorption for the untreated soil under Rh100. This means that for any given soil, the degree of water repellency required to sufficiently inhibit hygroscopic properties under an expected humidity condition can be determined and the corresponding dosage to achieve the same is calculated.

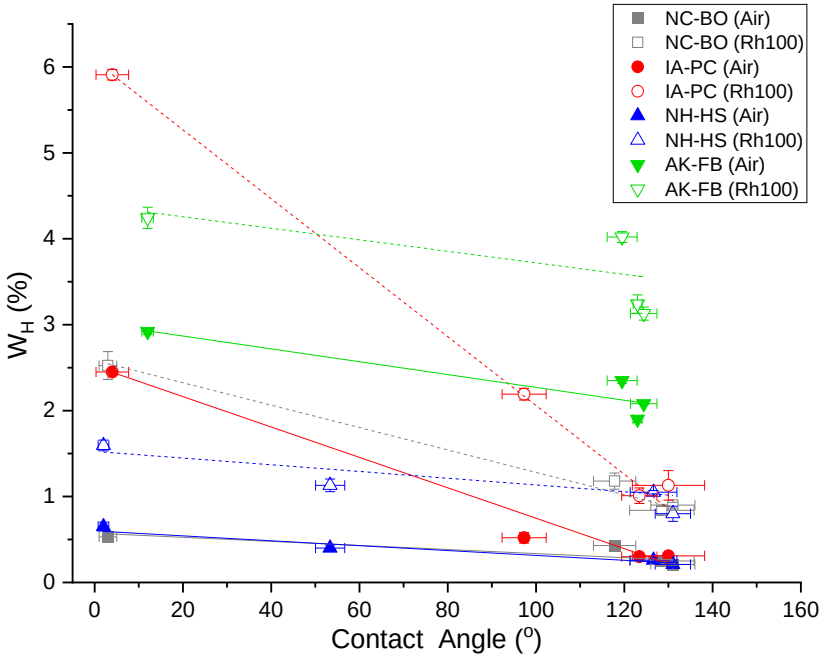

Figure 4-8 Contact angle – hygroscopic moisture content relationship for treated samples.

There is an increase in the Wh values after 1:100. This is due to excess OS in the soil absorbing moisture from the environment. Previous chapters have indicated EC and pH can be correlated to obtain the optimal amount of OS required to treat a given soil. When there is excess OS in the soil, the water-repellency properties and its effectiveness can be reduced due to increased osmotic potential from the excess ions present. Dumenu et al., 2017 carried out tests on EWR-treated Coal Combustion Residuals with the excess OS washed in a batch sorption process while measuring the COD until there were no more free ions in the solution. It was found that after repeated washing 5 times with deionized water, the unsorbed OS chemical was sufficiently washed out. Washing is not practicable for field applications, so there is a need to ensure the optimum dosage concentration is utilized. Finding the right amount of OS required will also lead to cost savings since there is no marginal improvement in performance with an increase in treatment dosage.

3.4 W_H - Effect of Different Grain Sizes

Untreated and soil treated at 1:10 were separated into grain size fractions using a set of sieves and the mass retained was subjected to the same process in air and under Rh100. The results indicate an increase in hygroscopic moisture content with a decrease in grain size regardless of treatment (Fig. 4-9). There is a higher W_h value for larger grain sizes for AK-FB because of the presence of organic materials. The effect of the excess OS is also observable with larger grain sizes of treated soil samples exhibiting close to or higher values compared to untreated soils. The hygroscopic property of fine-grained soil is an essential consideration for designing water-repellent soils containing a lot of fine or organic material since they are more susceptible to hygroscopy and may become wettable

within a shorter period compared to sandy coarse-grained material. Materials with high amounts of illite and montmorillonite groups (water absorbent) can affect the long-term water repellency of soils.

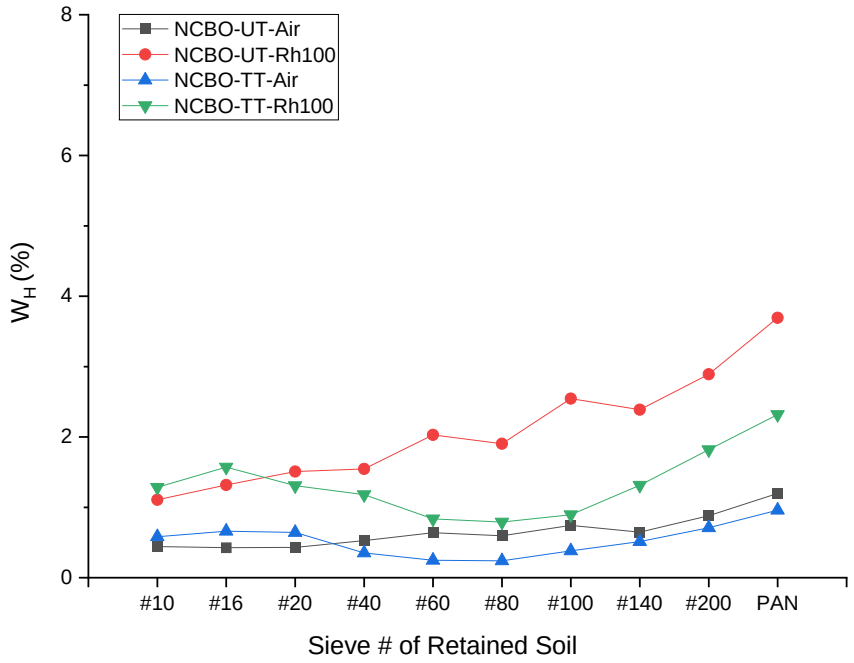

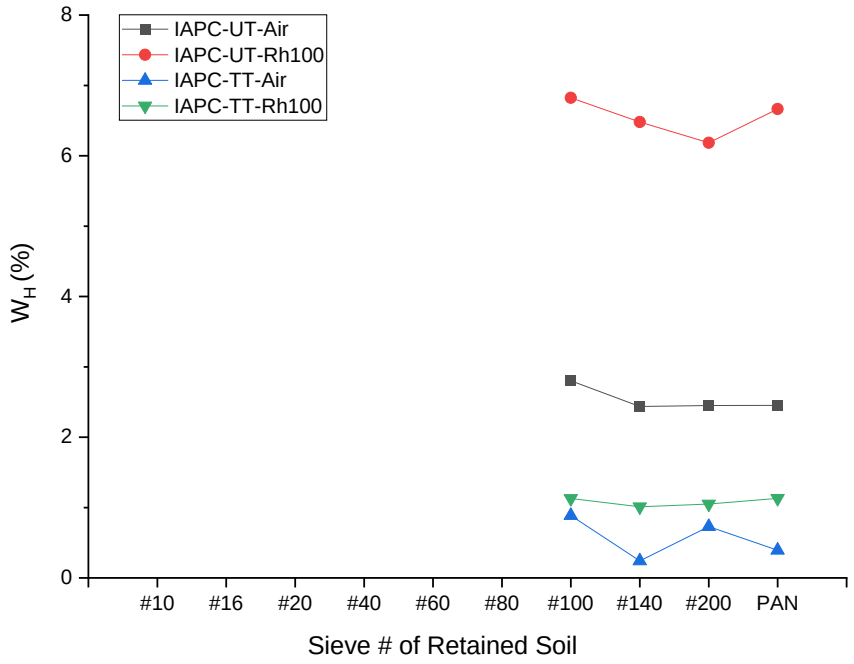

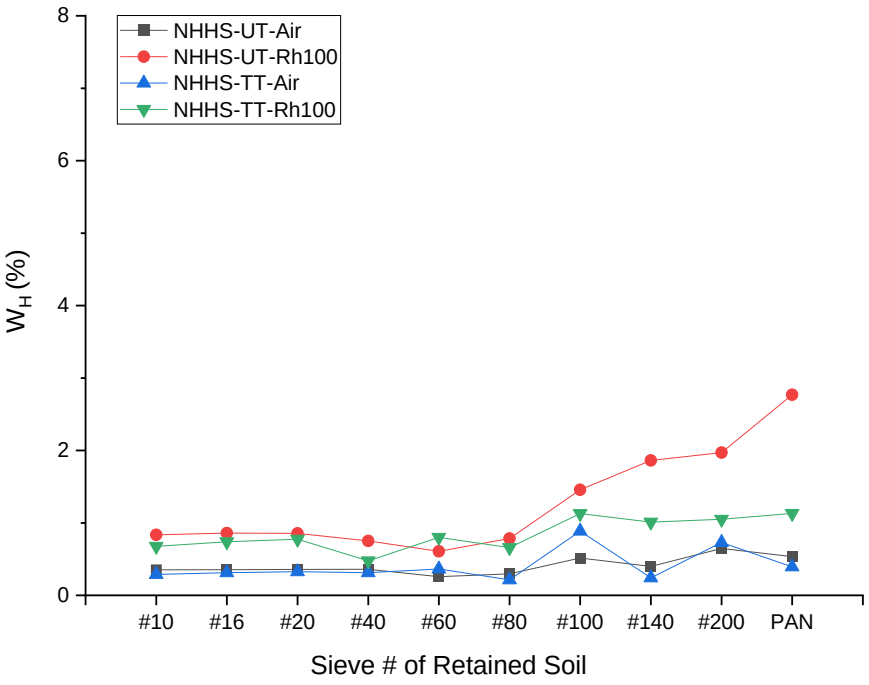

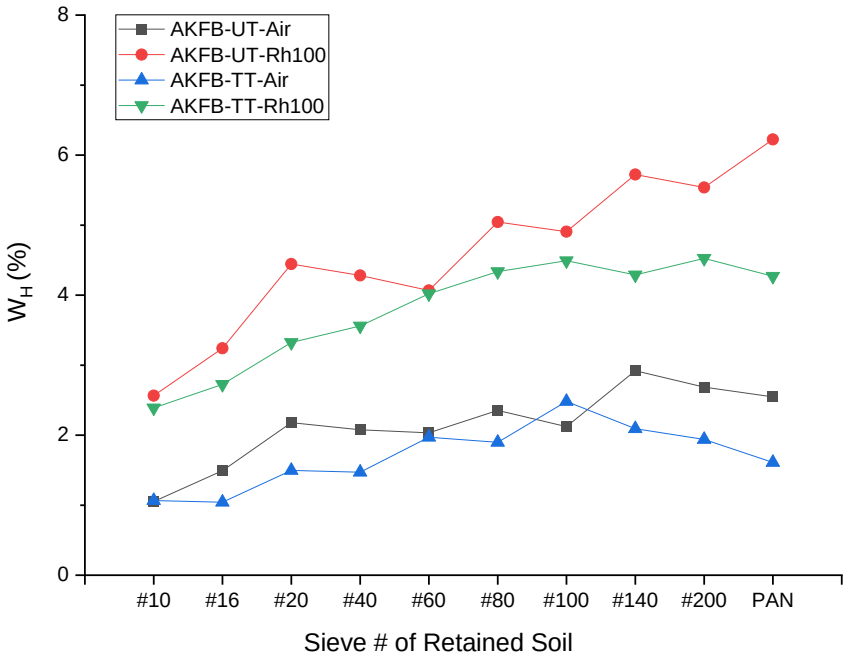

Figure 4-9 Hygroscopic moisture content grain size relationship for treated samples (1:10)

3.5 W_H- Effect of Washing Excess OS

To determine the effect of excess OS on hygroscopy, treated soil samples (1:10) were washed immediately after treatment to remove any excess OS. Each wash was carried out by mixing treated soil at a ratio of 1:3 with DI water in an HDPE bottle and shaking the mixture for 1 hour in a tumbler after which it was left to settle for 24 hours. The supernatant was decanted, and measurements of EC were obtained until they reached an asymptotic value. The values of EC measured with each wash are presented in Figure 9 below.

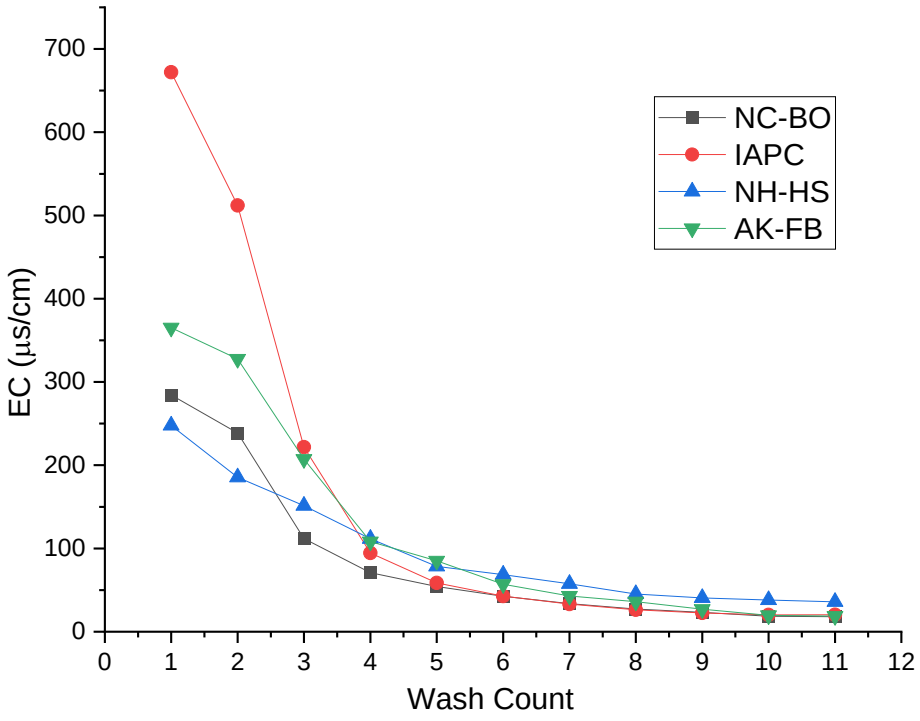

Figure 4-10 Change in Electrical Conductivity with repeated wash cycles

The results of washing the treated soil samples after treatment are observable in a reduced hygroscopic moisture content value (Fig. 10). There is a reduction in the Wh after washing (%) with larger reductions observed in IA-PC. The presence of organic material

in AK-FB makes it difficult to assert the relative contribution of the OS to the hygroscopic properties. The resulting reduction in hygroscopy due to washing is indicative that excess OS in the treated sample is responsible for some moisture absorption. Uduebor (2023) carried out optimization tests on treated samples to determine the optimal treatment dosages using EC and pH as indicators. It was observed that a ratio of 1:50 (OS: Soil) was optimal for all soils treated (indicated by significant increases and decreases in EC and pH respectively).

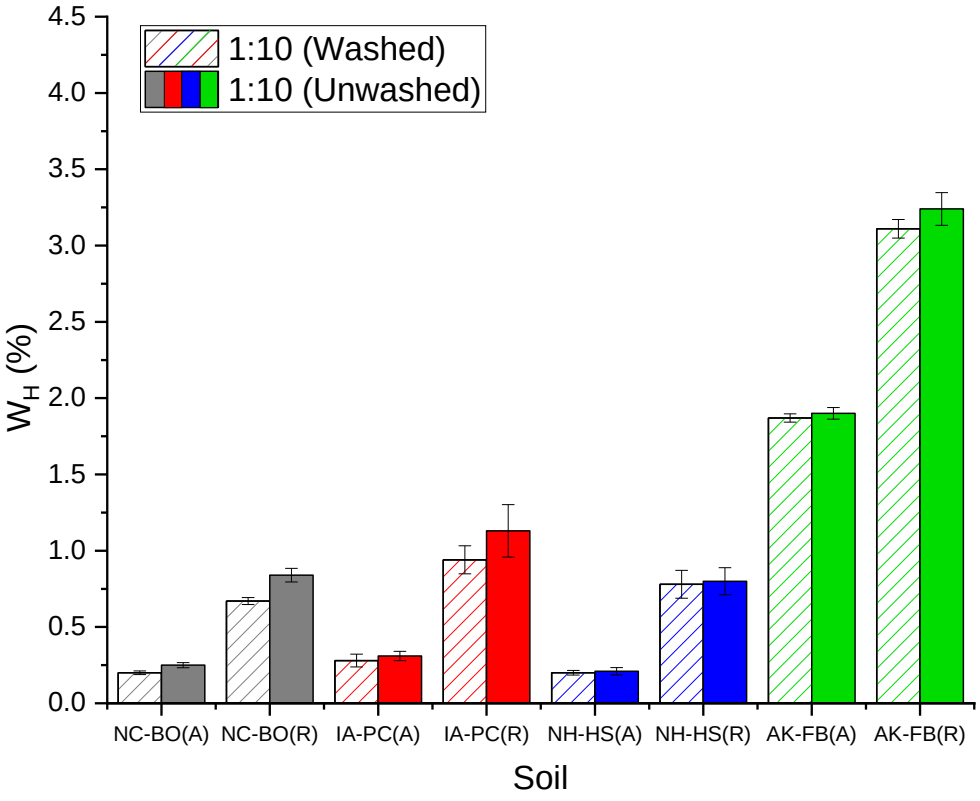

Figure 4- 11 Hygroscopic moisture content of treated samples before and after washing (A is the sample exposed to air, R is the sample exposed to Rh100)

4. Conclusion

Long-term moisture absorption of treated water-repellent fine-grained soils makes the exploration of hygroscopic behavior of paramount significance. This study investigates the relationship between water repellency and hygroscopy within fine-grained soils, particularly the effect of factors such as treatment dosage, drying conditions, grain size, and organic content. The results present the hygroscopic moisture content (W_h) as another pivotal parameter in characterizing the water-repellency of soils with the following summary.

- The Wh of soils is affected by water repellency treatment and reduces with increasing treatment dosage and concentrations. There is a clear relationship between Wh and other measures of water repellency (Contact angle, Water Drop Penetration Time), and is affected by factors including treatment concentration, drying conditions, and the presence of organic constituents.
- The implementation of silanes and siloxanes, which enable vapor migration, poses an inherent limitation on the complete eradication of moisture absorption. This revelation has profound implications for engineering applications, necessitating a nuanced understanding of the temporal behavior of treated soils under varying humidity conditions.
- Regardless of treatment, fine-grained soils, particularly those with clay minerals, still retain a degree of hygroscopic behavior. This challenges conventional assumptions that treatment can completely eradicate hygroscopy in such soils.

- The effect of grain size distribution and organic content on hygroscopicity emerges as a significant consideration for treated soils. The propensity for moisture adsorption is demonstrated to be more pronounced in finer-grained soils, potentially rendering them susceptible to wetting over a period under higher humidity values. Organic content further amplifies this effect, accentuating the hygroscopic nature even in treated soils.

Consequently, this study underscores the pivotal importance of incorporating these factors in the design and deployment of water-repellent soils, particularly those intended for engineering applications.

REFERENCES

Arkles, B., 2011. Hydrophobicity, Hydrophilicity and Silane Surface Modification. Morrisville, PA.

Arkles, B., Steinmetz, J.R., Zazyczny, J., Mehta, P., 1992. Factors contributing to the stability of alkoxysilanes in aqueous solution. J Adhes Sci Technol 6, 193–206. https://doi.org/10.1163/156856192X00133

ASTM, 2012. ASTM D698: Standard Test Methods for Laboratory Compaction Characteristics of Soil Using Standard Effort (12 400 ft-lbf/ft3 (600 kN-m/m3)). ASTM International 3.

Astm, 2000. D5084 - Standard Test Methods for Measurement of Hydraulic Conductivity of Saturated Porous Materials Using a Flexible Wall Permeameter. Astm D5084 04.

ASTM D 854, 2002. ASTM D854 Standard Test Methods for Specific Gravity of Soil Solids by Water Pycnometer. ASTM International 04.

ASTM D2974, 2020. Standard Test Methods for Determining the Water (Moisture) Content, Ash Content, and Organic Material of Peat and Other Organic Soils. ASTM International.

ASTM D7928, 2021. Standard Test Method for Particle-Size Distribution (Gradation) of Fine-Grained Soils Using the Sedimentation (Hydrometer) Analysis. ASTM International.

ASTM International, 2017a. ASTM D4318-17, in: Standard Test Methods for Liquid Limit, Plastic Limit, and Plasticity Index of Soils.

ASTM International, 2017b. D6913: Standard Test Methods for Particle-Size Distribution (Gradation) of Soils Using Sieve Analysis. ASTM International D6913.

ASTM International, 2010. Standard test methods for moisture, ash, and organic matter of peat and other organic soils, TA - TT -. ASTM International West Conshohocken, Pa., West Conshohocken, Pa. SE -. https://doi.org/LK - https://worldcat.org/title/741935120

ASTM International, n.d. D2166 Standard Test Method for Unconfined Compressive Strength of Cohesive Soil [WWW Document]. URL https://www.astm.org/d2166-06.html (accessed 6.15.23).

Behravan, A., Aqib, S.M., Delatte, N.J., Ley, M.T., Rywelski, A., 2022a. Performance Evaluation of Silane in Concrete Bridge Decks Using Transmission X-ray Microscopy. Applied Sciences (Switzerland) 12. https://doi.org/10.3390/app12052557

Behravan, A., Aqib, S.M., Delatte, N.J., Ley, M.T., Rywelski, A., 2022b. Performance Evaluation of Silane in Concrete Bridge Decks Using Transmission X-ray Microscopy. https://doi.org/10.3390/app12052557

Bowman, J.R., Ley, M.T., Sudbrink, B., Kotha, H., Materer, N., Apblett, A., 2012. EXPECTED LIFE OF SILANE WATER REPELLANT TREATMENTS ON BRIDGE DECKS FINAL REPORT ~ FHWA-OK-12-08.

Bray, M.T., Darrow, M.M., 2020. Frost Susceptibility and Strength of Cement-Treated Fine-Grained Soils.

Brooks, T., Daniels, J.L., Uduebor, M., Cetin, B., Wasif Naqvi, M., 2022. Engineered Water Repellency for Mitigating Frost Action in Iowa Soils. https://doi.org/10.1061/9780784484012.046

Carrillo, M.L.K., Yates, S.R., Letey, J., 1999. Measurement of Initial Soil-Water Contact Angle of Water Repellent Soils. Soil Science Society of America Journal 63, 433–436. https://doi.org/10.2136/SSSAJ1999.03615995006300030002X

Chamberlain, E.J., United States, Cold Regions Research and Engineering Laboratory (U.S.)., 1981. Frost susceptibility of soil review of index tests. U.S. Dept. of Transportation Federal Highway Administration Offices of Research and Development ; National Technical Information Service distributor. Hanover, NH 03755.

Chen, C., Hu, K., Arthur, E., Ren, T., 2014. Modeling Soil Water Retention Curves in the Dry Range Using the Hygroscopic Water Content. Vadose Zone Journal 13, vzj2014.06.0062. https://doi.org/10.2136/VZJ2014.06.0062/111668

Chen, C., Zhou, H., Shang, J., Hu, K., Ren, T., 2020. Estimation of soil water content at permanent wilting point using hygroscopic water content. Eur J Soil Sci 71, 392–398. https://doi.org/10.1111/EJSS.12887

Choi, Y., Choo, H., Yun, T.S., Lee, C., Lee, W., 2016. Engineering characteristics of chemically treated water-repellent Kaolin. Materials 9. https://doi.org/10.3390/ma9120978

Daniels, J.L., Hourani, M.S., 2009. Soil Improvement with Organo-Silane, in: U.S.-China Workshop on Ground Improvement Technologies 2009. American Society of Civil Engineers, pp. 217–224. https://doi.org/10.1061/41025(338)23

Daniels, J.L., Langley, W.G., Uduebor, M., Cetin, B., 2021. Engineered Water Repellency for Frost Mitigation: Practical Modeling Considerations. Geo-Extreme 2021 385–391. https://doi.org/10.1061/9780784483701.037--

DeBano, L., 1981. Water repellent soils: a state-of-the-art.

Ding, M., Zhang, F., Ling, X., Lin, B., 2018. Effects of freeze-thaw cycles on mechanical properties of polypropylene Fiber and cement stabilized clay. Cold Reg Sci Technol 154, 155–165. https://doi.org/10.1016/J.COLDREGIONS.2018.07.004

Doerr, S.H., Shakesby, R.A., Walsh, R.P.D., 2000. Soil water repellency: Its causes, characteristics and hydro-geomorphological significance. Earth Science Reviews 51, 33–65. https://doi.org/10.1016/S0012-8252(00)00011-8

Dumenu, L., Pando, M.A., Ogunro, V.O., Daniels, J.L., Moid, M.I., Rodriguez, C., 2017. Water Retention Characteristics of Compacted Coal Combustion Residuals. https://doi.org/10.1061/9780784480434.044

Edgar, T., Potter, C., Mathis, R., 2015. Frost Heave Mitigation Using Polymer Injection and Frost Depth Prediction. Proceedings of the International Conference on Cold Regions Engineering 2015-January, 416–427. https://doi.org/10.1061/9780784479315.037

Federal Highway Administration (FHWA), 1999. Quarter Century of Geotechnical Research, Chapter 4: Soil and Rock Behavior. Report Number: FHWA-RD-98-139, Turner-Fairbank Highway Research Center, McLean VA, USA. .

Feyyisa, J.L., Daniels, J.L., Pando, M.A., Ogunro, V.O., 2019. Relationship between breakthrough pressure and contact angle for organo-silane treated coal fly ash. Environ Technol Innov 14. https://doi.org/10.1016/j.eti.2019.100332

Fink, D.H., Myers, L.E., 1969. Synthetic Hydrophobic Soils for Harvesting Precipitation.

Ghazavi, M., Roustaie, M., 2010. The influence of freeze-thaw cycles on the unconfined compressive strength of fiber-reinforced clay. Cold Reg Sci Technol 61, 125–131. https://doi.org/10.1016/j.coldregions.2009.12.005

Henry, K.S., 1996. Geotextiles to mitigate frost effects in soils: A critical review. Transp Res Rec. https://doi.org/10.3141/1534-02

Johnson, A.W., 1952. FROST ACTION IN ROADS AND AIRFIELDS: A REVIEW OF THE LITERATURE, 1765-1951. Highway Research Board Special Report.

Keatts, M.I., Daniels, J.L., Langley, W.G., Pando, M.A., Ogunro, V.O., 2018. Apparent Contact Angle and Water Entry Head Measurements for Organo-Silane Modified Sand and Coal Fly Ash. Journal of Geotechnical and Geoenvironmental Engineering 144. https://doi.org/10.1061/(ASCE)GT.1943-5606.0001887

Kelley, W.P., Jenny, H., Brown, S.M., 1936. Hydration of minerals and soil colloids in relation to crystal structure. Soil Sci 41. https://doi.org/10.1097/00010694-193604000-00002

Kestler, M.A., Berg, R.L., Steinert, B.C., Hanek, G.L., Truebe, M.A., Humphrey, D.N., 2007. Determining When to Place and Remove Spring Load Restrictions on Low-

Volume Roads. https://doi.org/10.3141/1989-67 2, 219–229. https://doi.org/10.3141/1989-67

Khanzadeh Moradllo, M., Sudbrink, B., Ley, M.T., 2016. Determining the effective service life of silane treatments in concrete bridge decks. Constr Build Mater 116, 121–127. https://doi.org/10.1016/J.CONBUILDMAT.2016.04.132

King, P.M., 1981. Comparison of methods for measuring severity of water repellence of sandy soils and assessment of some factors that affect its measurement. Australian Journal of Soil Research 19. https://doi.org/10.1071/SR9810275

Ksaibati, Khaled, Armaghani, J., Fisher, Jason, Ksaibati, K, Fisher, J, 2000. Effect of Moisture on Modulus Values of Base and Subgrade Materials. Transp Res Rec 20–29.

Kuhn, S., 1932. . ~Jber die Beziehungen zwischen Hygroskopizit~it, adsorbierten Basen und einigen physikalischen Eigenschaften bei BiSden. Z. Pflanzenerniihr., Diing. 359–370.

Kuron, H., 1930. Versuche zur Feststellung tier Gesamtoberfl~iche an Erdb~den, Tonen und verwandten Stoffen. Z. Pflanzenerniihr., Dung 179–203.

Letey, J., Carrillo, M.L.K., Pang, X.P., 2000. Approaches to characterize the degree of water repellency. J Hydrol (Amst) 231–232, 61–65. https://doi.org/10.1016/S0022-1694(00)00183-9

Lourenço, S.D.N., Saulick, Y., Zheng, S., Kang, H., Liu, D., Lin, H., Yao, T., 2018. Soil wettability in ground engineering: fundamentals, methods, and applications. Acta Geotech. https://doi.org/10.1007/s11440-017-0570-0

Mahedi, M., Satvati, S., Cetin, B., Daniels, J.L., 2020. Chemically Induced Water Repellency and the Freeze–Thaw Durability of Soils. Journal of Cold Regions Engineering 34, 04020017. https://doi.org/10.1061/(ASCE)CR.1943-5495.0000223

Maisanaba, S., Ortuño, N., Jordá-Beneyto, M., Aucejo, S., Jos, Á., 2017. Development, characterization and cytotoxicity of novel silane-modified clay minerals and nanocomposites intended for food packaging. Appl Clay Sci 138, 40–47. https://doi.org/10.1016/J.CLAY.2016.12.042

Malisher, M., Daniels, J., Uduebor, M., Saulick, Y., 2023. Compaction and Strength Characteristics of Engineered Water Repellent Frost Susceptible Soils. Geo-Congress 2023 452–461. https://doi.org/10.1061/9780784484661.047

Moiseev, K.G., 2008. Determination of the specific soil surface area from the hygroscopic water content. Eurasian Soil Science 41, 744–748. https://doi.org/10.1134/S1064229308070089/METRICS

Muhammad, N., Siddiqua, S., 2021. Moisture-dependent resilient modulus of chemically treated subgrade soil. Eng Geol 285, 106028. https://doi.org/10.1016/J.ENGGEO.2021.106028

Naqvi, M.W., Sadiq, Md.F., Cetin, B., Adeyanju, E., Daniels, J.L., 2023. Development, Construction, and Instrumentation of Pilot Freeze–Thaw Resistant Granular Roadways Test Cells, in: 13th International Conference on Low-Volume Roads. Cedar Rapids, Iowa, pp. 3–9.

Nourmohamadi, M., Abtahi, S.M., Hashemolhosseini, H., Hejazi, S.M., 2022. Control of frost effects in susceptible soils using a novel sandwich geocomposite composed of geotextile-soil-nano silica aerogel-geotextile liners. Transportation Geotechnics 33, 100718. https://doi.org/10.1016/J.TRGEO.2022.100718

Oluyemi-Ayibiowu, B.D., Uduebor, M.A., 2019. Effect of Compactive Effort on Compaction Characteristics of Lateritic Soil Stabilized With Terrasil. Journal of Multidisciplinary Engineering Science Studies (JMESS) 5, 2458–925.

Prakash, K., Sridharan, A., Sudheendra, S., 2016. Hygroscopic moisture content: Determination and correlations. Environmental Geotechnics 3. https://doi.org/10.1680/envgeo.14.00008

Research Board, T., n.d. National Cooperative Highway Research Program NCHRP Synthesis 278 Measuring In Situ Mechanical Properties of Pavement Subgrade Soils A Synthesis of Highway Practice.

Robinson, D.A., Cooper, J.D., Gardner, C.M.K., 2002. Modelling the relative permittivity of soils using soil hygroscopic water content. J Hydrol (Amst) 255, 39–49. https://doi.org/10.1016/S0022-1694(01)00508-X

Roy, W.R.*., Krapac, I.G.*., Chou, S.-F.J.*., Griffin, R.A., 1992. Technical Resource Document: batch-type procedures for estimating soil adsorption of chemicals. Report.

Salem, H., 2005. Effect Of Seasonal Moisture Variation On Subgrade Resilient Modulus. Improving Pavements With Long-Term Pavement Performance: Products for Today and Tomorrow, November 2005 - FHWA-RD-03-049.

Saulick, Y., Lourenço, S.D.N., Baudet, B.A., 2019. Optimising the hydrophobicity of sands by silanisation and powder coating. Géotechnique 1–10. https://doi.org/10.1680/jgeot.19.p.108

Saulick, Y., Lourenço, S.D.N., Baudet, B.A., Woche, S.K., Bachmann, J., 2018. Physical properties controlling water repellency in synthesized granular solids. Eur J Soil Sci 69, 698–709. https://doi.org/10.1111/ejss.12555

Shah, P.H., Singh, D.N., 2006. Methodology for determination of hygroscopic moisture content of soils. J ASTM Int 3. https://doi.org/10.1520/JAI13376

Simonsen, E., Isacsson, U., 1999. Thaw weakening of pavement structures in cold regions. Cold Reg Sci Technol 29, 135–151. https://doi.org/10.1016/S0165-232X(99)00020-8

Taber, S., 1930. The Mechanics of Frost Heaving. J Geol 38. https://doi.org/10.1086/623720

Torrent, J., Del Campillo, M.C., Barrón, V., 2015. Short communication: Predicting cation exchange capacity from hygroscopic moisture in agricultural soils of Western Europe. Spanish Journal of Agricultural Research 13, e11SC01-e11SC01. https://doi.org/10.5424/SJAR/2015134-8212

Uduebor, M., Adeyanju, E., Saulick, Y., Daniels, J., Cetin, B., 2023. Engineered Water Repellency for Moisture Control in Airport Pavement Soils. Airfield and Highway Pavements 2023 92–102. https://doi.org/10.1061/9780784484906.009

Uduebor, M., Adeyanju, E., Saulick, Y., Daniels, J., Cetin, B., 2022a. A Review of Innovative Frost Heave Mitigation Techniques for Road Pavements. International Conference on Transportation and Development 2022. https://doi.org/10.1061/9780784484357

Uduebor, M., Daniels, J., Mohammad, N., Cetin, B., 2022b. Engineered Water Repellency in Frost Susceptible Soils 457–466. https://doi.org/10.1061/9780784484012.047

Uduebor, M.A., Daniels, J.L., Adeyanju, E., Sadiq, Md.F., Cetin, B., 2023. Engineered Water Repellency for Resilient and Sustainable Pavement Systems. International Journal of Geotechnical Engineering. https://doi.org/10.1080/19386362.2023.2241280

U.S. Army Corps of Engineers, 1965. Soils and geology- Pavement design for frost conditions. Department of the Army courses Department of Civil Engineering, University of New Technical Manual TM 5-818-2.

US Army Corps of Engineers, 1965. Soils and Geology – Pavement Design for Frost Conditions. Hanover, NH.

Wasif Naqvi, M., Sadiq, Md.F., Cetin, B., Uduebor, M., Daniels, J., 2022. Investigating the Frost Action in Soils. Geo-Congress 2022 257–267. https://doi.org/10.1061/9780784484067.027--

Wuddivira, M., Robinson, A., Lebron, I., Brechet, L., Atwell, M., De Caires, S., Oatham, M., Jones, S., Abdu, H., Verma, A., Tuller, M., 2012. Estimation of Soil Clay Content from Hygroscopic Water Content Measurements. Soil Science Society of America Journal 1529–1535. https://doi.org/10.2136/sssaj2012.0034

Zaman, M.W., Han, J., Zhang, X., 2022. Evaluating wettability of geotextiles with contact angles. Geotextiles and Geomembranes 50, 825–833. https://doi.org/10.1016/J.GEOTEXMEM.2022.03.014

CHAPTER 4: HYDRAULIC AND STRENGTH PROPERTIES OF ENGINEERED WATER REPELLENT SOILS

ARTICLE 5: AN AUTOMATED TECHNIQUE FOR MEASUREMENT OF WATER ENTRY PRESSURE IN HYDROPHOBIC SOILS

ABSTRACT

Water-repellent soils have been increasingly applied in solving civil engineering problems, with one of the most critical engineering properties being the Water Entry Pressure or Breakthrough Pressure (WEP/BP). The WEP/BP represents the pressure level at which water can permeate through the treated soil. Therefore, the breakthrough pressure is an essential parameter in determining the efficacy of water-repellent soil material as a moisture barrier in various engineering practices such as embankments and pavements, cover and liner systems for landfills, slopes, etc. While several methods have been proposed to measure WEP/BP in water-repellent soils, they often have limitations that impact their accuracy. Additionally, there is no consensus on the criteria for determining breakthrough pressure, making it difficult to define specifications for using water-repellent soils in engineering practice. This paper presents an automated test method for determining the breakthrough pressure of water-repellent soils while addressing limitations like side leakage, uneven compaction, and instrumentation constraints encountered in previous studies. It also provides a definition for breakthrough in water-repellent soils, and it establishes a basis for determining WEP based on volume, which can be utilized to specify the use of water-repellent soils in engineering applications. Two soils treated with a commercially available organosilane at varying dosages (1:1000, 1:100, 1:10) were found to be water-repellent with contact angles ranging from 102^{o} to 143^{o}. Breakthrough pressures of up to 36kPa are obtained for the soils. Hydrostatic creep tests revealed that treated soils can sustain a hydrostatic head below the breakthrough pressure. The improved accuracy of WEP/BP measurement via automation of the testing process using this method can aid in specifying the use of water-repellent soils in various civil engineering applications, particularly in controlling moisture penetration in construction applications.

Keywords

Water, Entry, Pressure, Breakthrough, Repellency, Soils, Volume, Test, Method

1. Introduction

Water-repellent soils – that prevent the normal infiltration of water via a hydrophobic surface coating are finding applications in solving civil engineering problems. While hydrophobicity in soils was first observed in soil science with studies carried out on its impacts on plant growth, soil erosion, and hydrology (DeBano, 1981; Debano, 2015), it has been embraced and engineered in soils to meet different engineering requirements and for a variety of engineering applications including barrier systems for reducing contaminant leaching (Dumenu et al., 2017; Feyyisa, Daniels, Pando, & Ogunro, 2019), stabilization of road pavements (Brooks, Daniels, Uduebor, Cetin, & Wasif Naqvi, 2022; Uduebor, Adeyanju, Saulick, Daniels, & Cetin, 2022), erosion mitigation (Daniels & Hourani, 2009a), cover for large bodies of water to prevent evaporation (Debano, 2015)

As solutions begin to be developed using water-repellent soils in engineering practice, it is essential to develop parameters for measuring the performance of these treated soils and provide specifications for their use. There are different methods to define the extent of water repellency in hydrophobic soils of engineering interest – Contact Angle (CA), Water Drop Penetration Time (WDPT), etc. but one crucial test, particularly important for using hydrophobic soils in barrier applications is the Water Entry Pressure or Breakthrough Pressure test (WEP/BP) - this is the critical pressure at which water can permeate through hydrophobic soil (Feyyisa et al., 2019). This pressure is theoretically equal to or greater than the negative value of capillary rise obtainable for water-repellent soils. This is due to intermolecular forces interacting between the hydrophobic soil surface, air, and water, creating a Laplace pressure that prevents water infiltration into the soil pores (Lourenço et al., 2018). Capillary water entry pressure can be defined in terms of the

Washburn equation (Washburn, 1921a, 1921b) which was initially designed for wettable surfaces.

$$BP(WEP) = -\frac{2\sigma cos\,(\theta)}{r} \qquad (1)$$

where σ is the surface tension between the wetting and non-wetting phase; θ is the contact angle (CA) formed between a liquid/gas and material surface, and r is the pore radius. Other relationships between the WEP and contact angle are available in the literature (Kloubek, 1981; Rigby & Edler, 2002), and are variations of Equation 1 above. Fig 1 shows the difference between the capillary rise in wettable and hydrophobic soils. Where d is the pore/capillary diameter; h_c is the height of capillary rise/fall; θ_P is the contact angle between the liquid and pore/capillary material. For wettable surfaces, the more wettable the surface or pore space, the higher the capillary rise, while capillarity reduces with increasing CA. This phenomenon contributes to resistance to infiltration and penetration into water-repellent soils.

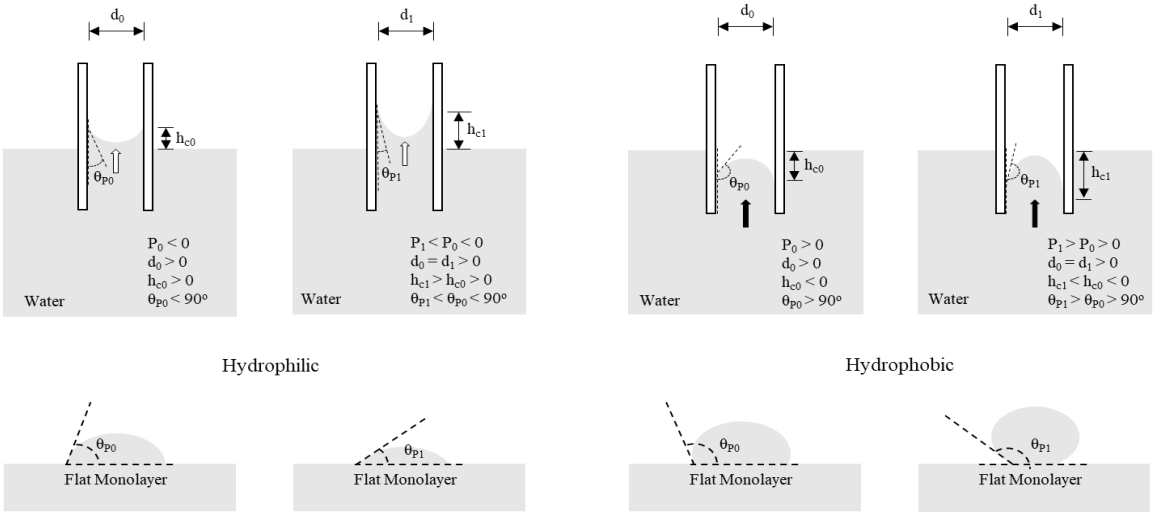

Figure 5-1 Idealized sketch of the difference in the capillary rise within hydrophilic and hydrophobic pore spaces.

Determination of the WEP is essential for civil engineering design because it determines the limits of usage and application of a particular treated soil material. Water-repellent soils will hinder and or prevent the infiltration and flow of water through them up to a critical pressure (WEP) beyond which flow is possible. So, it is essential to know the limits of the treatments carried out, define the extent of their use, and the factor of safety required in engineering applications. But all these can only be done if there is a standard method for testing such soils with a good amount of accuracy, and repeatability.

Several methods have been proposed for the measurement of WEP in water-repellent soils (Carrillo, Yates, & Letey, 1999; Feyyisa et al., 2019; Letey, Carrillo, & Pang, 2000; Lourenço et al., 2018; Watson CL & Letey J, 1970). While there is no consensus on what connotes water entry, the different test methods are mostly carried out to compare untreated and treated soils and/or soils at different levels of treatment to give a correlation between treatment and improved resistance to penetration of these soils. Many test methods in literature have also identified flaws and drawbacks - seepage through edges of a rigid wall, human error in visually monitoring the volume change, and uneven compaction of soils due to instrumentation – that make achieving accuracy, precision, and repeatability difficult, while also proffering creative solutions to mitigate the effects (Keatts, Daniels, Langley, Pando, & Ogunro, 2018; Saulick, Lourenço, & Baudet, 2016; Xing, Saulick, & Lourenço, 2022). All these coupled with an undefined measurement criterion for defining WEP make it difficult to present specifications for the use of water-repellent soils in engineering practice. This paper describes an automated test method for determining the WEP of water-repellent soils with accuracy and a lower margin of error. It also proposes a definition of a specified volume for the determination of

breakthrough/water entry for water-repellent soils and provides a basis for determining WEP with more consistent results.

2. Existing methods for measuring water entry pressure

Several test experiments have been carried out to determine the water entry pressure in hydrophobic soils. Table 1 below shows some of the different experiments carried out in the literature.

Table 5-1 Summary of some common WEP Test Methods

Authors	**Test Method**	**Rate**	**Material**	**Results (cmH_2O)**
(Carrillo et al., 1999)	Water Ponding (WP) - Constructed with polypropylene tube,	0.286 cmH_2O/sec	Two different Carsitas gravelly sand	2.4 - 13.4 cmH_2O
(Xing et al., 2022)	electrodes, and a pressure transducer	0.11 cmH_2O/s	Fujian sand, glass beads and crushed glass	2 - 33 cmH_2O
(Keatts et al., 2018)	Water Ponding (WP) - Rigid Wall Permeameter	1cmH_2O/10s (Sand) 5cmH_2O/10s (CFA)	Sand, Coal Fly Ash (CFA)	0 - 542 cmH_2O
(Feyyisa et al., 2019)	Water Ponding (WP) - Rigid Wall Triaxial setup	3.4kPa/s (Ramped)	Five types of Coal Fly Ash (CFA)	75-1000 cmH_2O
(Wang, Wu, & Wu, 2000)	Tension-pressure infiltrometer method	N/A	Sand, Loamy Sand	2-12 cmH_2O
Dumenu (2019)	Water Ponding (WP) - Flexible Wall Triaxial setup	3.4 kPa/s (Ramped)	Coal Fly Ash (CFA)	270 275cmH_2O

*N/A - not applicable

2.1 Water Ponding Method

The most widely used method is the water-ponding (WP) method (Carrillo et al., 1999; Keatts et al., 2018; Lourenço et al., 2018; Xing et al., 2022). The basic principle involves the application of a head of water on the hydrophobic soil surface, advancing it in small increments until infiltration into the soil. It is widely embraced because of its

simplicity and ease of design and different versions of the WEP abound in the literature. In many cases, the soil is packed into a rigid wall tube or permeameter mold, and pressure is applied using a transducer, Marriott tube or simply adding water to a burette or manometer. The infiltration of water into the soil is observed by a noticeable drop in head or pressure measured by placing transducers to measure a drop in the pressure (usually placed just above the soil water interface) or by visual observation of a drop in the volume of water within a burette, manometer, or Marriot tube after a particular head has been determined.

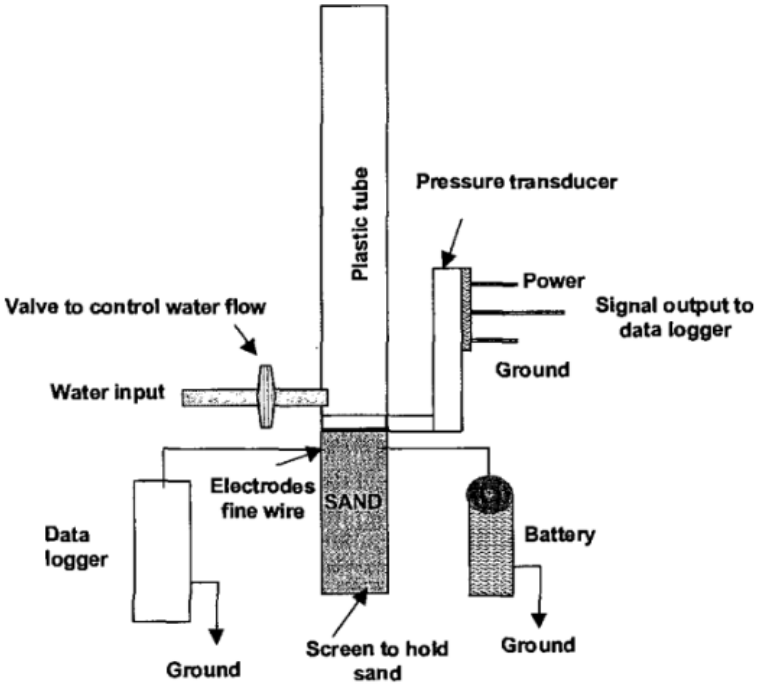

Figure 5-2 Schematic showing the Water Ponding test setup (Carrillo et al., 1999)

In many tests, sensors are placed within the soil, monitoring moisture content, dielectric constants, or electric conductivity to determine the moisture change and hence infiltration through the soil at successive head increments (Letey et al., 2000). The exact

positioning of these sensors varies from test to test, with each possessing its advantages and resulting issues. Sensors placed close to the test surface (Carrillo et al., 1999) generally give closer values to the actual WEP than sensors placed at the bottom of the soil (Lee, Yang, Yun, Choi, & Yang, 2015) which grossly overestimates the actual value because of the time taken for moisture to get to the sensor location.

While this test method is simple to carry out, several issues affect the repeatability of the results produced. In many cases, there is preferential infiltration through the edges of the walls of the containing chamber resulting in variations in results. In some tests, variations in results of up to 950cmH_2O (93.2kPa) have been observed for the same test sample. To mitigate this, the inside walls of the rigid tubes are made hydrophobic (Lee et al., 2015; Xing et al., 2022) or bentonite is added (Keatts et al., 2018) to limit leakage through the edge. Secondly, there is no standard for the positioning of pressure transducers and/or moisture detection sensors. Placing the sensors too close to the surface results in uneven compaction with the sensors themselves could provide a preferential point of infiltration when placed within compacted soil or compacted into the soil. Also placing the sensors at varying depths in the soil will result in different values of the WEP.

2.2 Tension-pressure infiltrometer method

Infiltrometers have also been utilized as well to determine the WEP (Brooks et al., 2022), whose principle is based on suction forces between the device and the soil. The test involves placing the infiltrometer directly on the soil surface with the saturated infiltrometer porous disk serving as an interface. The suction pressure in the infiltrometer is gradually reduced using a Marriot tube or bubble tower and the WEP is reached when

the suction pressure from the soil is greater than that in the tube, resulting in water infiltrating the specimen (observable by bubbles within the infiltrometer tube). Major challenges with this method include obtaining a perfect seal with the soil surface, particularly when testing coarse-grained soils (particularly suited for fine-grained soils), and the limited pressure head obtainable from these devices. WEP of up to 1000 cmH_2O has been obtained in literature (Feyyisa et al., 2019), which makes this method impracticable for a large variety of tests. Also, manual control of the Marriot or bubble tube introduces human error into the test setup.

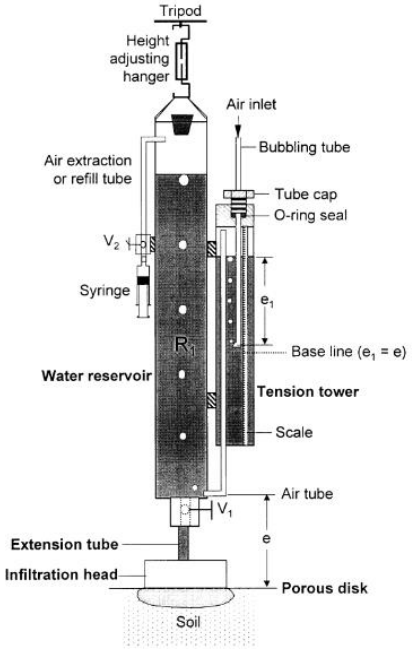

Figure 5-3 Tension-pressure infiltrometer method for measurement of water-entry value (Wang et al., 2000)

2.3 Triaxial Cell Pressure Method

Feyyisa et al., (2019) made use of a sealed rigid wall setup and a Flowtrac to ramp pressure (at a rate of 3.4kPa/s) through a water-repellent sample. The WEP was determined

as a function of pressure, with the maximum pressure determined from the maximum value in the change in the head with respect to time (dP/dT). The setup provides a repeatable test method and allows the use of compacted specimens without any intrusion by probes or sensors. It still has some flaws of utilizing a rigid wall for testing and the study reports several tests failing due to poor tightening of the top cover or sealant. Dumenu (2019) improved this method by placing the sample within a flexible wall permeameter and applying a confining pressure to ensure there is no leakage or preferential flow through the edges observed in rigid wall tests. The test is set up flexible wall permeameter setup as described in ASTM, D5084, with the difference being the soil sample is dry. The same principle of ramping pressure and determining the WEP as a function of the change in the head with respect to time is adopted.

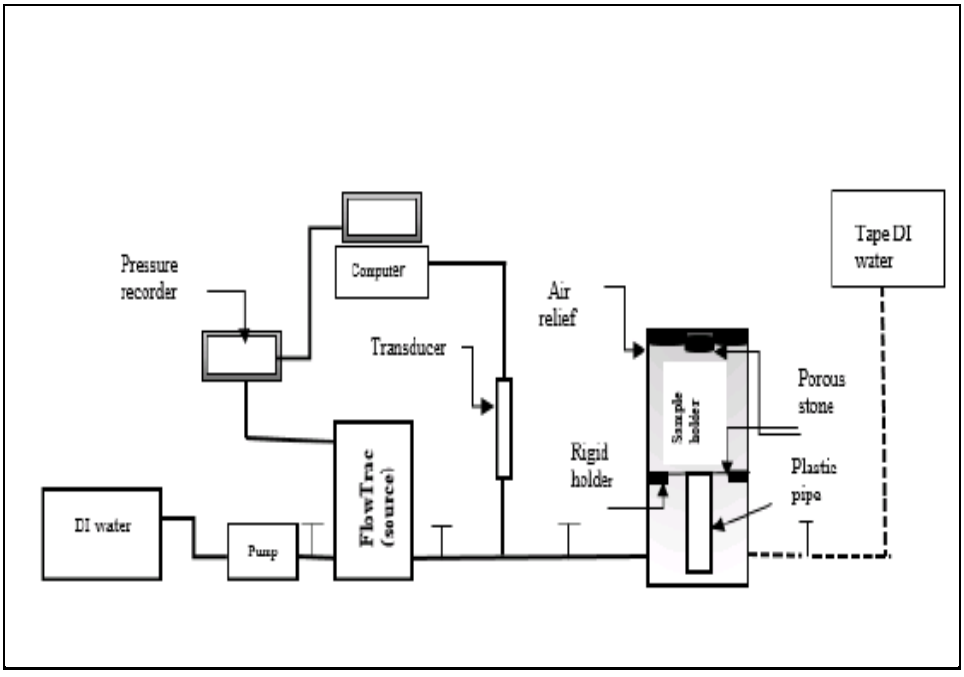

Figure 5-4 Triaxial Cell Pressure Method (Feyyisa et al., 2019)

While these tests serve as a significant improvement to the test method, quick ramping of the pressure gives a higher WEP than the true value of the WEP. Faster rates will

generally produce higher values because there is no radial equilibrium of the pressure over the sample area, instead, the pressure is advanced at points (finger flow) across the surface of the sample resulting in variations in results as pressure is advanced unevenly through the specimen. Lower flow rates (0.05 – 0.5 cmH_2O/s) are generally advised to allow for equilibrium across the tested area.

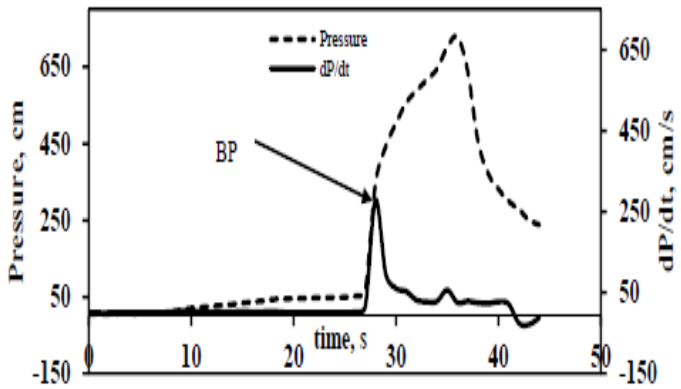

Figure 5-5 Pressure measurement and its rate of change to identify breakthrough pressure point.

Many tests make use of static pressure measurements – where a certain pressure is maintained for a time interval and then advanced further (Keatts et al., 2018), while others ramp up the pressure at a predefined rate using automated equipment (Feyyisa et al., 2019). While many water ponding tests described in literature utilize the former, they present the pressure sustained over a time period as a rate. The time interval selected affects the equilibration of pressure across the sample surface area. It also affects the determination of the effect of ponding time on infiltration through the specimen, which ultimately affects WEP results. There is no standard test interval for maintaining pressures before advancement or specific flow rates. Various tests have utilized various pressure increment durations (See Table 1). This issue can only be resolved by having a standard test method

for the determination of WEP from which further testing can be carried out to determine test duration effects on the results and determine a suitable interval for laboratory testing that will have engineering importance for field applications.

3. Determination of Breakthrough Volume

While traditional convention specifies breakthrough to be the hydrostatic pressure at which water permeates through a sample, it is as always been measured either by a change in pressure (ΔP) or a change in volume (ΔV). Many testing methodologies described earlier employ this change in pressure or volume under an applied hydrostatic head as an indication of flow into and through a tested sample. Many tests carried out either specify an arbitrary volume (or depth of infiltration) or a visible pressure drop (usually greater than 1mmH_2O).

While this concept is simple and practical for testing purposes, it creates another variable to consider while testing. For instance, a 0.1cm drop in the head from two burettes of different sizes will mean a different volume that has infiltrated into the soil sample, even though the pressure drop is the same. Also, because soil unlike other materials, like textiles and geosynthetics, soil is made up of non-uniform solids and voids (See Fig 6), the change in volume and resulting decrease in pressure can be a result of water filling up the top void space of the compacted soil grains. For there to be a breakthrough through a sample, all the void spaces within the top half of the filled space first need to be filled up. This volume filling the top void space could be misread as the breakthrough pressure due to a volume decrease in the reading tube, particularly for larger-grained soils which have a larger pore space. There is a need to determine the “Breakthrough Volume” above which breakthrough

has occurred respective to different soil samples.

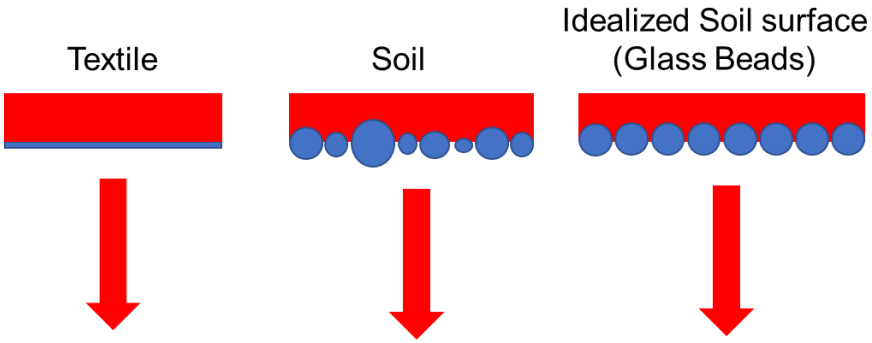

Figure 5-6 Schematic showing difference in void spacing over different materials.

To determine an appropriate breakthrough volume, consider a soil section made up of uniform soil grains below (Fig 7a). Initially, water under hydrostatic head ponds on the surface of the water-repellent soil grains (7b). As the pressure increases, water is forced into the void spaces on the top half of the soil grains, resulting in a decrease in the head, as well as a volume change (7c). This does not necessarily mean that water has broken through the soil. Breakthrough can only occur if water under an increased head passes through the void spaces beyond the soil grains, conservatively, a breakthrough can be achieved after half of the void space within the soil grains begin to be filled (7d)

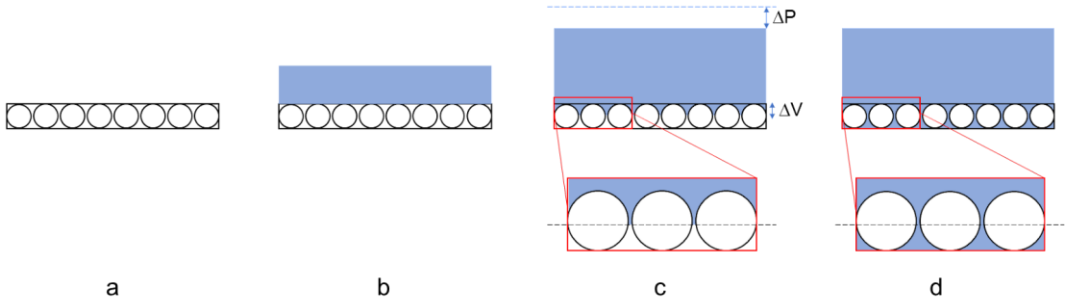

Figure 5-7 Idealized flow through water-repellent soil under hydrostatic pressure.

Considering the arrangement of soil grains within a cylindrical specimen below with radius, r_s, and maximum height being the diameter of soil grains of uniform diameter D_g

($2r_g$). If the total void space is denoted by V_v, the required volume for breakthrough is $0.5V_v$. V_v is calculated as

$$V_v = V_t - V_s \qquad (2)$$

Where V_t is the total volume and V_s is the volume of solids within the total volume. Total volume V_t is

$$Vt = \pi r_s^2 D_g \qquad (3)$$

The volume of solids is given as the sum of the volume of the individual uniform soil grains with diameter D_g ($2r_g$). The volume of one grain, V_g, (assuming a sphere) is given as

$$V_g = 1.333\pi r_g^3 \qquad (4)$$

The total number of grains, N_g, within the sample area is given as

$$N_g = 0.83(r_s^2/r_g^2) - 1.9 \qquad (5)$$

Volume of solids, V_s, is calculated as

$$V_s = [0.83(r_s^2/r_g^2) - 1.9] * [1.333\pi r_g^3] \qquad (6)$$

Therefore,

$$V_v = [\pi r_s^2 D_g] - [0.83(r_s^2/r_g^2) - 1.9] * [1.333\pi r_g^3] \qquad (7)$$

This can be rewritten as

$$V_v = [\pi r_s^2 D_g] - [3.32(r_s^2/(D_g)^2) - 1.9] * [10.664\pi(D_g)^3] \qquad (8)$$

Breakthrough volume can be calculated as

$$0.5V_v = 0.5* [[\pi r_s^2 D_g] - [3.32(r_s^2/(D_g)^2) - 1.9] * [10.664\pi(D_g)^3]] \qquad (9)$$

For non-uniform soil grains, either D_{60}, D_{30} or D_{10} can be utilized, representing the fraction of the soil. This can be selected based on the grain size distribution of the soil sample. D_{10} will give a conservative estimate of the breakthrough volume, while D_{60} will provide an

average estimate.

An alternative determination of the breakthrough volume based on user specifications can be utilized for engineering applications. Calculations based on breakthrough pressure test setups utilized in the literature place the average breakthrough volume at ~0.1cc (1mm drop in a burette with an internal diameter of 1cm). This can be utilized as performance criteria where calculations cannot be made. It can also be changed depending on criteria and the engineering use of the treated material.

4. Materials and Methods

4.1 Materials

4.1.1 Soils

Two frost susceptible soils selected from Pottawaine County, Iowa (IA-PC), and Boone County, North Carolina (NC-BO) were utilized in this study. Index property tests were carried out according to (ASTM D854; ASTM D7928; ASTM D4318) and the soils were classified as silty clay and silty sand respectively. Table 1 shows the summary of index tests carried out as well as the frost susceptibility based on (Chamberlain, United States, & Cold Regions Research and Engineering Laboratory (U.S.)., 1981)

Table 5-2 Summary of Soil Index Properties and Classifications

Soil Property	SOIL	
	IA-PC	**NC-AS**
Specific Gravity, Gs	2.74	2.65
% Passing #4 Sieve (4.75 mm)	100	89.51
% Passing #10 Sieve (2mm)	99.8	73.32
% Passing #40 Sieve (0.425 mm)	99.6	67.08
% Passing #200 Sieve (0.075 mm)	98.4	30.52
Silt content (%) (75μm–2μm)	86.67	26.47
Clay content (%) (< 2μm)	11.69	4.05
USCS Classification	CL	SM/SC
AASHTO Classification	A-6	A-4
Frost Susceptibility Classification	F3	F3

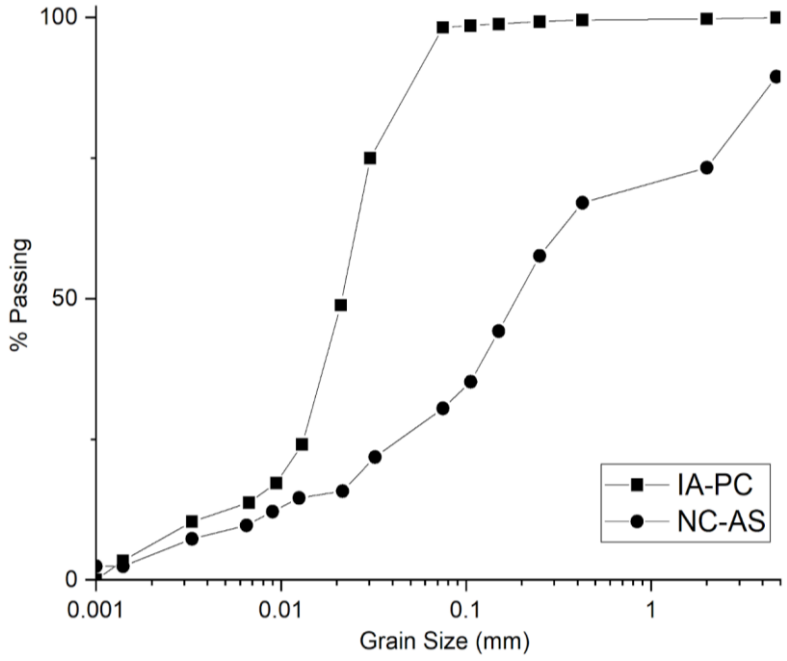

Figure 5-8 Grain Size Distribution of Soil Samples

Based on the calculations in equation 9, the values of breakthrough volume are given in Table 2 below based on D_{60}, D_{30}, or D_{10}. The breakthrough volumes are lower for the IA-PC because they contain finer soil grains than NC-BO which has larger grains.

Because over 90% of IA-PC passes through the #200 sieve, the values of the breakthrough volume using either D_{60}, $D_{30,}$ or D_{10} are smaller when compared to that of NC-BO. A user specification of 0.1cc is also selected for comparison.

Table 5-3 Breakthrough Volumes calculated.

Soil	**D_{60}(mm)**	**D_{30}(mm)**	**D_{10}(mm)**	**Breakthrough Volume (BTV), cc**			
				BTV_{60}	**BTV_{30}**	**BTV_{10}**	**User Spec.**
NC-AS	0.3	0.07	0.006	0.465	0.108	0.009	0.1
IA-PC	0.023	0.014	0.0012	0.036	0.022	0.002	0.1

4.1.2 Organosilane

The soil was treated with a commercial grade organosilane (OS) product. It is a viscous, water-soluble, and reactive soil modifier that permanently modifies the soil surface, making it hydrophobic (Malisher, Daniels, Uduebor, & Saulick, 2023). It has been also utilized in previous studies as a soil modifier and performance enhancer, particularly in stabilization for pavement applications (Brooks et al., 2022; Daniels & Hourani, 2009b; Oluyemi-Ayibiowu & Uduebor, 2019)

4.2 Method

4.2.1 Sample preparation and assessment

Samples were treated and prepared according to ASTM D5084 (Standard Test Methods for Measurement of Hydraulic Conductivity of Saturated Porous Materials Using

a Flexible Wall Permeameter), compacted at optimum moisture content and maximum dry density using a mixture of the OS at dosages of 1:10, 1:100 and 1:1000 (OS: Soil) mixed with deionized water (EC ~ 1µS/cm) and utilized as the molding moisture. Each sample specimen had an average diameter of 33mm and a height of 70mm. Both the diameter and height of sample specimens were more than six times greater than the largest particle size (4.75mm). After the preparation of the samples, the bulk density, as well as the moisture contents, were determined to ensure they met with at least 95% of the MDD. The samples were dried in an oven at 60^{o}C for 24 hours, to achieve maximum water repellency and afterward cooled and air dried for another 12 hours to ensure there is no pseudo-repellency due to drying in an oven.

About 40g of the treated sample was collected to determine the amount of hydrophobicity imparted. Contact Angle (CA) and Water Drop Penetration Time (WDPT) time tests were carried out. Contact Angle tests directly measure the soil-water contact angle based on the sessile drop method using a Goniometer (Brooks et al., 2022; Uduebor, Daniels, Naqvi, & Cetin, 2022), while the WDPT tests measure the persistence of hydrophobicity. Contact angle measurements less than 90^{o} are considered wettable/hydrophilic, while angles measured between 90^{o} and 150^{o} are considered hydrophobic. Angles above 150^{o} are taken to be super hydrophobic. Previous studies (King, 1981) categorize water repellency based on corresponding WDPTs as follows; non-repellent/Completely wettable (≤1s), slightly repellent (1-60s), strongly repellent (60-600s), severely repellent (600-3600s) and extremely repellent (≥3600s).

4.2.2 Specimen Setup

The sample was placed in a triaxial cell base fitted with saturated porous stones and filter paper (Figure 9). The porous stones and filter paper utilized at the top before the top platen is placed were not saturated to prevent restriction of airflow out of the specimen. A membrane expander was utilized to place a membrane around the specimen and O-rings were placed with an O-ring expander to seal the membrane to the base and the top cap. The permeameter cell was set up and filled with distilled water and a confining pressure was applied while the valve to the top cap remains open to allow the outflow of air from the sample within the membrane.

An initial "flushing" pressure (0.5kPa) is applied through the base of the setup using a FLOWTRAC II (Geocomp) to ensure there is no air trapped between the porous stones and the sample. This was done until there were no visible air bubbles within the base outflow flush line. A base pressure of 0.01kPa was also applied to the sample. This was to ensure that the entire base of the sample is duly saturated and to prevent any air pockets from forming below.

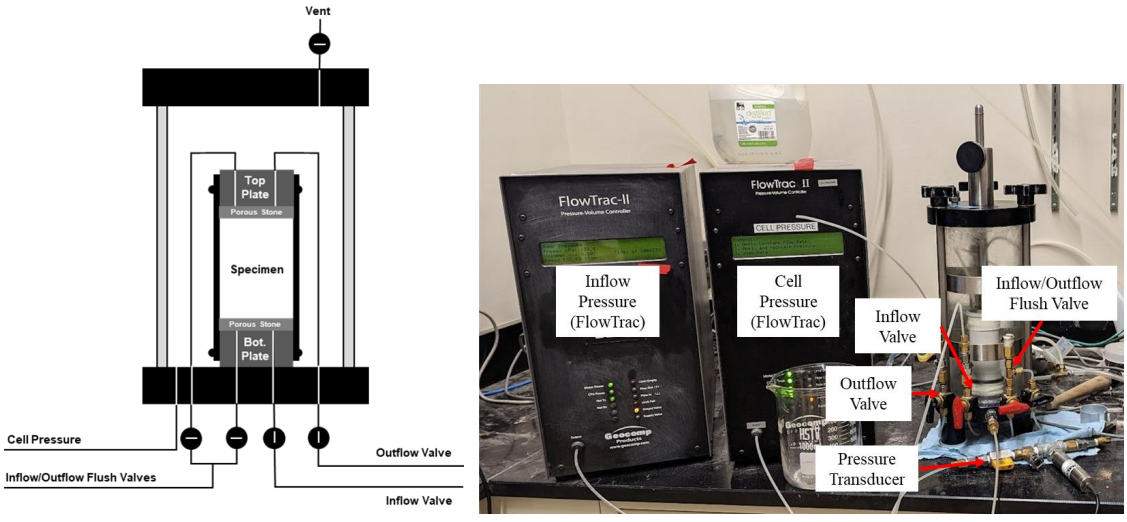

Figure 5-9 Schematic and assembly of Test Cell setup using flexible wall permeameter.

4.2.3 Specimen testing

A back pressure of 0.1kPa was applied to the sample using the FLOWTRAC II and kept constant for 5 minutes (selected to ensure there is equilibration of pressure over the surface of the sample) and the volume of water flowing into the specimen was measured. The pressure was incrementally increased at 0.1 kPa intervals till 1kPa and at 1kPa intervals till there was a breakthrough into the soil sample (smaller increments ~0.001kPa, are achievable with the equipment). When breakthrough occurs within the specimen, the previous pressure increment before water entry was selected as the breakthrough pressure. This was done because there is a large interval of 1kPa between pressure increments. The test was continued for another two pressure increments to confirm the breakthrough volume is exceeded and at set pressures (15kPa, 20kPa, 50kPa, and 100kPa) before the test was ended.

Samples were also tested under hydrostatic creep pressure loading to determine the effect of ponding overtime on the treated samples. The samples were tested at pressures of 0.5kPa, 1kPa, 5kPa, 10kPa, and 50kPa respectively for a duration of 24 hours (1440 minutes).

5. Results and Discussion

5.1 Water Repellency Assessment

Figure 10 below shows the result of contact angles and water drop penetration time test with varying OS concentrations. Treated samples had varying degrees of hydrophobicity after treatment. Contact angles correlated well with treatment dosages, with

a decrease in contact angle with decreasing OS concentration and all treated soil had very high contact angles (>102^{o}). The hydrophobicity imparted was persistent even at lower concentrations (1:1000), with results showing the treated samples as extremely water-repellent (>3600) at all levels of treatment.

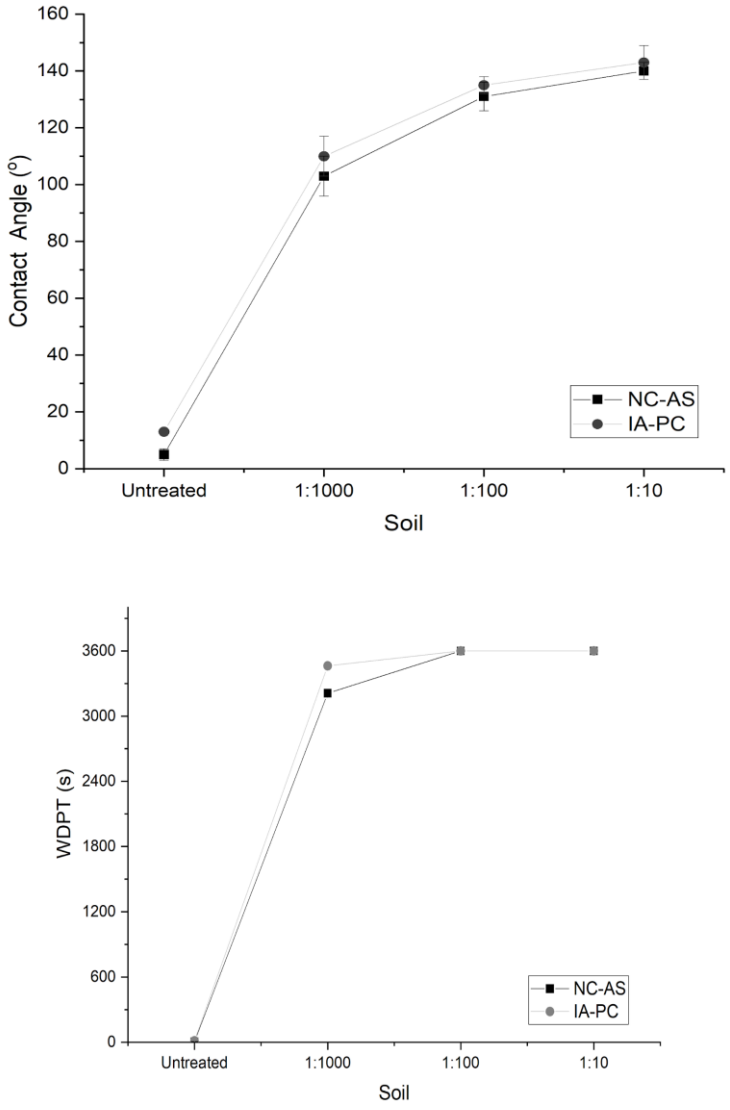

Figure 5-10 (a) Contact Angles and (b) Water Drop Penetration Time test results of soils with varying treatment dosage concentrations.

5.1.1 Sample Wettability

There is an observable difference in the wettability of treated samples when compared to untreated samples. Treated samples remain dry when mounted on the bottom platen, there is also a positive increase (+0.2kPa - +0.7kPa) in the pressure reading from the sensor indicating a positive pressure applied to the system. The reverse is observed for the untreated sample. There is noticeable wetting at the base of the sample and a reduction in the pressure reading on the sensor (-0.2kPa - -1.2kPa), indicative of suction forces within the capillary pores of the sample.

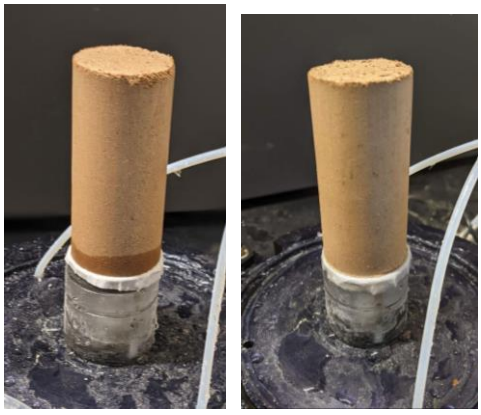

Figure 5-11 Samples showing wetting on the untreated and no wetting on the treated sample.

5.2 Breakthrough Pressure

A typical result from the breakthrough test is shown in Fig 12 below. There is an increase in the volume of water entering the treated sample with the rise in pressure. The corresponding volume increment with increasing pressure was calculated and the breakthrough pressure was selected based on the test protocol outlined previously.

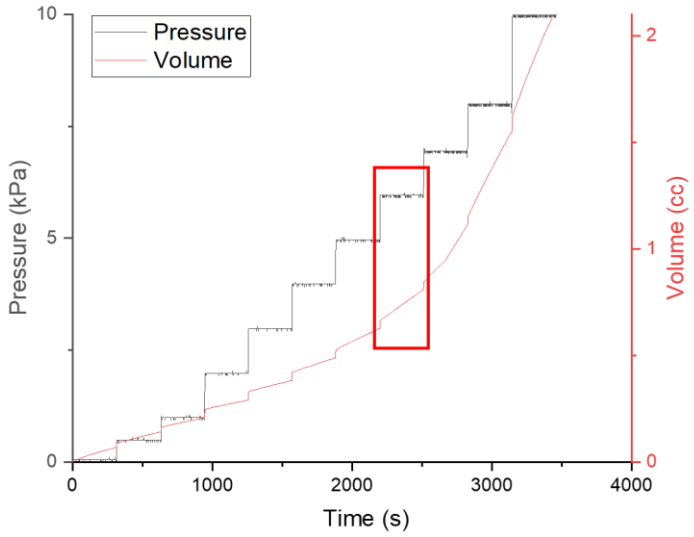

Figure 5-12 Test Result from Breakthrough Pressure Test (0.1cc volume is achieved at 6kPa, 5kPa is selected)

Figure 13 shows the volume of water entering the treated (at different treatment dosages) and untreated soils (NC-AS, IA-PC) with respect to pressure. The respective breakthrough criteria selected from Table 2 are also identified. The untreated sample has water entry exceeding any of the breakthrough criteria even at low pressures (0.1kPa), while for the treated sample there is an increase in the pressure required to break through the treated soil with an increase in organosilane treatment. Water repellency, characterized by reducing volume entry also improves with increasing dosage treatment at all pressures. This is largely due to an increase in the surface energy repelling the wetting of the soil particle surface. Previous studies have shown that at the same density or pore size, the contact angle, and water drop penetration time increase with respect to increasing surface treatment up to a maximum (Xing et al., 2022). There is also a marked difference between the breakthrough pressures of the silty sand and the clayey silt material, with IA-PC possessing higher breakthrough pressures compared to NC-AS. This is due to the smaller

grain sizes and equivalent pore size which improves the water repellency properties. Studies have shown that at constant treatment dosage, there is an increase in water repellency with decreasing pore size (Xing et al., 2022)

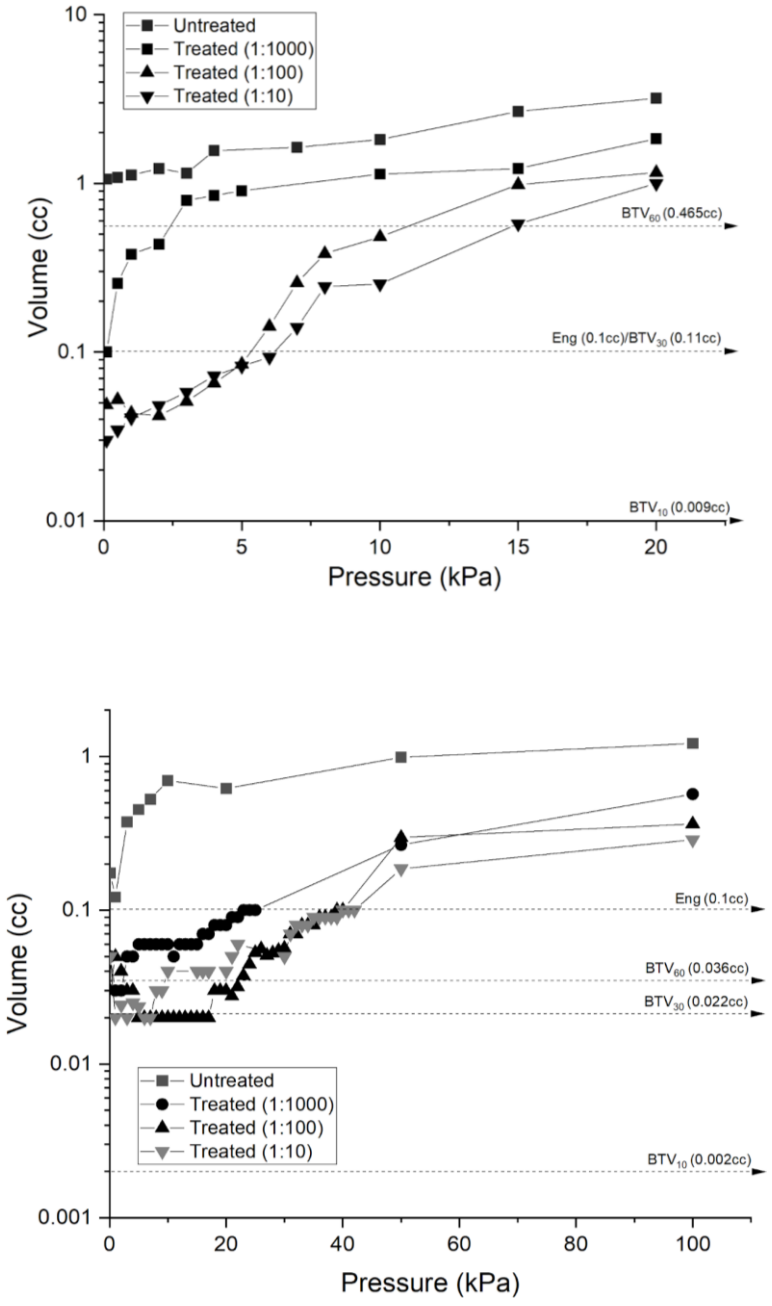

Figure 5-13 Breakthrough Pressure-Volume plots for (a) NC-AS and (b) IA-PC

5.3 Breakthrough pressure criteria

As discussed previously, breakthrough pressure obtained from tests will change based on different breakthrough volume criteria selected. Table 3 shows the final breakthrough pressure values of the tested soil samples based on the breakthrough volume criteria selected in Table 2. The breakthrough pressure values decrease with decreasing D values selected. For the silty Sand material (NC-AS), the selection of breakthrough pressure utilizing the D_{30} value matches values obtained from the user specification based on previous tests. This works because the soil is uniformly distributed. The results are not the same for the clayey silt material (IA-PC) which has extremely low values of breakthrough pressure even at a breakthrough volume criteria representative of 60 passing. This is because the selection of a smaller D-value will lead to smaller grain and pore sizes, resulting decrease in a breakthrough volume that may not be fully representative of the soil grains as evidenced by the values obtained for the soil which largely consists of fines (98.4% passing through #200). For such soils, a D value representing a larger proportion of the soil grains should be selected (90 - 95%).

Table 5- 4 Breakthrough pressure values of treated soils based on different BTV criteria.

Soil		**NC-AS**					**IA-PC**			
					Breakthrough Pressure (kPa)					
	BTV (cc)	UT	1:1000	1:100	1:10	**BTV (cc)**	UT	1:1000	1:100	1:10
User Spec.	**0.1**	<0.1	0.1	5	6	**0.1**	<0.1	23	39	40
BTP_{60}	**0.465**	<0.1	2	10	15	**0.036**	<0.1	<0.1	<0.1	8
BTP_{30}	**0.108**	<0.1	0.1	5	6	**0.022**	<0.1	<0.1	<0.1	1
BTP_{10}	**0.009**	<0.1	<0.1	<0.1	<0.1	**0.002**	<0.1	<0.1	<0.1	<0.1

Using the user-specified breakthrough volume criteria (0.1cc), test was repeated for treated soil samples and breakthrough pressure measurements obtained (Figure 14). Results obtained were repeatable with a maximum deviation of 6kPa. This high value was obtained because of the large increments in pressure (1kPa). More precision can be obtained by using a smaller pressure increment. Treated samples can sustain a hydrostatic head up to 6kPa for NC-AS and 36kPa for IA-PC. This has important significance because treated samples can be utilized in several engineering applications requiring the retention of water, and restriction of the transport of moisture through civil infrastructure systems (Capillary barriers for embankments and pavement systems, landfill cover systems, tunnels, and underground pipeline protection, etc.)

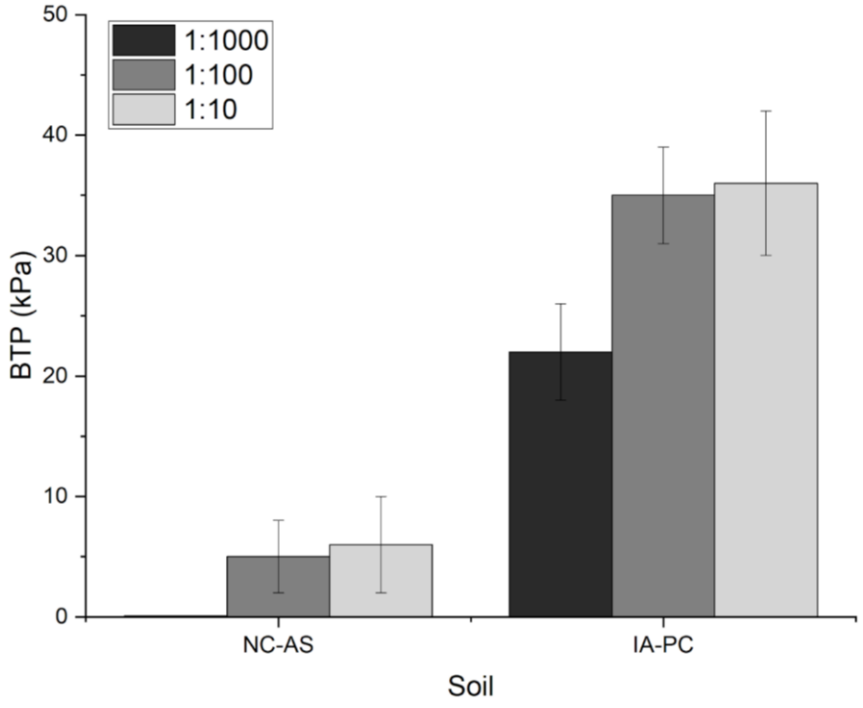

Figure 5-14 Breakthrough Pressure Test Results (Using user spec of 0.1cc BTV)

5.4 Hydrostatic creep tests

The results of ponding a head of water on the top of an untreated and treated sample (1:10) at different selected pressures are presented in Figure 15 below. For the untreated soil, there is immediate flow into the specimen and an increase in the volume of water infiltrating the specimen corresponding with an increase in the pressure. Volumes infiltrating into the sample are in excess of 10cc after 1440 seconds at all pressures tested. For the treated sample, it is observed that for pressures below the breakthrough pressure, the infiltration into the sample is below 1cc. Above the breakthrough pressure, the sample begins to behave like an untreated sample. This indicates that the sample is capable of restricting flow through it over a period. Values of volume infiltrating into the sample begin to plateau and could potentially stabilize to a consistent value over time.

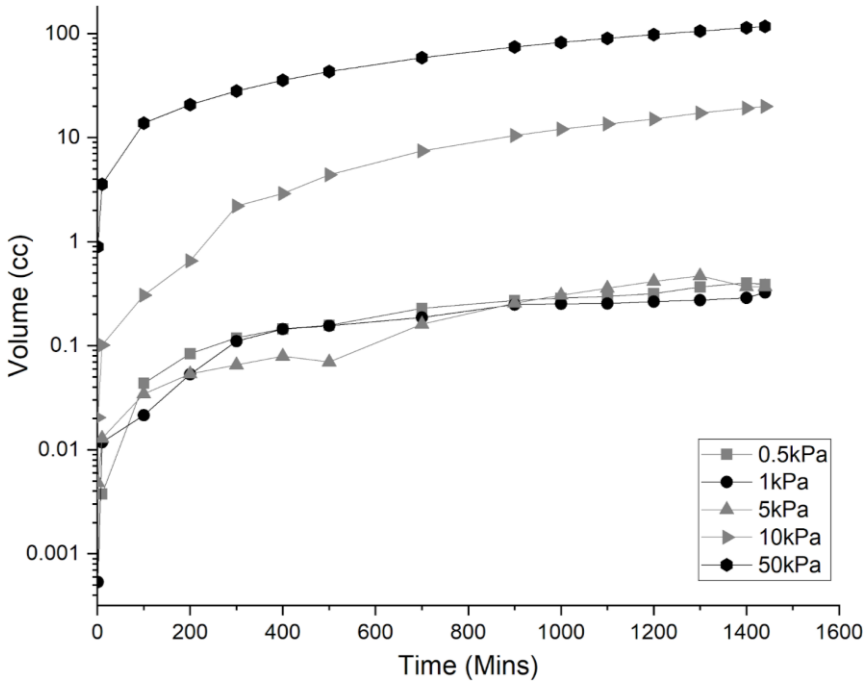

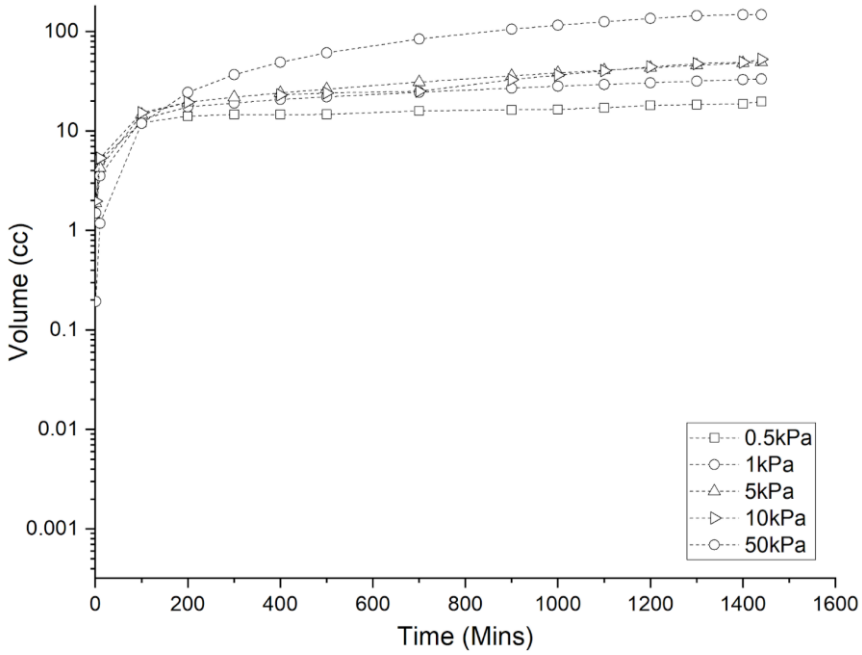

Figure 5-15 Time-Volume Plot for Creep Loading of Treated (1:10) and Untreated Soil (NC-AS)

6. Conclusion

This paper presents an automated technique for measuring the Water Entry Pressure (WEP) or Breakthrough Pressure (BP) in hydrophobic soils. The WEP/BP is a critical engineering property that represents the pressure level at which water can permeate through the treated soil. It discusses existing methods for measuring water entry pressure, including the water-ponding method, tension-pressure infiltrometer method, and triaxial cell pressure method, and highlights the limitations of existing methods for measuring WEP/BP, such as seepage through edges, human error in volume monitoring, and uneven compaction within the soil sample. It addresses the importance of test interval time in WEP/BP measurement and the determination of breakthrough volume. It emphasizes the need for a standard test method that considers these factors and provides consistent and reliable

results. It also proposes a novel automated test method that addresses these limitations and improves the accuracy of WEP/BP measurement.

The proposed test method involves determining the breakthrough pressure of water-repellent soils based on volume measurements. It provides a definition for breakthrough in water-repellent soils and establishes a basis for determining WEP based on a breakthrough volume criterion. Two soils treated with commercially available organosilane at varying dosages (1:1000, 1:100, 1:10) were found to be water-repellent with contact angles ranging from 102^{o} to 143^{o}. Also, results from WDPT tests characterize them as extremely water-repellent (>3600s). Results of the breakthrough test indicate that breakthrough pressures of up to 6kPa and 36kPa are obtained for the Silty Sand/Clayey Sand and Lean Clay respectively. Hydrostatic creep tests reveal that treated soils can sustain a hydrostatic head below the breakthrough pressure but behave like untreated soil above it.

The automation of WEP/BP measurement using this method can aid in specifying the use of water-repellent soils in various civil engineering applications, particularly in controlling moisture penetration in construction.

REFERENCES

ASTM. (2000). D5084 - Standard Test Methods for Measurement of Hydraulic Conductivity of Saturated Porous Materials Using a Flexible Wall Permeameter. *Astm D5084*, *04*(October 1990).

ASTM D 854. (2002). ASTM D854 Standard Test Methods for Specific Gravity of Soil Solids by Water Pycnometer. *ASTM International*, *04*.

ASTM D7928. (2021). Standard Test Method for Particle-Size Distribution (Gradation) of Fine-Grained Soils Using the Sedimentation (Hydrometer) Analysis. *ASTM International*, (May 2016).

ASTM International. (2017). ASTM D4318-17. In *Standard Test Methods for Liquid Limit, Plastic Limit, and Plasticity Index of Soils*.

Brooks, T., Daniels, J. L., Uduebor, M., Cetin, B., & Wasif Naqvi, M. (2022). Engineered Water Repellency for Mitigating Frost Action in Iowa Soils. https://doi.org/10.1061/9780784484012.046

Carrillo, M. L. K., Yates, S. R., & Letey, J. (1999). Measurement of Initial Soil-Water Contact Angle of Water Repellent Soils. *Soil Science Society of America Journal*, *63*(3), 433–436. https://doi.org/10.2136/SSSAJ1999.03615995006300030002X

Chamberlain, E. J., United States, & Cold Regions Research and Engineering Laboratory (U.S.). (1981). *Frost susceptibility of soil review of index tests.* U.S. Dept. of Transportation Federal Highway Administration Offices of Research and Development ; National Technical Information Service distributor. Hanover, NH 03755.

Daniels, J. L., & Hourani, M. S. (2009a). Soil Improvement with Organo-Silane. https://doi.org/10.1061/41025(338)23

Daniels, J. L., & Hourani, M. S. (2009b). Soil Improvement with Organo-Silane. In *U.S.-China Workshop on Ground Improvement Technologies 2009* (pp. 217–224). American Society of Civil Engineers. https://doi.org/10.1061/41025(338)23

DeBano, L. (1981). *Water repellent soils: a state-of-the-art*. Retrieved from https://books.google.com/books?hl=en&lr=&id=D_0TAAAAYAAJ&oi=fnd&pg=PA1&ots=SWVTEVJDWR&sig=vz2Yx4NP4Bzszu4B9xFLM6gkN6s

Debano, L. F. (2015). Infiltration, evaporation, and water movement as related to water repellency. *Soil Conditioners*, 155–164. https://doi.org/10.2136/SSSASPECPUB7.C15

Dumenu, L., Pando, M. A., Ogunro, V. O., Daniels, J. L., Moid, M. I., & Rodriguez, C.

(2017). Water Retention Characteristics of Compacted Coal Combustion Residuals, 403–413. https://doi.org/10.1061/9780784480434.044

Feyyisa, J. L., Daniels, J. L., Pando, M. A., & Ogunro, V. O. (2019). Relationship between breakthrough pressure and contact angle for organo-silane treated coal fly ash. *Environmental Technology and Innovation*, *14*. https://doi.org/10.1016/j.eti.2019.100332

Keatts, M. I., Daniels, J. L., Langley, W. G., Pando, M. A., & Ogunro, V. O. (2018). Apparent Contact Angle and Water Entry Head Measurements for Organo-Silane Modified Sand and Coal Fly Ash. *Journal of Geotechnical and Geoenvironmental Engineering*, *144*(6). https://doi.org/10.1061/(asce)gt.1943-5606.0001887

King, P. M. (1981). Comparison of methods for measuring severity of water repellence of sandy soils and assessment of some factors that affect its measurement. *Australian Journal of Soil Research*, *19*(3). https://doi.org/10.1071/SR9810275

Kloubek, J. (1981). Hysteresis in porosimetry. *Powder Technology*, *29*(1), 63–73. https://doi.org/10.1016/0032-5910(81)85005-X

Lee, C., Yang, H.-J., Yun, T. S., Choi, Y., & Yang, S. (2015). Water-Entry Pressure and Friction Angle in an Artificially Synthesized Water-Repellent Silty Soil. *Vadose Zone Journal*, *14*(4). https://doi.org/10.2136/vzj2014.08.0106

Letey, J., Carrillo, M. L. K., & Pang, X. P. (2000). Approaches to characterize the degree of water repellency. *Journal of Hydrology*, *231–232*, 61–65. https://doi.org/10.1016/S0022-1694(00)00183-9

Lourenço, S. D. N., Saulick, Y., Zheng, S., Kang, H., Liu, D., Lin, H., & Yao, T. (2018, February 1). Soil wettability in ground engineering: fundamentals, methods, and applications. *Acta Geotechnica*. Springer Verlag. https://doi.org/10.1007/s11440-017-0570-0

Malisher, M., Daniels, J., Uduebor, M., & Saulick, Y. (2023). Compaction and Strength Characteristics of Engineered Water Repellent Frost Susceptible Soils. *Geo-Congress 2023*, 452–461. https://doi.org/10.1061/9780784484661.047

Oluyemi-Ayibiowu, B. D., & Uduebor, M. A. (2019). Effect of Compactive Effort on Compaction Characteristics of Lateritic Soil Stabilized with Terrasil. *Journal of Multidisciplinary Engineering Science Studies (JMESS)*, *5*(2), 2458–2925. Retrieved from www.jmess.org

Rigby, S. P., & Edler, K. J. (2002). The Influence of Mercury Contact Angle, Surface Tension, and Retraction Mechanism on the Interpretation of Mercury Porosimetry Data. *Journal of Colloid and Interface Science*, *250*(1), 175–190. https://doi.org/10.1006/JCIS.2002.8286

Saulick, Y., Lourenço, S., & Baudet, B. (2016). Effect of particle size on the

measurement of the apparent contact angle in sand of varying wettability under air-dried conditions. *E3S Web of Conferences*, *9*. https://doi.org/10.1051/E3SCONF/20160909003

Uduebor, M., Adeyanju, E., Saulick, Y., Daniels, J., & Cetin, B. (2022). A Review of Innovative Frost Heave Mitigation Techniques for Road Pavements. *International Conference on Transportation and Development 2022*. https://doi.org/10.1061/9780784484357

Uduebor, M., Daniels, J., Naqvi, M. W., & Cetin, B. (2022). Engineered Water Repellency in Frost Susceptible Soils. https://doi.org/10.1061/9780784484012.047

Wang, Z., Wu, L., & Wu, Q. J. (2000). Water-entry value as an alternative indicator of soil water-repellency and wettability. *Journal of Hydrology*, *231–232*, 76–83. https://doi.org/10.1016/S0022-1694(00)00185-2

Washburn, E. W. (1921a). Note on a Method of Determining the Distribution of Pore Sizes in a Porous Material. *Proceedings of the National Academy of Sciences*, *7*(4), 115–116. https://doi.org/10.1073/PNAS.7.4.115/ASSET/2A938320-7284-4A7E-8413-61B527BA4960/ASSETS/PNAS.7.4.115.FP.PNG

Washburn, E. W. (1921b). The dynamics of capillary flow. *Physical Review*, *17*(3), 273–283. https://doi.org/10.1103/PHYSREV.17.273

WATSON CL, & LETEY J. (1970). INDICES FOR CHARACTERIZING SOIL-WATER REPELLENCY BASED UPON CONTACT ANGLE-SURFACE TENSION RELATIONSHIPS, *34*(6), 841–844. https://doi.org/10.2136/SSSAJ1970.03615995003400060011X

Xing, X., Saulick, Y., & Lourenço, S. D. N. (2022). Synergistic effects of density, gradation, particle size, and particle shape on the water entry pressure of hydrophobized sands. *Https://Doi.Org/10.1139/Cgj-2021-0585*, *59*(11), 1937–1949. https://doi.org/10.1139/CGJ-2021-0585

ARTICLE 6: EFFECT OF FREEZE-THAW CYCLES ON STRENGTH PROPERTIES OF ENGINEERED WATER REPELLENT SOILS

ABSTRACT

Frost-susceptible soils subjected to seasonal freeze–thaw action, experience changes in deformation, strain, and stress that impact their engineering properties. Frost heaving and thaw weakening are especially problematic, subjecting all elements of the soil system to significant changes in moisture content, stress, and strain. Engineered Water Repellency (EWR), a process in which soils are made hydrophobic has been utilized to convert in-situ soil material into suitable barriers limiting the transport of water through these soils, resulting in frost heave mitigation. While this solution is viable, very little is known about the impact of EWR treatment on the mechanical properties of soils, particularly under repeated freeze-thaw cycles. In this study, laboratory freezing experiments were carried out to assess the impact of engineering water repellency on soil performance. A frost susceptible soil from Fairbanks, Alaska was treated with organosilane, and the mechanical properties were investigated under multiple freeze-thaw cycles. Contact angle and water drop penetration tests were carried out to assess the level of water repellency imparted, and unconfined compressive tests were performed to determine the effect of treatment on the strength compared to untreated samples. Both treated and untreated samples were subjected to four freeze-thaw cycles and tested. The results show an improvement in the properties of the treated soil material even after several freeze-thaw cycles.

Keywords: Engineered Water Repellency, Freeze-thaw, Frost-susceptible soils, Unconfined compressive tests

1. Introduction

In cold regions around the world, particularly areas that experience seasonal freezing, pavement subgrade soils are significantly affected and fail because by frost heaving and thaw weakening (Mahedi et al., 2020; Uduebor et al., 2022a). Sub-zero temperatures result in the freezing of water within the pore spaces of soil causing it to expand by almost 10%. This expansion can exceed 100% or more in frost susceptible soils – soils in which significant ice lens formation occurs when there is access to moisture during specific freezing conditions. (Johnson, 1952). Under these conditions, segregated ices lens will continue to form and grow as water is drawn upward toward the freezing zone by capillary and osmotic gradients from a deeper water source (e.g., high, or perched groundwater table) (Taber, 1930; Chamberlain et al., 1981). These ice lenses may persist until the warmer ambient temperatures return. As temperatures rise, melting often occurs from the top, with lower layers of ice preventing the percolation and drainage of meltwater. The soils experience increases in moisture content and decrease in strength and bearing capacity (Simonsen and Isacsson, 1999). This process, in conjunction with traffic loading, leads to degradation in pavement performance, and recurrent annual maintenance costs, estimated nationally at over 2 billion dollars, in addition to ancillary economic impacts caused by related vehicle damage, road closures, and weight restrictions. (Federal Highway Administration (FHWA), 1999; Mahedi et al., 2020; Wasif Naqvi et al., 2022)

To mitigate the adverse effects of frost heaving on pavement subgrade soils, several strategies can be employed, including replacing frost susceptible soil with non-frost susceptible soils, polymer injection, placing polystyrene boards, restricting water transport through chemical stabilization, and the use of capillary barriers and geosynthetics, which

have been extensively studied (Henry, 1996; Edgar et al., 2015; Nourmohamadi et al., 2022). Although they provide relief, many of the methods listed can be cost and labor-intensive, particularly for low-volume roads often subjected to heavy agricultural traffic loads (Brooks et al., 2022; Wasif Naqvi et al., 2022) and constructed within tight budget restrictions. Low-volume roads account for an estimated 70% of the road networks in the United States with nearly half of them located in seasonal frozen areas affected by frost action (Kestler et al., 2007). Another major concern is the successful mitigation of the impacts of frost action in the long term. While the use of soil treatments like cement, fly ash, and lime can provide temporary relief from the detrimental effects of frost action, their efficacy diminishes over multiple free-thaw cycles resulting from moisture intrusion into widened pore spaces and cracks (Ding et al., 2018; Bray and Darrow, 2020). The loss of strength and stiffness after multiple freeze-thaw cycles coupled with the long and temperature-dependent curing time requirements, relatively expensive soil mixing operations, and required machinery make them less favorable alternatives for many entities (e.g., Counties in the U.S.) responsible for low-volume roads.

Engineered water repellency (EWR) is a process in which soils are made hydrophobic (water repellent) by covalently bonding soils with cost-effective and environmentally compatible organo-silane molecules. Previous (Daniels et al., 2021; Brooks et al., 2022; Uduebor et al., 2022a) have shown EWR – as an alternative approach to mitigating frost action in pavement soils. The primary design function of EWR is to act as a hydraulic barrier, which in this context involves limiting the transport of water toward the freezing zone (capillary barrier). Studies carried out have indicated a reduction in the frost heave, and heave rate, and an overall improvement in the freeze-thaw performance of

treated soils (Mahedi et al., 2020; Uduebor et al., 2022a). The use of these organosilanes has been found favorable due to their low cost, adaptability to existing construction methods and machinery, predictable behavior, and shorter curing periods (Brooks et al., 2022; Uduebor et al., 2022a).

While much is known about its effectiveness, nothing is known concerning the mechanical behavior and performance of these EWR-treated soils under repeated freeze-thaw cycles. There are few documented field studies of EWR for the purpose of mitigating frost action. Field tests carried out by (Naqvi et al., 2023) have only completed one freeze-thaw cycle and could take another 5-10 years to get a true field performance behavior of these treated soils under practical use conditions. Consequently, the primary objective of this study was to evaluate the durability of EWR-treated subgrade soil over multiple freeze-thaw cycles. Also, previous tests carried out to determine the strength properties of the treated soil samples were carried out on freshly prepared samples without the full development of water repellency in the samples (Uduebor et al., 2022a; Malisher et al., 2023) resulting in observable strength decrease due to reduced frictional angle. Results indicated a loss of strength from treatment (28.6% - 40.0%). These tests are not fully representative of field conditions because treated samples gain strength after developing full water repellency. Recent studies have shown that treated samples retain their strength gain after drying due to water repellent nature causing the soil matrix to remain unsaturated under wetting (M. Uduebor et al., 2023). Untreated soils on the other hand lose their strength due to increased moisture content upon moisture conditioning after drying.

The objective of this work is to evaluate the efficacy of EWR for mitigating frost action in frost-susceptible soil from Alaska. This will provide useful insights into the durability of

the treated pavement sections under multiple freeze-thaw cycles, particularly for low-volume roads where this innovative technology is currently being adopted.

2. Methods

2.1 Materials

2.1.1 Frost Susceptible Soil

Silt from Fairbanks in Alaska (AK-FB) was utilized for this study. The soil was mixed and quartered before being air-dried and prepared for testing and analysis. To ensure consistency in the soil specimens created, the soil was sieved through the #4 sieve (4.75mm) to remove gravel-sized fractions. Figure 1 shows the grain size distribution of the soil. Specific gravity test was carried out according to ASTM D854(ASTM D 854, 2002) and values ranged from 2.65 to 2.67. The particle size distribution was determined in accordance with ASTM D7928(ASTM D7928, 2021). The soil was classified as inorganic silt (ML) (USCS classification) with an AASHTO classification of A-5 (Silty Soil, fair to poor subgrade rating). Atterberg limits tests; plastic limit (PL) and liquid limit (LL), were performed in accordance with ASTM D4318(ASTM International, 2017a). The soil had a liquid limit of 41% and was classified as non-plastic (NP) (cannot roll into a thread). The sample also possessed some organic matter which was shifted and removed before testing. Organic content was determined by ASTM D2974(ASTM International, 2010) to be between 1.3 -1.4%. The maximum dry density (MDD) and optimum moisture content (OMC) of the soil were 14.1kN/m^3 and 20.7% respectively (ASTM D698(ASTM, 2012)). The soil has a frost susceptibility classification of F4 (High frost susceptibility) by

the US Army Corps of Engineers (US Army Corps of Engineers, 1965) based on the grain size distribution.

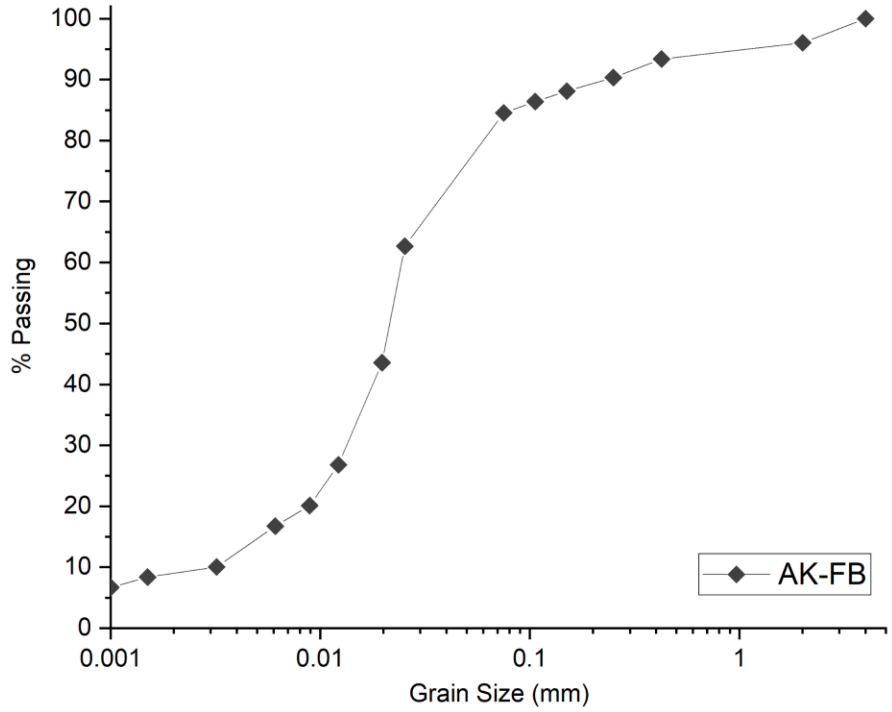

Figure 6-1 Grain Size Distribution of the Soil

2.1.2 Water Repellent Chemical

A commercially available organosilane (OS) product, Terrasil from Zydex Industries, was utilized for the treatment of the soil samples. It is a viscous, water-soluble, and reactive soil-modifying organosilane polymer with 65 -70% active ingredients (Alkoxy-Alkylsilyl Compounds) by weight. It has been used in previous research carried out by (Mahedi et al., 2020; Brooks et al., 2022; Uduebor et al., 2022b; Malisher et al.,

2023). Silanes provide a very stable bond to the surface of soil particles producing a hydrophobic surface. They also have the added benefit of an extra silicon atom which improves resistance to oxidation, and UV exposure and prevents any degradation (Arkles et al., 1992).

2.1.3 Treatment

The soil was treated at a uniform dosage concentration ratio of 1:40 (OS: Soil, batched by weight). This dosage was selected based on previous water-repellency studies (Brooks et al., 2022; Uduebor et al., 2022a; Malisher et al., 2023). The OS was first dissolved with deionized water (~1µs/cm) and utilized as the molding moisture during the compaction of the test specimens.

2.2 Compaction

Oven-dried soil was mixed with DI water or OS mixture (for treated specimens) at the optimum moisture content and then stored in a sealed plastic bag to allow for moisture equilibrium of the sample. Compaction of test specimens was done with the Harvard miniature compaction equipment (Humboldt Equipment). Samples were compacted in 5 lifts using a 9.07kg (20lbs) spring hammer to achieve a density close to the standard proctor compaction procedure utilized during the index testing. Compacted samples were within 95% of the maximum dry density. Prepared specimens were wrapped in nylon film to avoid loss of moisture within the sample. They were placed temporarily in a humidity-

regulated chamber (75%) while other samples were prepared before being placed in the environmental chamber for freeze-thaw tests.

2.3 Conditioning

To represent field conditions, samples were treated and allowed to dry. Another set of samples was subjected to a three-phase conditioning - Air drying; Humidifying; Freeze-Thaw cycling - with samples tested after each phase. Air drying (~25^{o}C, Rh ~45%, 3 days) occurred in a desiccator with a small opening to enable water-repellent properties to fully develop. After crushing the selected air-dried samples from the batch, the remaining air-dried samples are stored in a humidification chamber (~Rh100) for 7, 14, and 21 days after which another batch of samples is tested. Finally, samples were also taken for frost heave tests and then finally crushed. Figure 2 shows a schematic of the conditioning processes.

2.4 Contact Angle Tests

Contact angle measurement was carried out following protocols by (Uduebor et al., 2022b) Dried samples were placed on a double-sided adhesive tape and compressed for 10 seconds using a 10g weight after which excess material was removed. The process was repeated to create a monolayer of the sample on the tape. The soil specimen was placed on a goniometer (Ramehart Instruments, 260-U1, standard goniometer, #150512), and increasing drops of deionized water were placed on the surface of the specimen utilizing a FlowTrac II (Geocomp). Repeated horizontal image capturing and measurements were taken for each drop size until a stable contact angle is observed (apparent contact angle).

According to (Letey et al., 2000), contact angle measurements less than 90^{o} are considered wettable/hydrophilic, while angles measured above 90^{o} are considered hydrophobic. Tests were carried out for both treated and untreated samples before and after freeze-thaw cycles to determine the effect of water repellency treatment as well as the effect of freeze-thaw action on the hydrophobicity of the treated soils.

2.5 Water Drop Penetration Test

The water drop penetration test was also utilized to assess the water repellency of treated samples before and after freeze-thaw cycles. About 20g of dried sample was placed in aluminum cans and drops of deionized water (50 ± 1μL volume) were placed on the soil surface with a pipette. The time taken for the water droplets to infiltrate into the soil was recorded using a camera with a time stamp. All measurements were terminated after 1 hour (3600s). Water repellency categories based on (King, 1981) are as follows; ≤ 1s (Non-repellent/Completely wettable); 1–60s (Slightly repellent); 60–600s (Strongly repellent); 600–3600s (Severely repellent); ≥3600s (Extremely repellent).

2.6 Freeze-Thaw Tests

A closed-system freeze-thaw cycle approach was utilized in this study. Freeze-Thaw cycles were carried out using a Cincinnati Sub-Zero ZPH-16-1.5-H/A with a temperature range of −70 to 190°C. An RT-1 temperature sensor was utilized for monitoring the chamber temperature with readings logged on a Zentra ZL6 Datalogger. Treated and untreated specimens were placed into the chamber while wrapped in nylon

film to prevent any loss of moisture. A freezing regime of −12°C for 12h, followed by thawing at 12°C for 12 h at a regulated humidity of 75% (based on average for the Fairbanks area) was utilized in this study. These temperatures were selected based on previous studies carried out by (Wasif Naqvi et al., 2022) on the same soil. Samples were retrieved for further testing after 0, 5, 10, and 15 freeze-thaw cycles.

2.7 Strength Tests

After predefined freeze-thaw cycles have been reached, samples were retrieved from the chamber and transferred for strength testing. Unconfined compressive strength tests were carried out using a GeoJac automated load actuator (Geotac Geotechnical Test Acquisition and Control). Results were obtained and computed using the SIGMA UC software application. Unconfined compressive strength tests were carried out in accordance with ASTM D2166(ASTM International, n.d.). A strain rate of 1.25%/min was utilized, and testing stopped after 20% strain for samples without a uniformly defined peak.

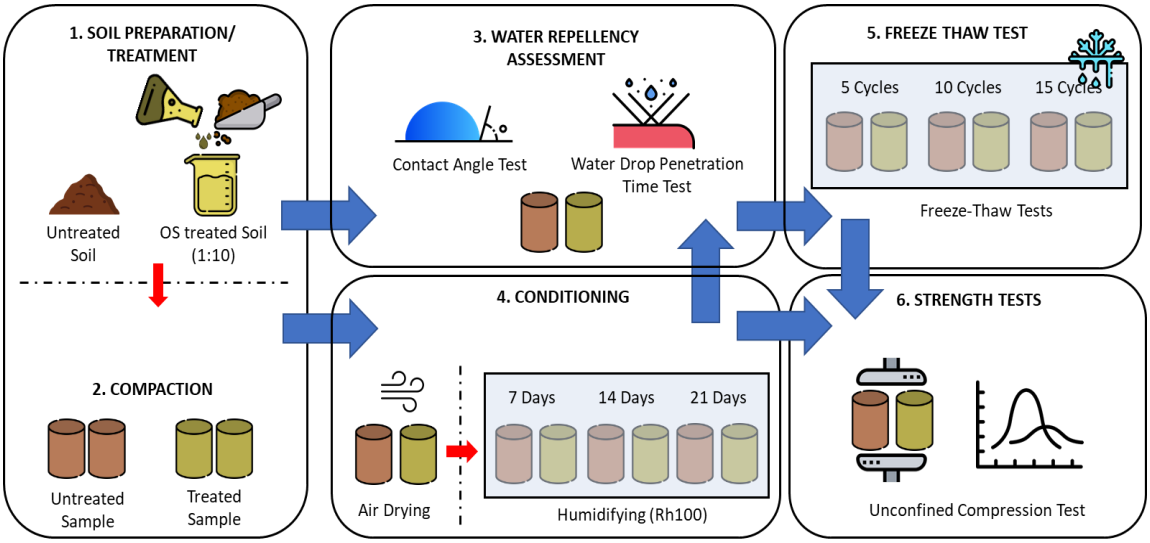

Figure 6-2 Graphical Summary of Soil Preparation and Testing Protocol

3. Results and Discussion

3.1 Contact Angle and Water Drop Penetration Test

Contact angle values obtained for untreated samples at all conditions were less than 10^o indicating the samples were hydrophilic (wettable). Treated samples possessed higher contact angles greater than 90^o; with values of samples before oven drying (as-is) being lower (16.1^o – 117.6^o) than the values obtained after oven drying (124.3^o – 127.6^o) (Figure 3a). This00 shows that the moisture condition of the sample after treatment has an impact on the repellent properties of the material. Even if the material surface is treated with sufficient moisture within the soil matrix, the treated soil behaves like a hydrophilic material. Other studies have shown an increase in the contact angle of oven-dried samples compared to air-dried samples (Uduebor et al., 2022b; M. A. Uduebor et al., 2023). Air-dried contact angle values are utilized for field specifications because the drying conditions closely match those obtainable in the field. It can be noted that after air-drying, there is no significant change in the contact angle under humidification for several days. This water-repellent property is corroborated by the results of the water drop penetration time test (Figure 3b) where samples at compaction (OMC) are completely wettable (~3s) and become severely repellent (~2875s) after air drying. All oven-dried samples exhibited extreme water repellency with penetration times exceeding 3600s and droplets drying out without any penetration into the sample. The material remains repellent even after being conditioned at Rh100 for up to 21 days.

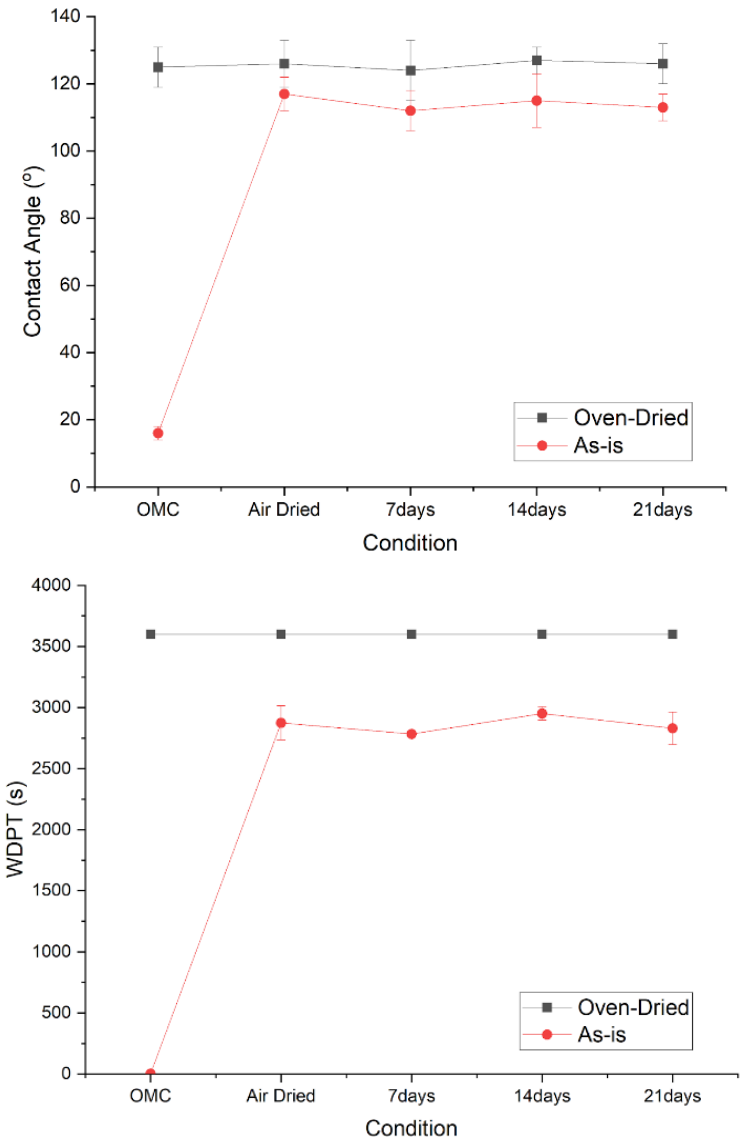

Figure 6-3 Results of (a) Contact Angle and (b) Water Drop Penetration Time on treated samples.

The development of water repellency after sufficient drying is important to note, particularly for construction purposes where there is a need to permit the sample to air-dry before commencing further construction activities. This constraint is like other methods of soil improvement which require a curing period, such as lime or cement stabilization. Previous tests (Uduebor et al., 2022a; M. Uduebor et al., 2023) carried out on water-

repellent treated soils indicate there is no increase in the moisture content of soils after treatment. Instead, there is a gradual decrease in the moisture condition as it dries out and becomes more water-repellent. Treated samples continuously decrease in moisture content via vapor moisture loss and develop water-repellent properties over time. Silane and siloxane treatments have the advantage of allowing air to pass them, permitting the escape of moisture vapor while repelling water from the outside (Arkles, 2011). This ensures there is a stable balance of the moisture condition within the samples, mitigating issues such as cracking or shrinkage from occurring.

3.2 Failure Strength Affected by Freeze-Thaw Cycles

The results of the unconfined compressive shear test are given in Figure 4 at various freeze-thaw cycles for both untreated and treated samples tested immediately after compaction. For the untreated soil, there is a reduction in the unconfined compressive strength of samples with increasing freeze-thaw cycles (~4.2% at 5 cycles, and ~12.0% at 10 cycles) as shown in Figure 5a. This is due to the expansion of water freezing within the pores of the soil during the freezing cycle. There is an increase in the volume of water by about 9% as it crystallizes into ice, resulting in a forced expansion of the pore space which is not fully recovered during thawing. The repeated freezing and thawing results in the expansion of pores between particles up to the maximum limit possible.

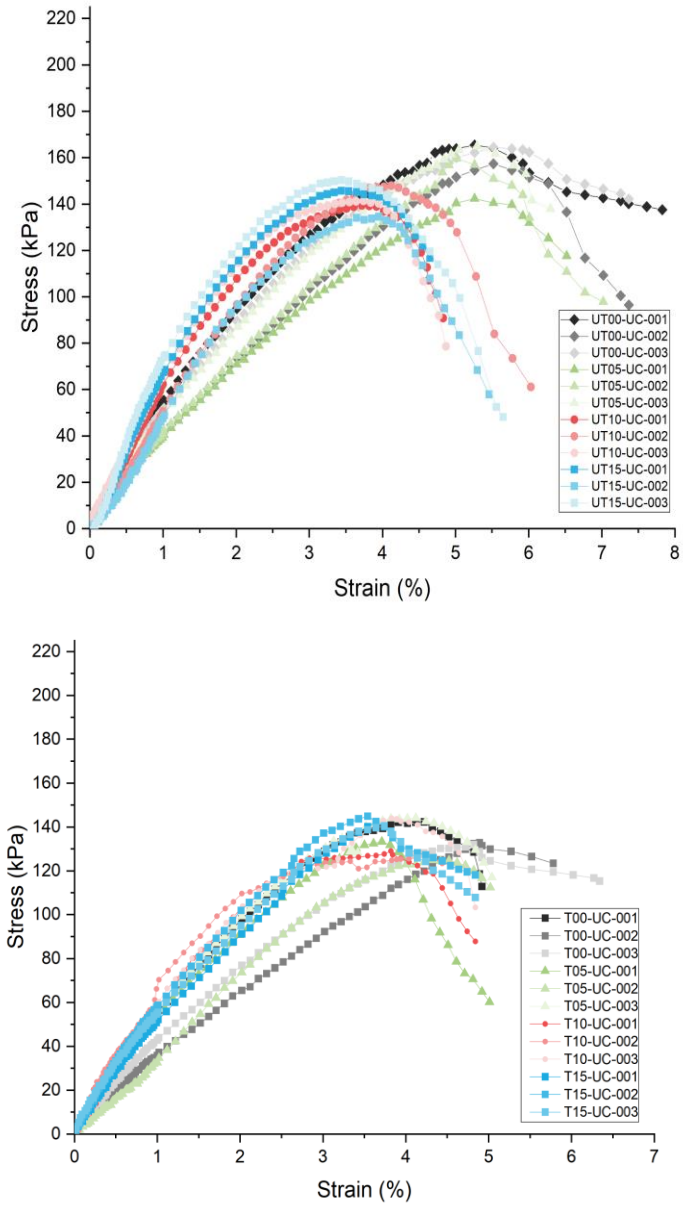

Figure 6-4: Stress-strain variation of (a) untreated and (b) treated samples after freeze-thaw cycles.

There is an observable increase in the shear strength after 10 cycles (~0.42% at 15 cycles), this is due to a combination of a decrease in the moisture content (Figure 6a), and a maximum limit reached on the expansion of the pore spaces due to successive freeze-thaw cycles. Compressive strength increases with a reduction in moisture content below

the optimum moisture content at uniform density, and for a given soil subjected to freeze-thaw cycles, a maximum pore volume limit is reached (corresponding to an increase in sample height in Figure 6b) after which the expansion of ice formed within them due to frozen pore water does not result in any further expansion of the pore (Ghazavi and Roustaie, 2010). This will result in the same sample structure even after multiple cycles.

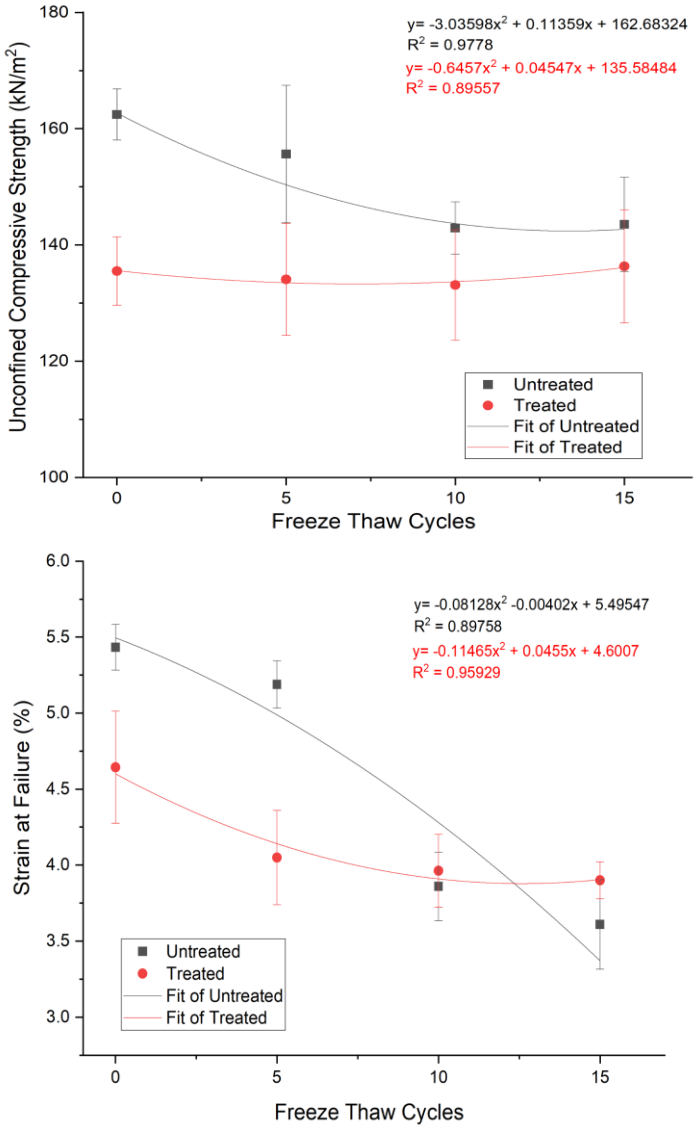

Figure 6- 5 Results of (a) unconfined compressive strength (b) failure strain for untreated and treated samples versus freeze-thaw cycles.

The UCS values for the treated sample before freezing are lower (~16.5%) than that of the untreated soil. This may be attributable to the lower friction between the particles due to the presence of the organo-silane molecules. Previous studies have shown improved densification, lower frictional angles, and lower strength resulting from similar soil treatments (*2*, *18*). With increasing FT cycles there is also an increase in the unconfined compressive strength of the soil (~1.18% at 5 cycles, ~2.70% at 10 cycles). This is due to a combination of the reduced water content at compaction (Figure 6a) and an increased density resulting from the reduced friction between the particles. There is also an increase in compressive strength after 15 cycles (Figure 5a).

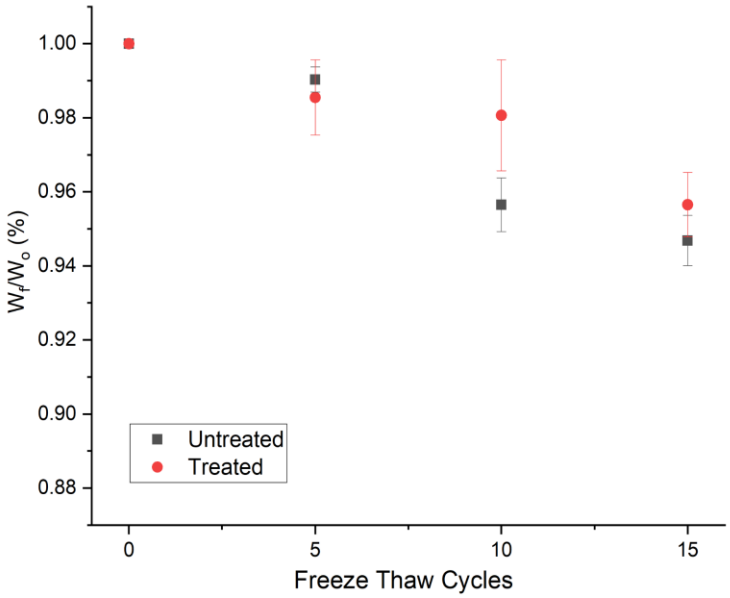

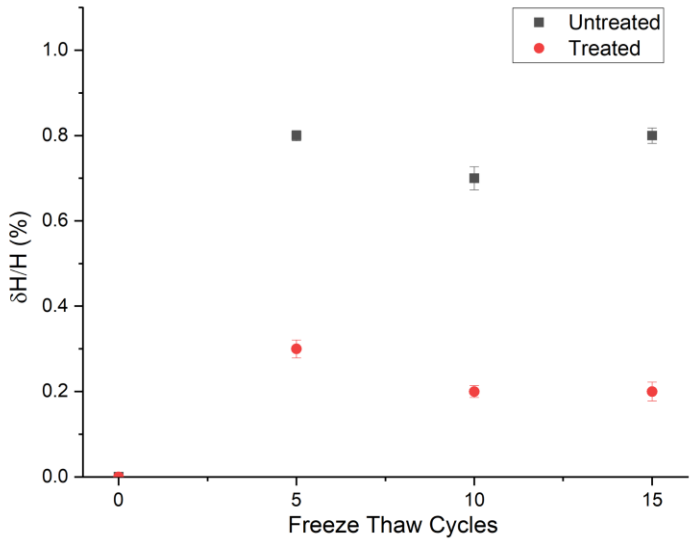

Figure 6- 6 Variation of (a) moisture content and (b) height of samples during freeze-thaw cycles.

Tests on air-dried specimens show an increase in strength of 300% and 333% for untreated and treated samples respectively compared to compacted samples at OMC (Figure 7). This strength gain is gradually lost with increasing moisture content in the untreated sample with final strength values at 290.0kN/m^2 after 21 days (59.4% decrease). This decrease in strength (moduli) with increasing moisture content has been observed in subgrade soil materials tested on the field (Salem, 2005; Muhammad and Siddiqua, 2021). (Ksaibati et al., 2000) also observed a reduction in moduli up to 29.4% for a 1% increase in moisture content. Treated samples do not lose significant strength after exposure to moisture, there is also no moisture gain in the treated samples, instead, there is a gradual loss of moisture over time.

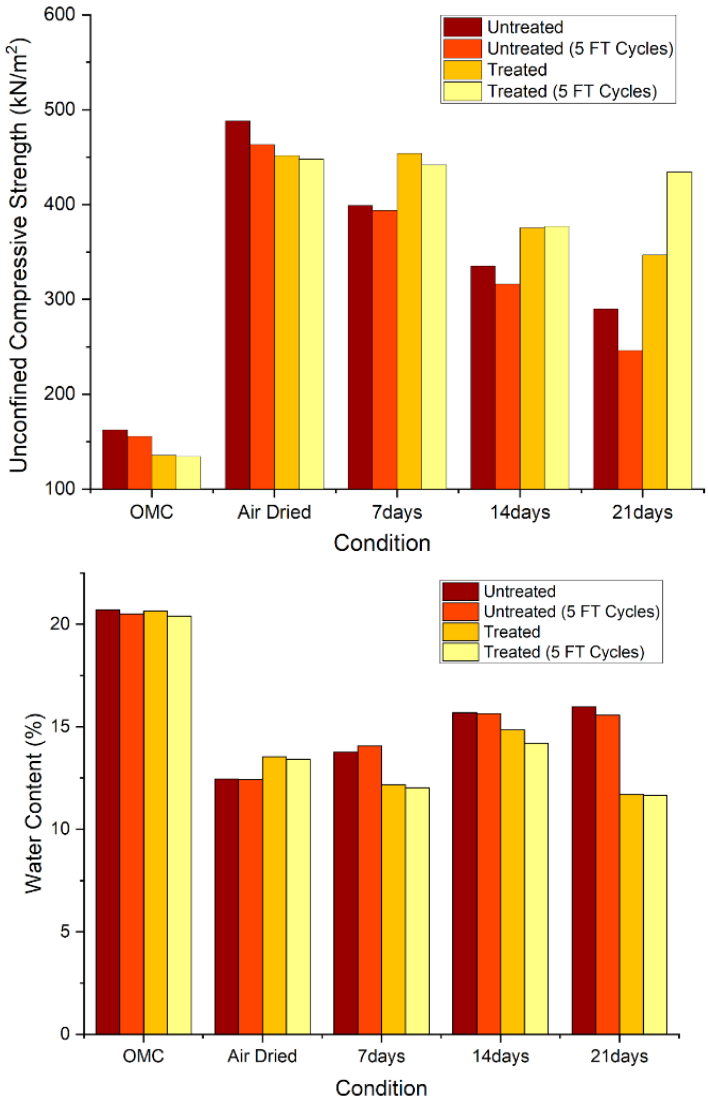

Figure 6- 7 Results of (a) unconfined compressive strength (b) water content for untreated and treated samples at various moisture conditions before and after 5 freeze-thaw cycles.

Treated sample strength and moisture content were relatively insensitive to varying wetting conditions, a likely benefit for field performance. Typically design CBR value is based on the soil strength/moduli values in a saturated state to account for moisture changes over the life of the pavement (Research Board, n.d.). By incorporating water repellency, pavement subgrade soils can retain their unsaturated

strength all year round resulting in a more reliable design. This can lead to a reduction in the design thickness of pavement sections resulting in a more cost-effective pavement aside from moisture protection and control. Previous use of organo-silane treatment indicates they last for decades, even with exposure to extreme conditions (Bowman et al., 2012; Khanzadeh Moradllo et al., 2016; Behravan et al., 2022b). When utilized in pavement applications underground, their lifespan should be considerably longer.

4. Conclusions

In cold regions experiencing seasonal freezing, pavement subgrade soils are susceptible to damage from frost heaving and thaw weakening, leading to significant changes in deformation, strain, and stress. Engineering Water Repellency (EWR) has emerged as a potential solution to mitigate the adverse effects of frost action in pavement soils. The process involves making the soils hydrophobic, limiting water transport, and improving resistance to frost degradation. This study investigated the mechanical behavior and performance of EWR-treated soils under repeated freeze-thaw cycles. Laboratory freezing experiments were conducted using frost-susceptible soil from Fairbanks, Alaska, treated with organosilane. Contact angle and Water Drop penetration tests confirmed the effectiveness of the water-repellent treatment, with treated samples exhibiting higher contact angles (117.6^{o} air-dried, 127.6^{o} oven-dried) and improved water-repellency (2875s air-dried, >3600s oven dried). Strength tests revealed that untreated soil samples experienced a reduction in unconfined compressive strength with increasing freeze-thaw cycles after moisture conditioning due to water freezing and expanding within the pore

spaces. In contrast, treated samples showed increased strength after multiple cycles, resulting from the induced water repellency within the soil matrix. The treated samples retained their unsaturated condition and strength properties even under varying wetting conditions, making them more suitable for construction where design is typically based on worst-case scenarios regarding subgrade strength with respect to moisture content. Incorporating water repellency in pavement subgrade soils can lead to more reliable pavement design, reduced pavement thickness specifications, and overall cost-effectiveness in pavement construction.

REFERENCES

Arkles, B., 2011. Hydrophobicity, Hydrophilicity and Silane Surface Modification. Morrisville, PA.

Arkles, B., Steinmetz, J.R., Zazyczny, J., Mehta, P., 1992. Factors contributing to the stability of alkoxysilanes in aqueous solution. J Adhes Sci Technol 6, 193–206. https://doi.org/10.1163/156856192X00133

ASTM, 2012. ASTM D698: Standard Test Methods for Laboratory Compaction Characteristics of Soil Using Standard Effort (12 400 ft-lbf/ft3 (600 kN-m/m3)). ASTM International 3.

Astm, 2000. D5084 - Standard Test Methods for Measurement of Hydraulic Conductivity of Saturated Porous Materials Using a Flexible Wall Permeameter. Astm D5084 04.

ASTM D 854, 2002. ASTM D854 Standard Test Methods for Specific Gravity of Soil Solids by Water Pycnometer. ASTM International 04.

ASTM D2974, 2020. Standard Test Methods for Determining the Water (Moisture) Content, Ash Content, and Organic Material of Peat and Other Organic Soils. ASTM International.

ASTM D7928, 2021. Standard Test Method for Particle-Size Distribution (Gradation) of Fine-Grained Soils Using the Sedimentation (Hydrometer) Analysis. ASTM International.

ASTM International, 2017a. ASTM D4318-17, in: Standard Test Methods for Liquid Limit, Plastic Limit, and Plasticity Index of Soils.

ASTM International, 2017b. D6913: Standard Test Methods for Particle-Size Distribution (Gradation) of Soils Using Sieve Analysis. ASTM International D6913.

ASTM International, 2010. Standard test methods for moisture, ash, and organic matter of peat and other organic soils, TA - TT -. ASTM International West Conshohocken, Pa., West Conshohocken, Pa. SE -. https://doi.org/LK - https://worldcat.org/title/741935120

ASTM International, n.d. D2166 Standard Test Method for Unconfined Compressive Strength of Cohesive Soil [WWW Document]. URL https://www.astm.org/d2166-06.html (accessed 6.15.23).

Behravan, A., Aqib, S.M., Delatte, N.J., Ley, M.T., Rywelski, A., 2022a. Performance Evaluation of Silane in Concrete Bridge Decks Using Transmission X-ray Microscopy. Applied Sciences (Switzerland) 12. https://doi.org/10.3390/app12052557

Behravan, A., Aqib, S.M., Delatte, N.J., Ley, M.T., Rywelski, A., 2022b. Performance Evaluation of Silane in Concrete Bridge Decks Using Transmission X-ray Microscopy. https://doi.org/10.3390/app12052557

Bowman, J.R., Ley, M.T., Sudbrink, B., Kotha, H., Materer, N., Apblett, A., 2012. EXPECTED LIFE OF SILANE WATER REPELLANT TREATMENTS ON BRIDGE DECKS FINAL REPORT ~ FHWA-OK-12-08.

Bray, M.T., Darrow, M.M., 2020. Frost Susceptibility and Strength of Cement-Treated Fine-Grained Soils.

Brooks, T., Daniels, J.L., Uduebor, M., Cetin, B., Wasif Naqvi, M., 2022. Engineered Water Repellency for Mitigating Frost Action in Iowa Soils. https://doi.org/10.1061/9780784484012.046

Carrillo, M.L.K., Yates, S.R., Letey, J., 1999. Measurement of Initial Soil-Water Contact Angle of Water Repellent Soils. Soil Science Society of America Journal 63, 433–436. https://doi.org/10.2136/SSSAJ1999.03615995006300030002X

Chamberlain, E.J., United States, Cold Regions Research and Engineering Laboratory (U.S.)., 1981. Frost susceptibility of soil review of index tests. U.S. Dept. of Transportation Federal Highway Administration Offices of Research and Development ; National Technical Information Service distributor. Hanover, NH 03755.

Chen, C., Hu, K., Arthur, E., Ren, T., 2014. Modeling Soil Water Retention Curves in the Dry Range Using the Hygroscopic Water Content. Vadose Zone Journal 13, vzj2014.06.0062. https://doi.org/10.2136/VZJ2014.06.0062/111668

Chen, C., Zhou, H., Shang, J., Hu, K., Ren, T., 2020. Estimation of soil water content at permanent wilting point using hygroscopic water content. Eur J Soil Sci 71, 392–398. https://doi.org/10.1111/EJSS.12887

Choi, Y., Choo, H., Yun, T.S., Lee, C., Lee, W., 2016. Engineering characteristics of chemically treated water-repellent Kaolin. Materials 9. https://doi.org/10.3390/ma9120978

Daniels, J.L., Hourani, M.S., 2009. Soil Improvement with Organo-Silane, in: U.S.-China Workshop on Ground Improvement Technologies 2009. American Society of Civil Engineers, pp. 217–224. https://doi.org/10.1061/41025(338)23

Daniels, J.L., Langley, W.G., Uduebor, M., Cetin, B., 2021. Engineered Water Repellency for Frost Mitigation: Practical Modeling Considerations. Geo-Extreme 2021 385–391. https://doi.org/10.1061/9780784483701.037--

DeBano, L., 1981. Water repellent soils: a state-of-the-art.

Ding, M., Zhang, F., Ling, X., Lin, B., 2018. Effects of freeze-thaw cycles on mechanical properties of polypropylene Fiber and cement stabilized clay. Cold Reg Sci Technol 154, 155–165. https://doi.org/10.1016/J.COLDREGIONS.2018.07.004

Doerr, S.H., Shakesby, R.A., Walsh, R.P.D., 2000. Soil water repellency: Its causes, characteristics and hydro-geomorphological significance. Earth Science Reviews 51, 33–65. https://doi.org/10.1016/S0012-8252(00)00011-8

Dumenu, L., Pando, M.A., Ogunro, V.O., Daniels, J.L., Moid, M.I., Rodriguez, C., 2017. Water Retention Characteristics of Compacted Coal Combustion Residuals. https://doi.org/10.1061/9780784480434.044

Edgar, T., Potter, C., Mathis, R., 2015. Frost Heave Mitigation Using Polymer Injection and Frost Depth Prediction. Proceedings of the International Conference on Cold Regions Engineering 2015-January, 416–427. https://doi.org/10.1061/9780784479315.037

Federal Highway Administration (FHWA), 1999. Quarter Century of Geotechnical Research, Chapter 4: Soil and Rock Behavior. Report Number: FHWA-RD-98-139, Turner-Fairbank Highway Research Center, McLean VA, USA. .

Feyyisa, J.L., Daniels, J.L., Pando, M.A., Ogunro, V.O., 2019. Relationship between breakthrough pressure and contact angle for organo-silane treated coal fly ash. Environ Technol Innov 14. https://doi.org/10.1016/j.eti.2019.100332

Fink, D.H., Myers, L.E., 1969. Synthetic Hydrophobic Soils for Harvesting Precipitation.

Ghazavi, M., Roustaie, M., 2010. The influence of freeze-thaw cycles on the unconfined compressive strength of fiber-reinforced clay. Cold Reg Sci Technol 61, 125–131. https://doi.org/10.1016/j.coldregions.2009.12.005

Henry, K.S., 1996. Geotextiles to mitigate frost effects in soils: A critical review. Transp Res Rec. https://doi.org/10.3141/1534-02

Johnson, A.W., 1952. FROST ACTION IN ROADS AND AIRFIELDS: A REVIEW OF THE LITERATURE, 1765-1951. Highway Research Board Special Report.

Keatts, M.I., Daniels, J.L., Langley, W.G., Pando, M.A., Ogunro, V.O., 2018. Apparent Contact Angle and Water Entry Head Measurements for Organo-Silane Modified Sand and Coal Fly Ash. Journal of Geotechnical and Geoenvironmental Engineering 144. https://doi.org/10.1061/(ASCE)GT.1943-5606.0001887

Kelley, W.P., Jenny, H., Brown, S.M., 1936. Hydration of minerals and soil colloids in relation to crystal structure. Soil Sci 41. https://doi.org/10.1097/00010694-193604000-00002

Kestler, M.A., Berg, R.L., Steinert, B.C., Hanek, G.L., Truebe, M.A., Humphrey, D.N., 2007. Determining When to Place and Remove Spring Load Restrictions on Low-

Volume Roads. https://doi.org/10.3141/1989-67 2, 219–229. https://doi.org/10.3141/1989-67

Khanzadeh Moradllo, M., Sudbrink, B., Ley, M.T., 2016. Determining the effective service life of silane treatments in concrete bridge decks. Constr Build Mater 116, 121–127. https://doi.org/10.1016/J.CONBUILDMAT.2016.04.132

King, P.M., 1981. Comparison of methods for measuring severity of water repellence of sandy soils and assessment of some factors that affect its measurement. Australian Journal of Soil Research 19. https://doi.org/10.1071/SR9810275

Ksaibati, Khaled, Armaghani, J., Fisher, Jason, Ksaibati, K, Fisher, J, 2000. Effect of Moisture on Modulus Values of Base and Subgrade Materials. Transp Res Rec 20–29.

Kuhn, S., 1932. . ~Jber die Beziehungen zwischen Hygroskopizit~it, adsorbierten Basen und einigen physikalischen Eigenschaften bei BiSden. Z. Pflanzenerniihr., Diing. 359–370.

Kuron, H., 1930. Versuche zur Feststellung tier Gesamtoberfl~iche an Erdb~den, Tonen und verwandten Stoffen. Z. Pflanzenerniihr., Dung 179–203.

Letey, J., Carrillo, M.L.K., Pang, X.P., 2000. Approaches to characterize the degree of water repellency. J Hydrol (Amst) 231–232, 61–65. https://doi.org/10.1016/S0022-1694(00)00183-9

Lourenço, S.D.N., Saulick, Y., Zheng, S., Kang, H., Liu, D., Lin, H., Yao, T., 2018. Soil wettability in ground engineering: fundamentals, methods, and applications. Acta Geotech. https://doi.org/10.1007/s11440-017-0570-0

Mahedi, M., Satvati, S., Cetin, B., Daniels, J.L., 2020. Chemically Induced Water Repellency and the Freeze–Thaw Durability of Soils. Journal of Cold Regions Engineering 34, 04020017. https://doi.org/10.1061/(ASCE)CR.1943-5495.0000223

Maisanaba, S., Ortuño, N., Jordá-Beneyto, M., Aucejo, S., Jos, Á., 2017. Development, characterization and cytotoxicity of novel silane-modified clay minerals and nanocomposites intended for food packaging. Appl Clay Sci 138, 40–47. https://doi.org/10.1016/J.CLAY.2016.12.042

Malisher, M., Daniels, J., Uduebor, M., Saulick, Y., 2023. Compaction and Strength Characteristics of Engineered Water Repellent Frost Susceptible Soils. Geo-Congress 2023 452–461. https://doi.org/10.1061/9780784484661.047

Moiseev, K.G., 2008. Determination of the specific soil surface area from the hygroscopic water content. Eurasian Soil Science 41, 744–748. https://doi.org/10.1134/S1064229308070089/METRICS

Muhammad, N., Siddiqua, S., 2021. Moisture-dependent resilient modulus of chemically treated subgrade soil. Eng Geol 285, 106028. https://doi.org/10.1016/J.ENGGEO.2021.106028

Naqvi, M.W., Sadiq, Md.F., Cetin, B., Adeyanju, E., Daniels, J.L., 2023. Development, Construction, and Instrumentation of Pilot Freeze–Thaw Resistant Granular Roadways Test Cells, in: 13th International Conference on Low-Volume Roads. Cedar Rapids, Iowa, pp. 3–9.

Nourmohamadi, M., Abtahi, S.M., Hashemolhosseini, H., Hejazi, S.M., 2022. Control of frost effects in susceptible soils using a novel sandwich geocomposite composed of geotextile-soil-nano silica aerogel-geotextile liners. Transportation Geotechnics 33, 100718. https://doi.org/10.1016/J.TRGEO.2022.100718

Oluyemi-Ayibiowu, B.D., Uduebor, M.A., 2019. Effect of Compactive Effort on Compaction Characteristics of Lateritic Soil Stabilized With Terrasil. Journal of Multidisciplinary Engineering Science Studies (JMESS) 5, 2458–925.

Prakash, K., Sridharan, A., Sudheendra, S., 2016. Hygroscopic moisture content: Determination and correlations. Environmental Geotechnics 3. https://doi.org/10.1680/envgeo.14.00008

Research Board, T., n.d. National Cooperative Highway Research Program NCHRP Synthesis 278 Measuring In Situ Mechanical Properties of Pavement Subgrade Soils A Synthesis of Highway Practice.

Robinson, D.A., Cooper, J.D., Gardner, C.M.K., 2002. Modelling the relative permittivity of soils using soil hygroscopic water content. J Hydrol (Amst) 255, 39–49. https://doi.org/10.1016/S0022-1694(01)00508-X

Roy, W.R.*., Krapac, I.G.*., Chou, S.-F.J.*., Griffin, R.A., 1992. Technical Resource Document: batch-type procedures for estimating soil adsorption of chemicals. Report.

Salem, H., 2005. Effect Of Seasonal Moisture Variation On Subgrade Resilient Modulus. Improving Pavements With Long-Term Pavement Performance: Products for Today and Tomorrow, November 2005 - FHWA-RD-03-049.

Saulick, Y., Lourenço, S.D.N., Baudet, B.A., 2019. Optimising the hydrophobicity of sands by silanisation and powder coating. Géotechnique 1–10. https://doi.org/10.1680/jgeot.19.p.108

Saulick, Y., Lourenço, S.D.N., Baudet, B.A., Woche, S.K., Bachmann, J., 2018. Physical properties controlling water repellency in synthesized granular solids. Eur J Soil Sci 69, 698–709. https://doi.org/10.1111/ejss.12555

Shah, P.H., Singh, D.N., 2006. Methodology for determination of hygroscopic moisture content of soils. J ASTM Int 3. https://doi.org/10.1520/JAI13376

Simonsen, E., Isacsson, U., 1999. Thaw weakening of pavement structures in cold regions. Cold Reg Sci Technol 29, 135–151. https://doi.org/10.1016/S0165-232X(99)00020-8

Taber, S., 1930. The Mechanics of Frost Heaving. J Geol 38. https://doi.org/10.1086/623720

Torrent, J., Del Campillo, M.C., Barrón, V., 2015. Short communication: Predicting cation exchange capacity from hygroscopic moisture in agricultural soils of Western Europe. Spanish Journal of Agricultural Research 13, e11SC01-e11SC01. https://doi.org/10.5424/SJAR/2015134-8212

Uduebor, M., Adeyanju, E., Saulick, Y., Daniels, J., Cetin, B., 2023. Engineered Water Repellency for Moisture Control in Airport Pavement Soils. Airfield and Highway Pavements 2023 92–102. https://doi.org/10.1061/9780784484906.009

Uduebor, M., Adeyanju, E., Saulick, Y., Daniels, J., Cetin, B., 2022a. A Review of Innovative Frost Heave Mitigation Techniques for Road Pavements. International Conference on Transportation and Development 2022. https://doi.org/10.1061/9780784484357

Uduebor, M., Daniels, J., Mohammad, N., Cetin, B., 2022b. Engineered Water Repellency in Frost Susceptible Soils 457–466. https://doi.org/10.1061/9780784484012.047

Uduebor, M.A., Daniels, J.L., Adeyanju, E., Sadiq, Md.F., Cetin, B., 2023. Engineered Water Repellency for Resilient and Sustainable Pavement Systems. International Journal of Geotechnical Engineering. https://doi.org/10.1080/19386362.2023.2241280

U.S. Army Corps of Engineers, 1965. Soils and geology- Pavement design for frost conditions. Department of the Army courses Department of Civil Engineering, University of New Technical Manual TM 5-818-2.

US Army Corps of Engineers, 1965. Soils and Geology – Pavement Design for Frost Conditions. Hanover, NH.

Wasif Naqvi, M., Sadiq, Md.F., Cetin, B., Uduebor, M., Daniels, J., 2022. Investigating the Frost Action in Soils. Geo-Congress 2022 257–267. https://doi.org/10.1061/9780784484067.027--

Wuddivira, M., Robinson, A., Lebron, I., Brechet, L., Atwell, M., De Caires, S., Oatham, M., Jones, S., Abdu, H., Verma, A., Tuller, M., 2012. Estimation of Soil Clay Content from Hygroscopic Water Content Measurements. Soil Science Society of America Journal 1529–1535. https://doi.org/10.2136/sssaj2012.0034

Zaman, M.W., Han, J., Zhang, X., 2022. Evaluating wettability of geotextiles with contact angles. Geotextiles and Geomembranes 50, 825–833. https://doi.org/10.1016/J.GEOTEXMEM.2022.03.014

CHAPTER 5: APPLICATION OF ENGINEERED WATER REPELLENCY IN FROST SUSCEPTIBLE SOILS

ARTICLE 7: ENGINEERED WATER REPELLENCY FOR FROST HEAVE MITIGATION

ABSTRACT

Frost action (heaving and thawing) is a perennial problem encountered in the design, construction, and management of civil engineering structures, particularly road pavements in cold regions and areas that experience seasonal sub-freezing temperatures. This paper reviews the existing methods for frost heave mitigation and proposes an innovative approach through engineered water repellency. Soil was collected from a test plot at the Charlotte Douglas International Airport and treated with a commercially available organosilane. Preliminary results indicate an increase in the maximum dry density from 17.54kN/m^3 to 17.66kN/m^3 and a decrease in the optimum moisture content from 17.36% to 11.75% after treatment. Data obtained from performance tests carried out under sub-freezing weather conditions indicated that the treatment was effective in limiting the infiltration and migration of water into the soil matrix when compared with the untreated soil. As such, engineered water repellency may be a viable solution for Airports and Departments of Transportation seeking methods to mitigate frost action.

1. Introduction

Frost heave is caused by the formation of ice lenses within the soil matrix of frost susceptible soils. The creation and subsequent melting of such lenses, combined with the effects of repeated traffic loads, (e.g. airport pavements), leads to long-term degradation. The uneven nature of this process adversely impacts utilities and leads to road closures, weight restrictions, and a reduction in the ride quality due to uneven heaving. This problem is exacerbated even further during the spring months when the thawing ice causes an increase in the moisture condition of road pavements, resulting in further reduction of pavement strength under imposed loads (thaw weakening). According to Doré et al (2005), seasonal freezing can contribute up to 75% of pavement degradation and it is estimated that over 2 billion is spent annually on pavement maintenance and restoration due to frost action in the US (FHWA,1999). To ensure good performance over the life cycle of the pavement, there is a need to explore alternative methods to mitigate the effects of frost heaving.

Traditional frost mitigation techniques focus on controlling either one or more of the three basic requirements for frost heaving; 1. The presence of frost-susceptible soils (FSS) (silt-sized fractions), which are soils that promote the migration of water towards a freezing front resulting in the formation of an ice lens. 2. Sub-freezing temperatures result in the freezing of water within the soil pores. The conversion of liquid water to solid ice has the effect of desaturating the pore space and increasing capillary suction, resulting in a negative pore water pressure. And as ice forms, it excludes ions that increase osmotic suction. 3. A continuous supply of water can result in continued ice formation and soil displacement. In the presence of sub-freezing temperatures, FSS would not heave if dry or

will experience limited heaving utilizing the in-situ moisture present. The degree to which ice lenses grow and heaving will occur within frost susceptible soils under sub-freezing temperature is a function of the availability of a water source, either as a groundwater table or perched water within the soil matrix.

This paper will focus on reviewing some of the methods and techniques used in frost heave mitigation in road pavements. It will also highlight the innovative, cost-effective solution of Engineered Water Repellency (EWR), a process where FSS are treated with Organo-Silane (OS) making them hydrophobic (water repellent). Preliminary results from characterization and performance tests carried out are presented and discussed, exploring the viability of EWR in pavement design.

2. Frost Heave Mitigation Techniques

2.1 Frost susceptibility of soils

According to Chamberlain (1981), many definitions of frost susceptible soil (FSS) fit only partially, failing to address relevant processes. One of the earliest definitions comes from Casagrande in 1932: "under natural freezing conditions and with sufficient water supply one should expect considerable ice segregation in non-uniform soils containing more than three percent of grains smaller than 0.02 mm, and in very uniform soils containing more than 10 percent smaller than 0.02 mm." However not all soils that satisfy this condition lead to frost heaving. Improved, yet not still all-inclusive definitions, combine grain size distribution and soil water interaction (capillary rise e.g more 2 m (Beskow (1935)), (Freden and Stenberg (1980)), hydraulic conductivity) or soil mineralogy (Atterberg limits e.g. plasticity index greater than 35%, clay content, and particle diameter

Vlad (1980)). Empirical classifications from direct observation in the field or through laboratory procedures are preferred because frost heaving is visible and tangible. However, empirical classifications are not standardized as different freezing setups could be used in the laboratory for FSS testing.

2.1.1 Replacing frost susceptible soil with non-frost-susceptible soils.

According to Christopher *et al.* (2006), frost heave mitigation procedures include FSS replacement, placement, and compaction of non-susceptible materials above FSS, elimination of soil fines by chemical stabilization, or drainage, as well as increased pavement thickness. These procedures aim at preventing frost heaving by eliminating one or two conditions required for frost heaving to occur. FSS replacement eliminates the soil variable in the frost heaving equation, even with sub-freezing temperature and water supply. The 1993 AASHTO Guide for pavement structures noted that removal of FSS is an acceptable practice towards frost heave mitigation. Removal of the FSS is governed by the depth of frost penetration and chosen approach (either Complete Frost Protection approach and Limited Subgrade Frost Penetration), grades, state Department of Transportation (DOT) policy, and other design considerations. Most DOTs in the USA have opted for a replacement, however, to varying depths (Schaus & Popik, 2011). Studies by Evans *et al.* (2011) indicated that the performance of FSS replacement is dependent on the excavation depth to frost depth. A more significant replacement depth with proper drainage translates to better performance, as observed with complete frost heave elimination at near-total frost depth replacement. A constant site survey showed that when

replacement is just about one-third of the frost depth, frost heave reduction is just about half (Evans *et al.*, 2011).

2.2 Temperature gradient

2.2.1 Polymer Injection

Given an FSS with a constant source of water supply, the temperature profile is the most dominant factor controlling frost heave in pavement structures. To impede the passage of subzero temperatures into the soil, polymer injection is used to create an insulation barrier below the road base material. This insulating blanket limits heat loss from the underlying subgrade layers. Therefore, the temperature of the subgrade remains higher, making it less likely to freeze (Edgar *et al.*, 2015). This technique involves the injection of a three-inch layer of polymeric or polyurethane foam into the subgrade. The appealing aspect of this method involves its application to any existing road pavement, as it does not require the removal of the overlying aggregate and surface layer within a short period. In addition, the foam supports the road surface. Edgar *et al.* (2015) tested Polymer injection successfully at the Battle Mountain Highway, Wyoming, where the temperatures below the polymer stayed at or above freezing, resulting in a decrease in the heave of 83 %.

2.2.2 Polystyrene boards

Synthetic insulation has been placed below a base to prevent the advance of freezing temperatures into the subgrade. Polystyrene, either expanded or extruded, is an excellent insulator, which thwarts freezing temperature from reaching the subgrade from the pavement. Extruded polystyrene boards were extensively used in Sweden from 1950 to

the 1980s to mitigate frost heaving (Gandahl, 1988). The application of expanded polystyrene insulation was tested in some road sections in Canada between 1962 and 1965, with 7.6 cm thickness achieving complete prevention. However, joints between treated and untreated sections developed bumps (solved by staggering the ends by 47 inches)). Guo *et al.* (2018) showed that Polystyrene boards of 12 cm could reduce frost heaving up to 92.6% and frozen depth by 10.1 cm. Polystyrene boards performance depends on the thickness. Municipality of Anchorage (MOA) and the Alaska Department of Transportation and Public Facilities (ADOT&PF), recommends High-density polystyrene board with a minimum compressive strength of 413 kPa with maximum water absorption of 0.10 by volume; a minimum of 45.7 cm of gravel fill over the insulation board to protect it from heavy wheel loads during construction and minimize frost formation on the pavement surface and extend the insulated section limits.

2.3 Supply of groundwater

Given an FSS and a freezing temperature, water availability is the most dominant factor controlling frost heave in pavement structures (Hermansson & Guthrie, 2005). The depth of the water table to the freezing front determines how much more water could be drawn to the frozen fringe. Numerous studies such as Hermansson (2000) and Guthrie and Hermansson (2003) have indicated that frost heaving in the soil is due to both freezing of free in-situ water presence in FSS- subgrade, (primary frost heave) and more importantly, from water inflow towards the freezing front (secondary frost heave). As long as the water table is within the capillary range of the groundwater table, the water supply is continuous.

The presence of water within 3 meters of frost penetration is considered a high frost hazard potential Oman and Lund (2018); Christopher et al. (2006). The influence of the water table is consistent with the studies by Hermansson and Guthrie (2005) and McGaw (1972), which indicated a reduction in frost heave and water uptake rates with decreasing water table height. The lower the water table, the lower the frost heave and water intake.

2.3.1 Techniques to the lower groundwater table

When FSS removal is not possible, the next step is to prevent continuous water supply. Water restriction could be achieved through various means, widely through the subsurface drainage systems. The core objective is to intercept and remove infiltrating water before it contributes to frost heave and curb water infiltration into overlying fine-pored unsaturated soil. Deep drains, capillary barriers, or a combination of both can be used to minimize water supply to the subgrade. Other methods include the utilization of Vertical Drains (Gravel mixed with sodium chloride or calcium chloride, rather than gravel alone) (Taivainen, 1963), improved ditching or ditch cleanout, or the installation of perforated sub drains beneath the shoulder of the highway.

Chemical Stabilization

Soil stabilization by additives has shown considerable performance in frost heave mitigation. Lime and cement are the most widely used additives for frost heaving control due to processes such as cation exchange, flocculation and agglomeration, cementitious hydration, and Pozzolanic reaction (Nourmohamadi, *et al.*, 2022). For lime application, an extended curing period is necessary to prevent the formation of FSS. Weakly cemented material usually has less capacity to endure repeated freezing and thawing without

degradation than firmly cemented material. Cement additive makes FSS less sensitive to moisture, and the hydration products will reduce frost heaving. But the impact of cement within the soil varies as the number of freeze-thaws increases (Lu *et al.*, 2020; Shidi and Kamei, 2014; Baldovino *et al.*, 2020). Other materials incorporated or used alone includes fly ash (Zhang *et al.*, 2016), cotton fiber (Liu *et al.*, 2020), jute fiber, steel fiber (Gullu and Khudir, 2014), polypropylene, basalt, glass, and microbially induced carbonate precipitation (MICP) (Sun *et al.* 2021; Gowthaman *et al.*, 2020). The major drawback is the long curing period. Furthermore, it is a time-consuming process with massive soil operations and machinery.

Capillary barriers

Capillary barriers include horizontal geocomposite drains (Henry and Holtz, 2001; Nourmohamadi, *et al.*, 2022) or an open-graded gravel layer sandwiched between two layers of geotextile separators, porous insulating layers (sand) (Rengmark, 1963). Studies have shown their effectiveness in preventing water from being drawn up to the ice front, yet frost heave could still occur. FSS can be replaced and compacted above the capillary break layer. In general, the thickness of the capillary break must supersede the height of the capillary rise of water. Then, the capillary break must be placed above the water table and as deep in the soil as possible below the depth of frost penetration. In addition, the drainage system must be placed below it, and lastly, clogging must be prevented using filters at the top and bottom (Henry, 1996).

Geotextiles

Geotextile in frost heave mitigation could serve as a capillary barrier, as filter layer (or as separator layer) (Roth, 1975; Roth, 1977; Clough and French, 1982), or to reinforce soil during freezing and thawing (Hoover *et al.*, 1981; Henry, 1996). They are good capillary breaks because of their relatively large pore sizes compared to FSS. Numerous experimental works, such as Allen *et al.* (1983) and Hoover et al., 1981, have shown that geotextiles can reduce frost heaving. Shoop and Henry (1991) indicated that when the water table was above the geotextile, the geotextile did not influence frost heave or the distribution of water in the soil. Studies by Zhang *et al.* (2014), Zhang and Belmont (2009), Galinmoghadam *et al.* (2019), and Zornberg *et al.* (2017), showed the efficiency of wicking fabric in preventing frost boiling as it absorbs water from surrounding soils and effectively drains it out.

Geofoam

Insulating materials can be used to lessen the heat exchange between the cooling surfaces and adjacent soils. The soil temperature can be maintained above the freezing point Liu *et al.* (2019). Recent studies are focusing on the application of geofoam as a thermal insulator to the culvert and transition sections. Studies such as Moussa *et al.* (2019), and Hua *et al.* (2014), recommended the utilization of geofoam of about 75 to 100 mm thickness. However, more studies need to be performed to standardize the geofoam's depth of placement and thickness.

2.4 Engineered Water Repellency

Every technique geared toward frost heaving reduction involves removing FSS, limiting or cutting water flow, and insulating the soil against freezing temperature. However, they do not provide a permanent solution as clogging, soil deposition, cost of implementation, and changing soil boundary temperature have reduced their efficiency (Henry, 1996). Also, many of these techniques are costly and labor-intensive, requiring extensive cost and life-cycle analysis. A new cost-effective approach is to make existing soil hydrophobic, thereby preventing water migration. To achieve hydrophobicity, the soil is treated with organosilane (O.S.), a silica-based organic coupling agent. The effectiveness of O.S., terms from the modification of the soil surface by grafting organic molecules without providing any interparticle bonding. Studies by Sage and Porebska (1993), Mahedi *et al.* (2020), and Daniels *et al.* (2021) have demonstrated that OS-treated soils achieve higher contact angles than untreated FSS corresponding to reduced water flow, indicating frost heave mitigation. These studies showed that hydrophobic soils take far less water than FSS layers. Therefore, the heaving rate or height is negligible; the treated soil is hence classified either as low or negligible potential FSS.

3. Materials and Methods

3.1 Material

The soil was collected from the currently constructed taxiway and de-icing pad on the south side of the Charlotte-Douglas International airport, North Carolina, USA, Soils were prepared and oven-dried at the geotechnical laboratory of the University of North Carolina at Charlotte. Index property tests were carried out according to ASTM standards.

The soil was classified as Silty Sand (SM) according to the Unified Soil Classification System (USCS) and A-6(2) based on the AASHTO classification system. Table 1 below gives the summary of the index property tests carried out on the soil sample.

Table 7- 1 Summary of Tests (Uduebor et al, 2023)

Properties	**Soil**
Specific Gravity, Gs (ASTM D854)	2.69
% Passing – #4	100
% Passing – #10	77.2
% Passing – #40	71.94
% Passing – #200	48.44
Liquid Limit, LL (ASTM D4318)	30.72
Plasticity Index, PI	10.16
Optimum Moisture Content (%) (ASTM D698)	17.19
Max. Dry Unit Weight (kN/m3) (ASTM D698)	17.08
USCS Classification	SM
AASHTO Classification	A-6(2)

3.2 Treatment

The soil was treated according to the protocol after Uduebor et al (2022). Commercial grade organosilane (OS) product was utilized for the treatment. It is a viscous, water-soluble, and reactive soil modifier that permanently modifies the soil surface, making it hydrophobic. Such chemicals have been used in food-grade applications (Maisanaba et al., 2017). It is also and has been utilized in previous studies as a soil modifier and performance enhancer, particularly in stabilization for pavement applications (Daniels & Hourani, 2009; Oluyemi-Ayibiowu & Uduebor, 2019)

A batch sorption treatment approach according to Bachmann (Bachmann et al., 2000, 2003) was utilized. Treatment was done using a mix ratio of 1:40 (OS to Soil), batched by weight. For 100g of soil, 2.5g of OS was mixed with deionized water (EC ~

1µS/cm) to make up 100g. The resulting OS mixture was utilized to completely saturate the specimen at a liquid/solid ratio of 1:1 (100g of soil to 100g of OS mixture). Where compaction was required, the OS mixture was utilized as the molding water used for the mixing of the soil samples.

3.3 Hydrophobicity Assessment

Treated soils need to be assessed for their level of hydrophobicity. Several methods abound to assess hydrophobicity in soils. Three methods were selected to assess the level of hydrophobicity in this study: contact angle, water drop penetration time and breakthrough head.

3.3.1 Contact Angle Test

Contact Angle (CA) tests directly measure the soil-water contact angle based on the sessile drop method using a Goniometer (Feyyisa et al., 2017; Keatts et al., 2018). A monolayer of soil was placed on a double-sided tape attached to a glass slide and the soil specimen was placed on a goniometer (Ramehart Instruments, 260-U1, standard goniometer, #150512). Drops of deionized water were placed on the surface of the specimen utilizing a FlowTrac II (Geocomp Products) with image capturing and measurements taken. The drop advancement was continued until a stable contact angle is observed which is taken as the apparent contact angle of the sample. Contact angle measurements less than 90^o are considered wettable/hydrophilic, while angles measured between 90^o and 150^o are considered hydrophobic. Angles above 150^o are taken to be super hydrophobic.

3.3.2 Water Drop Penetration Time Test

Water Drop Penetration Time Test (WDPT) is the most used because of its simplicity and versatility (Bachmann et al., 2003; Dekker et al., 2009). Treated samples were placed in aluminum cans and drops of deionized water (50 ± 1µL volume) were placed on the soil surface with a burette. The time taken for the drops to infiltrate into the soil samples is recorded. Any penetration less than or equal to 0.2 seconds was taken as instantaneous and measurements were terminated after 1 hour (3600s). Previous studies (Bisdom et al., 1993; King, 1981) categorize water repellency based on corresponding WDPTs as follows; non-repellent/Completely wettable (≤1s), slightly repellent (1-60s), strongly repellent (60-600s), severely repellent (600-3600s) and extremely repellent (≥3600s).

Figure 7-1 Contact Angle Test; Water Drop Penetration Test (Uduebor et al, 2023)

3.4 Field Performance Test

Two identical test setups were constructed for performance testing of both untreated and treated samples. An acrylic cylinder with a thickness of 1.27 cm, an internal diameter of 19.05 cm, and a height of 22.5cm was first filled with a sand layer to a height of 5 mm, after which soil samples (untreated and treated) were compacted using three lifts of 7.33 mm at the OMC and MDD using the standard proctor compaction effort. The soil samples

were compacted to a height of 22cm and instrumented with one TEROS 12 and TEROS 21 sensor (Meter Group) each at a depth of 11 cm into the sample. The TEROS 12 is a sensor for monitoring volumetric water content (VWC), the temperature in soil and soilless substrates, and Electrical Conductivity. The TEROS 21 Soil Water Potential Sensor measures soil water potential as well as soil temperature. The sensors were connected to the ZL6 Data Logger (Meter Group), and readings were logged at 10-minute intervals. Fig. 2 below shows a schematic drawing of the setup. The complete setup was placed out in the yard within the University premises, where a weather station was situated to monitor real-time precipitation temperature and other weather data. Data from Zentra was collected every day and results were analyzed.

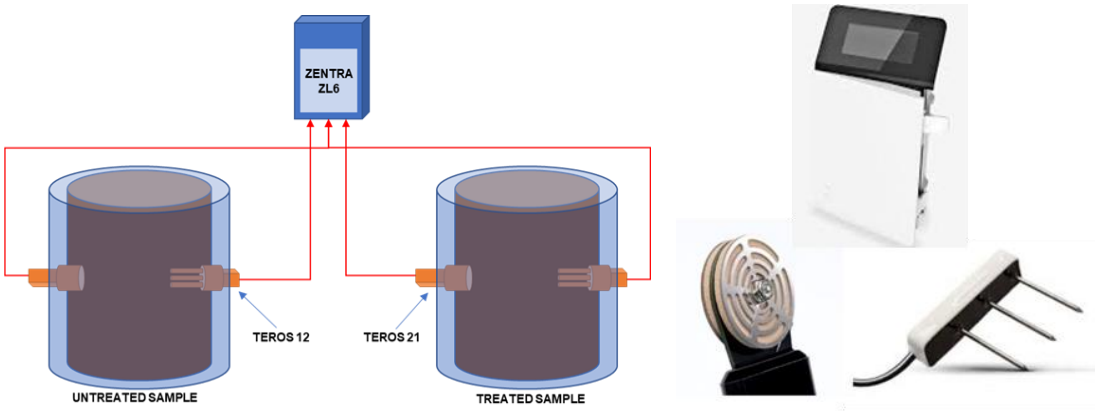

Figure 7-2 Schematic of the performance test setup; Teros 21, Teros 12 and Zentra ZL6 (Uduebor et al, 2023)

4. Results & Discussion

4.1 Compaction

The result of compaction tests carried out on the treated soil showed an increase in the maximum dry density from 17.08kN/m^3 to 17.56 kN/m^3 while the water content decreased from 17.19% to 12.13%. This improvement in density has also been reported in previous tests (Barbieri et al., 2020; Oluyemi-Ayibiowu & Uduebor, 2019; Uduebor et al., 2022), and results from the reduced friction, better lubrication, and bonding action of the coating layer of hydrophobic alkyl siloxane that allows for better compaction of the soil particles.

4.2 Hydrophobicity Assessment

The apparent contact angle was ~142^o (hydrophobic) compared to ~15^o for the untreated soil. The time taken for water droplets to infiltrate into the treated soil was >3600s (extremely water-repellent) compared to < 2s of the untreated soil (wettable). The results indicate that the treatment was effective (the soil is hydrophobic) and there is a reduced permeability through the soil. Correlations between apparent contact angle and water entry pressure, the pressure required to infiltrate the treated sample.

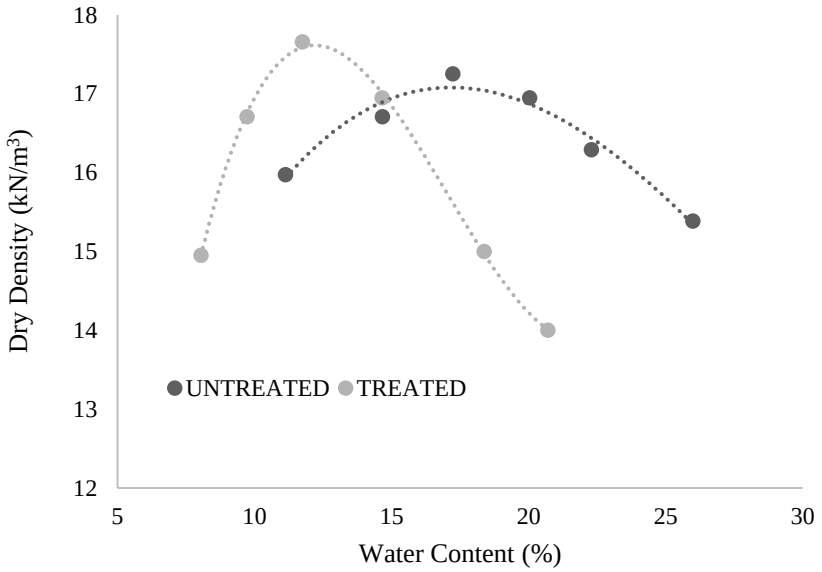

Figure 7-3 Compaction curve of untreated and treated soils (Uduebor et al, 2023)

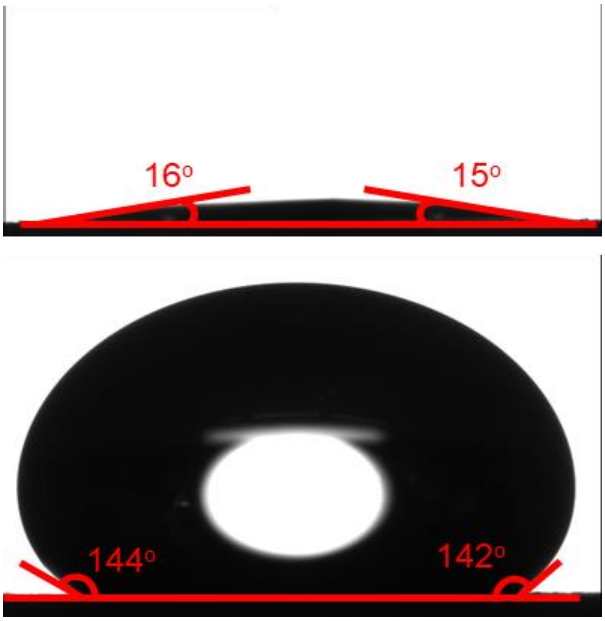

Figure 7- 4 Contact Angles for untreated and treated soils (Uduebor et al, 2023)

4.3 Field Performance Test

The results for the performance test carried out on both treated and untreated samples are given in Figure 5. Both setups were subjected to extreme weather conditions with snow cover, freezing, and thawing. It was observed that the temperature profiles within the two setups were similar indicating very little variation between the thermal conductivities of water-repellent treated and untreated samples. The readings also lag air temperature readings obtained from a weather station installed at the testing site.

Water content results indicated large variations correlating with precipitation, while the treated sample showed very little variation in water content. This stable reading also indicates that there is no migration of water through the sample and that the treatment is effective in limiting infiltration into the soil. Water content in the treated sample also declined gradually regardless of precipitation, indicating no infiltration into the soil. Instead, moisture was gradually removed by vaporization from the soil. This is because water-repellent soils can inhibit the permeation of water while remaining gas-permeable (Lourenço et al., 2018). It is expected that under drier conditions the soil will lose moisture resulting in a decrease in the moisture content and an increase in the matric suctions recorded. The resultant effect of this is a gradual “drying” effect of the treated soil up to a residual water content value and an accompanying ability to be unwettable. This means treated soils can be dry all year round regardless of prevalent moisture conditions. The untreated soil sample had large variations in water content, even getting completely saturated (Matric Suction = 0 kPa). This increment is due to the infiltration of water into the soil, while the decrement is due to evaporation. Larger matric suctions (values) were

recorded from the treated samples when compared to the untreated sample because of the lower moisture content of the treated sample.

Studies have shown that moisture condition is important to the performance of a pavement subgrade (Janssen & Dempsey, 1981). There is a correlation between the moisture content and shear strength and resilient modulus of pavement soils, with increasing moisture content resulting in a decrease in the strength properties (Black, 2015; Thompson & Robnett, 1976). Moisture also plays an important factor in frost heaving, particularly in areas subjected to seasonal sub-freezing temperatures. The moisture content limits the amount of heaving and flow based on the supply of water present within the soil or available below the depth of freezing (Beskow, 1948; Taber, 1930). Therefore, the ability to keep pavement systems and in particular subgrades dry is critical to performance. Moreover, pavements can be designed with smaller thicknesses resulting in considerable savings in construction costs.

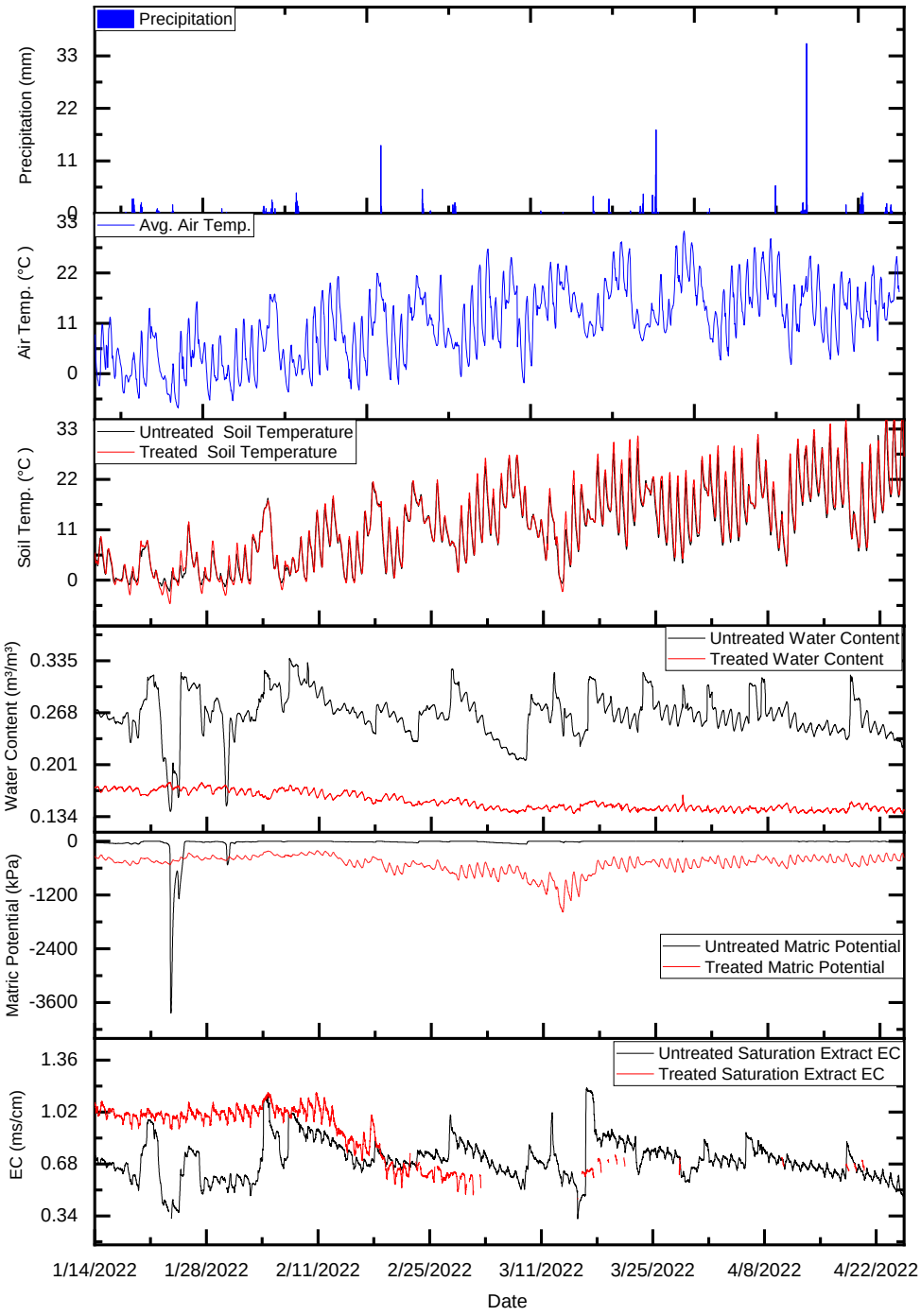

Figure 7-5 Results from Field Tests (Uduebor et al, 2023)

There were two winter storm events (Jan 20-23, 29-30) during the period, which provided a good opportunity for observing the performance of the samples under sub-freezing conditions. The untreated soil underwent a rapid reduction in moisture content due to the freezing of the pore water. This can result in shrinking and cracks that further reduce the strength of the pavement subgrade. The formation of ice and the resulting volumetric increase within the pore space also result in heave, a major problem for road pavements. There is also a potential loss in the bearing capacity of the subgrade due to the thawing of the ice (indicated by maximum water content after the thawing of the ice). A maximum heave of ~6mm was observed for the untreated soil sample after the two extreme winter storm events. Treated soil performed considerably better under sub-freezing conditions, without any large variations in moisture content or resulting heave (see Fig. 6)

Figure 7-6 a) Water beading on treated sample b) Treated sample without heave, d) Untreated sample showing heave (~6mm)(Uduebor et al, 2023)

5. Conclusion

There are several traditional and evolving methods for mitigating frost action, including engineered water repellency (EWR). EWR prevents moisture intrusion, increases dry density, and decreases the optimum moisture content. In this study, the maximum dry density increased from 17.54 kN/m^3 to 17.66 kN/m^3, while the optimum moisture content decreased from 17.36% to 11.75% after treatment with a commercially available organosilane. Performance tests indicated that there was no infiltration of water and little variation in the water content of the treated sample. Treatment also prevented moisture

migration within the soil matrix and limited the formation of pore ice and subsequent frost heaving of the soil. Treated samples also performed better under freezing conditions with no heaving compared to ~6mm of untreated soil. Water-repellent additives prove to be a useful tool for moisture control in road pavements, giving design engineers more confidence concerning soil behavior, allowing for easier design, reducing speculation of performance under unprecedented moisture impact events, and saving material and construction costs.

REFERENCES

AC 150/5380-6C - Guidelines and Procedures for Maintenance of Airport Pavements – Document Information. (n.d.). Retrieved November 24, 2022, from https://www.faa.gov/airports/resources/advisory_circulars/index.cfm/go/document.current/documentnumber/150_5380-6

Bachmann, J., Horton, R., van der Ploeg, R. R., Woche, S. (2000). Modified sessile drop method for assessing initial soil-water contact angle of sandy soil. *Soil Science Society of America Journal*, *64*(2), 564–567. https://doi.org/10.2136/SSSAJ2000.642564X

Bachmann, J., Woche, S. K., Goebel, M. O., Kirkham, M. B., Horton, R. (2003). Extended methodology for determining wetting properties of porous media. *Water Resources Research*, *39*(12). https://doi.org/10.1029/2003WR002143

Barbieri, D. M., Hoff, I., Mørk, M. B. E. (2020). Organosilane and lignosulfonate as innovative stabilization techniques for crushed rocks used in road unbound layers. *Transportation Geotechnics*, *22*, 100308. https://doi.org/10.1016/J.TRGEO.2019.100308

Bisdom, E. B. A., Dekker, L. W., Schoute, J. F. T. (1993). Water repellency of sieve fractions from sandy soils and relationships with organic material and soil structure. *Geoderma*, *56*(1–4). https://doi.org/10.1016/0016-7061(93)90103-R

Black, W. P. M. (2015). A Method of Estimating the California Bearing Ratio of Cohesive Soils from Plasticity Data*. *Https://Doi.Org/10.1680/Geot.1962.12.4.271*, *12*(4), 271–282. https://doi.org/10.1680/GEOT.1962.12.4.271

Brooks, T., Daniels, J. L., Uduebor, M., Cetin, B., Wasif Naqvi, M. (2022). *Engineered Water Repellency for Mitigating Frost Action in Iowa Soils*. https://doi.org/10.1061/9780784484012.046

Charlier, R., Hornych, P., Srešen, M., Hermansson, Å., Bjarnason, G., Erlingsson, S., Pavšič, P. (2009). Water influence on bearing capacity and pavement performance: Field observations. *Geotechnical, Geological and Earthquake Engineering*, *5*, 175–192. https://doi.org/10.1007/978-1-4020-8562-8_8

Daniels, J. L., Hourani, M., Harper, L. (2009). *Organo-silane chemistry : A water repellent technology for coal ash and soils*.

Daniels, J. L., Hourani, M. S. (2009). *Soil Improvement with Organo-Silane*. https://doi.org/10.1061/41025(338)23

de Jesús Arrieta Baldovino, J., dos Santos Izzo, R. L., Rose, J. L. (2021). Effects of Freeze–thaw Cycles and Porosity/cement index on Durability, Strength and

Capillary Rise of a Stabilized Silty Soil Under Optimal Compaction Conditions. *Geotechnical and Geological Engineering*, *39*(1), 481–498. https://doi.org/10.1007/S10706-020-01507-Y/FIGURES/12

Dekker, L. W., Ritsema, C. J., Oostindie, K., Moore, D., Wesseling, J. G. (2009). Methods for determining soil water repellency on field-moist samples. *Water Resources Research*, *46*(4). https://doi.org/10.1029/2008WR007070

dr. GUNNAR BESKOW, B. FIL. (1948). Soil Freezing and Frost Heaving with Special Application to Roads and Railroads. *Soil Science*, *65*(4). https://doi.org/10.1097/00010694-194804000-00015

Edgar, T., Potter, C., Mathis, R. (2015). Frost Heave Mitigation Using Polymer Injection and Frost Depth Prediction. *Proceedings of the International Conference on Cold Regions Engineering*, *2015-January* (January), 416–427. https://doi.org/10.1061/9780784479315.037

Feyyisa, J. L., Daniels, J. L., Pando, M. A. (2017). Contact Angle Measurements for Use in Specifying Organosilane-Modified Coal Combustion Fly Ash. *Journal of Materials in Civil Engineering*, *29*(9). https://doi.org/10.1061/(asce)mt.1943-5533.0001943

Feyyisa, J. L., Daniels, J. L., Pando, M. A., Ogunro, V. O. (2019). Relationship between breakthrough pressure and contact angle for organo-silane treated coal fly ash. *Environmental Technology and Innovation*, *14*. https://doi.org/10.1016/j.eti.2019.100332

Galinmoghadan, J., Zhang, X., Lin, C. (2019). *A Bio-Wicking System to Prevent Frost Heave in Alaskan Pavements: Phase II Implementation*. https://scholarworks.alaska.edu/handle/11122/10746

Gowthaman, S., Nakashima, K., Kawasaki, S. (2020). Freeze-thaw durability and shear responses of cemented slope soil treated by microbial induced carbonate precipitation. *Soils and Foundations*, *60*(4), 840–855. https://doi.org/10.1016/J.SANDF.2020.05.012

Guo, F., Shi, H., Cheng, M., Gao, W., Yang, H., Miao, Q. (2018). A study of the insulation mechanism and anti-frost heave effects of polystyrene boards in seasonal frozen soil. *Water (Switzerland)*, *10*(8). https://doi.org/10.3390/W10080979

Hamzah, M. O., Kakar, M. R., Hainin, M. R. (2015). An overview of moisture damage in asphalt mixtures. *Jurnal Teknologi*, *73*(4), 125–131. https://doi.org/10.11113/JT.V73.4305

Janssen, D. J., & Dempsey, B. J. (1981). Transportation Research Record 790 61 Soil-Moisture Properties of Subgrade Soils. *International Journal of Rock Mechanics and Mining Sciences and Geomechanics Abstracts*. https://doi.org/10.1016/0148-9062(82)91655-2

Keatts, M. I., Daniels, J. L., Langley, W. G., Pando, M. A., Ogunro, V. O. (2018). Apparent Contact Angle and Water Entry Head Measurements for Organo-Silane Modified Sand and Coal Fly Ash. *Journal of Geotechnical and Geoenvironmental Engineering*, *144*(6). https://doi.org/10.1061/(asce)gt.1943-5606.0001887

King, P. M. (1981). Comparison of methods for measuring severity of water repellence of sandy soils and assessment of some factors that affect its measurement. *Australian Journal of Soil Research*, *19*(3). https://doi.org/10.1071/SR9810275

Lourenço, S. D. N., Saulick, Y., Zheng, S., Kang, H., Liu, D., Lin, H., & Yao, T. (2018). Soil wettability in ground engineering: fundamentals, methods, and applications. In *Acta Geotechnica* (Vol. 13, Issue 1). Springer Verlag. https://doi.org/10.1007/s11440-017-0570-0

Mahedi, M., Satvati, S., Cetin, B., Daniels, J. L. (2020). Chemically Induced Water Repellency and the Freeze–Thaw Durability of Soils. *Journal of Cold Regions Engineering*, *34*(3). https://doi.org/10.1061/(asce)cr.1943-5495.0000223

Maisanaba S. Ortuño N. Jordá-Beneyto M. Aucejo S. Jos Á. (2017). Development characterization and cytotoxicity of novel silane-modified clay minerals and nanocomposites intended for food packaging. *Applied Clay Science* 40–47. https://doi.org/10.1016/j.clay.2016.12.042

Miah, M. T., Oh, E., Chai, G., Bell, P. (2022). Effect of Swelling Soil on Pavement Condition Index of Airport Runway Pavement. *Https://Doi.Org/10.1177/03611981221090517*, *2676*(10), 553–569. https://doi.org/10.1177/03611981221090517

Moses, T. L., Hulsey, J. L., Connor, B. (2009). *State of California • Department of Transportation Ca08-0564 2. Government Association Number 3. Recipient's Catalog Number 4. Title and Subtitle Airport Managers' Guide for the Maintenance of Asphalt Pavements of General Aviation Airports*.

Nourmohamadi, M., Abtahi, S. M., Hashemolhosseini, H., & Hejazi, S. M. (2022). Control of frost effects in susceptible soils using a novel sandwich geocomposite composed of geotextile-soil-nano silica aerogel-geotextile liners. *Transportation Geotechnics*, *33*, 100718. https://doi.org/10.1016/J.TRGEO.2022.100718

Oluyemi-Ayibiowu, B. D., Uduebor, M. A. (2019). Effect of Compactive Effort on Compaction Characteristics of Lateritic Soil Stabilized with Terrasil. *Journal of Multidisciplinary Engineering Science Studies (JMESS)*, *5*(2), 2458–2925. www.jmess.org

Omar, H. A., Yusoff, N. I. M., Mubaraki, M., & Ceylan, H. (2020). Effects of moisture damage on asphalt mixtures. *Journal of Traffic and Transportation Engineering (English Edition)*, *7*(5), 600–628. https://doi.org/10.1016/J.JTTE.2020.07.001

Rengmark, F. (1963). HIGHWAY PAVEMENT DESIGN IN FROST AREAS IN SWEDEN. *Highway Research Record*, *33*.

Rokitowski, P., Bzówka, J., Grygierek, M. (2021). Influence of high moisture content on road pavement structure: A Polish case study. *Case Studies in Construction Materials, 15*, e00594. https://doi.org/10.1016/J.CSCM.2021.E00594

Sage, J. D., & Porebska, M. (1993). Frost Action in a Hydrophobic Material. *Journal of Cold Regions Engineering*, *7*(4), 99–113. https://doi.org/10.1061/(ASCE)0887-381X(1993)7:4(99)

Savard, Y., Blois, K. de, Boutonnet, M., Hornych, P., Mauduit, C. (2005). Analysis of Seasonal Bearing Capacity Correlated to Pavement Deterioration in Cold Region. *Proceedings of the International Conferences on the Bearing Capacity of Roads, Railways and Airfields*. https://www.ntnu.no/ojs/index.php/BCRRA/article/view/2748

Schaus, L., Popik, M. (2011). Frost Heaves: A Problem that Continues to Swell. *Annual Conference of the Transportation Association of Canada*, 1201–1211.

Taber, S. (1930). The Mechanics of Frost Heaving. *The Journal of Geology*, *38*(4). https://doi.org/10.1086/623720

Thompson, M. R., Robnett, Q. L. (1976). *RESILIENT PROPERTIES OF SUBGRADE SOILS*.

Uduebor, M., Adeyanju, E., Saulick, Y., Daniels, J., Cetin, B. (2022). A Review of Innovative Frost Heave Mitigation Techniques for Road Pavements. *International Conference on Transportation and Development 2022*. https://doi.org/10.1061/9780784484357

Uduebor M.A., Adeyanju E., Saulick Y., Daniels J.L. (2023): Engineered Water Repellency for Moisture Control in Airport Pavement Soils. *ASCE International Conference on Transportation and Developmen 2023t*.

Zhang, X., Presler, W., Li, L., Jones, D., Odgers, B. (2014). Use of Wicking Fabric to Help Prevent Frost Boils in Alaskan Pavements. *Journal of Materials in Civil Engineering*, *26*(4), 728–740. https://doi.org/10.1061/(ASCE)MT.1943-5533.0000828

Zhang, Y., Johnson, A. E., White, D. J. (2016). Laboratory freeze–thaw assessment of cement, fly ash, and fiber stabilized pavement foundation materials. *Cold Regions Science and Technology*, *122*, 50–57. https://doi.org/10.1016/J.COLDREGIONS.2015.11.005

Zornberg, J. G., Azevedo, M., Sikkema, M., Odgers, B. (2017). Geosynthetics with enhanced lateral drainage capabilities in roadway systems. *Transportation Geotechnics*, *12*, 85–100. https://doi.org/10.1016/J.TRGEO.2017.08.008

CHAPTER 6: OSMOTIC POTENTIAL IN FREEZING SOILS

ARTICLE 8: MEASUREMENT OF OSMOTIC SUCTION IN FREEZING SOILS

ABSTRACT

Frost heave, a pivotal phenomenon in freezing soil systems, has historically garnered significant attention due to its influence on soil behavior. However, the role of osmotic potential, a crucial factor in this process, has remained enigmatic, largely due to equipment limitations. This study challenges the notion that osmotic potential is insignificant by investigating its dynamics in freezing soils. Naturally frost-susceptible soil from North Carolina was utilized in this study and was prepared by washing and treating it with various concentrations of NaCl (DI, 0.01, 0.1, 1M). A comprehensive methodology combining temperature, moisture content, and electrical conductivity measurements was utilized to assess the osmotic potential during freezing and thawing regimes. A multiple linear regression model was developed, showing strong correlations between temperature, moisture content, electrical conductivity, and molar concentration, with moisture content having a significant impact. The model's validity is confirmed through comparisons with actual freeze-thaw measurements, demonstrating its accuracy for positive temperatures. Below -10°C, its accuracy diminishes, indicating potential areas for further refinement. The study introduces an argument for the significance of osmotic potential in frost heave studies and provides a valuable model for estimating real-time molar concentration changes in freezing soils. These findings open new avenues for understanding the interplay of matric and osmotic potentials in freezing soil systems, shedding light on factors influencing water migration and frost heave. Further research and refinement of the model could yield deeper insights into freezing soil processes, with practical implications for geotechnical and environmental applications.

1. Introduction

The phenomenon of frost heave has captivated the attention of researchers for decades, as it plays a pivotal role in shaping the behavior of freezing soil systems. While the matric potential, which is largely responsible for water migration towards the frozen zone, has been a subject of extensive exploration, the osmotic potential remains an enigmatic facet of this intricate process. The relative obscurity surrounding the osmotic potential is primarily attributed to the limitations in equipment and testing techniques. Consequently, many existing models have relegated the osmotic potential to the realm of insignificance.

The total water potential (Ψ_{tot}) serves as the compass guiding water migration towards the freezing front, and it comprises two essential components: the matric potential (Ψ_m) and the osmotic potential (Ψ_o). While the matric potential is discerned through a complex interplay of factors such as particle size, pore size distribution, and the characteristics of soil particle surfaces (Hillel, 2005), the osmotic potential hinges on the concentration of solutes present in the soil water. These solutes, residing in the pore fluid, act as agents that lower the freezing point (Atkins, 1990), thereby inhibiting the formation of ice lenses and subsequently reducing or eliminating frost heaving. Nevertheless, a substantial variance in solute concentration can create a potential capable of driving the movement of water towards the frozen front.

Prior studies have studied the osmotic potential's significance in unfrozen water within frozen soil (Torrance and Schellekens, 2006). Suzuki's experimental investigations employing Nuclear Magnetic Resonance (NMR) and Time Domain Reflectometry (TDR)

led to the suggestion that the osmotic potential is a negligible force in this context. In contrast, Hillel (2005) countered this notion by arguing that if the matric potential alone determined the quantity of unfrozen water, it would theoretically result in smaller pore sizes. This, however, contradicts observations of pore space expansion just beneath the freezing front, due to the formation of ice within the pores, which should theoretically reduce the matric potential.

The ongoing discourse, marked by arguments and counterarguments, largely stems from a scarcity of laboratory and experimental tests designed to measure the evolution of the osmotic potential within freezing soils. This study, aiming to bridge this knowledge gap, introduces a model for the comprehensive assessment of osmotic potential dynamics in freezing soils.

2. Materials and Methodology

2.1 Soil

Naturally frost susceptible soil from Asheville in North Carolina (NC-AS) was utilized for this study. The soil was selected for its large amount of silt and low clay content. It also had a lower ionic concentration than other soils considered, which made processing it for testing easy.

2.1.1 Material Characterization

Index property and other tests were performed according to the standard ASTM procedures (ASTM D4318; ASTM D854; ASTM D7928; ASTM D698; ASTM D6913).

A summary of the index properties, material classifications, and frost susceptibility classification from the U.S. Army Corps of Engineers (U.S. Army Corps of Engineers, 1965) is given in Table 1.

Table 8-1 Summary of soil index properties and classifications

Soil Property	**NC-AS**
Specific Gravity, Gs	2.65
#4 Sieve (4.75 mm)	89.51
#10 Sieve (2mm)	73.32
#40 Sieve (0.425 mm)	67.08
#200 Sieve (0.075 mm)	30.52
Silt content (%) (75μm–2μm)	26.47
Clay content (%) (< 2μm)	4.05
Liquid Limit, LL	38.44
Plastic Limit, PL	NP
Optimum Moisture Content (%)	18.50
Max. Dry Unit Weight (kN/m^3)	15.02
USCS Classification	SM/SC
AASHTO Classification	A-4
Frost Susceptibility Classification	F3

2.1.2 Soil Preparation

To remove any antecedent salts and sufficiently achieve a uniformity in the pore fluid concentration, the soil sample was first washed. This was carried out by soaking the soil in buckets with distilled water at a ratio of (1:5, soil to water) for 4 days. The soil slurry was mixed daily using a stirrer to ensure uniform saturation and distribution of the pore fluid. Three samples of the soil slurry were collected after mixing and the pore fluid extracted over a vacuum. EC measurements were taken for each sample set collected. The

soil slurry was left to settle and afterward decanted. The process was repeated until EC values obtained reached an asymptotic value (with a standard deviation <10µscm). Fig xx below shows the values of EC measured with each wash carried out.

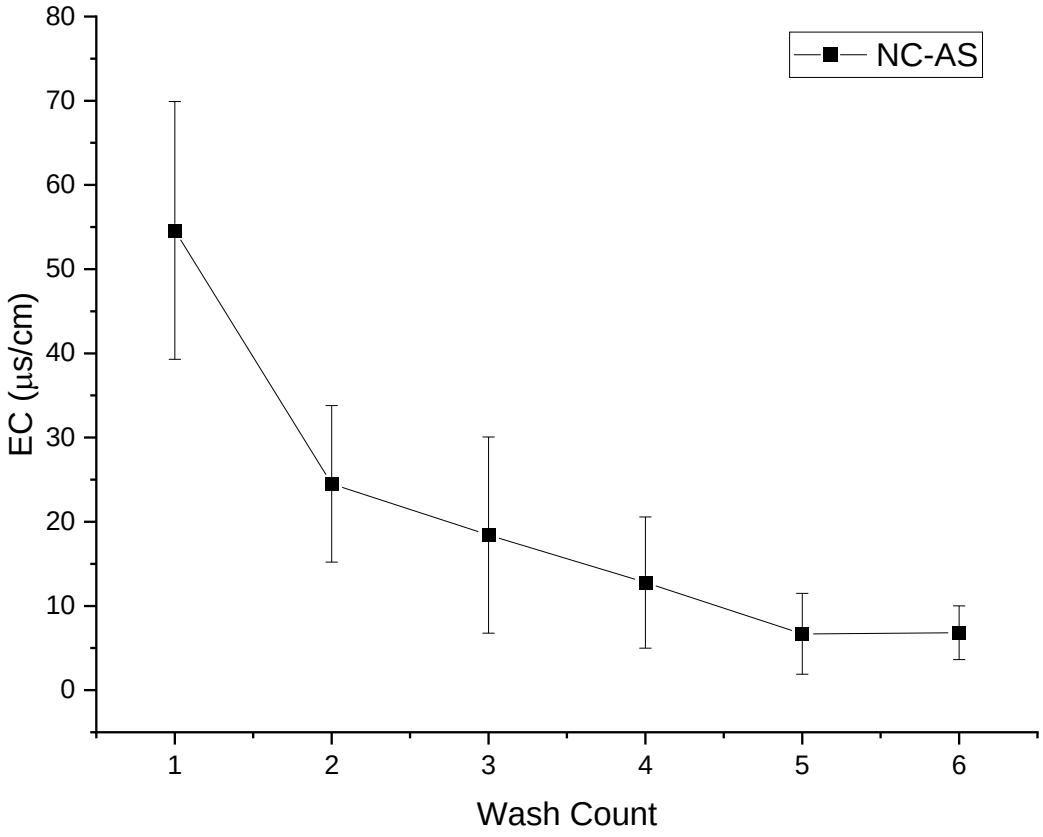

Figure 8- 1 Change in EC with wash count.

The washed soil was divided into four parts and treated with DI water (EC ~1µs/cm) and NaCl at three different molar concentrations (0.01M, 0.1M and 1M). For the salt concentrations, the respective molar solutions were prepared using DI water and mixed with the washed soil at a ratio of 1:1. The resulting mixture was mixed thoroughly with a stirrer and left to sit for 2 days with repeated stirring at 12-hour intervals. The soil-mixture was air-dried in trays and the dried soil bagged for further tests.

2.2 Methodology

A multiple linear regression model to estimate the equivalent molar concentration is derived from modified soil freezing tests measuring the temperature, volumetric water content and electrical conductivity carried out on soil samples at varying salt concentrations. The model is validated using samples prepared at different salt concentrations and utilized to determine the change in soil salt concentrations under freezing conditions.

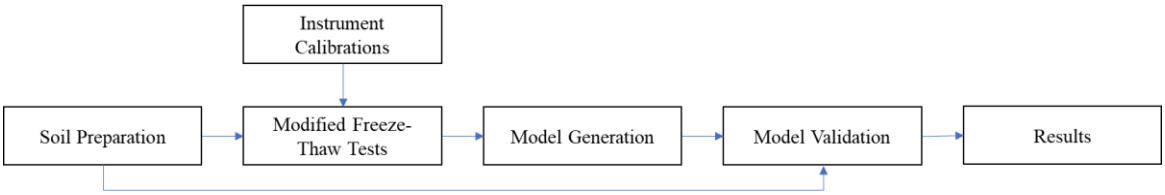

Figure 8- 2 Methodology workflow

2.2.1 Molar Concentration – EC -Suction Relationship

To determine the osmotic potential generated by increasing pore fluid concentration, an equivalent molar concentration – EC – Suction relationship was generated from measured samples. NaCl solutions at various molar concentrations (0.0001M, 0.001M, 0.01M, 0.1M and 1M) were prepared in the lab and tested to determine the electrical conductivity and suction values. The electrical conductivity was obtained using a Mettler Toledo probe, while the suction was obtained using a WP4C (Meter Group). Tests were carried out on triplicate samples. The results were plotted (Figure 9-3) and a polynomial trendline equation obtained for the relationship. The relationship will be utilized in

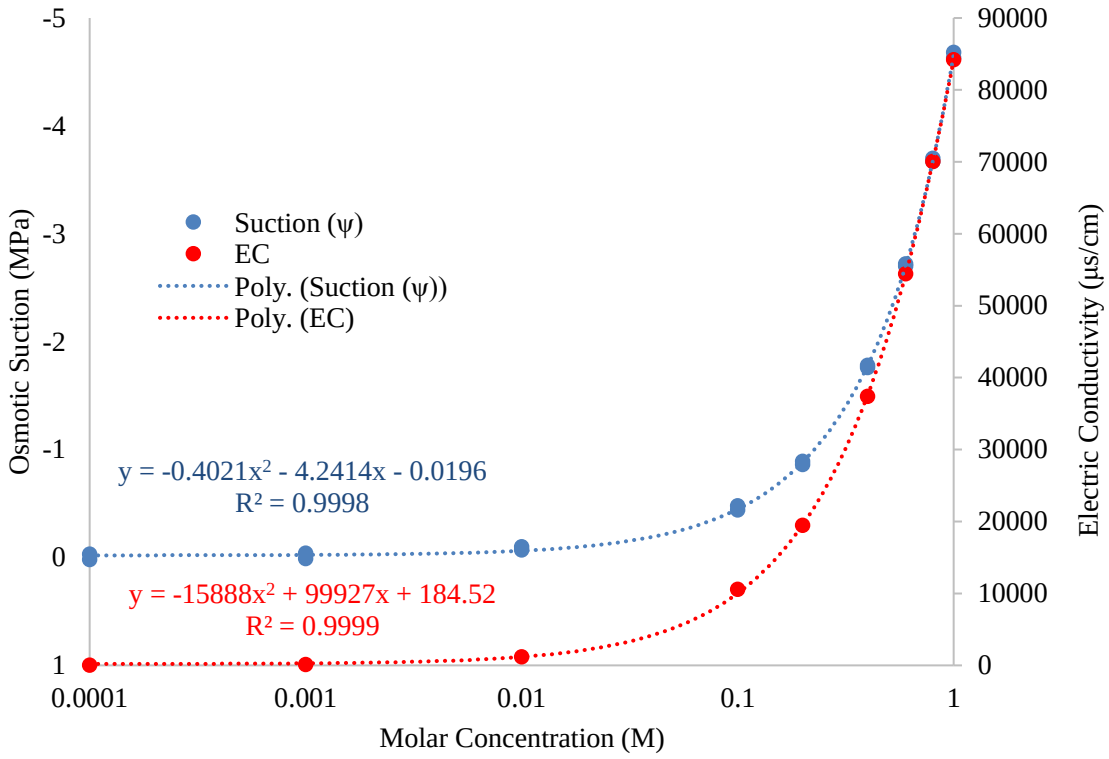

Figure 8-3 Relationship between NaCl molar concentration, Electrical Conductivity, and Osmotic Suction

2.2.2 Freezing Tests

Soil freezing tests after (Ren and Vanapalli, 2019) were modified to include EC measurements. For the tests, the soil was mixed and statically compacted at the optimum moisture content into 8mm thick cylindrical tubes (with small holes drilled, used to contain the lateral expansion of the soil). The compacted sample was submerged into a plastic bucket with a solution corresponding to the targeted pore fluid concentration with a weight (2kg) to prevent vertical expansion. The setup was left to stand for 3 days after which it was instrumented.

Figure 8-4 Compacted samples soaked in buckets.

The Teros 12 temperature, moisture, and electrical conductivity sensor, and the Zentra Logger (ZL6) Datalogger (both from Meter Group) were utilized for the tests. The Teros 12 determines the volumetric moisture content using capacitance/frequency domain technology on a 70-MHz frequency that minimizes textural and salinity effects (Meter Group, 2022). It has an accuracy greater than 0.03 m3/m3 in mineral soils. It measures the temperature using a thermistor (range -40^{o}C to + 60^{o}C, resolution of 0.1^{o}C) and the EC using a stainless-steel electrode array (0 – 20 dS/m, resolution of 0.001ds/m). The ability to obtain these measurements using one device made it the best choice for the tests. The Teros 12 was inserted into the bottom end of the specimen and complete coverage of the sensor was ensured. The sensor was connected to the ZL6 with reading logged at 5-minute intervals.

The setup was then wrapped in cling wrap to prevent moisture loss and the top and bottom insulated with insulating foam sprayed using a spray gun. The setup was placed in

a temperature and humidity-controlled chamber (Cincinnati Sub-Zero ZPH-16-1.5-H/A, -70 to 190oC, Rh 75%). The reading from the sensor was monitored to ensure a stable reading before the freeze-thaw tests were carried out. Three-dimensional freezing was carried out on the specimen by dropping the chamber temperature at intervals (25, 20, 15, 10, 5, 2, 0. -2, -5, -10, -15, and -20^{o}C) and thawing it out in the same sequence in reverse. Each temperature interval was sustained for 24 hours. The tests were carried out for samples at four different molar concentrations (DI, 0.01M, 0.1M and 1M). The values of temperature, moisture content and EC measured from the Teros 12 at each molar concentration were utilized to develop an equation that relates them together.

Figure 8-5 Test and calibration samples inside the controlled environment chamber

2.2.3 Calibration

For calibrating the temperature readings, the values from the Teros 12 sensor were compared with that of a thermometer at varying temperatures (-10, -5, 0, 2, 5, 7, 10, 15,

20, 25, 30 and 35ºC). Both were dipped into the soil samples with the readings of the thermometer obtained visually while that of the Teros 12 was retrieved from the datalogger. The results are plotted in fig 9-6. The values obtained for the Teros 12 are close to the thermometer reading with data points falling close to the 1:1 line. The Bulk EC measurements were calibrated with the Direct Soil Conductivity and Temperature Meter (Hanna Instruments, HI98331), while the pore EC was calibrated with the Mettler Toledo EC probe (Inlab 731-ISM) and the results presented in figure 9-6.

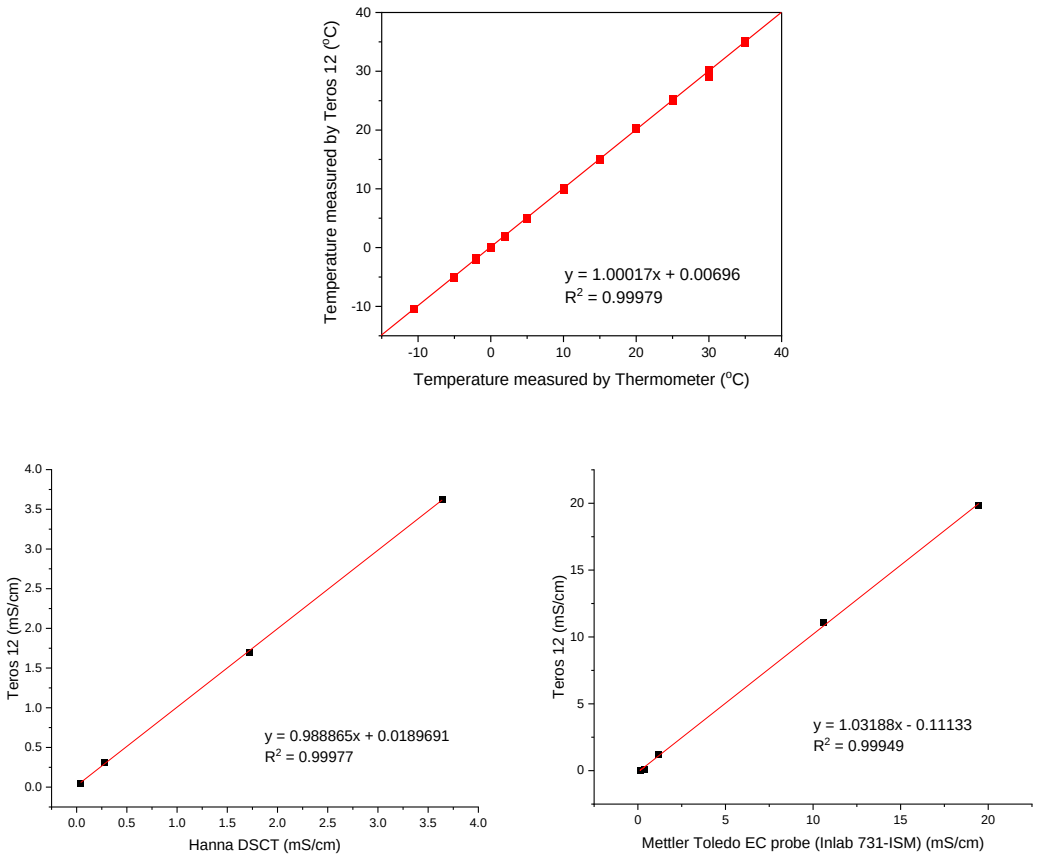

Figure 8-6 Calibration graphs and relationships Teros 12

A relationship between moisture content and temperature was obtained for the sensors by compacting soil three samples at OMC and conditioning them to varying

moisture content. While one was left at OMC, the other was saturated in a bucket filled with DI water and the third left in the lab to dry out for a day. All samples were wrapped with cling wrap after conditioning to prevent further moisture loss. The volumetric moisture content was obtained using the Teros 12 at various temperatures (25, 15, 5 and 2^{o}C) using the chamber.

Table 8- 2 Volumetric water content calculations

Sample ID	Gravimetric Water Content (%)	Dry density (g/cm^3)	Volumetric Water content (cm^3/cm^3)
1	20.41	1.52	0.310
2	17.02	1.50	0.255
3	13.57	1.52	0.206

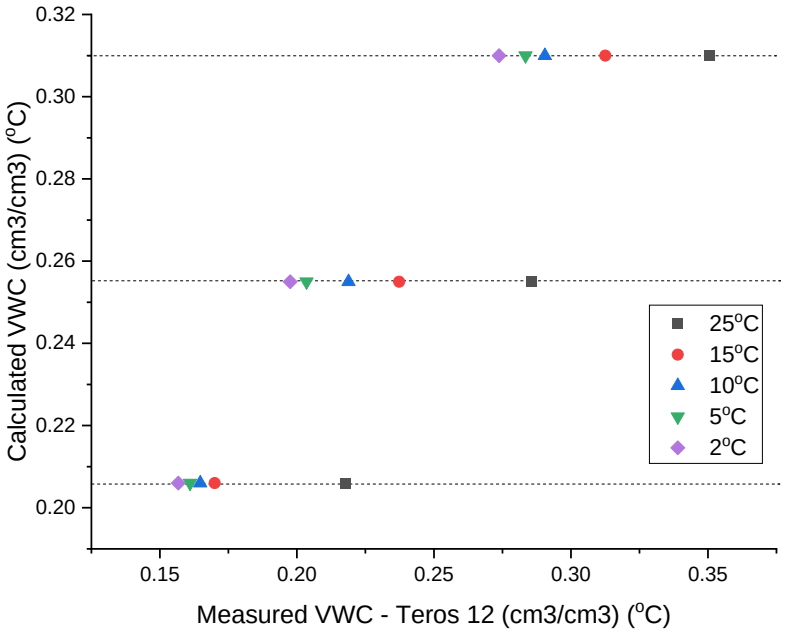

Figure 8- 7 Moisture content temperature relationship for Teros 12

From the results obtained, it was observed that there was a decrease in moisture content with temperature, suggesting that there is an influence of the temperature on the

moisture content. A linear relationship between the calculated and measured volumetric water content was derived at each temperature measurement above 0°C. For analysis of continuous measurements, the average of the relationships obtained was utilized.

Table 8-3 Calibration constants of measured and calculated Moisture content

Temperature (°C)	A	B	R^2
~25	0.78252	0.03432	0.99795
~15	0.72974	0.08189	1
~10	0.82366	0.07193	0.99778
~5	0.82863	0.07803	0.98029
~2	0.86691	0.07552	0.98061

Calculated VMC = A * Measured VMC (Teros 12) + B

For temperatures below zero, a general relationship between volumetric moisture content (θ_v) and the dielectric constant (K_a) developed by Smith and Tice (1988) for measuring the unfrozen water content in freezing soil using TDR and NMR was utilized. It was also compared with a similar relationship by Topp et al (1980) using electromagnetic determination using coaxial transmission lines. Their respective equations are presented below.

$$\theta_v = -1.458\,E-1 + 3.868E-2\,K_a - 8.502E-4\,{K_a}^2 + 9.920E-6\,{K_a}^3 \quad (1)$$

$$\theta_v = -5.3\,E-2 + 2.92E-2\,K_a - 5.5E-4\,{K_a}^2 + 4.3E-6\,{K_a}^3 \quad (2)$$

The dielectric constant was obtained from the Teros 12 raw output by using the equation below.

$$K_a = (2.887E-9 \times RAW^3 - 2.080E-5 \times RAW^2 + 5.276E-2 \times RAW - 43.39)^2 \quad (3)$$

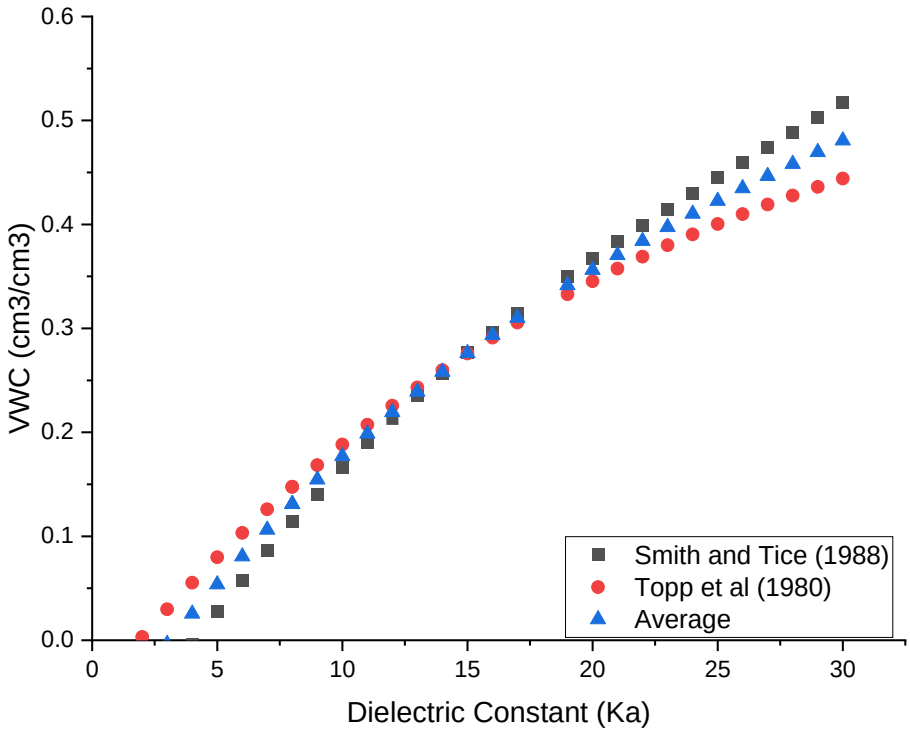

Figure 8- 8 Volumetric moisture content - Dielectric constant relationships

2.2.4 Freezing Point Depression

The freezing point determines the phase change of the soil matrix. Depending on the rate of change of temperature, a typical freezing curve can be groups into four stages (shown in figure xx). First the temperature reaches a supercooling value, at which point crystallization of pore water into ice begins (crystallization temperature). A latent heat (of fusion) is released during crystallization that raises the soil temperature. This can be observed if the latent heat is sufficient to raise the temperature instantaneously. The presence of ions and salts in the pore fluids causes a decrease in the freezing point, pushing this phase change to occur at a lower temperature value. This is known as the freezing point depression. If the pore fluid is treated as an ideal uniform solution, then the relationship between the freezing point and the concentration can be expressed in the equation below,

$$\Delta T_f = T_{fo} - T_f = k_r b_r \beta \qquad (4)$$

Where T_{fo} is the freezing point of water, T_f is the freezing point of the pore fluid, k_r is the cryoscopic constant (k_r = 1.853°C/mol.kg^{-1} for water, b_r is the mass molarity of the solute in mol.kg-1, β is the Van't Hoff factor (β = 2 for NaCl).

3. Results

3.1 Soil Freezing-Thawing Curves

A typical freezing-thawing curve is shown in Fig 9-10 below. Measurements were taken for Temperature, Water Content and Bulk EC (also convertible to Pore EC) at four different molar concentrations using DI water, 0.01M, 0.1M, and 1M NaCl solutions.

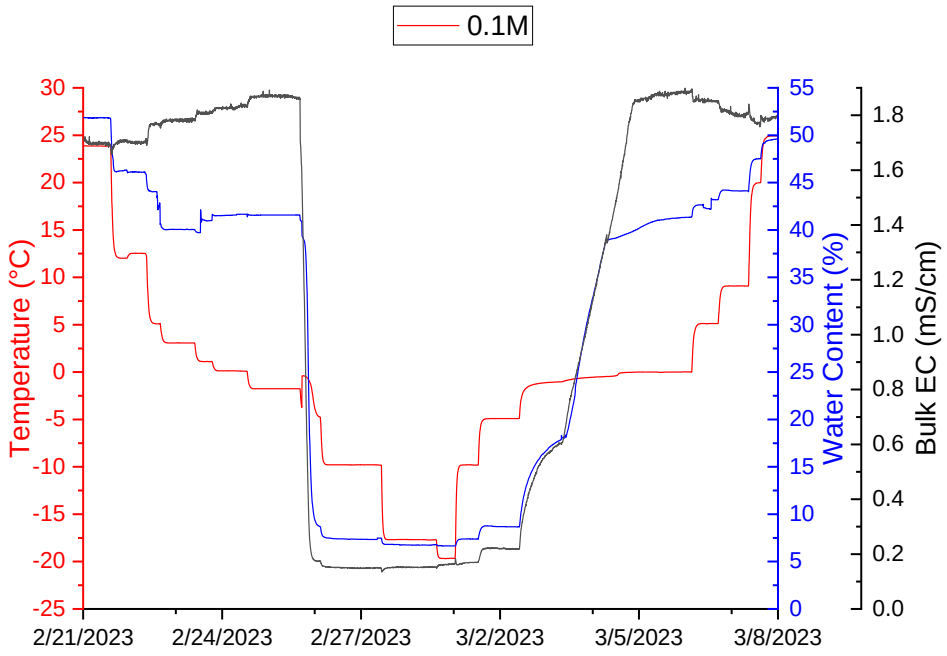

Figure 8- 9 Results of soil freeze-thaw tests (0.1M NaCl treatment)

Table 9-3 shows the targeted and actual molar concentrations (provided as NaCl equivalents), as well as the calculated and measured freezing point depressions for each sample.

Table 8-4 Molar concentrations, equivalent EC, suction, and freezing point depression at each concentration

Target Molar Conc. (NaCl eq), M	Actual Molar Concentration (NaCl eq)	EC @ 25ºC (µs/cm)	Suction @ 25ºC (MPa)	Freezing Point Depression (Calculated)	Freezing Point Depression (Measured)
0	0.00009	57*		0	0
0.01	0.017	1882.82	0.092	-0.037	-0.14
0.1	0.101	10260.95	0.444	-0.371	-0.4
1	0.914	90191.19	3.560	-3.706	-3.72

* Washed value

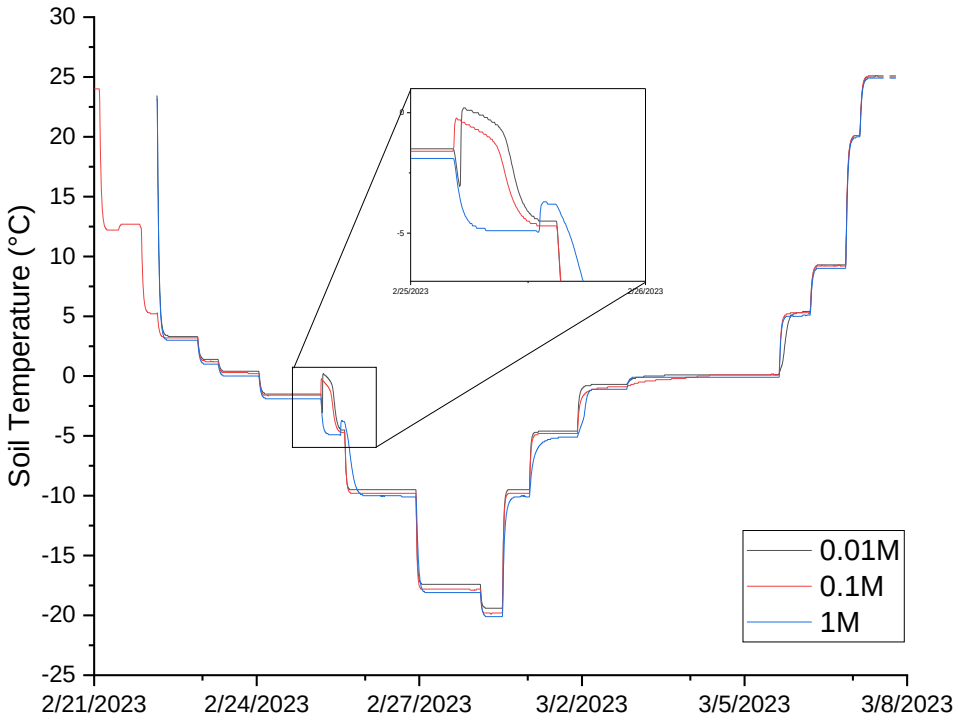

Figure 8- 10 Observed freezing point depression from tests.

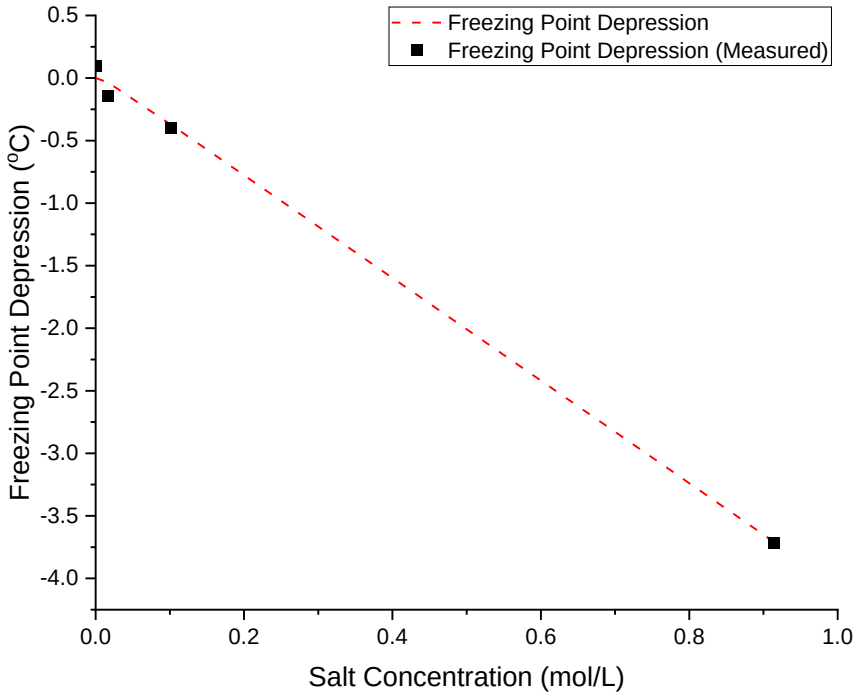

Figure 8- 11 Freezing Point Depression - salt concentration relationship

3.2 Model Development

Using the measured data obtained from the freeze-thaw tests carried out at different concentrations, a multiple linear regression model was computed using the linear model (lm()) function in R. Temperature, Volumetric Water Content and Electrical Conductivity were utilized as dependent variables, and their effect on the molar concentration of the pore fluid was determined. There was a strong correlation between the concentration and all the variables ($p=2e-16<0.05$), indicating their importance into the concentration. The moisture content also had the largest variance (mean square), indicating its major contribution to the change in molar concentration. Without adequate moisture, ions cannot be mobilized and there will be no measurement regardless of the presence of salt in the soil matrix.

Table 8-5 Model equations

Temperatures	Model Equation	R^2
<0°C	M = 0.02342+0.00007164*VMC-0.01848*T+0.05053*EC	0.9994
≥0°C	M = 0.02623-0.0007062*VMC+0.0005844*T+0.04846*EC	0.7924

*M = Molar Concentration, VMC = Volumetric Moisture Content, T = Temperature, EC = Electrical Conductivity

There is a good correlation for values above 0°C (0.9994) while for values below 0°C, the correlation is lower (0.7924). This is due to hysteresis between the freezing and the thawing portions of the test.

3.3 Model Validation

Results from the model were compared against freeze-thaw measurements of samples prepared at 0.02M, 0.05M, 0.1M and 0.5M. For positive temperatures, the calculated molar concentration was compared with the equivalent concentration of the pore fluid extract using the equations in figure xx above. For negative temperatures, the equation in Table 9-4 was utilized to obtain an equivalent EC to the observed EC from the tests using the solver tool in Microsoft® Excel. The results are presented in figure 9-13.

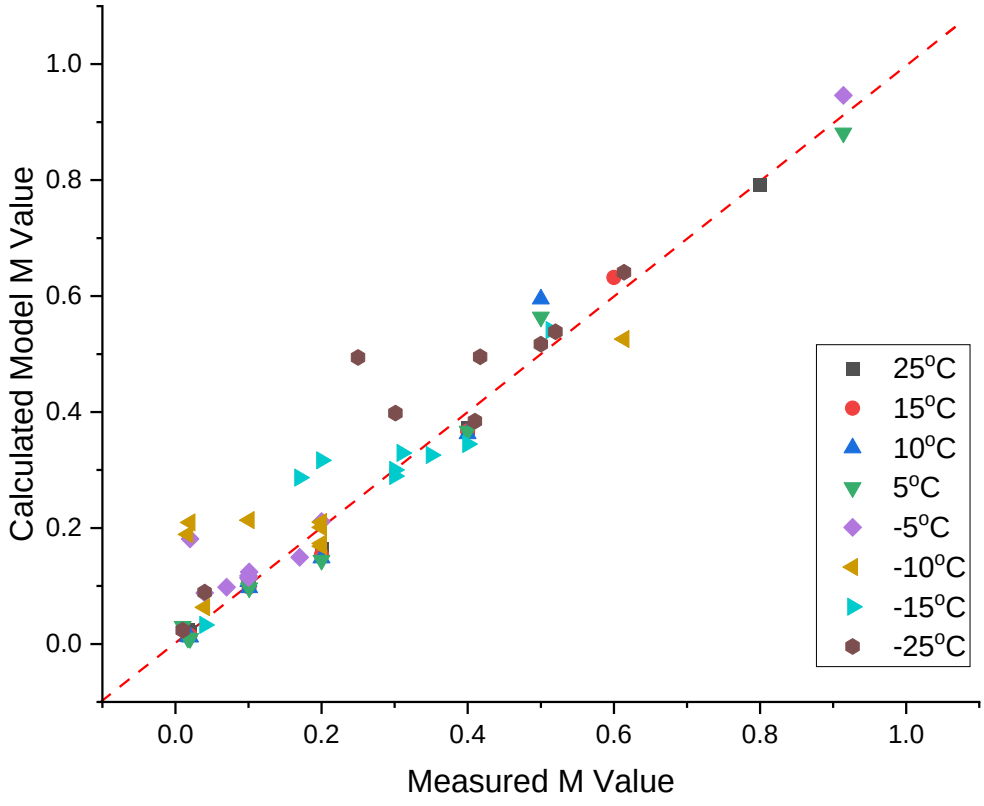

Figure 8- 12 Relationship between the measured and calculated molar concentration values

There is a very good correlation between the model calculated and observed values for the positive temperature values, while the for the negative values, the model overestimates the values, particularly for temperatures below -10°C. For higher salt concentrations, there is a good correlation for negative temperature values above the freezing point. Based on these observations, the model equation can be utilized with a good confidence up to -10°C.

4. Results

The model was utilized to determine the change in molar concentration in the soil matrix with decreasing temperatures. Figure 9-14 shows the model results for freeze thaw samples tested at 0.01M and 0.1M. Because of the confined space the increase in the salt concentration with decreasing temperature is measured as a stable reading under a uniform temperature. In an actual freezing soil, there will be a redistribution of the excluded ions over time to the zones of lower concentration, while causing a migration of water towards the more concentration zone.

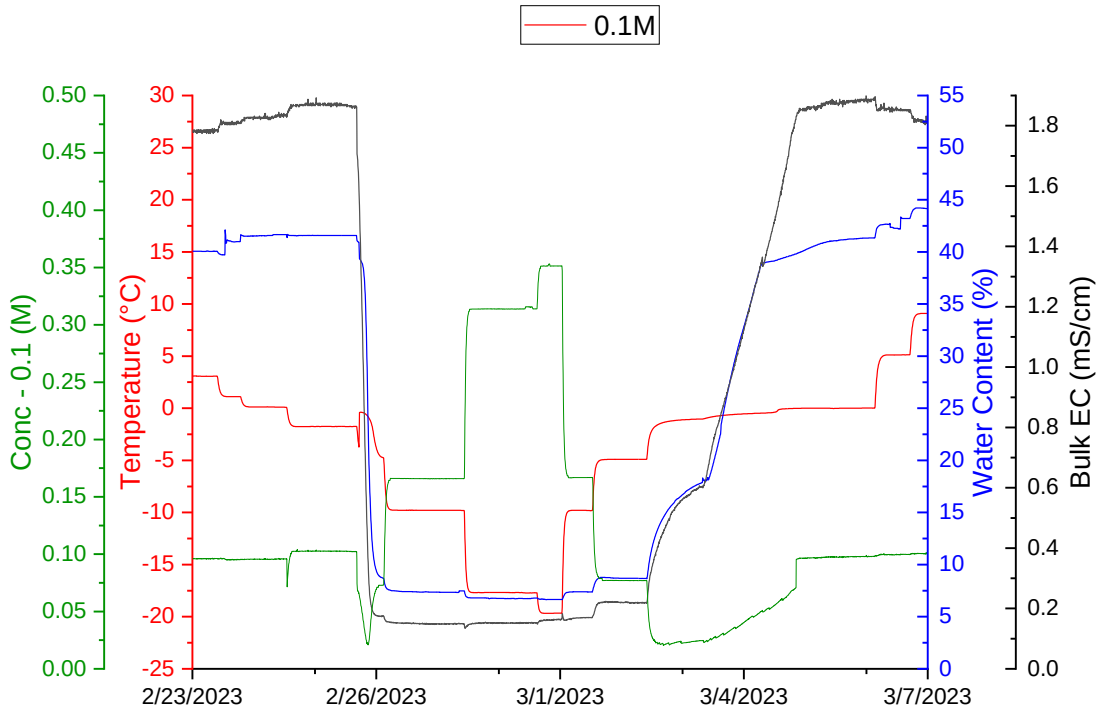

Figure 8- 13 Change in molar concentration of the sample (0.1M) under freezing and thawing

Figure 9-15 shows the change in molar concentration of samples treated at different concentrations under freezing and thawing. The values for thawing are shown in dashed lines. There is a difference in the molar values of the freezing curve and the thawing curve (hysteresis). This is due to a change in the chemical composition (concentration) of the pore fluid under those two regimes. Also, there is hysteresis observed in the moisture content under freeze-thaw which affects the EC results. Results above 0°C are uniform.

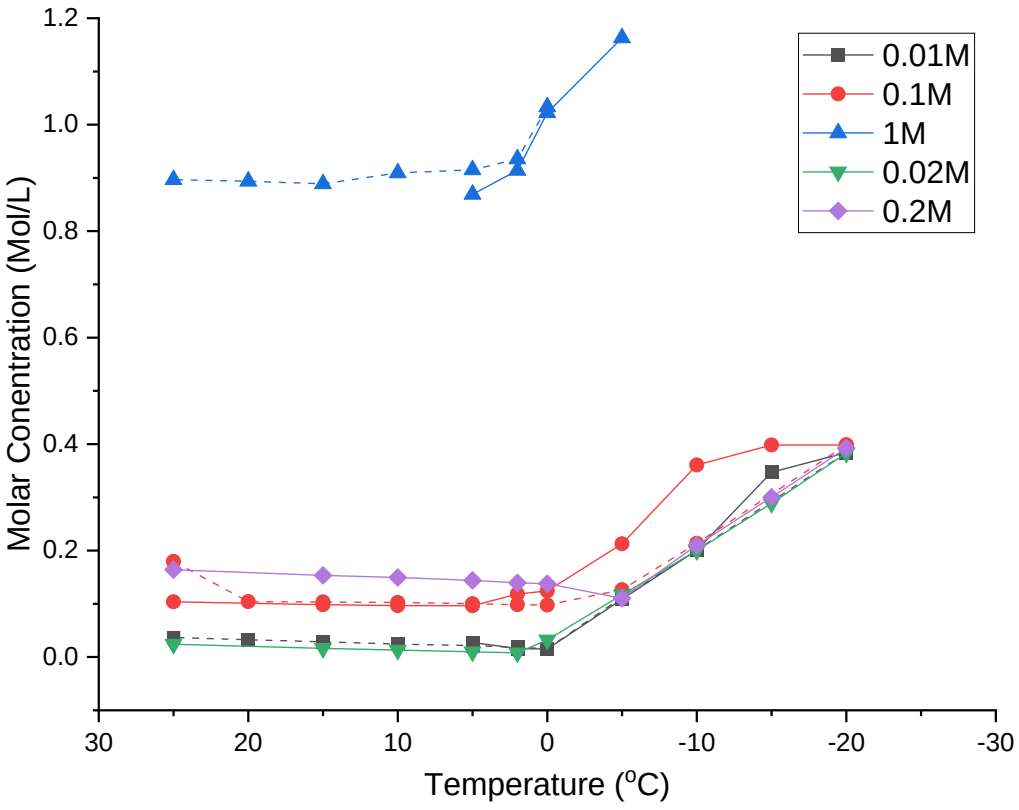

Figure 8- 14 Change in molar concentration of different samples under freezing and thawing (dash lines)

The resulting change in molar concentration of the freezing soil matrix will induce an osmotic potential. Utilizing the equation in Figure 9-3, the equivalent osmotic potential

within the soil at different temperatures are given in Table 9- 5 below. There is an observed increase in the osmotic potential from 3% (1M @ 2ºC) up to 850% (0.01M @ -20ºC). This signifies the occurrence of a dramatic increase in the potential at the frozen fringe which should contribute to the migration of water towards the freezing front.

Table 8-6 Equivalent osmotic potentials at different temperatures

Temperature	**0.01M**		**0.1M**		**1.0M**	
(ºC)	**Equivalent Suction (Mpa)**	**% change**	**Equivalent Suction (Mpa)**	**% change**	**Equivalent Suction (Mpa)**	**% change**
25	0.18	0%	0.46	0%	4.14	0%
15	0.16	-11%	0.44	-4%	4.13	0%
10	0.14	-22%	0.43	-7%	4.11	-1%
5	0.09	-50%	0.43	-7%	4	-3%
2	0.08	-56%	0.53	15%	4.23	2%
0	0.08	-56%	0.55	20%	4.77	15%
-5	0.49	172%	0.94	104%	5.5	33%
-10	0.89	394%	1.6	248%	ND	
-15	1.54	756%	1.77	285%	ND	
-20	1.71	850%	1.77	285%	ND	

*ND – Not Determined, EC values outside the measurable range of the device

5. Conclusion

This study investigates the change in osmotic potential within a soil matrix under freeze-thaw conditions, a phenomenon of great significance in freezing soil systems. While matric potential has traditionally received substantial attention as the primary driving force behind water migration in freezing soils, the osmotic potential's role has been largely underexplored due to limited equipment and testing capabilities. Many existing models have assumed that the osmotic potential is negligible, but these results challenge that

assumption. Osmotic potential can increase dramatically (up to 850%) causing a gradient and inducing the flow of ions and water to and from the freezing front.

A multiple linear regression model was developed to estimate the molar concentration of the pore fluid based on temperature, water content, and electrical conductivity. The model showed strong correlations between the variables, with the moisture content playing a substantial role in influencing molar concentration changes. Also, the freezing point depression, which determines the phase change of the soil matrix, is notably affected by the presence of ions and salts in the pore fluids. This, in turn, influences the migration of water in freezing soils. The model's validity was confirmed through comparison with actual freeze-thaw measurements, and it was found to provide accurate estimations for positive temperatures. For negative temperatures below -10°C, the model's accuracy diminished, suggesting potential areas for further refinement.

Overall, this study provides some basis for reestablishing the argument for osmotic potential in frost heave studies and presents a valuable model for estimating real time molar concentration changes in freezing soils. The findings open new avenues for understanding the complex interplay of matric and osmotic potentials in the freezing soil system, shedding light on the factors that drive water migration and frost heave in such environments. Further research and refinement of the model could yield deeper insights into the intricate processes at play in freezing soils, with practical implications for geotechnical and environmental applications.

REFERENCES

ASTM, 2012. ASTM D698: Standard Test Methods for Laboratory Compaction Characteristics of Soil Using Standard Effort (12 400 ft-lbf/ft3 (600 kN-m/m3)). ASTM International 3.

ASTM D 854, 2002. ASTM D854 Standard Test Methods for Specific Gravity of Soil Solids by Water Pycnometer. ASTM International 04.

ASTM D2974, 2020. Standard Test Methods for Determining the Water (Moisture) Content, Ash Content, and Organic Material of Peat and Other Organic Soils. ASTM International.

ASTM D7928, 2021. Standard Test Method for Particle-Size Distribution (Gradation) of Fine-Grained Soils Using the Sedimentation (Hydrometer) Analysis. ASTM International.

ASTM International, 2017a. ASTM D4318-17, in: Standard Test Methods for Liquid Limit, Plastic Limit, and Plasticity Index of Soils.

ASTM International, 2017b. D6913: Standard Test Methods for Particle-Size Distribution (Gradation) of Soils Using Sieve Analysis. ASTM International D6913.

ASTM International, 2010. Standard test methods for moisture, ash, and organic matter of peat and other organic soils, TA - TT -. ASTM International West Conshohocken, Pa., West Conshohocken, Pa. SE -. https://doi.org/LK - https://worldcat.org/title/741935120

ASTM International, n.d. D2166 Standard Test Method for Unconfined Compressive Strength of Cohesive Soil [WWW Document]. URL https://www.astm.org/d2166-06.html (accessed 6.15.23).

Torrance J. Kenneth and Fons J Schellekens. 2006 “Chemical Factors in Soil Freezing and Frost Heave.” Polar Record 33–42. https://doi.org/10.1017/S0032247405004894.

CHAPTER 7: CONTRIBUTIONS, AND RECOMMENDATIONS FOR FUTURE WORK

7.1 Research Contributions

This dissertation has explored the relevant considerations for executing water repellency in frost susceptible soils toward the mitigation of frost heave. Using an experimental approach, coupled with small-scale outdoor tests, the potential of organosilanes (OS) for use in imparting hydrophobicity in these soils has been established. The relevant contributions are discussed as follows:

a. *Article 1* establishes a systematic approach to the determination of the optimal dosage concentration of organosilane required for water repellency. Laboratory tests such as contact angle, water drop penetration, and breakthrough pressure are established as means to assess the degree of water repellency imparted. Electrical Conductivity (EC) and pH tests have been also highlighted as relevant metrics for identifying the optimal dosage concentration required. This is an important step for adoption by engineers and researchers looking to adopt EWR as a tool for implementing moisture barriers. Being able to identify the optimal dosage concentrations required will aid in proper design, and fiscal planning and prevent leaching due to excess OS. A comprehensive parametric study encompassing multiple variables was conducted on 216 samples. The results identified the primary factors influencing treatment efficacy - soil type, organosilane product, dosage, and drying condition – important conditions for consideration for field operations.

b. *Article 2* reviews the Contact Angle Test (Sessile Drop Method) test developed in soil science for engineering applications. While it is more suited for uniform-sized material to obtain repeatable and reliable results, engineering soil is a mixture of different grain-sized materials. This dissertation provides a method for determining the contact angle of bulk mass using that obtained from the sessile drop method. It highlights the effect of drying conditions on the contact angle as well as implications for field performance. It finally points out the flaws with utilizing this property for engineering design, presenting the Water Entry Pressure (WEP) influenced by the compaction density and pore size on the performance of the treated soil.

c. *Article 3* provides insights into the effect of salt on EWR treatment. Increasing salt content reduces the effectiveness of EWR treatment. This study highlights the crucial role of salt concentration in influencing the effectiveness of EWR treatment and the necessity of considering salt content, particularly in cold climate regions where salts are commonly applied. It also presents results on the durability and effectiveness of treated material under high saline conditions.

d. *Article 4* provides valuable information into the behavior of EWR-treated fine-grained soils. It shows the relationship between water repellency and hygroscopicity in fine-grained soils, shedding light on the influence of crucial factors such as treatment dosage, drying conditions, grain size, and the presence of organic content.

e. *Article 5* presents a new automated testing method for the determination of Water Entry Pressure (WEP) that fixes errors and large variations due to edge seepage,

human error in volume monitoring, and uneven compaction within the soil sample using a modified triaxial test method. It also provides a definition for breakthrough in water-repellent soils and establishes a basis for determining WEP based on a breakthrough volume criterion. This brings some uniformity in specifying the performance of water-repellent soils for use in various civil engineering applications, particularly in controlling moisture penetration in construction.

f. *Article 6* investigates the mechanical behavior and performance of EWR-treated soils under repeated freeze-thaw cycles. Strength tests revealed that untreated soil samples experienced a reduction in unconfined compressive strength with increasing freeze-thaw cycles after moisture conditioning due to water freezing and expanding within the pore spaces. In contrast, treated samples showed increased strength after multiple cycles, resulting from the induced water repellency within the soil matrix. The treated samples retained their unsaturated condition and strength properties even under varying wetting conditions, making them more suitable for construction where design is typically based on worst-case scenarios regarding subgrade strength with respect to moisture content.

g. *Article 7* presents the data obtained from performance tests carried out under sub-freezing weather conditions on EWR-treated soils. Test results indicated there was no infiltration of water and little variation in the water content of the treated sample. EWR treatment also prevented moisture migration within the soil matrix and limited the formation of pore ice and subsequent frost heaving of the soil. Treated samples also performed better under freezing conditions with no heaving compared to ~6mm of untreated soil.

h. *Article 8* presents a multiple linear regression model developed to estimate the molar concentration of the pore fluid based on temperature, water content, and electrical conductivity. It provides some basis for reestablishing the argument for osmotic potential in frost heave studies and presents a valuable model for estimating real-time molar concentration changes in freezing soils. The findings open new avenues for understanding the complex interplay of matric and osmotic potentials in the freezing soil system, shedding light on the factors that drive water migration and frost heave in such environments.

7.2 Recommendations for Future Research

a. While this study has investigated the variation of water repellency assessment results, there is still much to be learned about standard relationships between particle surface properties (Surface Energy, Contact angle, etc.), pore size, and engineering performance (WEP).
b. The study did not investigate the effect of salt concentrations after EWR treatment on its effectiveness. Also, the effect of washing was not explored.
c. The study was limited to hygroscopic moisture content in determining the effect of EWR treatment. Other effects on fine-grained properties relevant to practical implementation were not investigated.
d. While the study carried out extensive tests on the Water Repellency Assessment, including the development of an automated test method, it did not present information regarding a standard testing time based on material

behavior or natural phenomena. Variability in the test duration will yield varying results since the material is not waterproof.

e. The study did not carry out field strength tests to determine the performance of treated material under multiple freeze-thaw cycles.

f. While the study presents a model for estimating osmotic potentials in freezing soils, it still need to determine the effect of the same on the process of heaving.

REFERENCES

Adamson, A. W. (1990), Physical Chemistry of Surfaces, John Wiley, New York

Akagawa, S., Hori, M., & Sugawara, J. (2017). Frost Heaving in Ballast Railway Tracks. *Procedia Engineering.* 189, 547-553.

Andersland, O.B. and Ladanyi, B. (1994) Mechanical Properties of Frozen Soils. In: An Introduction to Frozen Ground Engineering, Springer, US, 121-150. https://doi.org/10.1007/978-1-4757-2290-1_5

Anderson, D.M., & Tice, A.R. (1972). Predicting Unfrozen Water Contents in Frozen Soils From Surface Area Measurements. *Highway Research Record*.

Bachmann J., Ellies A., Hartge K.H. (2000). Development and application of a new sessile drop contact angle method to assess soil water repellency. J. Hydrol. 2000;231–232:66–75. doi: 10.1016/S0022-1694(00)00184-0.

Bachmann, J., Woche, S. K., Goebel, M.-O., Kirkham, M. B., & Horton, R. (2003). Extended methodology for determining wetting properties of porous media. Determining Wetting Properties of Soil. *Water Resources Research.* 39.

Beskow, G. (1935). Soil freezing and frost heaving, with special applications to roads and railroads, Swedish Geological Society, Series C (375) (translated by J. O. Osterberg). In Historical Perspectives in Frost Heave Research, CRREL Special Report 91-23, 41157.

Boyd, D.W. (1976). Normal freezing and thawing degree-days from normal monthly temperatures. *Canadian Geotechnical Journal, 13*, 176-180.

Chamberlain, E. J. (1981). *Frost susceptibility of soil: review of index tests*. Hanover, N.H., U.S. Army Corps of Engineers, Cold Regions Research and Engineering Laboratory.

Chan C.S.H., & Lourenco S.D.N. (2016). Comparison of three silane compounds to impart water repellency in an industrial sand. *Geotechnique Letters.* 6.

Cass, L., & Miller, R.D. (1959). Role of the electric double layer in the mechanism of frost heaving.

Clark JI, Phillips R. 2003. Centrifuge modelling of frost heave of arctic gas pipelines. In Permafrost – 8th International Conference, Phillips M, Springman S, Arenson L (eds). AA Balkema: Zurich.

Daniels, J. L., and Hourani, M. S. (2009). Soil improvement with organo-silane. Advances in Ground Improvement. doi:10.1061/41025(338)23

Daniels, J.L., Ogunro, V.O., Pando, M.A., Dumenu, L., and Feyyisa, J.L. (2019) "Engineered water repellency: An evolving approach to infiltration control" World of Coal Ash Conference, St. Louis, MO, May 2019

Darrow, M. M. (2007). *Experimental study of adsorbed cation effects on the frost susceptibility of natural soils*.

Dekker, L. W., Ritsema, C. J., Oostindie, K., Moore, D., & Wesseling, J. G. (2009). Methods for determining soil water repellency on field-moist samples Measuring Water Repellency on Field-Moist Samples. *Water Resources Research.* 45.

Diehl, D., & Schaumann, G. E. (2007). The nature of wetting on urban soil samples: wetting kinetics and evaporation assessed from sessile drop shape. *Hydrological Processes.* 21, 2255-2265.

Doré, G., & Zubeck, H.K. (2008). Cold Regions Pavement Engineering.

Eigenbrod, K. D., Knutsson, S., & Sheng, D. (1996). Pore-Water Pressures in Freezing and Thawing Fine-Grained Soils. *Journal of Cold Regions Engineering.* 10, 77-92.

Everett, D. H. (1961). The thermodynamics of frost damage to porous solids. *Transactions of the Faraday Society.* 57, 1541.

Feyyisa, J. L., Daniels, J. L., & Pando, M. A. (2017). Contact Angle Measurements for Use in Specifying Organosilane-Modified Coal Combustion Fly Ash. *Journal of Materials in Civil Engineering.* 29, 04017096-04017096

Fowler, A. C., & Krantz, W. B. (1994). *A generalised secondary frost heave model*. 1650-1675. http://eprints.maths.ox.ac.uk/692/1/1994.4.pdf.

Freden, S. The Mechanism of Frost Heave and Its Relation to Heat Flow. Proc., 6th Int. Conf. on Soil Mech. and Found. Eng., 1966, pp. 41, 45; Nat. Road Res. Inst., Stockholm, Spec. Rept. 22, 1964.

Fukuda M., Strelin K., Shimokawa N., Takahashi N. Sone T. and Trombott D., 1992, Permafrost occurrence of Seymour Island and James Ross Island, Antarctic Peninsula region. Yoshida Y. et al. (ed.), Recent Progress in Antarctic Earth Science, 745-750

Genuchten, M. T. (1980). A Closed-form Equation for Predicting the Hydraulic Conductivity of Unsaturated Soils. *Soil Science Society of America Journal.* 44, 892-898.

Gold, L. W. (1957) A possible force mechanism associated with the freezing of water in porous materials, Highway Research Board Bulletin 168, p. 65-73

Gilpin R. R, 1980, A model for the prediction of ice lensing and frost heave in soils. Water Resources Research 16, 918-930

Hansson, K., J. Simunek, M. Mizoguchi, L.C. Lundin, and M.T. van Genuchten. 2004. Water flow and heat transport in frozen soil: Numerical solution and freeze-thaw applications. Vadose Zone J. 3:693-704.

Hallett, P. D., White, N. A., Ritz, K. 2006. Impact of basidiomycete fungi on the wettability of soil contaminated with a hydrophobic polycyclic aromatic hydrocarbon. Biologia61: S334-S338.

Henry, K. S. (1996). Geotextiles to mitigate frost effects in soils: a critical review. *Transportation Research Record.* 1996.

Hoekstra, P. (1969). Water Movement and Freezing Pressures. *Soil Science Society of America Journal.* 33, 512-518.

Hopke S. W., 1980, A model for frost heave including overburden. Cold Regions Science and Technology 3, 177-183

Horiguchi, K. (1977) Frost heave character in freezing of powder materials. In Proceedings, International Symposium on Frost Action in Soils, University of Luleä, Sweden, vol. 1, p. 67- 75.

Horiguchi, K., 1986. A solution model for soil freezing. Low Temp. Sci., Ser. A, 45: 69-82

Horiguchi K. 1987. An osmotic model for soil freezing, Cold Regions Science and Technology, Volume 14, Issue 1, Pages 13-22, ISSN 0165-232X, https://doi.org/10.1016/0165-232X(87)90040-1.

Jackson K. A. and Chalmers B., 1958, Freezing of liquid in porous media with special reference to frost heave in soils. J. Applied Physics 29, 1178-1181

Jackson K. A. and Uhlmann D. R., 1966, Particle sorting and stone migration due to frost heave. Science 152, 545-546

Japanese Geotechnical Society. 2003. Test Method for Frost Heave Prediction Test, JGS0171-2003

Jessberger, H L. 1973. Frost Susceptibility Criteria. 52nd Annual Meeting of the Highway Research Board. Washington District of Columbia, United States, 1973-1-22 to 1973-1-26

Keatts, M.I., Daniels, J.L., Langley, W.G., Pando, M.A., Ogunro, V.O., 2018. Apparent contact angle and water entry head measurements for organo-silane modified sand and coal fly ash. ASCE J. Geotech. Geoenviron. Eng. 144 (6), 1–9.

King P. M. (1981) Comparison of methods for measuring severity of water repellence of sandy soils and assessment of some factors that affect its measurement. Australian Journal of Soil Research 19 , 275–285. doi: 10.1071/SR9810275

Konrad, J. M. (1988). Influence of freezing mode on frost heave characteristics.

Konrad J. M., 1987, The influence of heat extraction rate in freezing soils. Cold Regions Science and Technology 14, 129-137

Konrad J. M., 1989, Influence of cooling rate on the temperature of ice lens formation in clayey silts. Cold Regions Science and Technology 16, 25-36

Konrad, J. M. (1994). Sixteenth Canadian Geotechnical Colloquium: Frost heave in soils: concepts and engineering. *Canadian Geotechnical Journal.* 31, 223-245.

Konrad, J.-M., And Morgenstern, N. R. 1980. A mechanistic theory of ice lens formation in fine-grained soils. Canadian Geotechnical Journal, 17, pp. 473-486.

1981. The segregation potential of a freezing soil. Canadian Geotechnical Journal, 18, pp. 482-491.

1982a. Prediction of frost heave in the laboratory during transient freezing. Canadian Geotechnical Journal, 19, pp. 250-259.

1982b. Effects of applied pressure on freezing soils. Canadian Geotechnical Journal, 19, pp. 494-505.

1983. Frost susceptibility of soils in terms of their segregation potential. Proceedings, 4th International Conference on Permafrost, Fairbanks, Alaska, July 18-22, 1983.

Konrad J. M. and Duguennoi C., 1993, A model for water transport and ice lensing in freezing soils. Water Resources Research 29, 3109-3124

Kujala K., 1991, Factors affecting frost susceptibility and heaving pressure in soil. Ph. D. Thesis, Acta Univ., Ouluensis

Kujala, K. 1997. Estimation of frost heave and thaw weakening by statistical analyses and physical models In: Proc. Int. Symp. on Ground Freezing and Frost Action in Soils. Lulea, Sweden, 15 - 17 April, 1997 pp. 31 -41.

Lamparter, A., Deurer, M., Bachmann, J., & Duijnisveld, W. H. M. (2006). Effect of subcritical hydrophobicity in a sandy soil on water infiltration and mobile water content. *Journal of Plant Nutrition and Soil Science.* 169, 38-46.

Lee, C., Yang, H.-J., Yun, T. S., Choi, Y., & Yang, S. (2015). Water-Entry Pressure and Friction Angle in an Artificially Synthesized Water-Repellent Silty Soil. *Vadose Zone Journal.* 14, 1-9.

Liu, H., Ju, Z., Bachmann, J., Horton, R., & Ren, T. (2012). Moisture-Dependent Wettability of Artificial Hydrophobic Soils and Its Relevance for Soil Water Desorption Curves. *Soil Science Society of America Journal.* 76, 342-349.

Liu, J., Cen, G., and Chen, Y. Study on frost heaving characteristics of gravel soil pavement structures of airports in Alpine regions. DOI: 10.1039/C7RA02151H

Loch, J.P. (1981). State-of-the-art report — frost action in soils. *Engineering Geology, 18*, 213-224.

Long, X., Cen, G., Cai, L., & Chen, Y. (2018). Experimental Research on Frost Heave Characteristics of Gravel Soil and Multifactor Regression Prediction. *Advances in Materials Science and Engineering.*

Lyazgin, A. L., Lyashenko, V. S., Ostroborodov, S. V., Ol'shanskii, V. G., Bayasan, R. M., Shevtsov, K. P., & Pustovoit, G. P. (2004). *Experience in the Prevention of Frost Heave of Pile Foundations of Transmission Towers under Northern Conditions*. Power Technology and Engineering. https://doi.org/10.1023/B:HYCO.0000036365.64731.4c.

Mackay, J.R., Konishchev, V.N. and Popov, A.I. (1978), Geologic controls of the origin, characteristics, and distribution of ground ice, Proc. Third Int. Conf. on Permafrost, Vol. 2, Nat. Res. Council Canada, Ottawa, pp. 1 18.

Mainwaring, K. A., Morley, C. P., Doerr, S. H., Douglas, P., Llewellyn, C. T., Llewellyn, G., Matthews, I., & Stein, B. K. (2004). Role of heavy polar organic compounds for water repellency of sandy soils. *Environmental Chemistry Letters.* 2, 35-39.

Michalowski RL. A constitutive model of saturated soils for frost heave simulations. Cold Regions Science and Technology 1993; 22(1):47–63

Michalowski, R.L. and Zhu, M. (2006), Frost heave modelling using porosity rate function. Int. J. Numer. Anal. Meth. Geomech., 30: 703-722. https://doi.org/10.1002/nag.497

Miller R. D., 1972, Freezing and heaving of saturated and unsaturated soils. Highway Research Record 393, 1-11

Miller R. D., 1978, Frost heaving in non-colloidal soils. Proceedings 3rd International Conference on Permafrost, 708-13

Miller R. D. and Koslow E. E., 1980, Computation of rate of heave versus load under quasi-steady state. Cold Regions Science and Technology 2, 243-252

National Research Council (U.S.). (1973). *Soils: loess, suction, and frost action: 7 reports prepared for the 52nd Annual Meeting*. Washington, D.C., Highway Research Board.

Nersesova, Z.A. and Tsytovich, A., 1963. Unfrozen water in frozen soils. Proc. 1st Int. Permafrost Conf., Purdue Univ.,Lafayette, Ind., pp. 230-234.

Nishimura, S., Gens, A., Olivella, S., and Jardine, R. 2009. THM-coupled finite element analysis of frozen soil: formulation and application, Géotechnique. Vol. 59 (3), pp. 159-171 URL https://www.scipedia.com/public/Nishimura_et_al_2009a 2

Nixon J. F., 1982, Field frost heave predictions using the segregation potential concept. Canadian Geotechnical J. 19, 526-529

Nixon J. F., 1991, Discrete ice lens theory for frost heave in soils. Canadian Geotechnical J. 28, 843-859

Noon, C. (1996). *Secondary frost heave in freezing soils*. Thesis / Dissertation ETD. http://eprints.maths.ox.ac.uk/27/1/noon.pdf.

O'Neill K. and Miller R. D., 1982, Numerical solutions for a rigid-ice model of secondary frost heave. CRREL Report 82-13,

O'Neill K. and Miller R. D., 1985, Exploration of a Rigid Ice model of frost heave. Water Resources Research 21, 281-296

Ozawa H. and Kinosita S., 1989, Segregated ice growth on a microporous filter. J. Colloid and Interface Science 132, 113-124

Penner E., 1966, Pressures developed during the unidirectional freezing of water saturated porous materials. Proc. Inter. Conf. Low Temperature Sci., 1402-141

Penner (1974). Uplift forces on foundations in frost heaving soils, Canadian Geotechnical Journal, 11, 323-338

Penner, E., & Goodrich, L. E. (1981). *Location of segregated ice in frost-susceptible soil*. Ottawa, National Research Council Canada, Division of Building Research.

Piercey, G., Volkov, N., Phillips, R., and Zakeri, A. (2011). Assessment of Frost Heave Modelling of Cold Gas Pipelines. PanAm CGS Geotechnical Conference

Rempel, A. W. (2007). Formation of ice lenses and frost heave. *Journal of Geophysical Research.* 112, F02S21.

Rempel, A. W., J. S. Wettlaufer, and M. G. Worster (2001), Interfacial premelting and the thermomolecular force: Thermodynamic buoyancy,Phys. Rev. Lett., 87, 088501.

Rempel, A. W., Wettlaufer, J. S., & Worster, M. G. (2004). Premelting dynamics in a continuum model of frost heave. *Journal of Fluid Mechanics.* 498, 227-244.

Sage, J. D., & Porebska, M. (1993). Frost Action in a Hydrophobic Material. *Journal of Cold Regions Engineering.* 7, 99-113.

Schulte, K., Culligan, P., & Germaine, J. (2007). Intrinsic sorptivity and water infiltration into dry soil at different degrees of saturation. Geotechnical Engineering, 1– 11. doi:10.1061/40907(226)5.

Schuyten, H. A., Reid, J. D., Weaver, J. W. & Frick J. G. Jr (1948). Imparting water-repellency to textiles by chemical methods. A review of the literature. Textile Res. J. 18, No. 7, 396–398.

Seto, J.T.C., and Konrad, J.-M. 1993. Pore pressure measurements during freezing of an overconsolidated clayey silt. Cold Regions Science and Technology. (In press.) Taber, S. 1929. Frost heaving. Journal of Geology, 37: 428-461.

Schreiner, O., and Edmund, C.S.. 1910. Chemical nature of soil organic matter. USDA Bur. Soils Bull. 74:2-48.

Smith, M.V. 1985. Observations of soil freezing and frost heave at Inuvik, Northwest Territories, Canada Can J Earth Sci V22, N2, Feb 1985, P283-290

Taber S., 1929, Frost heaving. J. Geology 37, 428-461

Taber S., 1930, The mechanics of frost heaving. J. Geology 38, 303-317

Takagi, S. 1979. Segregation Freezing as the Cause of Suction Force for Ice Lens Formation, Developments in Geotechnical Engineering, Elsevier, Volume 26, 1979, Pages 93-100, ISSN 0165-1250, ISBN 9780444417824, https://doi.org/10.1016/B978-0-444-41782-4.50013-0.

Takagi S., 1980, The adsorption force theory of frost heaving. Cold Regions Science and Technology 1, 57-81

Tiedje, E. (2015). *Characterization And Numerical Modelling of Frost Heave*. http://hdl.handle.net/11375/17198.

Torrance, J., & Schellekens, F. (2006). Chemical factors in soil freezing and frost heave. Polar Record, 42(1), 33-42. doi:10.1017/S0032247405004894

Tripp, C. P., & Hair, M. L. (1995). Reaction of Methylsilanols with Hydrated Silica Surfaces: The Hydrolysis of Trichloro-, Dichloro-, and Monochloromethylsilanes and the Effects of Curing. *Langmuir: the ACS Journal of Surfaces and Colloids.* 11, 149.

Vignes M. A., 1977, On the origin of the water aspiration in a freezing dispersed medium. J. Colloid and Interface Science 60, 162-171

Wilen, L. A., & Dash, J. G. (1995). *Frost heave dynamics at a single crystal interface*. [Woodbury, N.Y., etc.], American Physical Society.